Vysoké učení technické v Brně
Fakulta strojního inženýrství
Ústav konstruování

Brno University of Technology
Faculty of Mechanical Engineering
Institute of Machine and Industrial Design

# VOLUMETRIC WEAR ANALYSIS OF HIP JOINT IMPLANTS BY OPTICAL METHODS

**Ing. Matúš Ranuša**
Autor práce
Author

**doc. Ing. Martin Vrbka, Ph.D.**
Vedoucí práce
Supervisor

Disertační práce
Dissertation Thesis

Brno 2018

## STATEMENT

I hereby declare that I have written the PhD Thesis *Volumetric Wear Analysis of Hip Joint Implants by Optical Methods* on my own, according to advices from my supervisor doc. Ing. Martin Vrbka, Ph.D., and using the sources listed in references.

Brno, _____ …….

Matúš Ranuša

## BIBLIOGRAPHICAL REFERENCE

RANUSA, M. *Volumetric Wear Analysis of Hip Joint Implants by Optical Methods.* Brno, 2018, 125 p. PhD Thesis. Brno University of Technology, Faculty of Mechanical Engineering, Institute of Machine and Industrial Design. Supervisor: doc. Ing. Martin Vrbka, Ph.D.

## ACKNOWLEDGEMENT

I would like to express my special thanks to my Supervisor, doc. Ing. Martin Vrbka, Ph.D. and to Head of our Tribology Research Group, prof. Ing. Ivan Křupka, Ph.D. as well as our Department Director prof. Ing. Martin Hartl, Ph.D. for their support and consultations during my studies. Special thanks should go to prof. MUDr. Jiří Gallo, Ph.D., Prof. John B. Medley, Dr. Dipankar Choudhury and Ing. David Nečas, Ph.D. for their cooperation and help. Also, I would like to thank to all my colleagues at the Institute of Machine and Industrial Design for a friendly and creative atmosphere. Finally, I express my huge thanks to my family and specially to my great wife Veronika!

## ABSTRACT

This dissertation thesis deals with wear analysis of total hip replacements (THR) using optical methods. We introduced a new approach to volumetric wear assessments of polyethylene liners using a 3D optical scanner. The new approach brought benefits of time-efficient measurements, large number of points collected for post-processing, the possibility to create pre-worn models of retrieved samples as well as the possibility to exclude damages caused by surgeon during revision surgeries. The method was validated by gravimetric method according to the ISO 14242 Standard. The new approach was then used in three studies focusing on wear rate and mechanical changes of polyethylene liners. In the studies, the analysis of polyethylene liners geometry was followed by a detailed surface analysis of contact areas down to the microstructural level. Clinical history data for 23 retrieved liners combined with wear analysis showed several issues affecting failure of the polyethylene implants. We worked with Bicon-plus type implants, that are widely used in clinical practice in the Czech Republic. Structural surface analysis of the retrieved samples showed several different wear mechanisms such as adhesion/abrasion, pitting, delamination and plastic deformation. Analysis of material behaviour showed mechanical changes and chemical degradation in retrieved prostheses which mostly correlated with the wear depth. Investigated samples showed plastic deformations, an increased oxidation index and lower hardness to elasticity ratio compared to the new samples. Creep phenomenon or plastic deformation, which was investigated in the final part of thesis, occurred in all the retrieved samples. Further in vitro testing showed presence of creep in the run-in phase of implants.

This thesis aimed to introduce a new approach to wear analysis using the optical scanning method and to apply the new approach for investigations of surface geometry of retrieved polyethylene liners. The method proved to be a suitable method for investigations of retrieved polyethylene liners helping to better understand the processes leading to implant failures.

## KEYWORDS

Biotribology, Total Hip Replacement, Retrieval Analysis, UHMWPE, Wear Measurements, Optical Digitalization, Surface Analysis

## ABSTRAKT

Predložená dizertačná práca sa zaoberá analýzou opotrebenia totálnych bedrových endoprotéz za použitia optických metód. V práci bol predstavený nový prístup hodnotenia objemového úbytku materiálu pomocou 3D optického skeneru. Tento nový prístup je časovo efektívny, poskytuje veľké množstvo snímaných bodov na povrchu implantátu. Množstvo bodov umožňuje presnejšiu rekonštrukciu pôvodnej geometrie a prípadné rekonštrukcie nežiaducich poškodení polyetylénovej vložky pri extrakcii. Predstavené metóda bola validovaná za pomoci štandardizovanej gravimetrickej metódy v súlade s ISO 14242. Následne bol optická skenovacia metóda použitá v troch štúdiách zameraných na analýzu opotrebenia, mechanické zmeny artikulujúceho povrchu a mikroštruktúrne zmeny v dôsledku zlyhania implantátu. Analýza 23 extrahovaných polyetylénových vložiek typ Bicon - plus s rozšíreným použitím v Českej republike poukázala na niektoré problémy spojené so zlyhaním implantátu. Adhezívno - abrazívne opotrebenie bolo identifikované v oblasti penetrácie femurálnej hlavice a následné poškodenia ako delaminácia materiálu , plastické deformácie a pitting boli pozorované v okolí tejto oblasti. Analýza materiálových vlastností poukázala na degradáciu mechanických a chemických vlastností, čo bolo prevažne závislé od rozsahu opotrebenia implantátu. U implantátov boli pozorované výrazné plastické deformácie , nárast oxidačného indexu a nižší pomer tvrdosti voči modulu elasticity, v porovnaní s novými vzorkami. Tečenie materiálu a plastické deformácie, ktoré vykazovali všetky extrahované vzorky boli analyzované v závere predloženej dizertačnej práce, na základe testov na nových implantátoch v zábehovom cykle.

Cieľom práce je uviesť nový prístup analýzy opotrebenia polyetylénových vložiek za pomoci optických skenovacích metód a preukázať jeho použiteľnosť na analýze súboru extrahovaných implantátov. Výsledky získané pomocou tejto metódy sa ukázali ako vhodné a môžu viesť k lepšiemu pochopeniu procesov opotrebenia a zlyhávania implantátov.



## KĽÚČOVÉ SLOVÁ

Biotribológia, totálna bedrová endoprotéza, analýza extrahovaných implantátov, UHMWPE, analýza opotrebenia, optická digitalizácia, povrchová analýza.

# CONTENT

# 1 INTRODUCTION

Total hip replacement is one of the most common surgeries in modern medicine. During the total hip replacement surgery, failed femoral head and acetabulum are extracted and replaced with artificial components. Number of these surgeries increased on average by 30 % between years 2001 and 2017. According to the *Health at a Glance* statistics published by the Organisation for Economic Co-operation and Development (OECD) [1], the increased number of total hip replacement procedures (Fig 1.1). is related to changing lifestyle and age structure of population. Malfunction and pain are clinical indications of aseptic loosening caused by osteoarthrosis or joint fracture. Worldwide estimates show that 10% of men and 18% of women over 60 years suffer from symptomatic osteoarthritis. Osteoarthritis is one of the ten most disabling diseases in developed countries and one of the most frequent reasons for surgeries. In most cases, successful surgeries relieve the pain, however quality of life remains significantly affected. Despite many improvements, longevity of the implants is still limited to 10-20 years. Failed implants require revision surgeries with even more extensive interventions into the human body. Pelvis carrying a revised implant is more sensitive to fracture and the survival time of the revised implants is shorter than those of the primary surgeries.

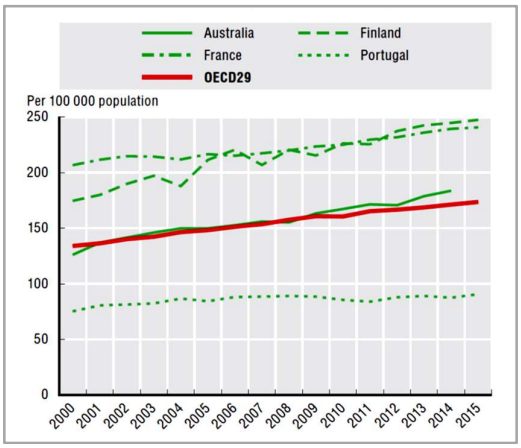


Fig 1.1 OECD Health Statistics 2017 [1]

Thanks to constant improvements of implants, there is a decreasing number of severe mechanical failures that require immediate revision, such as implant fracture, dislocation, or heavy delamination of the implant material. However, failures caused by aseptic loosening are increasing. Aseptic loosening is caused by osteolysis - resorption of bone tissue initialized by presence of foreign debris. Foreign particles interacting with the hip environment can cause inflammation reactions, tissue degradation and subsequent loosening of the implant. Loose implants do not provide sufficient stability and must be revised.

Certain threshold number of foreign particles released into the human body can lead to health problems. Probability of revision surgery rises with rising number of the particles. Therefore, wear reduction is identified as a high priority goal in

contemporary implants research and development. To understand the implant properties and behaviour better, it is necessary to use a high performing measurement method for analysis of the retrieved cups. The thesis focused on implants composed of hard on soft materials, i.e. Metal-on-Polyethylene (MoP) and Ceramic on Polyethylene (CoP) implants. Hard on soft implants are being increasingly used, reaching 58,4% of all the primary surgeries in 2016 according to the National Joint Registry for the United Kingdom [2]. These types of replacements are the most common bearing constructs used for cemented, uncemented and hybrid hip replacements. (Fig 1.2) Hard materials are represented by very stiff femoral heads (CoCrMo alloys, Ceramics) and soft materials are represented by compliant acetabular cups (Ultra-high Molecular Weight Polyethylene - UHMWPE, Highly Cross-linked Polyethylene - HXPE).

Although information on wear rate (affecting especially the soft materials) may be very important to understand longevity of implants, we need a better description of other parameters related to complex geometrical changes of the implant, too. Therefore, we focused on various methods of wear analysis and their mutual comparison. In general, two different approaches can be used for wear analysis: reverse analysis of the extracted cups and prediction analysis using a hip simulator or a mathematical model. Combination of these methods can lead to a better understanding of the wear mechanism.

The aim of this thesis is to provide a methodology for wear analysis of polyethylene liners on micro and macro level using optical methods.

Most literature reports on a direct correlation between one input wear parameter, such as amount of wear or volume loss, and implant failures. Very few studies show a complex approach to description of geometrical and surface changes of the articulating components. For this purpose, a novel methodological approach has been developed.

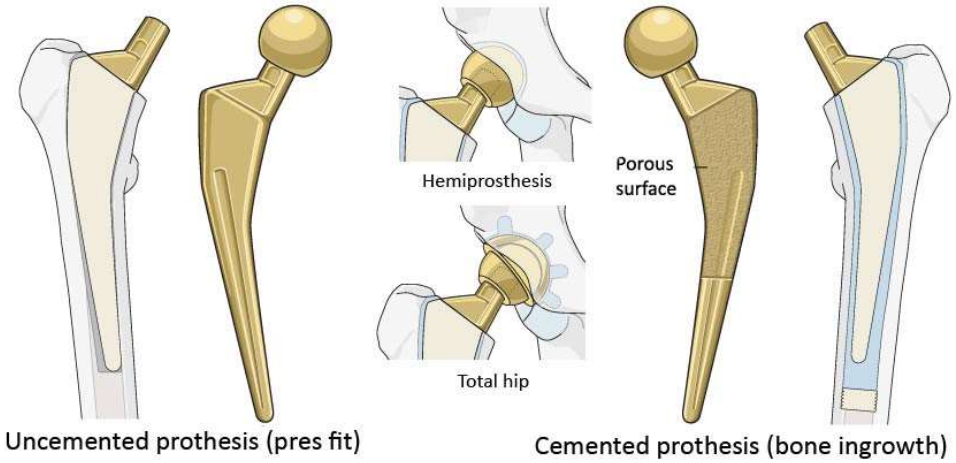


**Fig 1.2 Types of Total hip replacements (www2.aofoundation.org)**

# 2 STATE OF THE ART

The hip joint is the second largest joint of the human body. Main elements of a natural synovial joint are: the underlying bone, articular cartilages, synovial fluid, tissues that constrain and articulate the joint, ligaments, and tendons as shown in (Fig 2.1) of a lower limb joint [3]. The hip joint transmits high loads of up to five times the body weight while permitting motions in all six degrees of freedom (DOF). It is actuated by numerous muscles (active structures) that are attached to bones by tendons. The muscles, along with articular cartilage, ligaments, and joint capsule provide joint with stability. In case of a functional defect of the joint, it is necessary to perform a joint surgery. A partial hip replacement surgery replaces the surface of a femoral head by an artificial one. This procedure is also called hip resurfacing. On the other hand, a total hip replacement surgery replaces all components of a human joint. The total hip replacement provides a higher locomotion and longevity of implants, but the surgeries are much more invasive.

## 2.1 Clinical aspects of hip joint

The hip joint (*articulatio coxae*) is the connection between the femur and acetabulum of the pelvis. The hip represents a conduit through which the weight of the rest of body is transmitted to the lower extremities. In this role, the hip must be able to carry and transmit both the gravitational forces of the body and the ground reaction forces of the lower extremity throughout a large range of positions. This is accomplished through a combination of both static and dynamic stabilizers such as tissues and tendons that help to prevent joint dislocation and to maintain mechanical efficiency. The hip must, at the same time, be highly dynamic, allowing for a large degree of motion to enable various movements required for the wide range of activities of a human body. In case of the hip joint replacement surgeries, the effort is to get as close to this functionality as possible to minimize negative effects on quality of life.

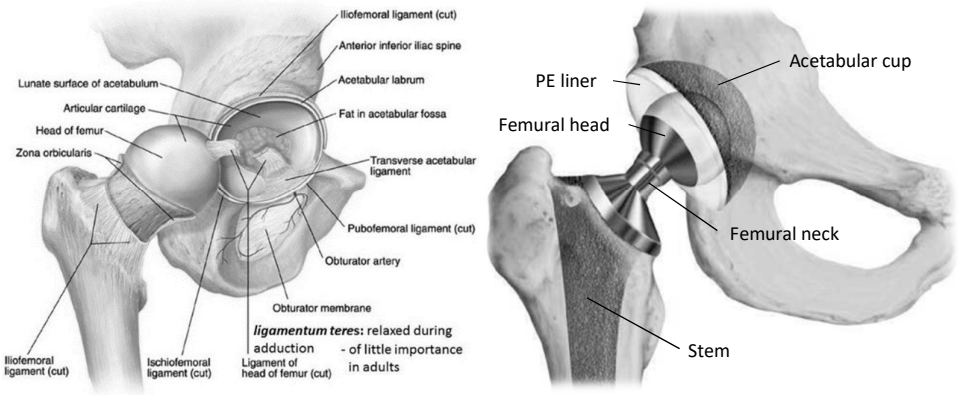


Fig 2.1 Hip joint and total hip replacement (www.boneandspine.com)

### 2.1.1 Anatomical positioning of hip joint

The most often used reference system that is suitable for various biomechanical investigations, including a gait analysis, a radiograph analysis, in vitro studies and wear description can be described as follows. The scheme below (Fig 2.2) shows three general planes of the joint: sagittal, frontal and transverse. These planes serve as a reference motion and position system of the hip joint. Position of each hip component is defined by perpendicular directions against each plane. Medial and lateral directions are perpendicular to the sagittal plane located in the coordinate system of the joint. Anterior and posterior directions are perpendicular to the frontal plane and finally superior and inferior directions are perpendicular to the transverse plane. The centre of the motion system is usually placed in the centre of a femoral head in a neutral position against the acetabular cup, even if a measurable incongruity of ball and socket does exist. Motion of the hip joint is then defined from the centre of the coordinate system in directions of each plane. Rotation around *the medial – lateral axis* is defined as a flexion – extension motion. Rotation around *the superior – inferior axis* is defined as an internal – external motion. Rotation around *the anterior- posterior* axis is defined as an abduction – adduction motion.

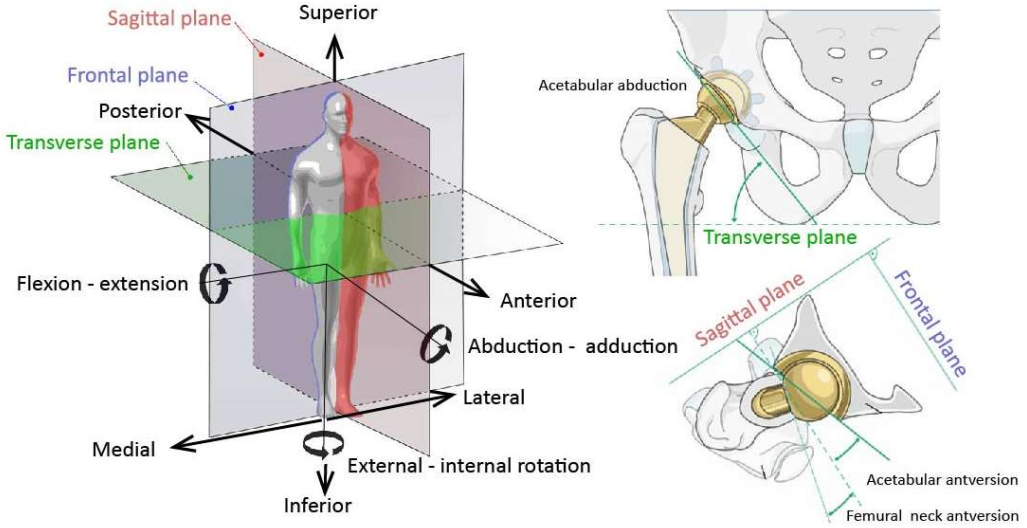


Fig 2.2 Anatomical positioning of the hip joint

The gait cycle is the key physiological movement for the hip joint. This complex movement can be divided according to the three anatomical planes as described above: flexion /extension, abduction/adduction and inner/outer rotation. The gait cycle defines range of movement for the lower limb and it creates an elliptical trajectory from the perspective of a point located on the articulating surface of a hip joint implant. This mechanism causes multidirectional shear stress that correlates with patient's weigh [4]. Changes, fluctuations and peaks of the shear stress can influence wear degradation of the articulating surface.

### 2.1.2 Kinematics of hip joint during gait

Kinematic and load parameters for in vitro testing of hip implants are specified in the ISO 14242 Standard to ensure comparable test results [5]. The Standard defines movements and load cycles during the gait. There are two maximum load peaks of 3000 N during the gait: heel strike and toe-off. They are derived from the human gait which can be divided to two main phases: a stance phase and a swing phase. The stance phase begins with the heel strike, a moment when the heel begins to touch the ground, but the toes do not touch the ground yet. What follows is settlement of the foot at the lateral border. When the stance phase ends, the swing phase begins. This is the phase between the toe-off phase and the heel strike phase. In the swing phase we can recognise two more phases - acceleration and deceleration. The acceleration phase goes from the toe-off to a midswing, while the deceleration goes from the midswing to the heel strike. In the acceleration phase, the swing leg makes an accelerated forward movement to propel the body weight forward. The deceleration phase brakes the velocity of this forward body movement to place the foot down under control. Understanding principles of the gait cycle and weight transmission during the gait is crucial for understanding the kinematic and load conditions of a hip replacement.

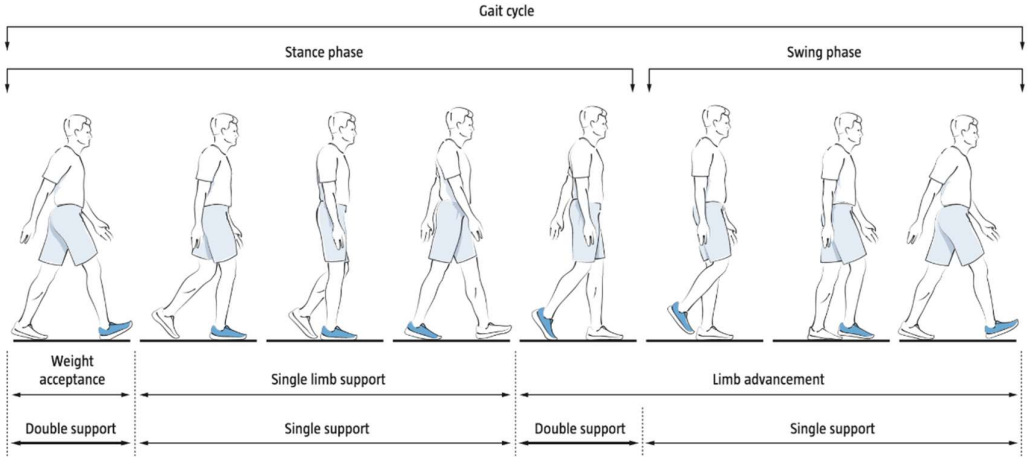


Fig 2.3 The Gait Cycle (www.wddty.com)

Gait analysis of a hip joint was carried out by Tsai et. al.[6] The aim of this study was to quantify the 6-degrees of freedom kinematics of in-vivo hips during a gait cycle in patients with total hip replacement. The analysis was performed on 28 patients without dislocation, subluxation or any other surgical complications. Each subject was asked to perform a level walking on a treadmill at a self-selected speed. Series of image frames were captured during their gait to obtain the 3D kinematics of the movement. A non-invasive dual fluoroscopic imaging system (DFIS) based tracking technique was used to measure an accurate 6-degrees of freedom kinematics. Results showed ranges of angular and translation movements for each plane of the hip joint.

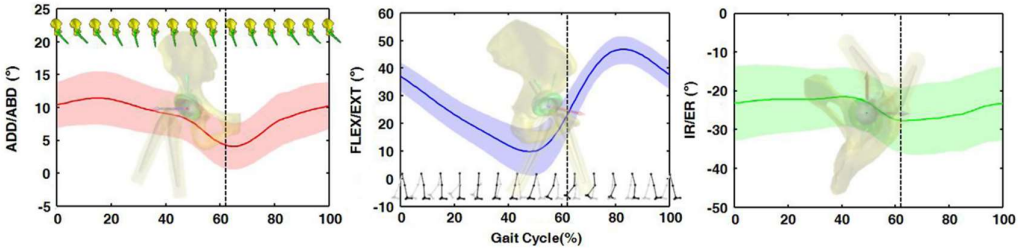


Fig 2.4 Averages and standard deviations of in-vivo hip translations and rotations of 28 THA during gait [6]

Tab. 2.1 Averages of maximum hip rotation angles of THR [6]

| Hip rotations | Maximum angle |
|---|---|
| Flexion/extension | 8.7deg to to 47.6deg |
| Adduction/abduction | 3.5deg to to 12.5deg |
| Internal/external rotation | -29.7deg to to -19.2deg |

### 2.1.3 Wear debris and implications on health of patient

As the hip joint implants wear out, the wear debris is released into the surrounding tissues of the joint. Most of the implanted pairs consist of a metal or a ceramic femoral head articulating with a polyethylene liner and it is mostly the soft polyethylene material that wears out. Recent observations indicate that the wear of the articulating surfaces might be substantially influenced also by the third body particles - either bone cement debris particles or particles released from the surfaces as was demonstrated in study Pokorny et. al.[7, 8]. The biological response of the surrounding tissues to the released particles can influence lifecycle of implants and potentially influence also the mechanical and chemical behaviour of the materials. Size and shape of the particles play a crucial role. Shibo. et al. [9] studied debris and found debris fractions of tens of microns in four different shapes: round, flake, twig and stick particles (Fig 2.5). The authors also observed a detailed debris release process on the UHMWPE surface (Fig 2.6). The debris release was studied under various ranges of load, motion and bovine serum lubrication conditions. If we assume that the wear rate and the surface topography might be influenced by the particles behaviour, it is worth noting that only a small number of studies examine the relationship between the particle shape and wear of an implant.

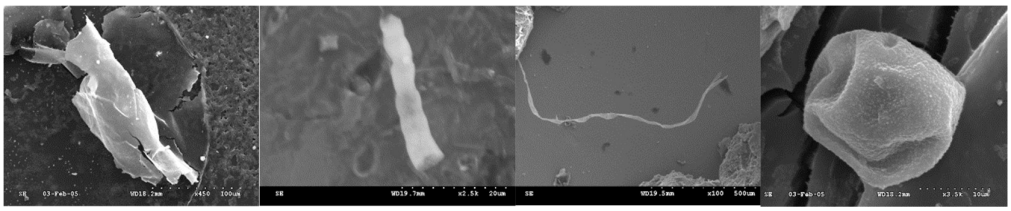

Fig 2.5 SEM images of UHMWPE debris

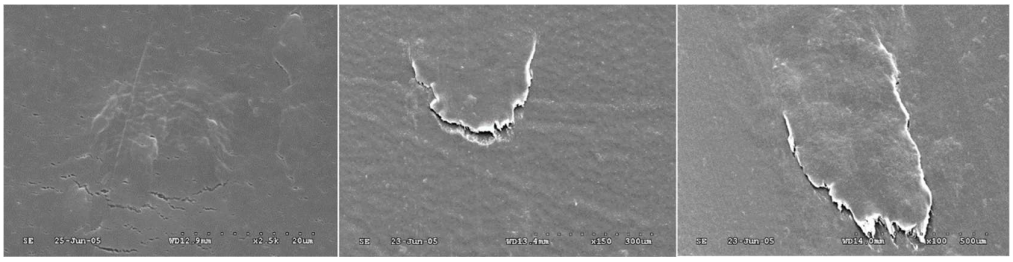

Fig 2.6 SEM observation on the detachment of fragment on UHMWPE surface: shear cracking, initial generation and debris enlargement before fracture.

One the other hand, there are several studies dealing with the amount of debris released into human body that is critical from the clinical perspective. Clinical studies suggest that the incidence of osteolysis increases with an increased wear rate. The literature review by Dumbleton et. al. [10] indicates that osteolysis is rarely observed at wear rates of < 0.1 mm/y of linear wear. Authors concluded that the threshold wear rate of 0.05 mm/y would eliminate the osteolysis. This wear rate threshold suggests that the new cross-linked polyethylene could reduce osteolysis, provided that the in vivo wear rates mirror those observed in vitro. The main limitation of the reviewed studies is that they suggest the wear rate threshold based on the linear wear. However, different sizes of the implants can lead to different results because the larger heads release higher volumes of wear than the smaller heads showing the same linear penetration values as the larger heads. The studies also do not consider plastic deformations and rim delaminations influencing especially the volumetric wear of the liners. Oparaugo et. al. [11] investigated correlation between the volumetric wear and osteolysis for 3 various groups of patients. (Tab. 2.2).

Tab. 2.2 Correlation between volumetric wear rate and osteolysis

| | |
|---|---|
| 0 - 80 $mm^3$/year | Rare osteolysis |
| 80 - 140 $mm^3$/year | osteolysis ranged from 6% to 31% |
| > 140 $mm^3$/year | osteolysis ranged from 21% to 100%. |

### 2.1.4 Materials of implants

Polyethylene acetabular cups with articulating metal femoral components were first used for total hip replacement surgeries in 1950s. Surgeons used ultra-high molecular weight type of polyethylene (UHMWPE) that was made by catalysing chaining polymerization and then sterilized without any further modifications. The material had sufficient tribological properties and was biocompatible. Later the material has been further enhanced in different ways, but the basic combination of materials is still used today. UHMWPE has low resistance against wear in interaction with significantly harder materials such as cobalt-chrome-molybdenum (CoCrMo) alloys and ceramics that are used in femoral heads. At the end of 1990s, wear resistance of UHMWPE was improved by linking the amorphous fractions of the material using gamma irradiation. Irradiation forms bonds between long hydrocarbon chains and creates free radicals. Highly reactive radicals interact with each other and form bridges between each chain. As a result, new generation of polyethylene, so called

Cross Linked Polyethylene (XLPE), is created. This material is more resistant against wear thanks to its limited chain mobility and increased density of chemical bonds between adjacent molecular chains. The density of chemical bonds makes it difficult for molecules to split from each other. UHMWPE was reported to develop gravimetric wear rates below 56 $mm^3$/year, while XLPE was reported to develop wear rate around 2.8 $mm^3$/year. The values are multiple times lower for hard materials such as metal or ceramics, reaching up to 0,004 - 0,9 $mm^3$/year [12].

What remains problematic are the residual radicals accelerating the oxidative degradation of the XLPE polyethylene. Residual radicals are usually eliminated by recast or annealing of polyethylene. Recast modification is risky, because it can change polyethylene properties. Heat treatment influences strength of the material what can lead to acetabulum fractures. Moreover, annealing does not remove radicals properly. There are efforts to apply sequential irradiation and several steps of annealing to improve the results. Alternatively, vitamin E as antioxidant can be applied for elimination of free radicals instead of the heat treatments [13]. The final implant is then gamma-radiation sterilized (cobalt-60) while sealed in a threefold pouch in a nitrogen atmosphere. In general, crosslinking makes the UHMPWE more isotropic.[14]

**Tab. 2.3 Typical average physical properties of UHMWPE**

| | |
|---|---|
| Molecular weight | 2 . . . 6 $10^6$ g/mol |
| Melting temperature | 125 . . . 138 °C |
| Poisson's ratio | 0.46 |
| Specific gravity | 0.932 . . . 0.945 |
| Tensile modulus of elasticity (at 23°C) | 0.8 . . . 1.6 GPa |
| Tensile yield strength | 21 . . . 28 MPa |
| Tensile ultimate strength | 39 . . . 48 MPa |
| Tensile ultimate elongation | 350 . . . 525 % |
| Degree of crystallinity | 39 . . . 75 % |

## 2.2 Methods of analysis for hip joint implants

2.2

### 2.2.1 Main approaches to wear determination

There are two main approaches to wear determination: determination of *linear wear* and determination of *volumetric wear*. Volumetric wear, linear wear and wear rates are the most widely used and recognised parameters of a THR joint performance. *Linear wear* is often defined as penetration of the head into the acetabular cup and it is usually defined in relation to the lifecycle of the implant, i.e. the laboratory test results are reported in *mm per year* or *mm per number of cycles*. This approach does not consider the total volume of the released material. Liner wear analysis is not suitable for investigating the implant position or damages outside of the articulating surface [15-17]. The advantage of this method is that it is easily comparable with results of standard in vivo analyses, such as radiograph. *Volumetric wear* determines

the amount of debris released from the implants. This allows for more accurate results both in terms of linear wear as well as volume of the material released into the body.

Data on linear wear, volumetric wear, wear rates and wear direction together with basic information on creep and geometrical changes of the implants can help us better understand the complex wear mechanism and advance our predictions of wear behaviour.

### 2.2.2 In vivo wear determination

Several different methods have been developed to determine wear under in vitro or in vivo conditions. Current clinical practice evaluates in vivo wear using non-destructive and contactless methods that can recognize position and shape of implants in human body. *Radiographic and stereographic examinations* are the most often used clinical routines after a total hip replacement surgery. These methods are also used for tracking the lifecycle of the implant to support medical decisions regarding arthroplasty [17-19]. *Computer tomography (CT)* is used less often. Though it provides more detailed data, including data on the surrounding environment of the implant, it is more expensive and has negative health consequences for patients [20-22].

*Radiographic method* is one of the clinically most widely used methods of linear wear analysis that is routinely performed with each hip replacement. The results are usually available in patients' health records. Linear head penetration is determined by image processing. One possible approach is to simply use a geometrical analysis of clear edges of implants to assess the femoral head penetration. This approach can be supported be an image processing software that recognizes the edges and calculates the wear accordingly. One of the available computer assisted techniques has been developed by Martel et al.[15]. Martell's method determines vector of wear and rate of linear wear (Fig 2.7). Martell's analysis demonstrated superior repeatability and accuracy compared to manual analysis. Better repeatability and accuracy in determination of the polyethylene wear leads to more reliable investigations of various factors influencing diagnosis of the implants.

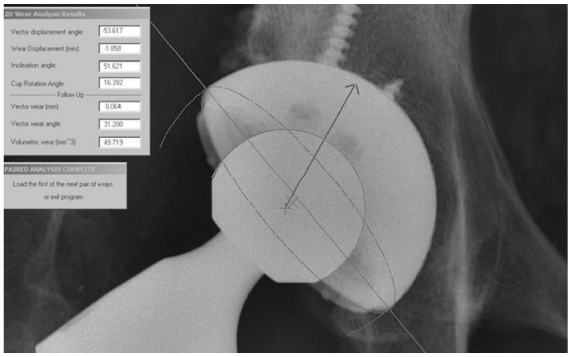


**Fig 2.7 The Martell method of linear wear measurement shown on this radiograph [23].**

Computer assisted radiographic methods has been discussed by many authors. An approach described by Livermore et al.[24] and EBRA method (Ein Bild Röntgen Analyse) [25] are often used for wear assessment. There are also other more precise methods to detect the wear [17, 26, 27]. A study on accuracy of various clinical radiograph methods was carried out by Ebramzadech et. al. [16]. The results shown in figure (Fig 2.8) represent the errors of radiographic measurements. The true value of wear was assumed to be that directly measured with the coordinate measuring machine from the retrieved components and subtracted from each measurement to calculate error.

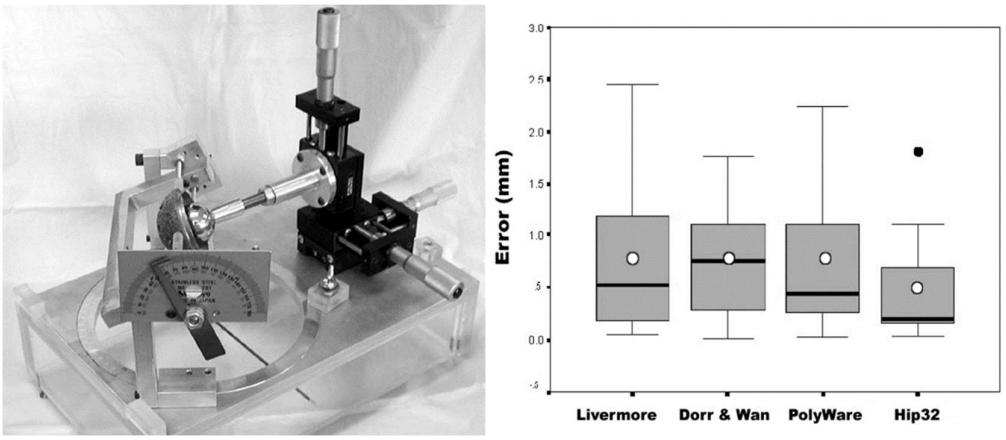


**Fig 2.8 The phantom apparatus that was used for creating the different three-dimensional displacements and errors of radiographic measurements.**

*Radiostereometric analysis* (RSA) is the second approach to head penetration analysis. The method was developed by Selvik et. al. in the early 1970s as a technique for accurate measurements of small displacements of the implant body or implant segments in vivo [28]. The method has been used to evaluate fracture healing, growth plate viability, joint kinematics and spinal fusion stability. The radiostereometric analysis has been also extensively used to evaluate migration of the THR components [29].

Despite many improvements in radiographic methods, the methods do not determine wear with satisfying accuracy. Radiologic measurements are based on geometric principles and require number of simplifications and compromising steps to acquire approximately precise values. More accurate measurement techniques are needed for in vitro analysis.

The inherent 2D nature of many radiographic methods can cause errors in determination of wear based on implant positioning. Therefore, it is interesting to compare the results of radiographic methods with more precise methods of in vitro analysis that can provide complex information on liner surface. In vitro methods are used for retrieved liners or for wear tests carried out on new samples. Therefore the

in vitro methods as described below are used mostly for validation or for better understanding of tribological interactions of implant surfaces.

### 2.2.3 In vitro wear determination

Hu et al. [30] developed a geometric method for in vitro measurements. A contacting roundness machine (Carl Zeiss, Germany, ±0.03 µm for wear depth and ±0.436 µm for angle measurement) was used to measure the depth and angle of the wear patch. The measured values had a high resolution (<0.1 µm) but were 2D in their nature. The results were processed using a numerical model developed to calculate the wear volume for both the femoral head and the acetabular cup. The method was applied on samples worn by a wear simulator and later compared with the gravimetric method. Authors consider the method as a valid, and error as a statistically significant.

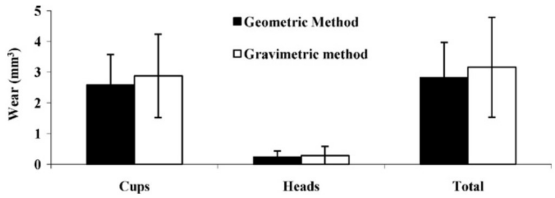


**Fig 2.9 Wear comparison between the geometric and gravimetric methods [30].**

Joyce et al. [31] used another method for wear analysis of retrieved metal-on-metal liners to compare the out of roundness results with clinical complications of patients. The wear was analysed in three planes and results diverged from circularity (Fig 2.10 Maximum out of roundness values of the explanted components and the associated clinical data [32]. The analysis showed that failures associated with effusion and pain in patients were associated with out of roundness values far higher than the manufacturing tolerances. These results were supported by the high ion levels seen in the blood of patients. In addition, all these failures were associated with cups positioned at high angles of inclination and anteversion.

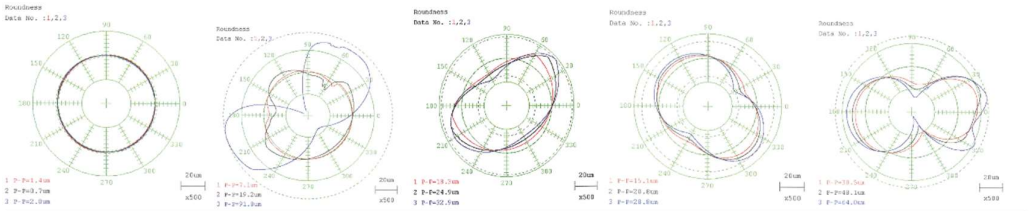

| Patient | Head OOR (µm) | Cup OOR (µm) | Reason for revision | Duration (months) | Cr (µg/l) | Co (µg/l) | Cup inclination (°) | Cup anteversion (°) |
|---|---|---|---|---|---|---|---|---|
| 1 ♀ | 31.3 | – | Pain, effusion | 28 | – | – | 62 | 26 |
| 2 ♀ | 17.7 | 14.8 | Pain, effusion | 18 | – | – | 58 | 29 |
| 3 ♀ | 91.8 | 64.0 | Pain, effusion | 8 | 36 | 88 | 65 | 39 |
| 4 ♀ | 38.0 | 28.8 | Pain, effusion | 27 | 5 | 8 | 50 | 32 |
| 5 ♀ | 32.9 | 23.1 | Pain, effusion | 17 | 15 | 19 | 51 | 18 |
| 6 ♀ | 1.8 | – | Fracture | 2 | – | – | – | – |
| 7 ♂ | 3.1 | – | Fracture | 5 | – | – | 46 | 31 |
| 8 | 2.5 | – | Fracture | | | | | |
| 9 ♂ | 1.7 | – | Fracture | 8 | – | – | – | – |
| 10 ♂ | 2.0 | – | Fracture | 1 | – | – | 47 | 7 |

**Fig 2.10 Maximum out of roundness values of the explanted components and the associated clinical data [32].**

As mentioned above, the main advantage of linear wear analyses is that they enable comparison with clinical radiologic methods as well as comparisons across various studies. However, there are limitations that do not allow us to describe the whole process of material loosening during implants' lifespan in greater detail. 3D in vitro methods such as the coordinate measuring method, the micro CT method and optical methods can provide complex information on wear and surface changes.

#### 2.2.3.1 Coordinate measuring method

One of the frequently used methods for the articulating surface wear analysis is the *coordinate measurement method (*CMM) as described by ISO Standard 14242-2 [5].

Coordinate measuring machines are mechanical systems designed to move a measuring probe to determine coordinates of points on a surface. The machines are comprised of three main components: the machine itself, the measuring probe, and the control or computing system with a measuring software. The resulting point cloud measured with a coordinate measuring machine is post-processed using a modelling software (e.g. CAD) and regression algorithms for further analysis.

The method provides satisfactory measurement accuracy at each isolated measured point that is declared to be at levels with maximum axial-position error of measurement D, in micrometres, of:

$$D = 4 + 4\mathrm{l} \times 10^{-6} \tag{2.1}$$

where l is the numerical value of the dimension in meters [5].

The wear rate is calculated using the equation for the least squares linear relationship between wear volume and number of cycles.

$$\mathrm{V}_n - V_o = a_V.n + b \tag{2.2}$$

$V_o$ – original volume
$V_n$ – acetabular cavity
n – number of cycles
b – constant using a least square fit
$a_V$ – wear rate

Thanks to its accuracy and reliability, the coordinate measurement method has become a reference method for validation.

Major limitation of the method is that it uses only a limited number of measurement points for reconstructing the original geometry from the unworn parts of the articulating surface when measuring volumetric wear of a liner with an unknown original geometry. Limited number of points poses problem with mash spacing of distributed surface points. The accuracy of the CMM measurements is also compromised by the fact that the retrieved components can be extensively damaged what can influence precision of the coordinates and cause problems with analysis of these areas of the surface geometry.

Despite these problems there are still efforts to reconstruct the original geometry using the unworn parts of the articulating surface. Several studies describe an algorithm of data processing and reconstruction for metal-on-metal, metal-on-polyethylene or metal-on-ceramics implant pairs [33-35]. Though this process entails geometric error, the coordinate measurement method provides good results in volumetric wear determination.

Usability of the coordinate measurement method was demonstrated by Galvin et al. [36] who compared wear of the UHMWPE acetabular cups against surface-engineered femoral heads. The wear was determined volumetrically by using a coordinate measuring machine (Kemco 400 3D, Keeley Measurement Co. UK). The three-dimensional geometry of the cups was measured before the test and then every million cycles of the wear test (Fig 2.11). Geometrical mapping allowed a three-dimensional reconstruction of the cup surface to show the maximum areas of wear and penetration.

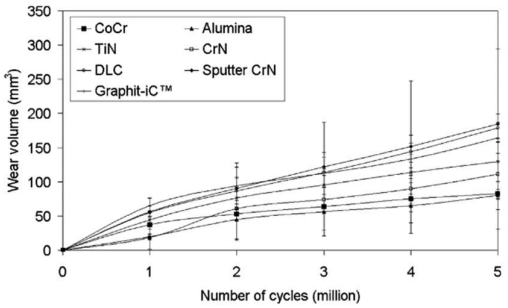


**Fig 2.11 Volumetric wear of UHMWPE published by Galvin et al. [36]**

Another study published by Wang et al. [37] aimed to determine volumetric wear and spatial distribution for polyethylene acetabular liners. Authors used the coordinate measurement method, (Global Classic SR 757) with probe diameter of 1mm and accuracy of 1.9 µm. The number of collected points was 3720 for each sample. The method was used on retrieved liners with no original referential surface data. The authors developed algorithms to process data from the point cloud to evaluate the volumetric wear and to determine the original geometry from the unworn area. The algorithms are equally applicable to other kinds of measuring methods.

Measurement errors of the coordinate measuring method were described by Bills et al. [38]. The study analysed the uncertainties associated with measurements of spherical geometries and applied them to both the measurement of wear in retrieved bearings and metal hip resurfacing components. The influence of measurement uncertainty was showed to be of a significant order for the coordinate measurement method. The study showed that the grid definition and performance of the meshing algorithms can significantly influence the results (Fig 2.12). It is therefore also suggested that the grid spacing should be adapted to component size. The analysis was carried out on six explanted metal-on-metal hip replacements.

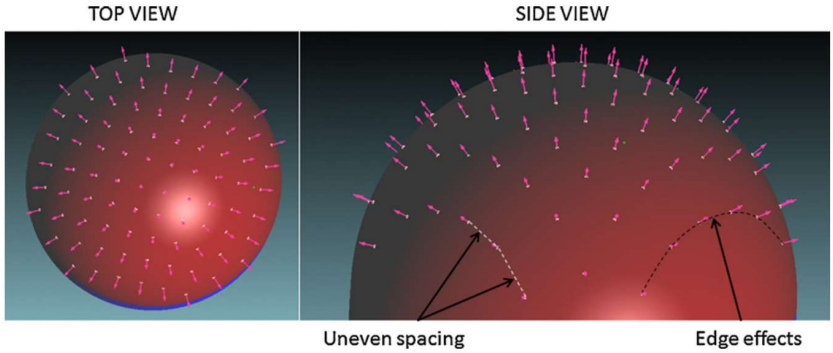


Fig 2.12 Effect of mesh spacing

The measurement error demonstrated for the volumetric wear was between 1,145 and 1,859 $mm^3$.

Another study quantifying uncertainty of measuring methods was published by Carmignato et al. [39], who compared the results of the coordinate measurement method with gravimetric measurements. Wear weight was divided by the material density 3.98 ±0.02$mg/mm^3$ for ceramics to obtain the volumetric wear for validation. Gravimetric measurements were carried out according to the ISO/IEC98-3 Standard [40] taking into consideration the uncertainty of weightings (derived from the expanded uncertainty of the balance, which was ±0.1mg in their case) and the uncertainty of material density (±0.02mg/mm3) using this equation:

$$E_N = \frac{|Value(CMM) - Value(Gravimetric)|}{\sqrt{U_{CMM}^2 + U_{Gravimetric}^2}} \quad (2.3)$$

Uncertainty contribution for each method was counted separately and the resulting value U was counted as sum of these values. Differences between the volumetric

wear measurements using the coordinate measurement method and gravimetric method as reported in (Fig 2.14) defined the so called normalized error $E_N$, which is a parameter typically used to evaluate the metrological compatibility of two different measurement results. The authors discussed the measured point spacing (Fig 2.13) as one of the reasons of the measurement uncertainty.

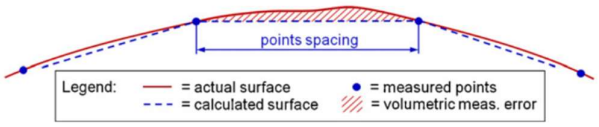


Fig 2.13 Schematic representation of a section of the measured surface[39].

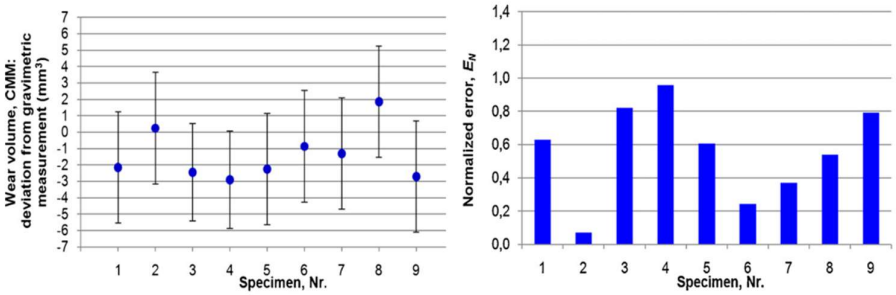


Fig 2.14 Deviations between wear volume measurements from CMM and gravimetric method [39].

Similar principles under different measurement conditions were used for the polyethylene liners analysis by Uddin et al. [41]. The authors used the coordinated measurement method on conventional crosslinked polyethylene (XPE) and second-generation highly cross-linked polyethylene (X3) retrieved liners.

An initial coordinate measurement method probing of at least ten random points was performed on the unworn regions between the rim and the pole of the cup to define the original reference geometry. The whole worn surface of the retrieved cups was then CMM probed on predefined scanning paths with 0.25 mm × 0.25 mm mesh of measurement points to determine the worn geometry. The difference between the reference geometry and the worn geometry defined the actual wear. The results were validated with gravimetric method. The normalized error was always below 1, with maximum volumetric uncertainty of ±3.12 $mm^3$ (95% confidence interval, Fig 2.15) hence proving the usability of coordinated measurement method also for polyethylene surfaces.

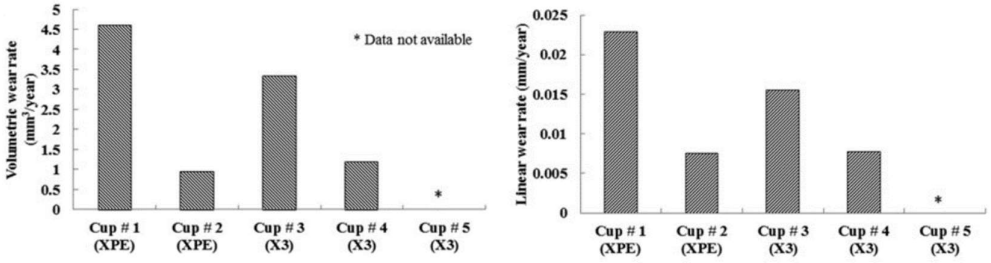


| Method | Wear Amount ($mm^3$) First Stage | Second Stage | Third Stage | Fourth Stage | Fifth Stage |
|---|---|---|---|---|---|
| Mean gravimetric (mg) | 56 | 82 | 128 | 153 | 177 |
| Mean gravimetric ($mm^3$) | 7.65 | 10.83 | 16.53 | 19.54 | 22.51 |
| Mean CMM ($mm^3$) (SD) | 7.01 (0.81) | 10.27 (0.72) | 16.02 (0.62) | 19.17 (0.46) | 22.18 (0.29) |
| Normalized error, $E_N$ | 0.32 | 0.28 | 0.24 | 0.18 | 0.16 |

**Fig 2.15 Comparison of wear rate between liners: linear and volumetric wear**

### 2.2.3.2 Micro CT methods

The coordinate measurement method is relatively time consuming and requires mathematical algorithms for post-processing due to limited amount of measured points. Thanks to its high accuracy, it is more suitable for hard materials. More significant damages on polyethylene liners such as a delamination, pitting or broken parts can be difficult to measure using the coordinate measurement method.

MicroCT methods can serve as an alternative for polyethylene materials. Chen et al. [42] developed an effective approach to tomographic image processing for computing volumetric wear of polyethylene and pelvic osteolysis after a total hip arthroplasty. In his approach, he worked with edge detection and volume computation using a 3-D image reconstruction method. Bowden et al. [43] provided a more detailed study describing the whole process and validation of this innovative approach. Six UHMWPE acetabular liners with in situ time ranging from 2.7 to 14.4 years were collected and evaluated using a high-resolution micro-CT scanner (SCANCO Medical AG, Switzerland). The method was then combined with 3D rigid image registration of geometric primitives to identify deviations of the articulating surface of the extracted implants from the expected unworn geometry. High volumetric resolution of the image data was required for accurate volume measurements. The detection limit of the present micro-CT method was calculated to be 140 $mm^3$.

Teeter et. al. [44] described the process of volumetric wear determination. Authors used the micro-CT (eXplore Vision 120) for measurements and Geomagic software (Geomagic Inc, Research Triangle Park,NC) for data analysis and for reconstruction of scans at the isotropic resolution of 0.05 mm. Comparison was made on the articular and backside surface of a sample extracted after 16.7 years in situ. As the original geometry of the implant was unknown, the authors used geometry of a new implant of the same type (Hexloc, Biomet Inc, Warsaw, Ind) as a reference geometry. 3D

deviation of the articular surface was −2.48 ± 0.02 mm, with maximum backside deviation of 0.46 ± 0.02 mm.

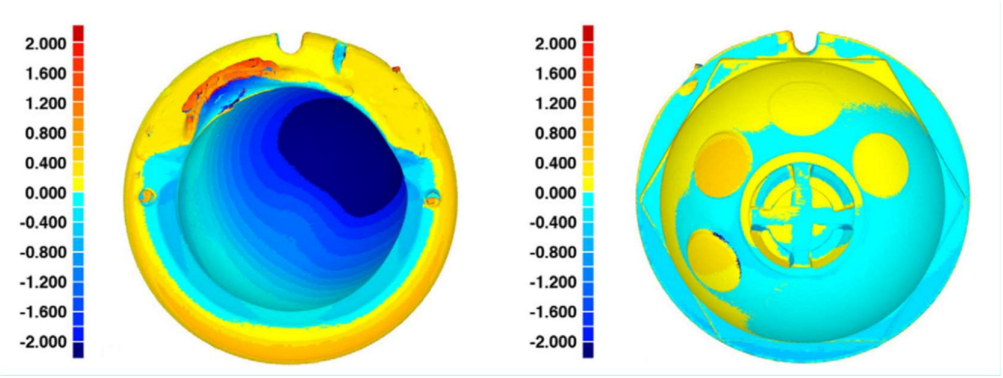


**Fig 2.16 Three-dimensional volume images of the retrieved acetabular liner scanned using micro-CT [44]**

One of the limitations of the method is the uncertainty associated with detection of low wear volumes. This limitation could be tackled by increasing the voxel resolution of the micro-CT scan; however, this can lead to longer scanning times and larger datasets for post processing.

#### 2.2.3.3 Optical methods

Wear analysis methods as described above do not fully solve the problems of prosthetic wear measurement such as extensive damages and geometrical surface changes caused by significant plastic deformations or creep. Optical 3D methods and their application for quantification of the volumetric wear can be explored in this context.

The optical 3D wear measurement is based on creating a 3D profile map of a retrieved cup. A pilot study in this field was conducted by Zou et al. [45] who referred to a novel principle of optical scanning. The study described sequential hemisphere measurement method using an optical non-contact measurement system with a laser probe (OP2, Renishaw, UK) working on the principle of optical triangulation. The OP2 laser probe was designed to be used with a Motorised Probe Head (PH9, Renishaw, UK), and held in a coordinate measuring machine (CMM, Merlin II, International Metrology System Ltd., UK). The study introduced strategy of surface alignment with a crucial influence on the complex error of volume wear determination. Zou et al. assembled partial scans, which in turn allowed analysis of the whole geometry (Fig 2.17). Reproducibility was tested on this novel approach. Volumetric differences were measured over a rectangular area of 400 $mm^2$ with the mean volumetric difference of 1.4 $mm^3$. Next, two cups were tested before and after a half million cycles wear tests and the volumetric difference was found to be 5.3 $mm^3$. The method also allowed to determine the direction of maximum removal of the material which is important for determining depth of femoral head penetration and linear wear. The study showed precise results, however alignment of scans during post-processing remained problematic.

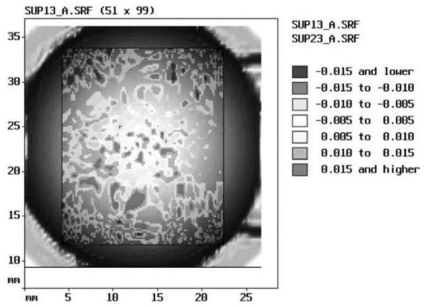


**Fig 2.17 The wear pattern after a half million cycles wear test [45]**

Rosller et al. [46] introduced 3 types of wear analyses: (a) a contact microscopy method (VEB, Carl Zeiss Jena, Germany) using 3D coordinates on the surface of the implants, (b) non-contact method, called Fourier or phase-shifting profilometry and (c) scanning profilometry (Fig 2.18). All measurements were performed on polyethylene liners that were worn under different angles of wear direction. A milling cutter used for wear simulation was set to obtain wear perpendicular (α=0°) and oblique to the mouth of the cup (directions of 30° and 50°). For each direction, the depth of milling was chosen to simulate three clinically important values of the total wear – low, medium and high wear conditions.

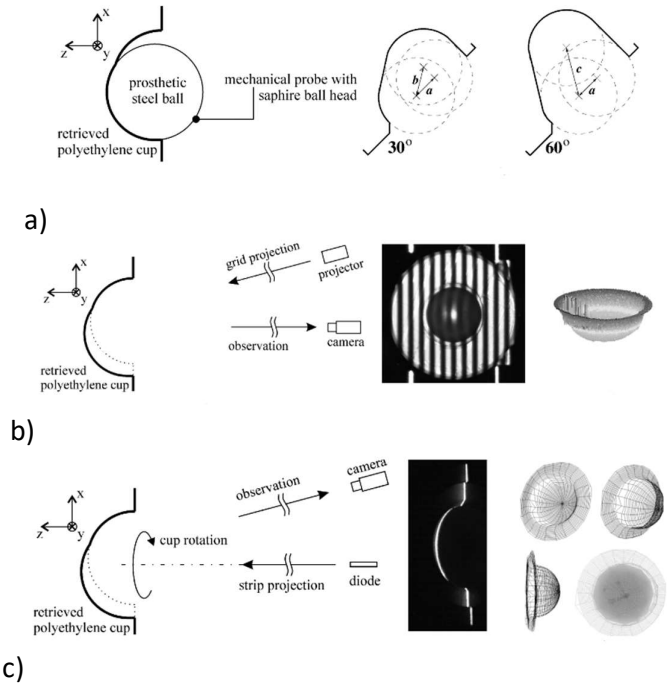


**Fig 2.18 Principle of measurement by a) universal measuring microscope; b) phase-shifting profilometry c) scanning profilometry [46]**

With known diameter of the cup and the head, it was possible to calculate the linear and volumetric wear using a geometrical "two-sphere model" and a computational algorithm described in study. Tab. 2.4. shows results of the study.

**Tab. 2.4 Absolute values of measured wear [46].**

| METHOD | angle [deg] | 0 | | | 30 | | | 50 | | |
|---|---|---|---|---|---|---|---|---|---|---|
| | depth [mm] | 0.5 | 1.5 | 2.0 | 0.5 | 1.0 | 2.0 | 0.5 | 1.5 | 2.5 |
| GR* | wear [mm³] | 253.4 | 865.5 | 1147.6 | 259.5 | 510.6 | 1084.6 | 234.3 | 730.0 | 1269.2 |
| UM* | | - | - | - | - | 316.0 | 484.0 | 222.0 | 620.0 | 1263.0 |
| SP* | | 268.3 | 843.7 | 1197.6 | 276.4 | 465.2 | 998.7 | 218.5 | 658.0 | 1224.1 |
| FP* | | 278.0 | 911.4 | 1226.7 | 281.6 | 495.8 | 1136.7 | 241.5 | 719.0 | 1238.7 |

*legends: GR=gravimetry; UM=universal measuring microscope; SP=scanning profilometry; FP=fourier profilometry

This innovative approach had two important limitations. First, the contact microscopy method shows worse or no results at all under small angles of wear direction. The lower the angle was, the smaller part of the original unworn surface was available for the fitting reference sphere inside the cup in one of the two positions. The second limitation was dispersion of the results of both the phase-shifting method and the scanning profilometry in 10% range. Despite these limitations, the study provided a solid base for further explorations of using the optical methods for wear analysis and for a better description of the mechanical degradation processes.

Another novel approach to volumetric wear determination was introduced by Tuke et al. [47]. The method known as the RedLux Artificial Hip Profiler (AHP) (RedLux Ltd., Southampton, UK) combined the high resolution of the roundness measuring method with the high coverage of the coordinate measurement method, while using an automated, non-contact sensor for increased speed of measurements. The sensor could scan spherical objects covering the whole bearing surfaces in a single measurement taking only few minutes. The resulting cloud of points measured by the artificial hip profiler was the raw data and described the form of the sphere in 3D with a resolution of 20nm. The artificial hip profiler used a point sensor, based on the chromatically encoded confocal measurement and the method was applied on metal femoral head implants.

Authors studied influence of the temperature on the accuracy of the method. The influence of temperature on the measurement of sphericity and wear was negligible. The total error of measured volume was established at 0,033 mm$^3$.

**Tab. 2.5 Results of validation of methods [47]**

| Component Id | AHP measurement time (min and s) | Diameter (laser micrometer) mm | Diameter (AHP) mm | Linear wear (roundness) μm | Linear wear (AHP) μm | Volume loss (gravimetric) mm³ | Volume loss (AHP) mm³ |
|---|---|---|---|---|---|---|---|
| 1 | 1′53–2′07 | 41.8484 (0.0024) | 41.849089 (0.00083) | 10.3 (0.3) | 10.7 (0.3) | 0.313 (0.006) | 0.280 (0.022) |
| 2 | 1′51–2′06 | 41.8499 (0.0019) | 41.850737 (0.00251) | 23.3 (0.4) | 22.9 (0.3) | 0.600 (0.004) | 0.575 (0.016) |
| 3 | 1′52–2′06 | 41.8477 (0.0013) | 41.849245 (0.00193) | 2.0 (0.1) | 2.6 (0.1) | 0.069 (0.004) | 0.047 (0.005) |
| 4 | 1′51–2′07 | 41.8478 (0.0013) | 41.847964 (0.00036) | 9.3 (0.2) | 11.0 (0.1) | 0.306 (0.005) | 0.293 (0.001) |
| 5 | 1′52–2′07 | 41.8518 (0.0023) | 41.852021 (0.00153) | 11.7 (0.3) | 12.2 (0.2) | 0.404 (0.002) | 0.392 (0.012) |
| 6 | 1′53–2′07 | 41.8453 (0.0023) | 41.846755 (0.00144) | 3.6 (0.1) | 3.9 (0.2) | 0.067 (0.006) | 0.064 (0.003) |

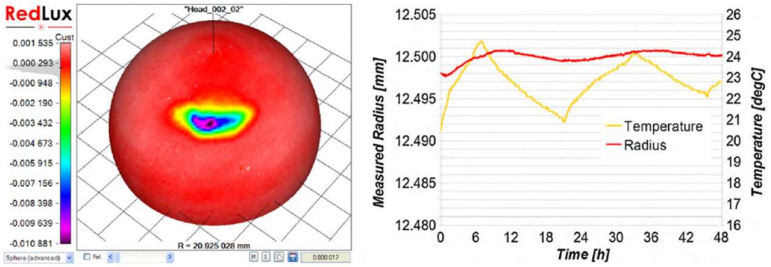


**Fig 2.19 Artifical Hip Profiler - deviation of surface include temperature influence**

RedLux method is one of one of the high performing methods providing reliable data of the whole surface. The method has a wide range of applications; however, the time efficiency remains a limiting factor. The RedLux method could be also interesting for analysis of polyethylene liners, though in case of more extensive surface damages, polyethylene liner might diverge from the spherical shape what may complicate the RedLux measurements.

Collecting clinical data on retrieved implants from high numbers of patients requires a simple and accurate method. At the same time soft material implants can suffer more extensive wear damages making it difficult for some methods to measure the wear accurately. Both issues were addressed by Yun et al. [48] who used the optical scanning method for analysis of retrieved polyethylene cups. The authors introduced a novel approach to volumetric measurement. Though the study does not describe each step of the analysis in detail, it gives a decent overview of the basic measuring principles. Measurements were performed on 17 polyethylene liners collected from 16 patients during revision surgeries. The samples were scanned using a triangulation 3D scanner (Rexcan III; Solutionix, Seoul, South Korea). The three-dimensional technique involved using two cameras to capture the object under the white light. The mean scan time was 30 minutes (ranging from 25-34 minutes), showing time efficiency of the 3D scanning method. An image processing software (Geomagic, Morrisville, NC) was used to generate the 3D reconstruction images. Wear volume for each of the retrieved liners was measured by subtracting the interior volume of a new liner from the interior volume of a retrieved liner of the same size. The results were compared with the Dorr method of radiographic analysis [49]. Digitalized images of prerevision non-weight bearing hip anteroposterior radiographs were acquired. Radiographs were exported into PowerPoint (2007 Version; Microsoft, Redmond, Wash).

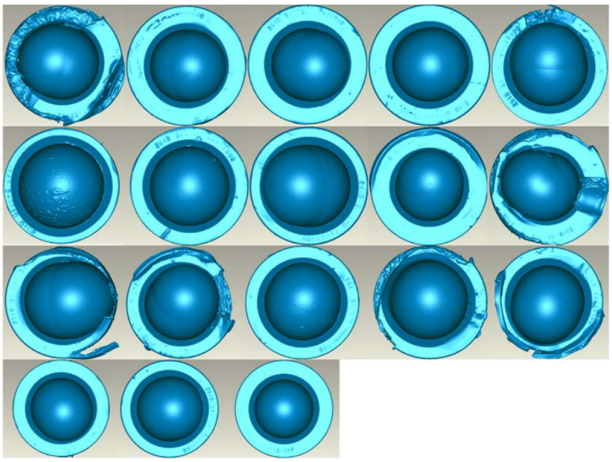

**Fig 2.20 Three-dimensional reconstructed images of 17 retrieved PE liner [48]**

The mean interior volumes of the 17 retrieved PE liners measured by 2 sets of 3D laser scans were 9172.19 ± 574.70mm$^3$ (range, 8344.88-10480.71mm$^3$). The mean interior volumes of the 7 unused PE liners measured by 2 sets of 3D laser scans were 8016.23 ± 0.13 mm$^3$ (Tab. 2.6).

| | 3D Laser Scan (Scan 1/Scan 2) | PowerPoint Method (A-1/A-2/B-1/B-2/C-1/C-2) | Dorr and Wan Method (A-1/A-2/B-1/B-2/C-1/C-2) |
|---|---|---|---|
| 1 | 1554/1450 | 2077/2077/2077/2077/2007/2077 | 1667/1512/1677/1506/1601/1627 |
| 2 | 1142/1092 | 1730/1800/1800/1800/1730/1800 | 1509/1512/1558/1537/1601/1767 |
| 3 | 928/928 | 953/953/953/953/953/953 | 63/286/415/123/607/261 |
| 4 | 339/339 | 415/484/484/484/346/484 | 315/377/677/426/238/666 |
| 5 | 988/988 | 1038/1315/969/1246/1038/1246 | 330/718/658/870/664/733 |
| 6 | 1864/1864 | 1923/2200/1923/2200/1923/2338 | 1698/2126/2030/1732/2043/1821 |
| 7 | 328/328 | 276/553/276/553/276/553 | 404/512/166/310/541/650 |
| 8 | 992/956 | 1077/938/1008/1008/1077/1008 | 2160/2140/2195/2089/2348/2157 |
| 9 | 785/785 | 1038/1107/1107/1107/969/1038 | 1144/1127/826/1141/1246/1015 |
| 10 | 747/683 | 915/707/984/707/846/638 | 1211/1689/1531/1589/1711/1764 |
| 11 | 1845/1845 | 2077/2007/2077/2077/2077/2077 | 1787/1997/1513/1717/2221/1860 |
| 12 | 1149/1149 | 1453/1453/1523/1523/1523/1453 | 1749/1790/1755/2106/2114/1892 |
| 13 | 2464/2403 | 2531/2115/2600/2600/2462/2669 | 2317/2498/2734/1729/2342/2746 |
| 14 | 689/689 | 1177/1177/1107/1107/1107/1107 | 1241/1178/1263/1201/1303/1390 |
| 15 | 1417/1417 | 1515/1307/1446/1307/1446/1238 | 1326/1330/1307/1530/1277/1369 |
| 16 | 1645/1645 | 1723/1723/1723/1723/1723/1653 | 1801/1832/1915/1980/2024/2106 |
| 17 | 771/771 | 815/815/815/815/746/746 | 733/773/840/875/692/875 |
| Mean | 1156/1137 | 1337/1337/1345/1370/1354/1354 | 1262/1376/1356/1321/1445/1453 |

**Tab. 2.6 Individual Wear Volume (mm$^3$) of 17 Retrieved Polyethylene Liners Measured by 3D Laser Scanning Method, the PowerPoint Method, and the Dorr and Wan Method.**

Study results showed that wear volumes determined by the PowerPoint method strongly correlate with wear volumes determined by the 3D laser scan. The 3D laser scan methodology provides a basic framework for using the optical scanning to determine volumetric wear. For further application of the optical scanning method, it is necessary to provide validation of the method and analysis of the unworn parts of the retrieved liner. The unworn parts analysis is key for determining the original geometry of the liners. Many approaches use new liners with corresponding dimensions as a reference geometry, neglecting the manufacturing error or manufacturing tolerances. Another challenge of volumetric wear determination is the distinction between plastic deformation and material loosening. Finding a border line between these two is difficult, especially with the unknown original geometry and original weight of the liner.

### 2.2.4 Factors influencing wear analysis

Current methods used for wear analysis enable wear investigations in wide spectra of failures cases. There are several factors that can influence the analysis results. Each of the methods has various limitations as described in the literature review above. To select the most suitable method for analysis, factors such as range of wear, type of implant and type of failure need to be considered carefully. Before analysing the wear, it is important to identify the wear mode and to exclude parameters that do not cause material loosening, such as a plastic deformation and damages caused by surgeon during extraction. It is also useful to consider surface damages appearing at levels below the recognition ability of the selected method. The paragraph below focuses on several factors that influence the optical methods.

#### 2.2.4.1 Wear mode

To find a suitable approach to wear analysis, it is necessary to recognize different wear modes that lead to material loosening of the implant. McKellop et al. [50] recognized four basic mechanisms (modes) of implant failing (Fig 2.21). Mode-1 describes a normal wear, where only the intended bearing surfaces are in contact and undergoing wear. This mode is the main interest and subject of investigation with the optical scanning methods. Mode-2 describes micro-separation wear, where the bearing surface is worn against a non-bearing surface, e.g. due to subluxation of the ball from the socket. Mode-3 describes 3-body abrasive wear between the two primary bearing surfaces, but with third-body abrasive particles interposed. Mode-4 wear occurs between two non-bearing surfaces, examples being (4A) neck–socket impingement and (4B) backside wear between the polyethylene cup and the metal shell.

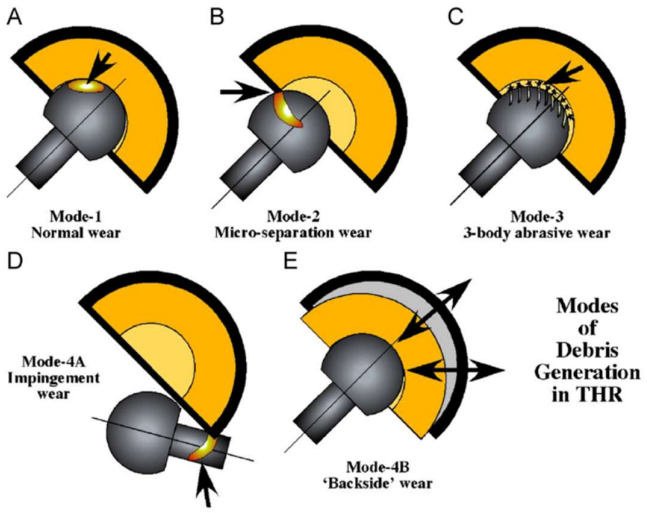


Fig 2.21 Schematic illustration of the four wear modes for a total hip prosthesis [50]

Retrieved liners very often show combinations of the above-mentioned wear modes. Therefore, it is necessary to differentiate them and take them into account when determining the overall volumetric wear and related plastic deformations.

#### 2.2.4.2 Polyethylene creep

Plastic deformation (creep) is an important factor influencing quantification of the polyethylene wear. The difficulty lies in distinguishing wear, in which the PE material is lost, from the plastic deformation in which the polymer is distorted in shape but without significant loss of material. Polyethylene is a material with mechanical properties that are time dependent. When a constant load (not higher than the yield stress) is applied, polyethylene deformation increases with time. This process is known as creep. Many studies fail to differentiate material wear from plastic deformations. The authors often do not specify the amounts of creep and wear exactly and both processes are being simply referred to as wear. This is especially true for older studies where this simplification was usually clearly articulated. Puloski et al. [51] went on to state that ''*although the use of the term wear to describe all forms of surface and subsurface deformation may be semantically imprecise, we will continue to use it in this study, acknowledging that the damage can occur without the subsequent generation of debris*.'' The same approach was taken by Sychterz et al. [52]. This basic approach to wear identification is sufficient for clinical purposes. However, for a better overall understanding of wear, it is necessary to distinguish these two wear mechanisms. Relatively few studies and publications do so, and their results provide us only with basic insights into the problem.

One of the studies in this field published by Lee et al [53] observed creep deformations of UHMWPE over time. The tests were performed for various doses of gamma irradiation according to irradiation during manufacturing process. The samples were loaded with a constant static strain. Creep processes were observed during loading with subsequent relaxation of the materials.

Variable load that better simulates the real load in the human body was applied in another study published by Meyer et al. [54]. Test samples were loaded with cyclic strain. Certain time for relaxation of material was allowed between the individual cycles. The figure shows similar behaviour of creep deformation for various doses of irradiation (Fig 2.22). An increasing deformation with logarithmic behaviour was observed in the first 200 minutes of the test, when 90% of deformations occurred. A slower increase with a linear function behaviour followed. Relaxation of materials after removing the load showed similar behaviour. Results of this study show increasing plastic deformation and point out on microstructural changes of surface. Residual plastic strain was found to increase with an increasing amount of true strain and number of cycles. Density was found to decrease linearly with increasing residual plastic strain. Initiation of gap in crystal grid was also found, leading to lamella alignment. This phenomenon was also observed with increasing amount of true strain and number of cycles. The study clearly shows changes in polyethylene

morphology during plastic deformation what influences wear of the polyethylene implants. The study applied load without considering kinematics of the movement. Currently, there is no research in polyethylene implants considering the kinematics of movement when studying plastic deformation. However, it is possible to predict the development of plastic deformation using finite element analysis predictions.

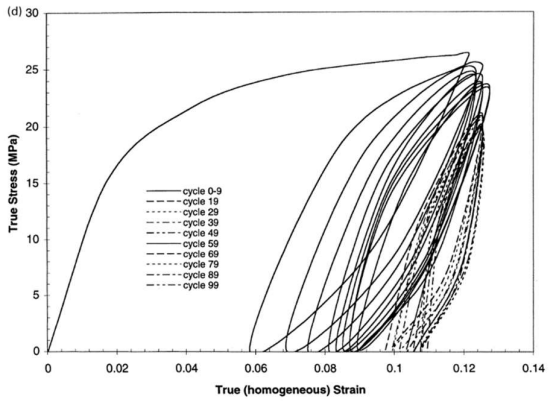


Fig 2.22 Cyclic true stress - strain curve from non-sterile UHMWPE [54]

One of the significant studies performed by Bevill et al. [55] on creep and wear predictions shows that while 40% of all wear happens in the first two years of an implants life, 56% of all linear penetration happens in the first 3 or 4 months of this period (Fig 2.23).

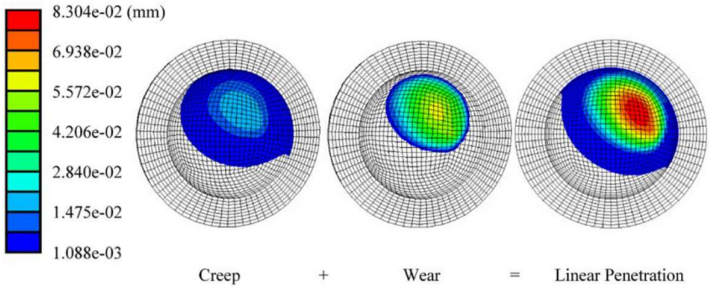


Fig 2.23 . Contours of creep and wear penetration calculated by FEM [55]

A follow up study on creep published by Penmetsa et al. [56] used the finite elements method (FEM) to simulate wear and plastic deformations of cups. The calculated creep strains were modelled as inelastic. The model was applied to a mathematical model of wear simulations. Results showed the same direction of plastic deformations and head penetration. Creep occurred quickly upon loading with approximately 85% of the total creep penetration occurring within the first 150,000 cycles. Maximum creep penetrations calculated from the full creep analyses ranged from 0.032 to 0.055 mm depending on geometry (Fig 2.24).

Creep poses two major challenges for wear analysis: (1) it leads to distortion of wear rate determined by a selected measuring method and (2) creep changes the contact areas between the articulating surfaces of implant components. Larger contact areas

decrease contact pressure what can influence determination of wear scare and a correct identification of the unworn and worn areas of the articulating surfaces.

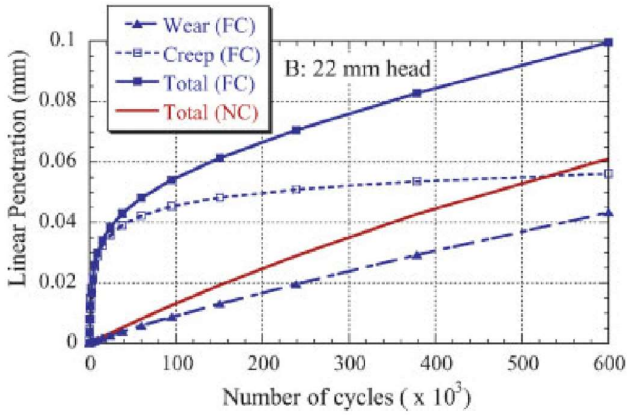


**Fig 2.24 Creep and wear penetration levels using full creep properties (FC) and no creep (NC).**

The study provided a useful tool for predicting total creep and its development. However, its numerical model implied several simplifications. One of the main limitations is exclusion of the lubrication parameter. The authors also used non-stop hip joint loading, what does not exactly correspond with the human joint environment. With evolving technologies, it is necessary to enhance the models with experimental parameters. A different approach was chosen by Estok et al. [57] , who compared two types of materials: UHMWPE a XPLE. Authors applied load similar to the load in human joints on hip joint liners.

The load was derived from the gait cycle. Frequency was set at 2Hz with maximal load of 3330N. The experiment was designed as a static one, without using articulating head and cup. This approach enabled to observe the creep separately from the wear. Results of similar articulating pairs showed linear wear of 38 µm after 10 000 cycles. Creep deformation gradually increased, reaching 132 µm after 4 million cycles. In a follow up study published by Affatato et al. [58] the phenomenon of plastic deformations was studied by observing microstructural changes and oxidation changes of the surface. The study showed influence of surface changes on the amount of wear.

### 2.2.4.3 Surface analysis

Volumetric wear analysis needs to be complemented with a surface analysis of failed implants for a complex wear analysis. In total hip replacements, where the articulating geometries consist of conforming spherical surfaces, the wear mechanism occurring at a microscopic scale (µm or less) has been associated with polyethylene resistance to multidirectional stress. The multidirectional stress depends on kinematic conditions, load and material of the implants and causes various types surface damages that can indicate various types of wear.

Identification of the unworn areas is another important aspect of the surface analysis. The unworn part of the articulating surface is the remaining area of the liner that can provide information on the original geometry of the liner. A correct identification of the unworn area provides important data for reconstruction of the original shape of the liner. The more accurate the reconstruction of the original geometry is, the more accurate is determination of the volumetric wear.

A study provided by Edidin et al. [59] showed basic type of surface damage called multidirectional scratching, including abrasive/adhesive wear mechanism, micro-contact fatigue such as micro-pitting and delamination. Authors focused on the influence of clinical factors on the surface morphology. Surfaces of nine extracted samples of the same size and material were analysed by optical profilometry using the white light interferometry. Surface roughness ranged from 0.142 to 1.7 µm for seven samples that showed multidirectional scratching. Surface roughness for fatigue type of wear showed higher values.
Kurtz et al. [60] studied the initial phase of wear of 21 retrieved implants with short lifecycle using white light interferometry. The unworn surface areas of the liner were recognized by scoring caused by manufacturing machines. Trommer et al. [61] made a similar observation when analysing surface of UHNWPE liners in in vitro conditions. The authors observed interesting scratches caused by third bodies – being either residuals of bone cement used to fix the metal back of the cup or the released material expelled from the contact area between the two surfaces. The authors also observed existence of areas on stainless steel/CoCr femoral heads with apparent material deposition and cracks suggesting brittle behaviour of the deposited material, which may cause appearance of the abrasive third body particles (Fig 2.25).

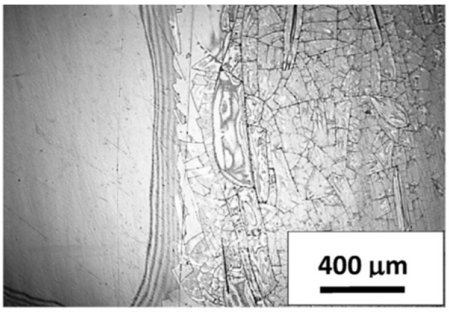


**Fig 2.25 Images from optical microscope of the top view of a CoCr alloy**

The calculated linear wear rates were 0.16 mm/year. Three different topographies and morphologies were observed in the region associated with wear: (Fig 2.26 c, d) showed the unworn surface with the machining marks, (Fig 2.26 b) smooth surface with ripple-like morphology resulting from adhesion/fatigue mechanism and cyclic plastic strain accumulation and finally (Fig 2.26 a) showed scratched regions resulting from ploughing mechanism by protuberances of the hard-counter face, with transverse cracks to the ploughing direction.

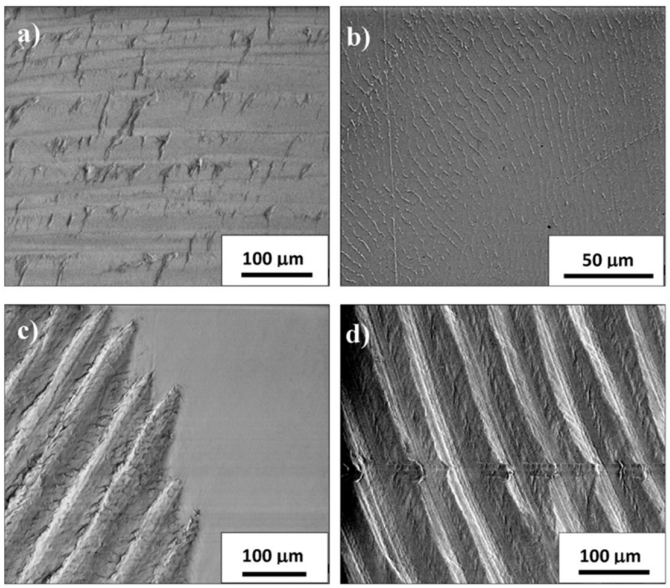


**Fig 2.26 SEM images of a UHMWPE cup showing: (a) scratch with transversal cracks; (b) ripples in the polished zones; (c) rough surface with remaining machining marks; (d) unworn surface [61]**

## 2.3 In vitro testing of hip implants



Functionality of hip joints is influenced by various factors such as individual pelvis geometry, age, sex and weight of patient. Levels of activity and lifestyle also play an important role and have a direct impact on wear of the implants. Different load rates and kinematic variations complicate predictions regarding implant wear and failures. Clinical practice of hip joint replacements treats each patient individually.

In case of in vitro investigations, there are two main approaches. The first approach focuses on analysis of retrieved implants and on retrospective reconstruction of the processes and interactions leading to implant failure, including the human environment. The second approach seeks to unify the parameters for new implants testing as defined in an International Standard ISO 14242. The Standard describes measurement procedures, loading and displacement parameters for wear-testing machines and environmental conditions for tests. ISO 14242 [62] is used as a reference for comparability of performance tests of the implants.

### 2.3.1 Kinematic of testing

ISO 14242 defines individual phases of human gait as described above in the chapter on the kinematics of the hip joint. The complex movement of human gait is defined in three basic planes of movement: flexion /extension, abduction/adduction and inner /outer rotation. The multidirectional shear stress between the implant components is obtained by imitating combination of these three movements and by simulating load on the hip joint. Omitting some of the planes of movement would lead to one-directional shear stress [4] without an elliptical movement of the contact point between the articulating surfaces, what may influence the overall wear behaviour. Wear resistance of polyethylene acetabular liner changes with different amounts of shear stress due to the linked character of polyethylene. This effect can also distort results of wear tests.

Two types of simulators are usually used for long-term testing of hip implants: three axes simulator and two axes simulator. The three axes simulator allows 6 degrees of freedom to simulate the kinematic cycles according to the ISO 14242 Standard. It can also simulate certain movements such as a climbing the stairs, running, jumping and several other more specific movements. The two axes simulator has two rotation axes driven by one actuator (Fig 2.27). During testing, one of the tested components is placed in a waterproof jig to allow for flooding the contact with a lubricant. The jig usually allows rotational movement on the platform. The rotation axes are inclined about 23 degrees to each other according to the ISO 14242 Standard (Fig 2.27). The simulator is relatively simple in its design and principles. The main limitation of the machine lies in the missing third axis. The third plane of movement can be compensated by a phase shifting of the other two planes of movements as suggested by Turell et al. [4]. This approach allows to use the two axes simulator as equivalent

to the simulator with six degrees of freedom. Another disadvantage of the two axes simulator is that it allows only gait kinematic testing.

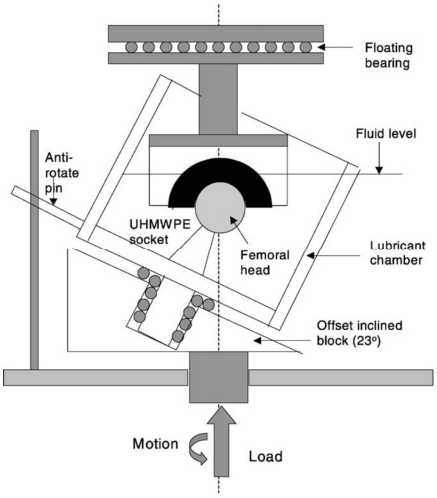


**Fig 2.27 Schematic diagram of the MTS hip joint simulator [63].**

The ISO 14242 Standard supports two-axes simulator test by defining phase shifting and testing conditions.

### 2.3.2 Positioning of acetabular cup

Spatial orientation of the acetabular cup in a patient's body is determined by anteversion and abduction angles. There are surgically recommended intervals for both of these angles, being 20 degrees for anteversion and 40 degrees for abduction according the study published by Scheerlinck et al. [64]. Altering the abduction angle significantly affects the properties of the contact area. Increasing the abduction angle shifts the contact pressure area closer towards the acetabular rim and at the same time decreases its overall size and increases its maximal contact pressure as described by Hua et al. [65].

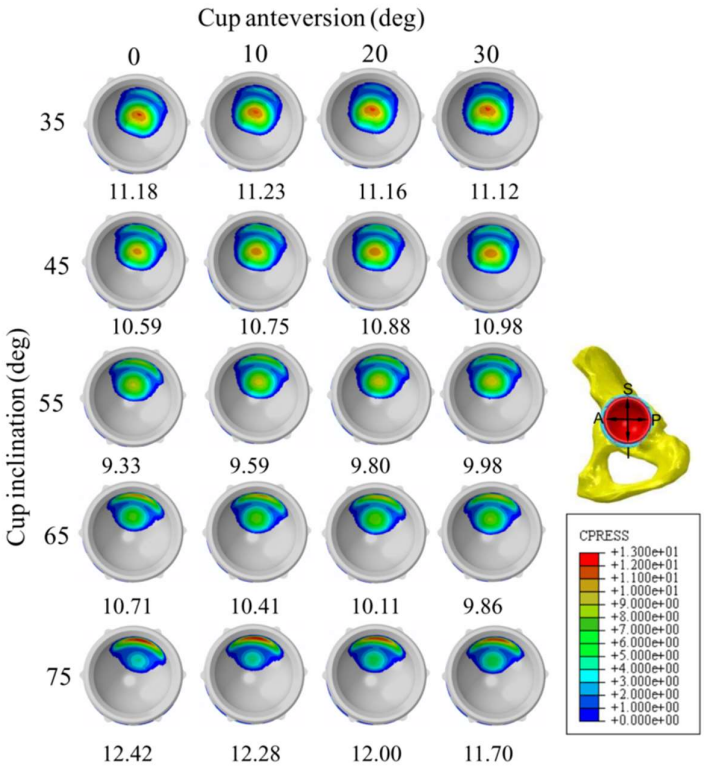


Fig 2.28 Influence of cup inclination on contact pressure

While influence of the acetabular orientation on the contact stress is well documented, a direct relationship between the contact pressure (Fig 2.28) properties and wear mechanism is not fully understood yet. Older studies found no significant correlation between higher contact stress, wear rate and higher abduction angles as suggested by Patil et al. [66] (Fig 2.30). Some more recent studies such as Halma et al. [67] or Korduba et al. [68] showed decreasing wear rates with increased abduction angles.

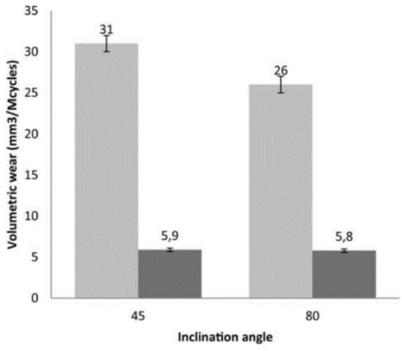


Fig 2.29 The in vitro wear rates of different inclination angle [67]

Generally higher wear rates are measured when using the radiography compared to simulator wear tests as observed by Kang et al. [69]. These rather significant

differences between numerous studies can be caused by multiple factors. For example, simulator studies with strictly controlled conditions do not consider loose third body particles of bone void fillers or bone cement. There are also various approaches to wear measurement methods used in the studies - ranging from radiography used in clinical practice to gravimetry, coordinated measurement method or optical methods.

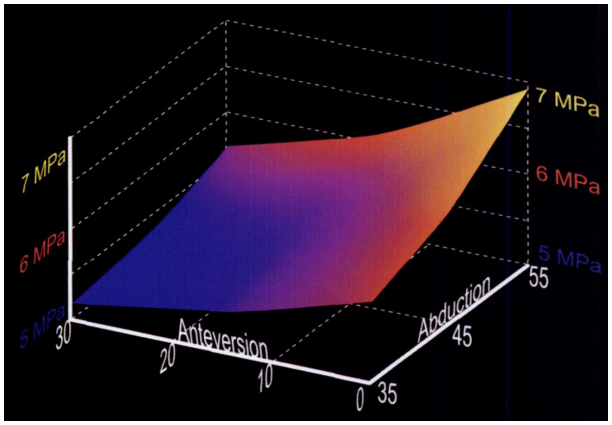


**Fig 2.30 Increase in the abduction angle increase peak contact stress according FME analysis [66].**

# 3 ANALYSIS AND CONCLUSIONS OF LITERATURE REVIEW



Better understanding of wear mechanisms is one of the main goals of biotribology and wear of articulating surfaces has been historically the focus of biotribological studies. With better observation technologies and improved implants, more studies started to focus on lubrication and behaviour of implants in human body using clinical data, laboratory simulations and mathematical simulations. However, the material loosening analysis, as one of the key parameters in the process, remains an important research topic. The literature review shows that we still need a better understanding of the articulating surfaces behaviour. With constant enhancements of the implant materials, it is equally important to advance the methods for observation of their interactions.

Several different methods have been developed to determine wear in vitro or in vivo. Radiographic method has been one of the first methods of linear wear analysis. The method is still quite common. X-ray is a routine procedure conducted before and after the revision surgeries for a follow-up examinations and observation of the lifecycle of the implants. Several researchers used software recognition of radiographs identifying edges of implants to determine the linear wear with a better accuracy [15-17, 24, 27]. However, the accuracy was not higher than 2.5 mm. The method has other limitations as well. Volumetric wear analysis based on radiographs yields inaccurate results and the method does not allow for a clear surface recognition. The method is also not able to recognize material loosening from plastic deformations (creep). Despite these limitations, there is still an effort to improve the radiographic method as it is one of the few methods that enables observation of changes directly in the human body while having additional clinical data available for a more comprehensive analysis.

Radiographic methods are not suitable for in vitro testing and there has been an increasing demand for more precise methods providing complex information on wear, including parameters such as direction of wear (wear scare) and surface recognition. The coordinate measuring method has been developed for investigation of artificial wear using wear simulator. The method was initially designed as a contact method [36, 37] with the pointing stylus defining coordinates in different points of the articulating surface of implants. This approach has several limitations as well. One of them is point spacing that causes polygonization error [70] during post-processing. Another issue is geometry distortion caused by neglecting the plastic deformation of the implant.

Nevertheless, the coordinate measuring method remains one of most important methods for in vitro testing. Coordinate measuring method procedures and their usage for hip joints implants are described in Standard ISO 14242, Part 2 [5]. The method has been modified by replacing the touching stylus with an optical sensor. One of the well-known modifications of the coordinate measuring method is the RedLux method [47]. Majority of authors using the RedLux method focus on hard

materials such as metal and ceramics. Polyethylene liners have not been investigated much using this method. Hence, little is known about limitations of this method for polyethylene liners with more extensive damages. Pioneer research in this field was carried out by Rossler et. al. [46] showing potential of the optical methods in analysis of failures of polyethylene liners. According to author's knowledge, there is no similar study dealing with suitability of 3D optical scanning methods for analysis of volumetric wear and recognition of the creep so far.

Various factors influencing wear rate are often mentioned in context of wear analysis methods. We focused on methods enabling 3D surface analysis and wear determination, where creep is one of the major factors contributing to distortion of the wear analysis. Range of the creep deformations depends on positioning of the acetabular cup and on wear modes involved. Reviewed studies showed that major development of creep deformation occurs in the run-in phase of the implant. Representation of the creep strains was inelastic. In vitro simulation experiments involved continuous loading that allowed a more limited creep recovery than in vivo loading. Simulations showed that around 85% of the creep occurs in first 150 000 load cycles [53]. Authors argued that the creep of polyethylene liners quickly changed the head–liner contact mechanics and increased an early head–liner penetration what could distort wear analysis based on surface investigation. Though, according to the authors, the creep properties of the liner did not affect volumetric wear. There are relatively few studies investigating the creep process.

Volumetric wear analysis needs to be complemented with surface analysis of failed implants for a complex wear analysis. The surface analysis involves two areas: (1) study of tribological processes in the contact areas and (2) study of the unworn parts of the extracted implants. Various types of wear occur in the contact areas of the implants, such as abrasion, third-body debris, adhesion/fatigue disclosed by micro-scale ripples and cyclic plastic strain accumulation as described by Trommer et. al. [61]. Identification of the unworn parts of the surface is important for reconstruction of the original reference geometry that is then compared with the current surface geometry to determine the values of volumetric wear. The unworn parts can be identified by scoring caused by manufacturing machines identifiable up to 10 years after the replacement surgeries.

Technical standards are important to ensure comparability of measurements and testing. ISO 14242, Part 1 [62] describes kinematic conditions and dynamic loading for in vitro tests in three planes of movement: flexion /extension, abduction/adduction and inner /outer rotation. Two axes orbital testers are also frequently used in in vitro testing, replacing one plane of the gait cycle by phase shifting the other two planes of movement as described in the Standard ISO 14242, Part 3 [71]. This simplified option is well-founded by research showing that a point on articulating surface performs an identical trajectory both in case of two phase-shifted planes and in case of three planes. The loci or trajectory of motion at the point of contact between a femoral head and an acetabular cup during a gait cycle can be

described generally as quasi-elliptical or rectangular. Differences were tested by Turell at at. [4].

Ensuring the general quasi-elliptical trajectory of the contact point is important for preserving the shear stress conditions. Range of shear stress and resulting wear of polyethylene liners are affected by various influences such as lubricants, clinical conditions, patient activities and positioning of the acetabular cup in the pelvis.

The final part of the literature review studies effects of liner position in human body on the material loosening. Various investigations on relationship between the wear progress and inclination angle of liners showed different results. Earlier publications documented influence of cup positioning using radiographic records. These - mostly clinical - studies recommended abduction angle of 40 degrees and anteversion angle of 20 degrees to avoid complications. However, some patients with anatomic variations or with afunctional pelvic orientation outside the normal range would require a customized cup position. [64]

Finite elements analysis proved influence of the abduction angle, which significantly changes the contact pressure on the liner surface influencing the volume of material loosening [65]. Two different allegations can be found in literature on this issue. The first study investigated clinical radiographs of conventional UHMWPE cups and found that an increasing abduction angle led to an increased contact pressure and hence increased the volumetric wear [66].

More recent studies describe an opposite relationship between the abduction angle and volumetric wear. Tests examining the conventional UHMWPE samples using the gravimetric method found decreasing volumetric wear with an increasing abduction angle [68]. The authors explained this phenomenon by smaller contact area for abduction angles above 55 degrees. On the other hand, higher abduction angles showed higher risk of the edge load effect. Though the edge load effect does not influence the volumetric wear significantly, it entails higher risk of liner fracture and luxation.

The literature review shows that measurement methods that are currently used for wear analysis are not suitable for analysis of retrieved polyethylene liners. It is necessary to seek new approaches. Optical methods seem to offer a promising direction in this respect – providing advantages such as time efficiency, large number of measuring points and the possibility of complete geometry reconstruction. However, the accuracy of the methods remains questionable and has not been investigated yet. Developing a new approach opens new ways to obtain information on retrieved implants which are a good source of material for investigation of the relationship between the material loosening and position of the liner and for a better understanding of the wear mechanisms in general.

# 4 AIMS OF THE THESIS

The aim of this doctoral thesis is to establish a new approach to volumetric wear assessment for acetabular polyethylene liners using optical methods. The aim is to develop and validate an optical method that is suitable for wear analysis of polyethylene liners. Surface topography and mechanical properties of the polyethylene liners will be explored to describe the changes of the articulating surface of the retrieved implants and to expand the wear analysis of the implants. To achieve the main goal of this thesis, following steps were taken:

- Development of a volumetric wear assessment method for retrieved polyethylene implants using an optical scanner.
- Validation of the method according to the ISO 14242 Standard.
- Demonstration of usability of method on liners retrieved during the revision surgeries
- Surface topography analysis of the samples.
- In- vitro tests to observe the run-in phase of the samples under various inclination angles.
- Data analysis.
- Conclusions and discussion of the results.

## 4.1 Scientific questions

Q1 How can the accuracy of the optical scanning method and errors during data post-processing influence wear determination of retrieved polyethylene liners?

Q2 What is the influence of wear rate on mechanical properties and surface structures of polyethylene liners?

Q3 What is the influence of liner position on plastic deformation of the liner?

## 4.2 Hypotheses

H1: The optical method will be able to approximate the original surface geometry with a better accuracy than current methods that use new lines for approximation of the original geometry and hence will be more accurate in determining the wear – in correlation with the gravimetric measurements.

H2: Retrieved polyethylene liners that survived longer time in situ will show lower rate of material loss per year with no extensive changes of their surface structures.

H3: Retrieved liners with lower abduction angle will have lower wear rate and lower plastic deformations due to decreasing contact pressure in the articulating area.



## 4.3 Thesis layout

This doctoral thesis is composed of three papers published in journals with impact factor (Paper A, B, C). The main aim of this thesis is to develop a new approach to optical measurements and to prove usability of this method for volumetric wear determination. Paper A introduces the new method. Optical scanner was used to gather surface data for both new and worn polyeth ylene liners. The paper describes liner geometry reconstruction and creation of 3D models for volumetric wear determination. The new method was validated by a standard gravimetric method that is usually used for this purpose. Finally, the new method was applied to determine volumetric wear of 13 UHMWPE liners retrieved during revision surgeries. Results of the volumetric wear analysis were compared with clinical data.

As the optical scanning method can analyse the samples down to the micrometer scale, we supplemented the optical method with a surface analysis to examine a more detailed microscopic structure of failed liners. We worked with the 13 UHMWPE Bicon-plus polyethylene implants (Plus Endoprothetik AG, Switzerland) that are commonly used in total hip replacement surgeries in the Czech Republic. The surface analysis was carried out using a profilometer with a positioning stage allowing determination of topography areas (Appendix A). The resulting microstructure of the surface showed extensive mechanic damages that were further examined using chemical and mechanical analysis and then summarized in Paper B. The measurements were performed in cooperation with the University of Arkansas in the USA. The final part of this doctoral thesis, Paper C, focuses on the relationship between liner position, plastic deformations and volumetric wear of the liner.

**A.** RANUŠA, M., J.GALLO, M.VRBKA, M.HOBZA, D.PALOUŠEK, I.KŘUPKA and M. HARTL. Wear Analysis of Extracted Polyethylene Acetabular Cups Using a 3D Optical Scanner. *Tribology Transaction,* 2017, 60(3), 437–447.
*Author's contribution 80%*
**Journal impact factor = 1.723, Quartile Q2, CiteScore = 1.57**


**B.** CHOUDHURY, D., M.RANUŠA, R.A.FLEMING, M.VRBKA, I.KŘUPKA, M.G.TEETER, J.GOSS and M. ZOU. Mechanical wear and oxidative degradation analysis of retrieved ultra high molecular weight polyethylene acetabular cups. *Journal of the Mechanical Behavior of Biomedical Materials,* 2018, 79, 314-323.
*Author's contribution 50%*
**Journal impact factor = 3.239, Quartile Q1, CiteScore = 3.49**


**C.** ZEMAN, J., M.RANUŠA, M.VRBKA, J.GALLO, I.KŘUPKA and M. HARTL. UHMWPE Acetabular Cup Creep Deformation during the Run-in Phase of THA's Life Cycle. *Journal of the Mechanical Behavior of Biomedical Materials,* 2018, In Press.
*Author's contribution 50%*
**Journal impact factor = 3.239, Quartile Q1, CiteScore = 3.49**

# 5 MATERIALS AND METHODS



## 5.1 Experimental devices



Several different devices were used for the wear analysis in this thesis. An optical scanner ATOS Triple Scan was used to develop the novel measurement method. An optical profiler was used to analyse the surface topography, Raman spectrometer was used for chemical analysis and a nanoindenter for mechanical analysis of the surface. A customized hip joint simulator was used to investigate various inclination angles and plastic deformations of polyethylene liners.

### 5.1.1 Optical scanner

Acetabular cups were measured using the 3D optical scanner ATOS Triple Scan (GOM,GmbH). The optical system is based on an active fringe projection and triangulation. The ATOS Triple Scan uses the "Blue Light Technology" in three viewing angles between a stereo camera and a projector. Thanks to this approach, the measurements are not dependent on environmental factors and therefore it is not necessary to maintain constant environmental conditions during the measurements. A fringe pattern is projected on the measured object and the image is acquired using a two-camera system (Prosilica GX 3300, Allied Vision). The cameras use chip KAI-08050 with resolution of 3296 x 2472 px. Final scan is comprised of several partial scans that are aligned according to software-detected reference points.

For measurement of the acetabular cups, reference points with diameter of 0.8 mm were positioned on the surface of the cups outside the measured surface areas [72]. The measurement was carried out using MV170 lenses with measurement volume of 170 × 130 × 130 mm calibrated in a small object (SO) arrangement. The lenses complied with the VDI/VDE 2634 - Part 3 [73]. Detailed parameters of the measuring equipment, including basic calibration results are shown in (Tab. 5.1).

**Tab. 5.1 Parameters of the ATOS Triple scan and results of calibration**

| | |
|---|---|
| Camera pixels | 2 × 8 Mpx |
| Measuring volume (mm) | 170 × 130 × 130 mm |
| Measuring distance (mm) | 490 mm |
| Reference points diameter (mm) | 0.8 mm |
| Camera position | Small object (SO) |
| Angles of cameras | 27.2 ° |
| Type of calibration object | CP40-170-40346 |
| Deviation of calibration (170 x 130 x 130 mm) | 0.033 pixel /0.001 mm |
| Point distance (mm) | 0.055 mm |
| Repeatability of method - validation | 0.005 mm |

Surface of the measured polyethylene acetabular cups was too transparent for scanning and it was necessary to apply a layer of TiO2 coating. An airbrush system was used to apply the coating of approximately 3 µm. [74]. The acetabular cup was fixed in the middle of a rotary measurement table. The scanner was focused on the centre of the acetabular cup in the scanning distance of 490 mm. Each individual scan consists of many isolated points, technically described as a point cloud. Approximately six partial scans were used to comprise the final scan for post processing. The resulting polygonal data of each cup liner were saved in a stereolithographic file format (STL).

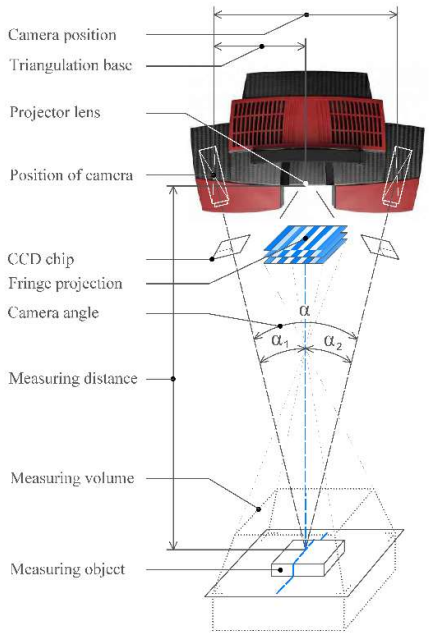


**Fig 5.1 Principle of the ATOS 3D optical system**

### 5.1.2 3D optical profiler

The initial surface topography of all tested samples was analysed in a greater detail using a 3D optical profiler contour GT-X8 (Bruker, USA). The measurements were based on the phase shifting interferometry technique. The range of the vertical axis is down to 0.1 nm which is completely sufficient for the purposes of this thesis, since the surface roughness of the tested femoral heads and acetabular liners is in the range of units of µm or higher. The commercial machine was customized by installing a rotational stage allowing to position the samples in a polar coordinate system (Fig 5.2).

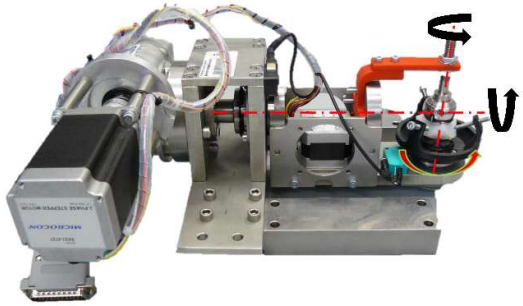

Fig 5.2 Rotational stage allowing to position the samples

### 5.1.3 Raman analysis and nanoindentation

Confocal Raman microscope (inVia™, Renishaw) was used to observe microstructures of the retrieved UHMWPE liners, particularly variations in the orthorhombic crystalline phase fraction and oxidation indices. Measurements were carried out in cooperation with the University of Arkansas, USA. The excitation source had a 785 nm wavelength, yielding a power of approximately 1.5 W, with an exposing time of 30 seconds and a spot size of ~100 µm in diameter. The generated Raman spectra (800-2000 cm-1) were processed in the Origin software and the integrated peaks were measured around 1293, 1305, and 1414 cm-1 Raman shift: $I_{1293}$, $I_{1305}$, and $I_{1414}$. $I_{1293}$ and $I_{1305}$ of the Raman bands of UHMWPE are associated with –CH2– bond wagging, whereas $I_{1414}$ represents –CH2– twisting vibrations [75]. The volume fraction of orthorhombic crystalline phase and the oxidation index were calculated based on the following equations [75, 76]:

$$\alpha_c = \frac{I_{1414}}{0.14(I_{1293}+I_{1305})} \tag{5.1}$$

$$OI = \exp\{1.19\, x\, tan\left[14.26\left(\frac{I_{1414}}{I_{1293}+I_{1305}} - 0.26\right)\right] - 0.13\} \tag{5.2}$$

The Raman investigations were conducted in two different phases. In the first phase, a 5X lens was used due to the curvature (~28 mm diameter) of the prosthesis cup liners. A schematic view of such measurement is shown in the Fig 5.3. A total of nine (9) points on each liner were measured.

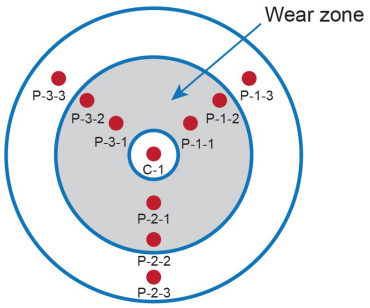


**Fig 5.3 The schematic diagram for confocal Raman (non-destructive) assessments of oxidation index in UHMWPE**

The hardness and modulus of elasticity were measured using an instrumented nanoindenter (TriboIndenter, Hysitron Inc. Minneapolis, MN) with a diamond Berkovich tip having a 100 nm tip radius. Normal loads of 500 µN were chosen for the nanoindentation with 5 indentation tests under the same test conditions that were used for the Raman spectroscopy.

### 5.1.4 Wear simulator for hip joint testing

Hip simulator was used to subject hip implants to physiological loading and motions. We used a customized, fully servo-driven hip simulator featuring uniaxial load and two motion axes. The physiological load was applied through spring compression using twin peak 3000 N load gait cycle with 1 Hz frequency according to the ISO 14242-1. (Fig 5.5) displays a scheme and basic measurement principles of the simulator.

Orientation of the two motion axes relative to the load line was chosen to simulate the flexion/extension (applied on the femoral head, range -18° / +25°) and the inner/outer rotation (applied on the acetabular cup, range -10° / +2°) motions. Lack of the third abduction/adduction motion axis as specified in ISO 14242-1 was compensated by a phase shift of the flexion/extension and inner/outer sinusoidal motion curves by 90° according to ISO 14242-1 (Fig 5.4). A sleeve sealing on the heating platform of the simulator is necessary for fully flooded contact pairs. Platform can be heated up to a tested temperature using heating patrons.

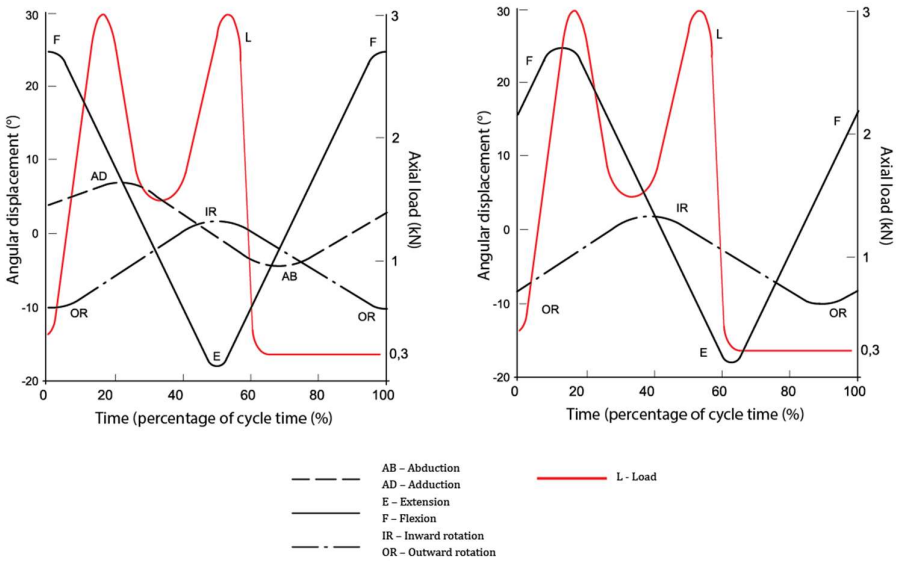


Fig 5.4 Phase shifting cycle of kinematic conditions

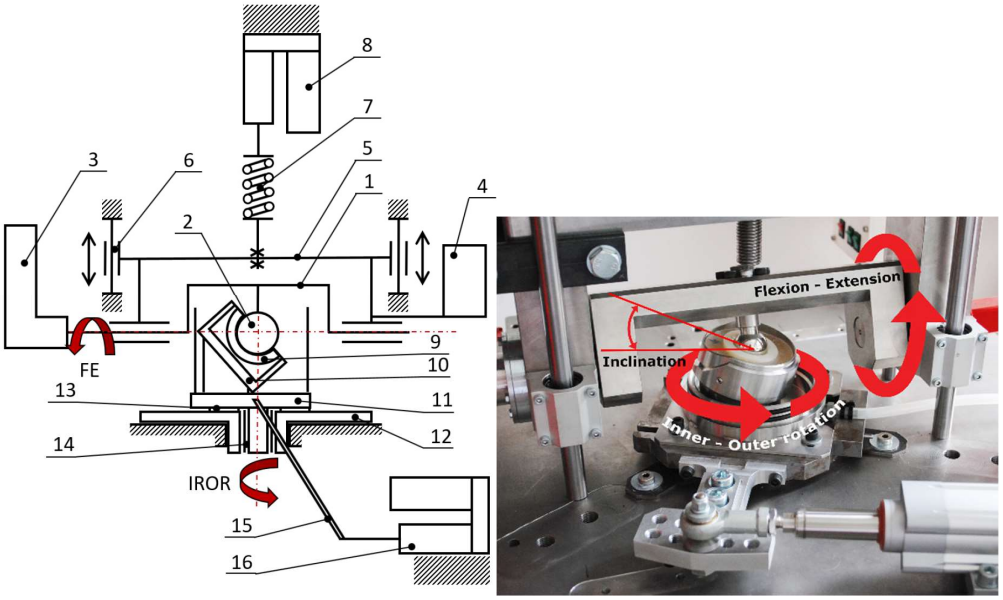


Fig 5.5 Design of the hip joint simulator

Tab. 5.2 Description of simulator components

| | | | |
|---|---|---|---|
| 1 | Swinging frame flexion - extension | 9 | Acetabular liner |
| 2 | Femoral head | 10 | Holder cup |
| 3 | Actuator | 11 | Heating platform |
| 4 | Stationary frame | 12 | Base |
| 5 | Load frame | 13 | Axial bearing |
| 6 | Linear bearing | 14 | Radial bearing |
| 7 | Compensating spring | 15 | Leaver |
| 8 | Load actuator | 16 | Linear actuator |

## 5.2 Measurement methods

Optical scanning method is the key method used in this thesis. One of the main advantages of this method is that it allows to observe geometry of the whole liner to identify the unworn parts of the liner and direction of the wear scare. These parameters can be then used to reconstruct the original geometry for comparison with the clinical data.

### 5.2.1 3D geometry analysis

Scanned data were post-processed using the software GOM Inspect (GOM mbH). First, the scan was polygonised and smoothed with surface tolerance of 3 µm to remove the surface roughness and possible coating defects that could distort the measurements. The process can be described in following steps:

- **Removing of damages** caused by surgeon. In some cases, surgeon caused more extensive damages to polyethylene liners during the revision surgery, what could complicate further analysis. However, thanks to large number of scanned points it was possible to reconstruct the damaged areas.
- **A reference coordinate system** for liner geometry was created using three fitting elements: a line, a point and a plane. The line represented a direction of the wear path (also described as a wear scar) and was used to identify the unworn parts of the samples. The direction of the wear scar was obtained by an initial comparison of the scanned data with nominal data of a new acetabular cup using the best fit function of GOM Inspect. This comparison rendered a map of deviations that enabled us to infer the final direction of the wear scar. The point was defined by the centre of a sphere with a diameter corresponding to the original dimensions of the acetabular cup defined by the unworn part of cup. The plane was defined by the rim of the acetabular cup.
- **Wear vector determination**. Polygonal data with the defined coordinate system were then used to determine the wear vector as a vector originating from the centre of the unworn cup geometry to the most worn point on the inner surface of the cup.
- **Reconstruction of the original geometry.** A 3D model of the articulating surfaces of the original geometry was created using the unworn parts of the liner.
- **Surface and volume creation.** Polygonal data were exported to a STL format for further post-processing with the Geomagic Design X (3D Systems GmbH) software. First, the surface model was generated from the polygonal data using the Geomagic Surface Tool. Quality of this

transformation was evaluated by comparing the rendered surface model with the polygonal data. We found that the uncertainty was under 2 µm. Volumetric model of the retrieved samples was created after a complete reconstruction of the surface geometry.

- **Wear determination.** Volumetric wear of the samples was determined by comparing the volumetric model of retrieved samples with their reconstructed original geometry.

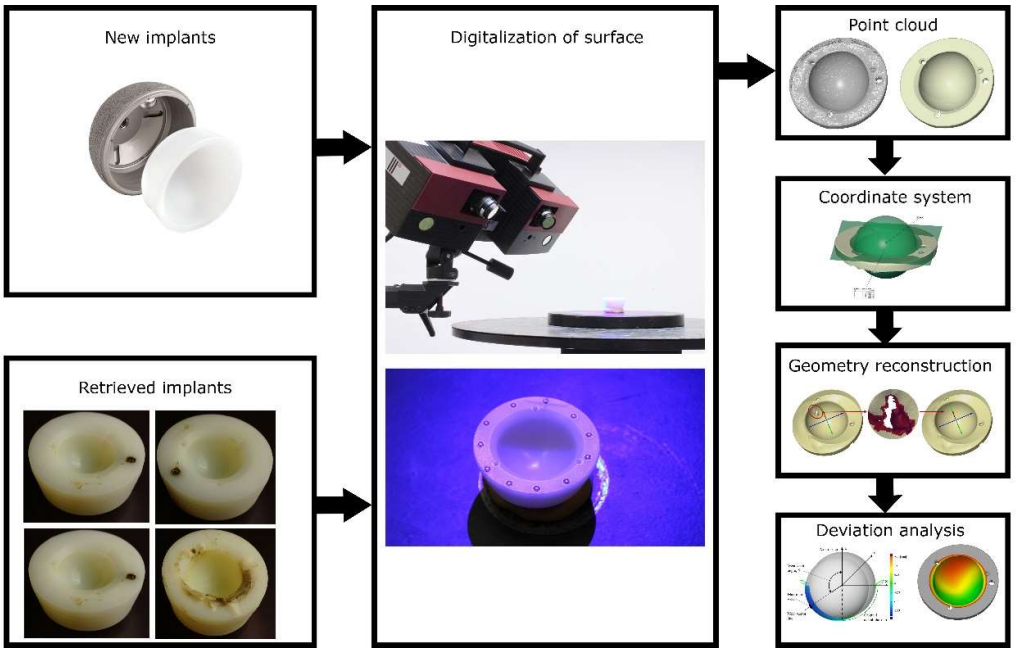


Fig 5.6 Geometry evaluation

### 5.2.2 Surface analysis

A 3D optical microscope ContourGT-X (Bruker, USA) was used to analyse the surface topography of 13 retrieved cups with various extent of wear. Topography measurements were evenly distributed around the articulating surface with 79 points (Fig 5.7). Each measurement position was defined by polar coordinates and compared with the wear distribution obtained by the optical scanning method. Ra value was evaluated as an arithmetic average value a of filtered roughness profile determined by deviations from the centre line. The roughness values were sorted according their frequency and compared with the individual categories of wear mechanism. Several surface areas with different wear mechanisms were identified: abrasive wear, adhesive wear, delamination and surface smoothening. The unworn areas were identified by scoring from manufacturing machines.

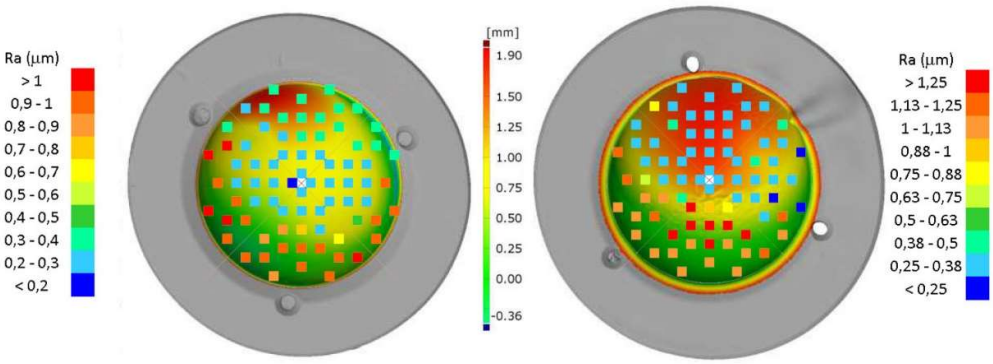


**Fig 5.7 Roughness distribution on wear surface**

## 5.3 Test samples and experimental conditions



New test samples, as well as samples retrieved during revision surgeries, were provided by the Faculty Hospital in Olomouc in cooperation with Professor Jiří Gallo, who was the main surgeon performing all the revision surgeries. Professor Gallo shared with us his surgery procedures and protocols that served as a valuable input for further analysis.

### 5.3.1 Retrieved liners

The optical scanning method was demonstrated on 23 polyethylene acetabular liners with the diameter of 28 mm. Thirteen of the extracted acetabular liners were part of the Bicon-plus cups (Plus Endoprothetik AG, Rotkreuz, Switzerland; later Smith and Nephew, USA). Ultra-high molecular weight polyethylene (UHMWPE) was made of RCH-1000 Chirulen (Quadrant PHS Deutschland GmbH, Vreden, Germany) according to ISO 5834-2 and ASTM F648. The UHMWPE liners were gamma-radiated (2,5 mrads), sterilized (cobalt-60) while sealed in a threefold pouch in a nitrogen atmosphere. The dose adopted was between a minimum of 25 kilogray (kGy) and a maximum of 37 kGy [77]. The other ten retrieved liners were of a newer type Bicon Sulene. Cups were made of the newest generation of compression molded GUR 1020. The extracted cups were produced in two designs. The first design was a standard acetabular cup and the second design was an acetabular cup with an elevated rim - the so-called antiluxation modification. The prostheses were obtained during revision surgeries between 2010 and 2016. All surgeries were performed by the same surgeon. The component´s survival time in situ was on average 8.75 years (0.1-16.8; standard deviation (SD) 4.1 years). After the extraction, all PE liners were mechanically cleaned, immersed in a disinfectant for 24 hours, and then sterilized routinely for 2 hours. All retrieved cups were obtained under standard conditions with a written informed patient consent, and the study was approved by the local Ethics Committee as a part of the project NT11049-5 under Ministry of Health of the Czech Republic.

### 5.3.2 New liners

All the new acetabular liners had the diameter of 28 mm, the same diameter as in case of the retrieved liners. Three new liners manufactured by Zimmer, type Durasul Low Profile Cups, size 50/28 were used as reference samples for validation of the optical scanning method. As the optical scanning method is based on surface reconstruction, validation did not depend on the material or type of the implant. It was the volume loss that was important. The new liners used for comparison tests with the retrieved liners were produced from the same material as the retrieved liners as defined above.

### 5.3.3 Test conditions

Experimental conditions and procedures varied with different measurement methods and experimental devices. First, the new 3D optical scanning method was validated to prove its suitability for volumetric loss measurements. Next, an experiment was designed to investigate the relationship between the inclination angle and plastic deformations using a custom build hip simulator.

#### 5.3.3.1 Validation of the 3D scanning method

The 3D optical scanning method was validated by a gravimetric comparison according to ISO 14242 using analytic balances Kern ABS 320-4N with resolution of ±0.1 mg. The wear of the extracted cups was simulated simply by removing the material from new cups. The wear was simulated on a hip pendulum composed of two main parts: a base frame with acetabular cup and a pendulum with femoral head. The pendulum oscillated freely in the flexion-extension plane. The pendulum set-up is described in details elsewhere [78]. The material loss of new cups was measured in six simulated wear cycles, each cycle lasted 15 minutes and the process was replicated on three cups. As the surface damage was not intended for validation investigations, femoral head was damaged extensively to increase the wear and to decrease the time of experiment. The amount of removed material was within the range corresponding to the average natural material loss in human body for similar type of implants (21 – 74 $mm^3$) as showed by radiographs of the patients [79]. Liner fixation was performed on the outer rim that was sealed into the epoxy resin mixture (Dentacryl). All tests were performed with this fixation; each cup was thoroughly cleaned before weighing and scanning according to ISO 14242. Repeatability was evaluated based on the software-determined value of the inner diameter using the best-fit function. The method was set to the Gaussian statistic method using point filtration three sigma. Measurements were repeated 10 times. Results of the experiment were published in article A.

**Tab. 5.3 Parameters of the validation experiment**

| | |
|---|---|
| Load | 2080 N |
| Frequency | 0.48 Hz |
| Density of used UHMWPE | 0.940 g/cm3 |
| Acetabular cup liner | Durasul, size 50/28 mm (Zimmer) |
| Femoral Head (significant damage) | CoCrMo alloy, size 28 mm (Zimmer) |
| Duration | 6 cycle / 15 minutes |
| Temperature | 22 – 23 deg |

### 5.3.3.2 Experimental conditions for creep test

The creep experiments were conducted using a custom hip joint simulator as described above. Three physiological orientations with different abduction angles were tested. Abductions of 30°, 45° and 60° were chosen to represent the whole surgically recommended abduction interval. Anteversion angle remained unchanged at 15 degrees (approximately in the middle of the recommended interval) for all three cases to isolate the influence of abduction. The hip replacement components were submerged in pseudo-synovial fluid during simulator testing. The fluid was based on phosphate-buffered saline serum with addition of Albumin (28 mg/ml) and γ-globulin (9.4 mg/ml) proteins. The whole containment with the flooded hip articulating components was heated to 37 °C with accuracy of ± 2 °C according to the ISO 14242-1 using heating elements in the containment's bed.

The simulator ran for total of 50 000 gait cycles with series of measurements starting in the initial brand-new state of the implants and then repeated after every 10 000 gait cycles to observe development of liner deformations in the run-in phase. Results of the experiment were published in the article C.

**Tab. 5.4 Parameters of the creep experiment**

| | |
|---|---|
| Load, kinematic | According ISO 14242 |
| Abduction angle | 30deg, 45deg, 60deg |
| Anteversion angle | 15deg |
| Lubricant | PBS + non-stained proteins (albumin, γ-globulin). |
| Temperature | 37± 2 °C |
| Acetabular cup liner | UHMWPE, (B-Braun, Aesculap AG ) |
| Femoral Head | CrCoMo alloy (B-Braun, Aesculap AG ) |

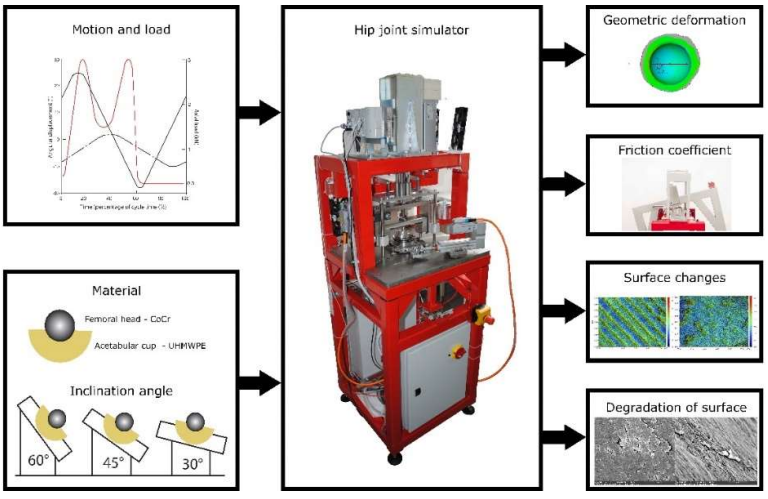


**Fig 5.8 Design of the run-in phase experiment**

# 6 RESULTS AND DISCUSSION

We have introduced a new optical scanning approach to measurements of the polyethylene hip joint acetabular liners wear. Thanks to their time efficiency and accuracy, optical scanning methods are used widely across many industries. Application of the method for wear analysis required two steps: first the liners were conventionally scanned and then the scanned data were post-processed accordingly to yield inputs for the wear analysis.

The method was demonstrated on thirteen retrieved polyethylene liners and validated on three new liners according to the ISO 14 242 Standard defining standard testing requirements based on kinematic of human gait for other wear measurement methods such as gravimetric method and coordinate measuring method.

In case of the retrieved liners, the post processing and further analysis were complicated by the unknown original geometry of the samples. However, it was still possible to reconstruct the original geometry using the unworn areas with negligible damages of the retrieved liners. The unworn areas could be identified by scoring from manufacturing machines.

Design of the new wear analysis approach including measurements, data post-processing, demonstration on retrieved liners and validation on new liners is described in paper A. High number of collected points (191 500 surface points) ensured high quality of surface transformations with deviations less than 0.002 mm and thus solved problems described by as a point spacing problem, curvature of the elements or problems related to the latitudinal and longitudinal mesh pattern [39].

Despite the high-quality surface data, the problem of cold flow phenomenon, called also creep or plastic deformation, remained. Plastic deformation without release of actual wear can cause distortions in volumetric wear analysis, especially when using methods other than gravimetry. The creep process usually takes place in the first few months after total hip replacement surgeries when material loss is negligible yet.

The problem of creep was partially eliminated during the validation phase, when the extensive damages of the head allowed material loosening from the beginning of the whole process, while the material could relax in between the measurements. Despite this, there were still differences between the volumetric wear values inferred from the surface data and volumetric wear values inferred directly from the weight of the samples. As shown by the validation measurements, the volumetric wear obtained by the 3D scanner was significantly higher that the wear obtained by the gravimetric method.

During the validation phase, material loss of new cups was measured in six simulated wear cycles using both the gravimetric and 3D optical methods. Each cycle lasted 15 min and the process was replicated on three cups. Validation was performed by

gravimetric method according to the ISO 14 242 Standard as mentioned above. Results of the validation showed deviation of 0.0040 g, 0.0021 g and 0.0029 g, corresponding with 2.2 – 4.3 $mm^3$ of material loss. Repeatability of the optical scanning method was evaluated on the inner diameter of a new cup. Ten various measurements showed deviation of 0.005 mm.

From the accuracy perspective, coordinate measuring method or RedLux method proved to be more accurate than the optical scanning method [47]. However, they have limited use for analysis of liners showing more extensive damages. Due to its lower precision, the optical scanning method is not suitable for analysis of hard components. On the other side, the accuracy of optical scanning method is fully acceptable when it comes to the analysis of polyethylene components, especially those with extensive damages. The ability to measure the whole geometry of a liner, including its rim and any possible extensive damages is one of the main advantages of the optical scanning method. Number of collected points is also significantly higher compared to other methods. This is important especially for reconstructions of damages caused by surgeon during extraction that, when left unnoticed, may distort the volumetric wear determination. High number of collected points enables to replace the surgeon damage with a new surface during post processing, while the curvature is calculated based on the surrounding elements.

As the surface structure is one of the parameters influencing correct volumetric wear determination, we conducted a surface analysis of 13 retrieved UHMWPE Bicon- plus implants (Smith and Nephew, Switzerland). The results are discussed in greater detail Appendix A. The Bicon- plus implants are still relevant in clinical practice in the Czech Rebublic, even though being increasingly replaced by newer generations of implants. The 13 liners were extracted during revision surgeries. Liners were scanned by an optical scanner to determine the wear rate. Then we analysed surface roughness with Contour GT-X8 profiler using the principle of phase shifting interferometry. Wear scare of the articulating surface was determined according to the wear vector and angle of penetration and surface roughness was then compared with the clinical results.

The average linear wear was 0.13 mm/year (ranging from 0.06 to 0.3 mm/year), and the mean value of total volumetric material loss was 44.37 $mm^3$/year (ranging from 9.98 to 125.85 mm3/year). Using the optical profilometer, a map of roughness distribution of the individual cups was created. For each implant, 76 values of roughness were measured, and each measurement was evaluated on an area of 0,22$mm^2$. Based on their roughness and topography, liner surfaces were then sorted into several different categories of wear mechanisms: surface polishing, abrasive-adhesive wear, surfaces with preserved grooving, surfaces with substantial plastic deformation and delamination. The abrasive-adhesive surface wear was between 0.1 – 0.3 μm and was observed mostly in patients without loosened implant components.

The abrasive wear was defined by typical and significant scratches corresponding with direction of the wear scare. Character of scratches suggested presence of third body particles in the contact areas. The adhesive wear was distinguished by polished surface and decreased roughness compared to the original surface that was preserved in the unworn parts of the liner. The abrasive wear was accompanied with pitting – a process assigned to fatigue of polyethylene. This effect was observed in patients with longer lifespan of implants, on average 10,5 year (SD 2,5 year). Damages such as cracks, significant plastic deformation or delamination were also observed in implants with a longer lifespan. Extensive surface damages could have been caused by changing material properties and chemical degradation of the surface. As expected, extensive damages of liners correlated also with higher linear wear and – except for the extreme causes such as implant fractures – also with a higher abduction angle in pelvis. Linear wear rate exceeding 0.1 mm/year correlates with an increased risk of osteolysis formation as mentioned in several studies [10, 11, 80]. The examined implants resisted osteolysis even though the above-mentioned conditions were met. Though the number of samples was not statistically significant to make valid conclusions, the results may serve as hypotheses for future research.

Issues outlined in appendix A such as surface degradation and influence of the abduction angle on wear/creep were further examined in Papers B and C. Paper B focused on mechanical and chemical degradation of ten extracted polyethylene Bicon-plus liners with the same specifications as the 13 liners studied in paper A and appendix A. The 10 samples were extracted during revision surgeries between 2015 and 2016 and their survival time in vivo was on average 9.52 years (range: 0.1–16.76 years, SD 4.69 year). Measurements and analyses were carried out in cooperation with the University of Arkansas in the USA due to availability of measurement devices and knowledge in this field.

All 10 samples were divided into three groups according to the reason of revision: (1) aseptic loosening and extensive wear, (2) pain and (3) other reasons such as a dislocation, articular ossification and osteolysis. Surface deviation measurements were carried out for each liner to determine the linear wear and deviation map. Positive values on the deviation map indicated material inflation and negative values indicated wear and creep. Direction of penetration was relative to the axis of liner and was defined by the wear vector. Samples 1–3 from the group 1 had smaller wear vector angle, 16 degrees on average, and corresponded with the lowest rate of linear wear, on average 0.09 mm/year.

Samples in groups 2 and 3 had obviously higher wear vector angles of around 73.7 degrees and likewise showed increasing linear wear of 0.45mm/year. Changes in wear rate could indicate changes in the material behaviour of the surface. All liners were analysed using Raman spectroscopy. Oxidation indices showed a clear sign of chemical degradation in the retrieved prostheses, and these mostly correlated with wear depth. Oxidation index and volume fraction of orthorhombic phase are very significant, since both are closely related to the oxidative degradation of tribo-

corrosion process. Hardening and stiffening were also identified in the liners. Samples representing each type of failure were chosen for hardness and modulus of elasticity measurements using nanoindentation on the surface of the samples (indentation depth is below 2 μm). All the measured samples showed an increased hardness and stiffens range compared to new samples. Several studies showed that the hardness and elastic modulus is a key material property that is related to tribological performance [81]. The advantage of the above-mentioned approach is the possibility to match measurements of hardness and stiffens with the map of surface deviations. Thanks to wear scare and angle of head penetration, position of the retrieved liner in human body can be identified in reverse.

Results outlined in appendix A and paper B indicated a possible relationship between the wear rate, creep and position of the acetabular cup in pelvis. The literature review showed influence of the abduction angle on load distribution and hence on wear and creep. Confirmation of this relationship can influence both the wear rate of the implants and quantification of wear using optical scanning methods. Therefore, we continued to study the liner position in the run-in phase of its lifecycle.

Paper C investigated three new samples tested on a hip simulator to study creep deformations and influence of the abduction angle. We investigated several angles of acetabular abduction that are frequently used in the clinical practice. Three main deformation regions of the cups' bearing surface were distinguished. The first deformation region was the region affected directly by head's penetration with most *profound compression deformations*. This oval-shaped region was positioned in the direction of applied force, moving closer to the superior quadrant of the acetabular rim with an increasing inclination angle. However even in case of the liner with the highest tested inclination angle of 60-degrees, this deformation region did not involve the cup's rim itself. The first region of the most profound deformations was surrounded by the second region of *shallow compression deformations* ranging up to the inferior quadrant of the cup's rim. The third region of *plastic deformations* was in the posterior-superior quadrant of the acetabular rim. Inflation areas (or plastic deformations) were observed also in liners that were analysed in paper B. Rim deformations cause potential risk of liner cracking in this area as demonstrated by Brazier et. al. [82], and corresponds with the predicted distribution of contact stress as described in an earlier finite elements analysis study [65]. The elevated rim increases radial clearance of the hip replacement with possible consequences for lubrication processes [78]. In addition to the methods described earlier in this thesis, the damaged surfaces of the tested liners were also observed using scanning electron microscopy after the performing of tests.

The brand new acetabular cups showed spherical articulating surface with distinctive circular marks from the manufacturing process. These marks were evened out to a smooth finish with the femoral head during the first 10 000 to 20 000 gait cycles. Development of fine multidirectional scratches replacing the initial bearing surface structure was observed at up to 50 000 gait cycles. The 45° and 60° inclination angles

specimens showed a similar steady increase of head roughness from the average Ra of 10.2 nm - 11.2 nm at the initial measurement, to the final measurement of Ra of 12.7 - 13.0 nm. The main factor contributing to the surface degradation was development of occasional fine multi-directional scratching. On the contrary, the lowest inclination angle specimen of 30° showed decrease of the initial roughness from Ra 9.0 nm to Ra 7.7 nm with the smoothening effect.

The maximal depths of compressive creep deformation were between 0.04 – 0.05 mm and are generally on the lower end of those predicted by previous studies. This supports usage of creep model parameters taken over from static creep tests for creep depth measurements [54]. Neglecting the elastoplastic nature of creep deformations in favour of a purely plastic creep model, however, could be the cause of the slightly more profound deformations found in the previous studies compared to our study. On contrary, the bearing surface area affected by deformation was notably larger than values found in previous studies [55]. This could be caused by omitting the cross-shear factor in creep model in previous FEM studies. The results are also influenced by irregular load cycles in line with the ISO 14242 Standard simulating gait cycle of a patient.

The relaxation periods allowed not only to observe just the irreversible plastic creep deformation, but the cyclic applying and relaxing of the elastic strain could also support both the processes of strain-induced recrystallization of UHMWPE and lamellae alignment perpendicularly to the applied load. The increased crystallinity and aligned crystalline phase increase the elastic modulus and hence improve the creep resistance. On the other hand, an increased elastic modulus increases maximal value of the Hertz contact stress, making the acetabular cup prone to fracture and delamination.

As for the limitations of this study, we used the conventional polyethylene cups as test samples, while nowadays XLPE acetabular cups are more common. On the other hand, the crosslinking itself does not affect creep mechanism, not nearly as much as the wear resistance does. Moreover, the conventional polyethylene is better comparable with the liners retrieved during the revision surgeries nowadays. This can lead to better understanding of wear mechanism in the human body and the resulting knowledge can be applied for the newest generation of polyethylene cups.

TRIBOLOGY TRANSACTIONS
http://dx.doi.org/10.1080/10402004.2016.1176286

stle
Society of Tribologists and Lubrication Engineers

# Wear Analysis of Extracted Polyethylene Acetabular Cups Using a 3D Optical Scanner

Matúš Ranuša[a], Jiří Gallo[b], Martin Vrbka[a], Martin Hobza[b], David Paloušek[a], Ivan Křupka[a], and Martin Hartl[a]

[a]Faculty of Mechanical Engineering, Institute of Machine and Industrial Design, Brno University of Technology, Brno, Czech Republic; [b]Department of Orthopaedics, University Hospital Olomouc, Faculty of Medicine and Dentistry, Palacky University, Olomouc, Czech Republic

**ABSTRACT**

Wear analysis of total hip replacements (THRs) is considered one of the most relevant research areas helping to improve the longevity and overall design of THRs. The coordinate machine method (CMM) and Fourier profilometry are the most common methods for measuring THR wear. This article presents optical scanner digitalization as a new method for measuring the wear of polyethylene (PE) acetabular cups. The aim of this article is to explore the potential of this method for the PE wear measurements. Optical scans for the purposes of this study were produced using an ATOS Triple Scan 3D optical scanner. The optical scanner is efficient and it can measure a large number of points for polygonization and for further development of the preworn models. In this study, the scanner first generated point clouds on a sample of 13 retrieved ultra-high-molecular-weight polyethylene (UHMWPE) acetabular cups. Next, volumetric models of the cups were created by polygonizing the point clouds. Reverse engineering was used to develop models of the original acetabular cups using the geometry of the unworn parts of the retrieved cups. A comparison of the two models then showed the total volume of the PE debris. The optical scanning method was validated against the gravimetric method using three new acetabular cups that were worn out on a hip pendulum simulator. Validation shows that the optical scanning method is a valid method for wear analysis of the retrieved UHMWPE acetabular cups.

**ARTICLE HISTORY**
Received 15 December 2015
Accepted 5 April 2016

**KEYWORDS**
Total hip replacement; polyethylene; wear measurement; optical digitalization; volumetric wear

## Introduction

Total hip replacement (THR) is currently the most effective treatment of a number of hip afflictions that helps to alleviate pain and improve quality of life. This surgical procedure consists of removing the damaged joint surfaces and replacing them with artificial ones—an acetabular cup articulating surface with femoral head on a femoral stem. The most common combination of bearing materials is a polyethylene (PE) acetabular cup articulating with a metal or ceramic head.

Along with a growing number of THRs, there is a growing need for revision surgeries due to prosthesis failure. Projected estimates made for the United States show that by 2030 the demand for primary THA will grow by 174% for primary surgery and 137% for revision surgery compared to the levels in 2005 (Kurtz, et al. *(1)*). By far, the main reason for a revision surgery is aseptic loosening followed by infection and dislocation. Aseptic loosening is causally associated with liberation of huge amount of prosthetic wear particles from the bearing surfaces. These particles stimulate the receptors of innate immunity to trigger a foreign body host response driven predominantly by macrophages and fibrocytes (Gallo, et al. *(2)*). That is why manufacturers and researchers are motivated to develop bearing materials with increased resistance to wear.

In order to measure the amount and rate of prosthetic wear, various in vivo and in vitro methods have been developed offering clinicians as well as researchers the ability to determine damage to the prosthetic cup liner (Patel, et al. *(3)*). In vivo wear measurement methods rely on the assumption that a definite relationship exists between a quantifiable X-ray penetration of the prosthetic head in the cup and the true amount of wear. However, this article focuses only on in vitro methods. Gravimetric methods are suitable for evaluation of the cups tested under repetitive load cycle in special hip joint simulators when the pretest weight of a cup is known. The gravimetric method is also suitable for assessment of artificially worn components in experimental settings. The approach is defined by international standards ISO 14242 (Affatato, et al. *(4)*). The accuracy of this method is a minimum of 0.1 mg according to ISO 14242–2 *(5)*.

However, this method is not useful for the analysis of extracted hip implants because the weight of the original cup in a preworn stage is not known. Therefore, development of alternative methods allowing the measurement of volumetric wear in a retrieved cup without knowledge of its weight before its use is needed (Bills, et al. *(6)*).

One of these methods is the analysis of surface geometry by a coordinate measurement machine (CMM). It is the most common method for measuring the geometry in manufacturing practice for control of the shape and dimensions of product elements. Use of this method has also become a correct standard method for the measurement of THR volumetric wear during in vitro tests (Bills, et al. *(7)*; Martell, et al. *(8)*). A precise description of

**CONTACT** Matúš Ranuša ranusa@fme.vutbr.cz

Color versions of one or more of the figures in the article can be found online at www.tandfonline.com/utrb.

Review led by Thierry Blanchet

© 2016 Society of Tribologists and Lubrication Engineers

this method is clearly summarized in ISO 14242-2 (5), where a particular focus is dedicated to the maximum axial position error of measurement, which is described as $D = 4 + 4l \times 10^{-6}$ ($D$ = volumetric position error in micrometers, and $l$ = measuring length of the work envelope in millimeters). A location change of specimen must affect the volume by no more than 0.05%, and the point mesh spacing should be <1 mm. This standard offers a fundamental basis for the volumetric wear analysis with defined uncertainty of THR measurement (ISO 14242-2 (5)).

There are many studies describing the uncertainty and postprocessing algorithm related to this method. Kothari, et al. (9) published one of the first studies discussing the use of a CMM method to evaluate 22 retrieved THR components. Three hundred and twenty-five points were measured on the surface of a sample. The analysis was carried out in vitro and the examined implants were from metal material (Kothari, et al. (9)). The declared accuracy of this method was ±5 $\mu$m, with the definition described in geometrical product specification for CMM system declaration by ISO 10360-2 (10). Becker and Dirix (11) evaluated the precision of this method in the study comparing two CMM methods with a standard precision of 2.6 $\mu$m and a high precision of 1.2 $\mu$m. Lord, et al. (12) assessed metal-on-metal THR components, analyzing 32 femoral heads and 22 acetabular cups. The aim was to evaluate the effectiveness of the CMM method against a conventional gravimetric method. To determine the volumetric wear, a program using mathematical software was created. This program aimed to identify the origin of the spherical components from as wide an area of the articulating surface as possible. Then the worn area was localized. Results of this study were verified by the gravimetric method. A validation procedure compared the mathematical and the gravimetric method. In Lord, et al. (12), three stages of mean absolute error—0.53, 0.50, and 0.24 mm$^3$—were reported for metal components. Another study examined distribution of the scan lines. The results deal with the impact of the scanning method (polar, planar, etc.), distances between the scan lines, and distribution of points along a single scan line (Bills, et al. (6)).

An innovative surface analysis methodology is the optical method. A noncontact analysis provides simplification of measurements and postprocessing analysis. On the other hand, it offers new possibilities for postprocessing the scanned geometry. The main method used for complex analysis of THR geometry is based on reflectivity of the surface. Reflection of the incident beam is processed by an active or passive triangulation.

One of the studies focused on the use of a noncontact scanning method using Fourier profilometry (Rossler, et al. (13)). The study deals with a sinusoidal grating projector that creates an optical pattern on the object. This pattern is deformed by refraction on the surface, which is reflected in changes of its phase. The image is recorded by a digital camera. Information about the geometry and topographic depth is obtained by the image processing and by the mathematical algorithm computing the phase shift toward the reference plane. A relative percentage difference of this method compared to the gravimetric method is approximately 6.3% depending on the rate of volumetric wear (Rossler, et al. (13)).

Another approach, called scanning profilometry, uses only a one-strip projection. For the analysis of all surfaces, the object is rotated. The sensitivity and accuracy of this method depends on the size of the angle of object rotation. As a result, the whole profile is created by connecting the individual linear scans. The third coordinate is determined from the equal compared reference plane and the plane of refraction. The relative percentage difference of this method compared to the gravimetric method is about 10% (Pochmon, et al. (14)).

Zou, et al. (15) studied the macrostructure surface of acetabular cups. To establish an accurate method for digitizing a convex hemispherical shape, a laser probe fitted on a CMM machine is used. The principle of this optical method is based on triangulation. The surface was digitized at 0.1-mm intervals in $X$ and $Y$ directions divided into six scans. Then discrete points were merged into one surface data. Reproducibility of the method shows a volumetric difference of 1.411 mm$^3$ (Zou, et al. (15)).

Yun, et al. (16) used 3D optical scanning for validation of the reliability of a power point method to recognize volumetric wear in vivo from radiographs. This method is applied on 17 retrieved PE acetabular cups. A 3D laser scanner used for the analysis of the cup has a resolution of 2.0 megapixels and precision less than 0.01 mm. Data are postprocessed using special software (Geomagic, Morrisville, NC). The mean wear volume achieved by the 3D laser scanning method is 1,146.72 ± 576.59 mm$^3$. The main message is to show that the power point method correlated well with the 3D scanning method (Yun, et al. (16)).

The aim of this article is to demonstrate the optical method as a method suitable for determination of volumetric wear and material loss. This method is applicable for retrieved PE acetabular cups at various stages of wear. The data obtained from the 3D digitizing process by the optical scanner are processed and evaluated using computer-aided design (CAD). Using a postprocessing algorithm, it is possible to determine the amount of volumetric wear. A particular focus is given to validation of this method by the standard gravimetric method. This method ranks among the most innovative methods in the respective field to determine the volumetric wear of PE acetabular cups. Information on volumetric wear can be used to suggest an effective modification of geometry that would lower the friction and wear by effectively moving the lubrication regime away from the boundary regime toward the mixed and hydrodynamic lubrication regimes (Dougherty, et al. (17); Choudhury, et al. (18)).

As indicated above, the CMM and the gravimetric method are the two most widely used methods for determining the volumetric wear on acetabular cups in vitro. These methods are very precise and have high confidence levels. In recent years, these methods have been supplemented with optical methods to obtain a more comprehensive and time-efficient analysis. The main advantage of the approach described in this article is its ability to reconstruct the unworn geometry of the cup. The analysis of geometry is made on the basis of a large number of points forming the point clouds. This advantage opens new opportunities for analytic and statistical approaches for determination of volumetric wear.

**Table 1.** Characteristics of the patients enrolled in the study.

| Patient | Gender | Weight (kg) | Body ms index | Age (years) | Side | Date of revision | Duration (months) | Type of patient[a] | Reason for revision |
|---|---|---|---|---|---|---|---|---|---|
| 1 | M | 66 | 24.24 | 67 | Right | January 27, 2015 | 145 | B | Periprosthetic fracture, wear |
| 2 | F | 48 | 19.23 | 48 | Right | October 10, 2011 | 126 | B | Aseptic loosening[b] |
| 3 | F | 75 | 27.55 | 55 | Left | November 5, 2012 | 120 | B | Aseptic loosening–stem |
| 4 | F | 63 | 24.01 | 61.5 | Right | September 11, 2013 | 131.5 | B | Aseptic loosening |
| 5 | M | 103 | 32.51 | 52 | Right | January 30, 2012 | 75 | A | Painful hip |
| 6 | F | 88 | 34.38 | 77 | Right | January 22, 2014 | 48.5 | B | Aseptic loosening |
| 7 | M | 100 | 30.86 | 73 | Left | May 14, 2013 | 89.5 | A | Aseptic loosening–stem |
| 8 | F | 58 | 21.05 | 43 | Left | October 20, 2010 | 92.2 | B | Fracture of the cup |
| 9 | F | 56 | 23.31 | 63 | Right | October 30, 2013 | 164 | B | Aseptic loosening |
| 10 | F | 72 | 26.77 | 53 | Right | September 24, 2014 | 53.6 | A | Aseptic loosening |
| 11 | F | 77 | 26.96 | 69 | Left | March 12, 2014 | 61.9 | A | Aseptic loosening |
| 12 | F | 60 | 22.04 | 77 | Right | September 14, 2010 | 43 | B | Aseptic loosening |
| 13 | F | 68 | 29.05 | 59 | Left | April 20, 2011 | 114.6 | B | Aseptic loosening |

[a]The Charnley classification tries to estimate the level of walking capacity, with class A having no disturbance in locomotion, class B with bilateral hip disease (or hip and knee) and normal findings in other weight-bearing joints, and class C with severe compromise of locomotion due to multiple joint involvement.
[b]Both components.

## Materials and methods

### Components

The new method of wear evaluation was demonstrated on 13 acetabular cups with a diameter of 28 mm (Table 1). All extracted acetabular cups were part of the Bicon-plus cup (Plus Endoprothetik AG, Rotkreuz, Switzerland; later Smith and Nephew). Ultra-high-molecular-weight polyethylene (UHMWPE) was made of RCH-1000 Chirulen (Quadrant PHS Deutschland GmbH, Vreden, Germany) according to ISO 5834-2 and ASTM F648. The UHMWPE liner was gamma radiation sterilized (cobalt-60) while sealed in a threefold pouch in a nitrogen atmosphere. The dose adopted was between a minimum of 25 kGy and a maximum of 37 kGy (Milosev, et al. *(19)*). There is a consistent agreement in clinical studies that the UHMWPE represents an improvement in wear over conventional PE (Williams, et al. *(20)*). The extracted cups were produced in two designs. The first design was a standard acetabular cup and the second design was an acetabular cup with an elevated rim (the so-called antiluxation modification). Retrieved prostheses were obtained at revision surgeries between 2010 and 2015. All surgeries were performed by one surgeon. The component's survival time in situ was on average 97.29 months (range = 43–145, SD = 37.83 months). After prosthesis extraction, all of the PE liners were mechanically cleaned, immersed in a disinfectant for 24 h, and then sterilized routinely for 2 h. All retrieved cups were obtained under standard conditions with written informed patient consent, and the study was approved by the local Ethics Committee (as a part of project NT11049-5, Ministry of Health, Czech Republic).

New acetabular cups with a diameter of 28 mm were used as reference samples for validation of the method. The new acetabular cups were Durasul Low Profile Cups produced by Zimmer (size 50/28). Validation was replicated on three independent samples to eliminate measurement and manufacturing random errors.

### Optical scanning method

Acetabular cups were measured using an 3D ATOS Triple Scan optical scanner (Fig. 1). This optical system is based on active fringe projection and triangulation. The ATOS Triple Scan uses blue light technology in three viewing angles between the stereo camera and projector. With this approach, the measurements are not dependent on environmental factors and therefore it is not necessary to maintain constant environmental conditions during the measurements. A fringe pattern is projected on the object to be measured and the image is acquired using a two-camera system (Fig. 2). The final scan is composed of multiple partial scans that are aligned according to the reference points detected by software.

For measurement of the acetabular cups, the reference points with a diameter of 0.8 mm were positioned on the surface of the cups outside their evaluated areas (GOM *(21)*). The measurement was carried out with MV170 lenses with a measurement volume of 170 × 130 × 130 mm calibrated in a small object arrangement. The lenses complied with VDI/VDE2634-3 *(22)*. Further parameters of the measuring equipment are shown in Table 2.

The scanner was calibrated according to the procedures as defined by the producer. Results of calibration are shown in Table 3.

The surface of PE acetabular cups was too transparent for scanning and it was necessary to apply a layer of $TiO_2$ coating. An airbrush system was used to apply an approximately 3 $\mu$m coating (Palousek, et al. *(23)*). The acetabular cup was fixed in the middle of a rotary measurement table. The scanner was focused on the center of the acetabular cup at a scanning

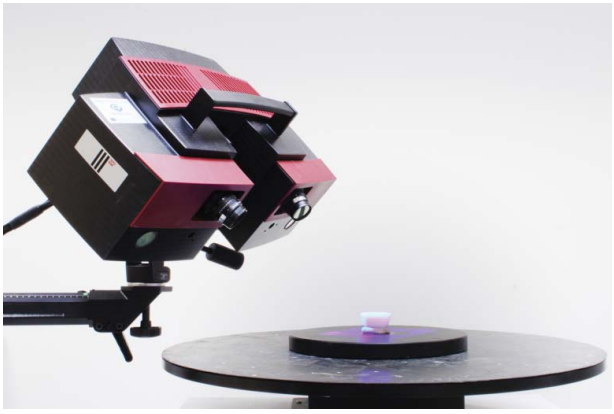

**Figure 1.** Measuring by ATOS III Triple Scan 3D optical scanner.

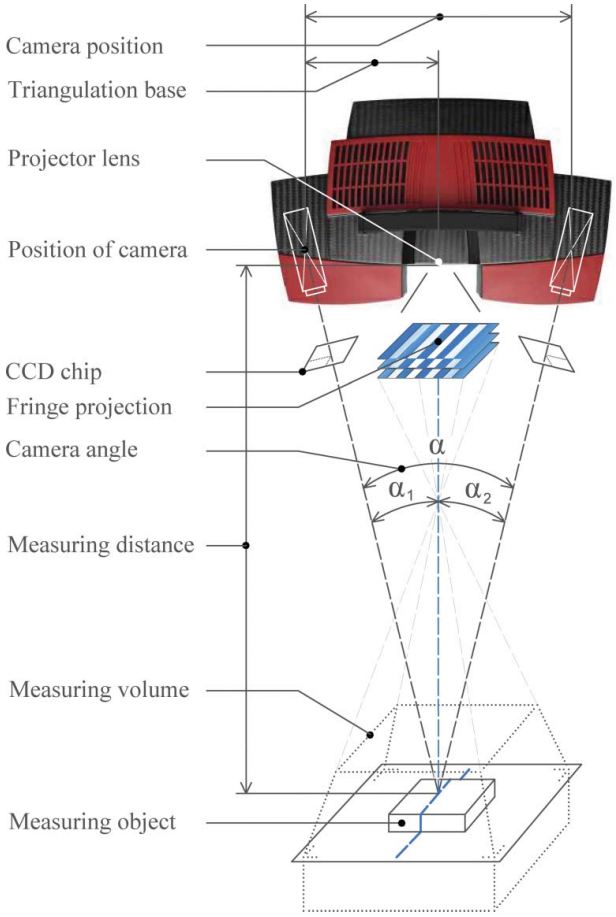


**Figure 2.** Principle of ATOS 3D optical system.

distance of 490 mm. Each individual scan consists of a large number of isolated points, technically described as a point cloud. Approximately six partial scans were used for the final scan to be used in postprocessing.

## *Polygonization and definition of coordinate system*

After the measurement, the data were postprocessed using the software GOM Inspect (GOM mbH). First, the scan was polygonized. For the purpose of further analysis, only the articulating surface and its close surroundings were necessary; redundant data were removed. Next, the polygonized object was reconstructed by removing and filling in damage caused by the surgeon during extraction of THR components (Fig. 3). Surgical damage was identified after analyzing and considering

**Table 2.** Parameters of GOM ATOS III Triple Scan 3D scanner (Palousek, et al. (23)).

| Parameters | ATOS Triple Scan |
|---|---|
| Camera pixels (Mpx) | 2 × 8 |
| Measuring volume (mm) | 170 × 130 × 130 |
| Measuring distance (mm) | 490 |
| Lamp | LED |
| Focal length camera lenses (mm) | 40 |
| Focal length projector lens (mm) | 60 |
| Point distance (mm) | 0.055 |
| Reference points diameter (mm) | 0.8 |
| Camera position | Small object |

**Table 3.** Results of calibration.

| Parameters | Results of calibration |
|---|---|
| Deviation of calibration (pixels) | 0.033 |
| Optimized deviation of calibration (pixels) | 0.020 |
| Calibration of projector (pixels) | 0.118 |
| Optimized calibration of projector (pixels) | 0.019 |
| Angles of cameras (°) | 27.2 |
| Temperature (°C) | 24 |
| Type of calibration object | CP40-170-40346 |

the procedures used for extracting of THR implants. After these modifications, the polygonized geometry was smoothed with a surface tolerance of 3 $\mu$m to remove the surface roughness and possible coating defects that could distort the measurements.

A reference coordinate system for cup geometry was created using three fitting elements: a line, a point, and a plane.

The line represented the direction of the wear path (also described as a wear scar) and was used to identify the unworn parts of the samples. The 3D model was created on the basis of the nominal value of the acetabulum diameter. The direction of the wear scar was obtained by an initial comparison of the measured data with the nominal data of the new acetabular cup using the best-fit function of GOM Inspect. This comparison rendered a map of deviations that enabled us to infer the final direction of the wear scar (Fig. 4).

The point was defined by the center of a sphere with a diameter corresponding to the original dimensions of the acetabular cup. The sphere itself was created using the Gaussian best-fit method on a cloud of points of the unworn region. A selection of points defining the unworn region is made manually according to the deviations from the ideal model. Cups with higher wear volumes have a clearly identifiable line between the worn and unworn regions. The selected points were then evaluated with three sigma statistical criteria enabling use of 99.73% of the points.

The plane was defined by the rim of the acetabular cup. A selection of points was performed automatically. A different method of point selection was used for antiluxation cups where the definition points were located only on the outer edge of the rim.

Polygonal data with the defined coordinate system were then used to determine the wear vector as a vector originating from the center of the unworn cup geometry to the most worn point on the inner surface of the cup. The center of the unworn region is defined by the point in the center of the coordinate system as described above. The center of the worn region is defined by the best-fit function applied to the selection of data in the direction of the wear scar. This can be calculated using the basic linear algebra equation for the angle between the two vectors (Fig. 5; Uddin *(24)*).

The surface of the original acetabular cup was defined by fitting the primitives on unworn parts of the extracted acetabular cup as described above (Fig. 6d). The original unworn model was created on the basis of the dimensions of the primitives from the unworn parts of the samples by means of reverse engineering (Fig. 6e). This method assumed that the original unworn surface was truly spherical and without roughness after machining.

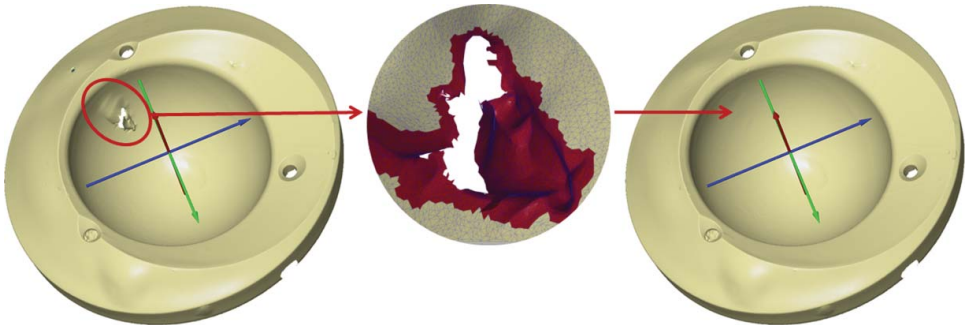

**Figure 3.** Reconstruction of extracted acetabular cup (GOM Inspect).

### *Surface and volume creation*

Polygonal data were exported to STL (STereoLitography) format for further postprocessing with Geomagic Design X (3D Systems GmbH) software (Fig. 6b). First, the surface model was generated from the polygonal data using the Geomagic autosurface tool. The quality of this transformation was evaluated by comparing the rendered surface model with the polygonal data. This comparison showed a maximum deviation of 2 $\mu$m, which is a negligible uncertainty (Fig. 7).

Next, the scanned geometry was trimmed and closed with a cylindrical geometry. Dimensions of the geometry were specified with respect to the extent of the volumetric wear. The cylindrical geometry had to include the whole articulation surface showing any material loss. The resulting surface model was suitable for transformation to the volumetric model using Geomagic tools (Fig. 6c).

In the next step, the volumetric model was compared with the model of the original acetabular cup. The resulting comparison shows the volume of material released to a human body during the life cycle of the cup (Fig. 6f).

### *Validation of method*

The 3D scanning method was validated by a gravimetric comparison. Wear of the extracted cups was simulated simply by removing the material from new cups. The method specification and preparation of specimen can be found in ISO 14242-2 *(5)*. The samples were cleaned of the PE particles to avoid loosening of the particles during scanning.

A Kern ABS 320-4N analytic balance was used to determine the weight loss. Reproducibility of the balance was 0.2 mg and the linearity was ±0.3 mg. The resolution was ±0.1 mg, which results in the volumetric uncertainty of ±0.106 mm$^3$ for PE analysis. Gravimetric measurements were performed at temperatures between 22 and 23°C at a constant humidity level. Gravimetric measurements were taken five times in order to reduce a random error. The average of the measurements was used for the gravimetric comparison.

The volume of the acetabular cup was multiplied by the density of UHMWPE (0.940 g/cm$^3$; McKellop, et al. *(25)*). The validation samples consisted of three noncemented new acetabular cups with a size of 50/28.

Wear was carried out on a hip pendulum composed of two main parts: a base frame with an acetabular cup and a pendulum with a femoral head. The pendulum was allowed to oscillate freely in the flexion–extension plane. The simulator setup is described in detail elsewhere (Vrbka, et al. *(26)*). The parameter of weight loss was defined as the decisive parameter for validation. The articulating surface of the metal (CoCrMo) femoral head was scratched to increase the material loss (Fig. 8). One test of volumetric wear lasted 1.5 h with a frequency of approximately 0.48 Hz. The test was performed without lubrication. Weights on pendulum arms ensured a total load of 2,080 N. The weight loss of the cups was measured in six cycles. The average weight loss after the sixth cycle was 0.075 g (80 mm$^3$). This material loss simulates the wear rate as discussed in previous research (Dumbleton, et al. *(27)*).

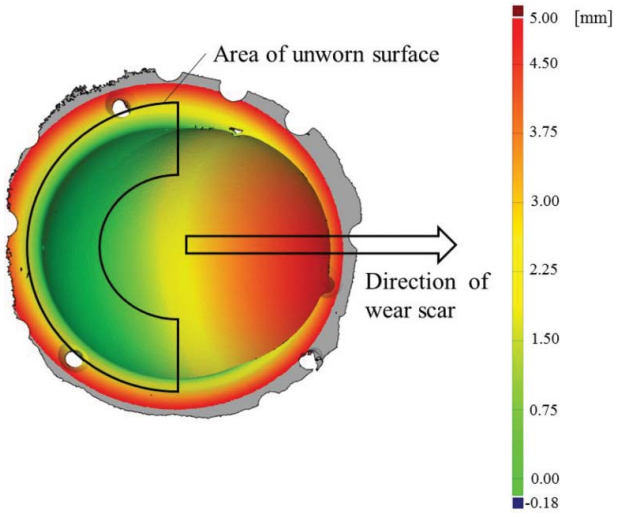


**Figure 4.** Definition of wear scar direction and coordinate system.

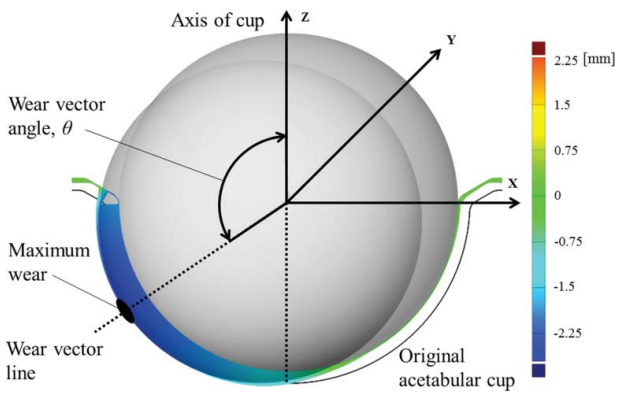


**Figure 5.** Determination of wear vector.

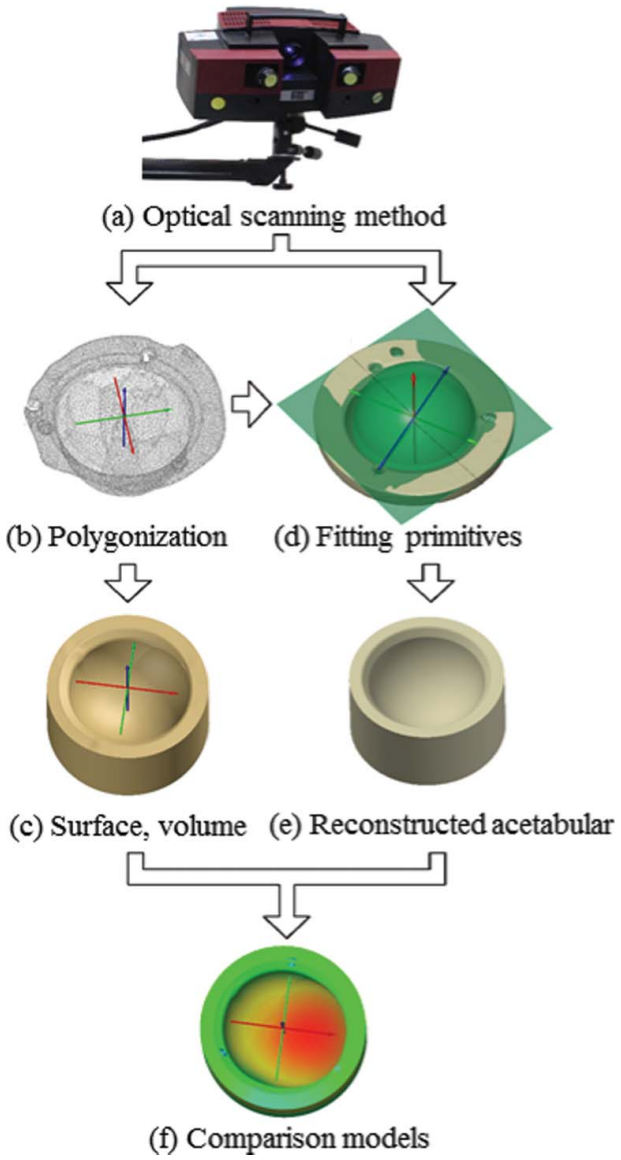


**Figure 6.** Process of evaluation of volumetric wear.

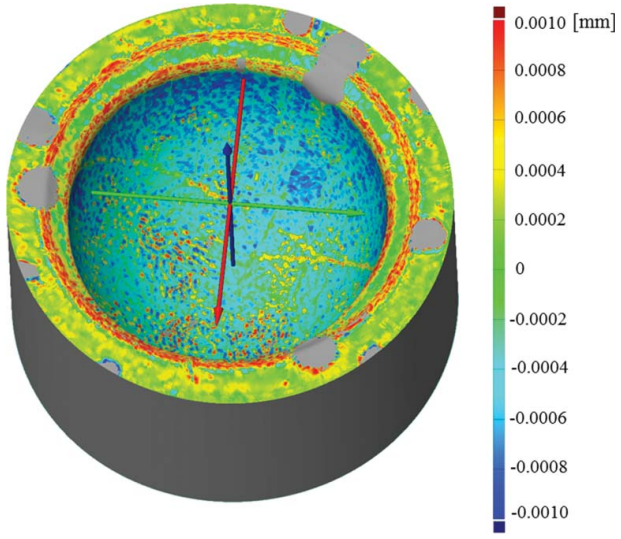


**Figure 7.** Comparison of 3D scan and reconstructed geometry.

**Figure 8.** Validation test by hip pendulum.

The sample was weighed before and after testing. In order to mount the acetabular cup on the hip pendulum, it was necessary to fix the outer rim into the epoxy resin mixture. All tests were performed with this fixation; each cup was thoroughly cleaned before weighing and scanning.

## Results

### *Validation of 3D scanning method by gravimetric method*

The material loss of the cups was measured in six cycles using both the gravimetric and 3D optical methods. Each cycle lasted 15 min and the process was replicated on three cups. Validation results are shown in Figs. 9a–9c. As can be seen, the mean difference between the reference gravimetric method and the optical scanning method was

- −0.0040 g (range −0.0352 to 0.0089 g) for cup 1 (Fig. 9a).
- −0.0021 g (range −0.0159 to 0.0051 g) for cup 2 (Fig. 9b).
- −0.0029 g (range −0.0286 to 0.0067 g) for cup 3 (Fig. 9c).

A significant difference in volumetric wear values measured with the gravimetric method and optical scanning method was present after the first 15-min cycle. This difference may have occurred due to the plastic deformation process. Polygonal data for each measurement were created on average from 191,500 points. This number of points ensures a high quality of surface transformation with deviations less than 0.002 mm as shown in Fig. 7. A volume calculation based on surface data was carried out using the CAD system calculation algorithm. The calculation was replicated using three independent software systems. The difference was less than 0.1 $mm^3$; hence, the deviation of the calculation algorithm is considered negligible.

In order to demonstrate the time efficiency of the method, the duration of each step in the measurement process was recorded. Results are shown in Table 4.

### *Analysis of extracted acetabular cups*

This study analyzed 13 extracted acetabular cups using the optical scanning method based on the principle of fringe

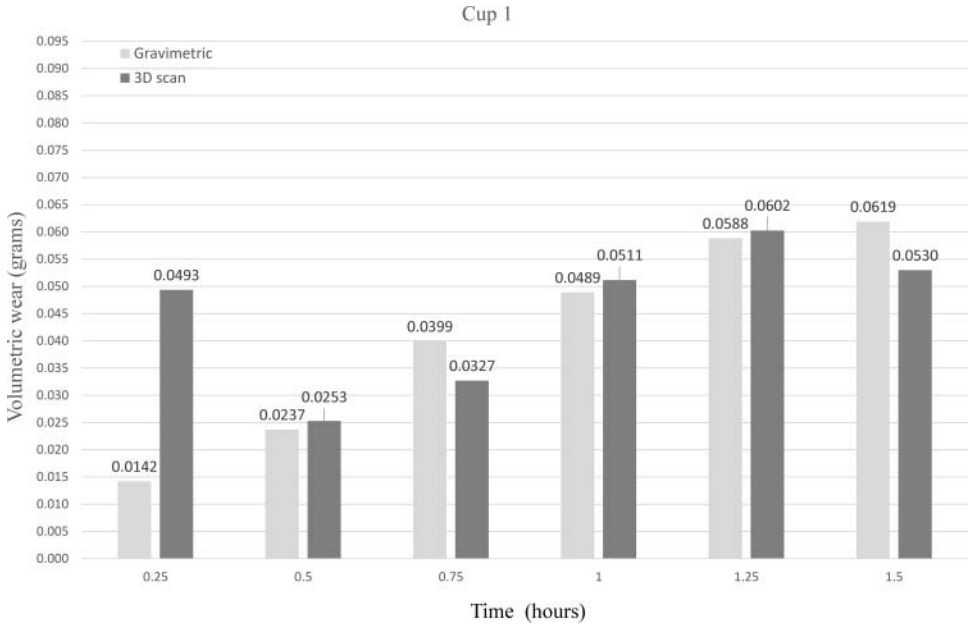


**Figure 9a.** Comparison of validation test results of 3D scan and gravimetric method—Cup 1.

projection and triangulation. The cups were scanned using the ATOS III Triple scan to create digital representations of articulating surfaces of cups. Results of measurements and the analysis of 13 extracted UHMWPE bearing cups are shown in Table 5.

The nominal inner diameter of the extracted acetabular cups was 28 mm. The outer diameter varied; however, this had no influence on the results. Acetabular cups exhibited a mean volumetric wear of 395.53 $mm^3$ (range = 51.80–1,119.70 $mm^3$). The mean wear rate was 44.37 $mm^3$/year (range = 9.98–125.85 $mm^3$, SD = 32.45 $mm^3$). Each measurement was replicated twice in order to eliminate scanning errors. Small differences between the measurements had no impact on quantification of volumetric wear. This can be supported by the repeatability analysis of measurement. The results were supported by a study of survival of replacements produced by Bicon-plus where the mean linear wear of the Bicon-plus PE was 1.8 mm, which corresponds to 0.12 mm/year (Ottink, et al. *(28)*). Another study validates the results of the scanning method with a widely used radiographic method where the volumetric wear of the failed replacement ranged from 730 to 813 $mm^3$ (Ilchmann, et al. *(29)*).

A new acetabular cup produced by the same producer as the extracted cups (Endoplus GmbH) was used as a reference sample for repeatability of the optical scanning method. Results of the repeatability test are shown in the graph below (Fig. 10). Repeatability was evaluated on the basis of the software-determined value of the inner diameter using the best-fit function.

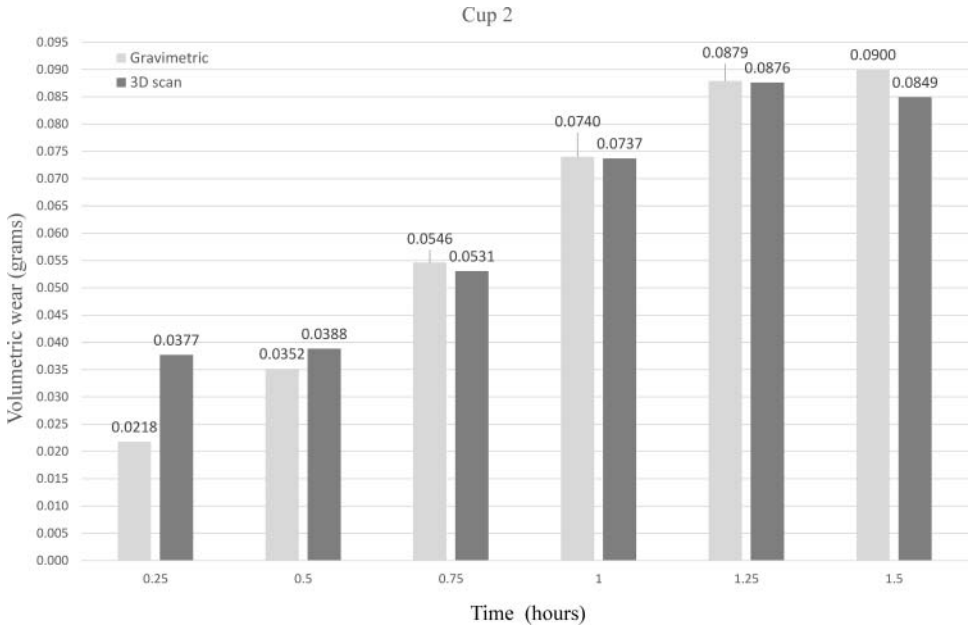


**Figure 9b.** Comparison of validation test results of 3D scan and gravimetric method—Cup 2.

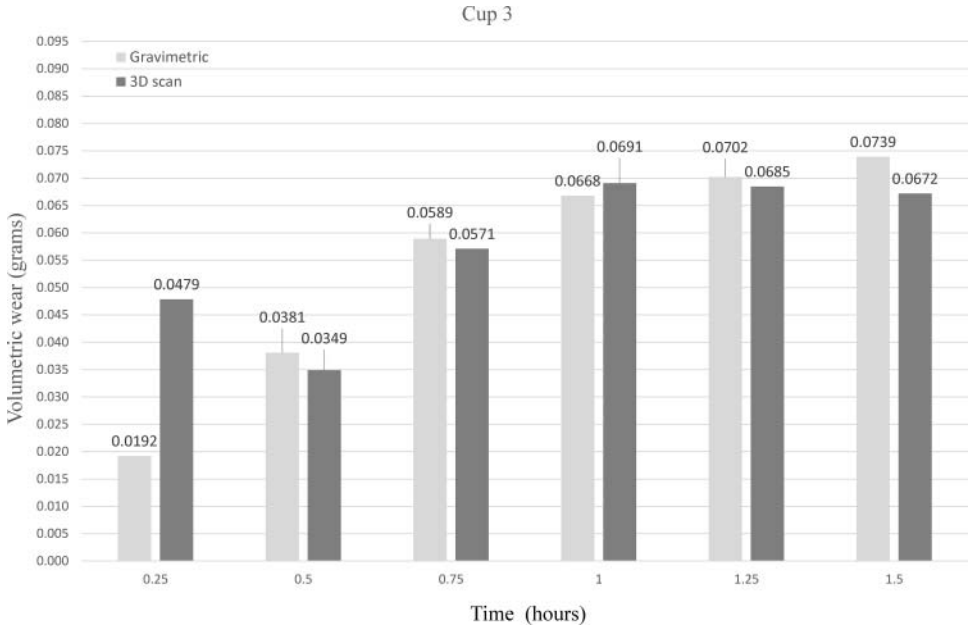


**Figure 9c.** Comparison of validation test results of 3D scan and gravimetric method—Cup 3.

The method was set to the Gaussian statistic method using point filtration three sigma. Measurements were replicated 10 times. Results of measurement were obtained only from the articulating surface; the rim and the outer diameter were not taken into account when determining the volumetric wear. Roughness and roundness of the measured object were neglected. The mean variation of the inner diameter was 0.005 mm (range = 28.624–28.643 mm, SD = 0.005 mm).

## Discussion

The results show that the 3D optical method is suitable for measuring the THR wear of PE acetabular cups and thus it represents an effective alternative to the CMM method, which has, in some cases, reached the limits of its use.

One of the major limitations of the CMM method is a limited number of measured points collected for designing the geometry. Collecting a larger number of surface points using the CMM method is relatively time consuming. However, larger numbers of collected points are crucial for credible reconstruction of the unworn geometry and hence for a more precise analysis of wear. Previous studies showed that the mesh definition and performance of the meshing algorithms can significantly influence the obtained results (Bills, et al. *(6)*; Lord, et al. *(12)*; Carmignato, et al. *(30)*).

This limitation of the CMM method can be solved by the optical scanning method, which allows for collecting a larger number of points in a shorter time. Approximately 191,500 points collected on a single 28-mm acetabular cup can help to create a better surface visualisation. The resulting close point spacing solves the problem of curvature of the elements (Lu and McKellop *(31)*) and the problems related to the latitudinal and longitudinal mesh pattern (Bills, et al. *(6)*). Moreover, the ability to produce fully three-dimensional wear contours allows us to locate the wear scar with high reliability. The direction of the wear scar helps to define the unworn area of the acetabular cup. A right selection of points in the unworn area can then have a significant influence on the obtained result.

It is therefore important to carefully select the measured points of the unworn area to create the original geometry and to define the diameter. One of the options is to use GOM Inspect software. This approach was used in this study, taking advantage of compatibility of the results with the CAD software for further analysis. Another option is to use a fitting histogram for a precise selection of the unworn area points (Uddin *(24)*).

**Table 4.** Time efficiency of scanning method.

| Operation | Approximate time (min) |
|---|---|
| Cleaning of acetabular cup | 10 |
| Application of titanium coating | 15 |
| Placement of a reference points | 10 |
| Scanning process | 12 |
| Polygonization | 5 |
| Repair of geometry | 10 (depends on rate of damage) |
| Transformation on surface | 20 |
| Transformation on volume | 8 |
| Total | 90 |

**Table 5.** Quantification of volumetric wear explanted acetabular cup.

| Patient | Duration (months) | Size of implants | Type of implant | Material loss ($mm^3$) | Material loss per year ($mm^3$) |
|---|---|---|---|---|---|
| 1 | 145 | 4/28 | PE insert standard | 1,119.7 | 92.66 |
| 2 | 126 | 5/28 | PE insert standard | 528.97 | 50.38 |
| 3 | 120 | 4/28 | PE insert antiluxation | 99.81 | 9.98 |
| 4 | 131.5 | 4/28 | PE insert standard | 752.01 | 68.63 |
| 5 | 75 | 6/28 | PE insert standard | 170.98 | 27.36 |
| 6 | 48.5 | 4/28 | PE insert standard | 162.63 | 40.24 |
| 7 | 89.5 | 5/28 | PE insert standard | 299.66 | 40.18 |
| 8 | 92.2 | 4/28 | PE insert antiluxation | 966.92 | 125.84 |
| 9 | 164 | 3/28 | PE insert standard | 584.86 | 42.80 |
| 10 | 536 | 5/28 | PE insert antiluxation | 69.46 | 15.55 |
| 11 | 61.9 | 4/28 | PE insert antiluxation | 152.98 | 29.66 |
| 12 | 43 | 7/28 | PE insert standard | 51.80 | 14.46 |
| 13 | 114.6 | 4/28 | PE insert standard | 182.05 | 19.06 |

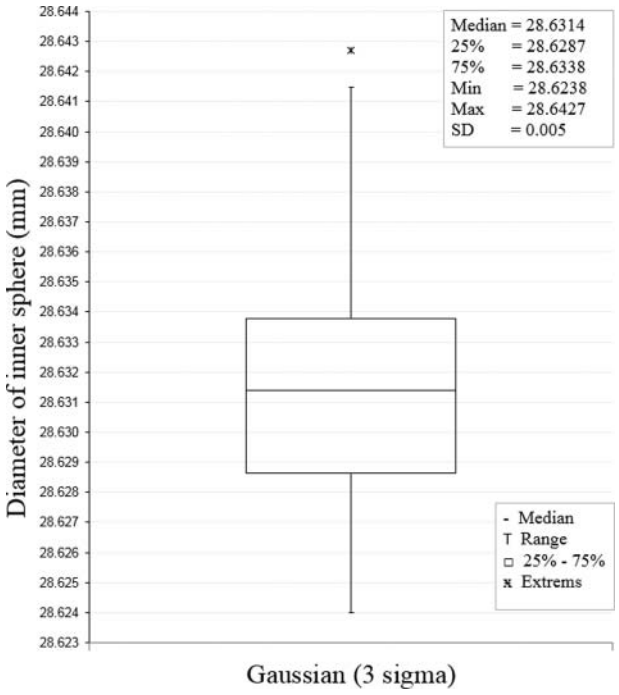


**Figure 10.** Repeatability of 3D scanning measurement.

Another advantage of the optical 3D method is the ability to define the wear vector on the basis of decentration of the worn region position against the original, software-generated geometry (Fig. 5). Parameters of the resulting wear vector can be then compared with the results obtained by medical methods (Dai, et al. *(32)*).

Data collected through the optical scanning method can be also suitable as input parameters for finite element prediction models (Uddin and Zhang *(33)*).

Despite the clear advantages of the optical scanning method, this method poses some challenges and limitations. The main limitation is the precision of the optical 3D scanner, which was established by repeatability of the measurement and parameters of the device. The optical scanning precision as established for the purposes of this study did not reach the levels of accuracy of the CMM method. The maximum accuracy of CMM is approximately $\pm 1$ $\mu$m. An evaluation of measurement method uncertainty, following ISO/IEC98-3 *(34)*, is fundamental for both establishing a metrological traceability and allowing a proper comparison to the reference gravimetric method. The CMM method finds its application for the analysis of small amounts of material loss. Therefore, it is often used for metal femoral heads, which have a wear rate of approximately 1–40 mm$^3$ (Bills, et al. *(6)*; Lu and McKellop *(31)*). The method of measurement is defined by standard ISO 14242-2 *(5)*.

The lower precision of the optical scanning method makes the method inadequate for the analysis of hard components. On the other hand, the accuracy of the optical scanning method is fully acceptable when it comes to the analysis of PE components.

When evaluating the quantitative wear of PE acetabular cups by volume loss, it is also necessary to consider the cold flow phenomenon. This process takes place in the first few months of implant use and results in plastic deformation of PE cup without generation of wear debris (McKellop *(35)*). This phenomenon and effect of radial clearance of hard prostheses can be analyzed and specified by the finite element method (Shankar and Nithyaprakash *(36)*).

The analysis of PE components using the optical scanning method poses the problem of the correct selection of the unworn area of the components, which is important for further reconstruction of the original geometry as stated above. The optical scanning method takes into account neither the problem of the surface roughness nor the problem of nonsphericity of the cups. This issue is particularly evident in the initial phases after implanting the acetabulum when the material loss is relatively low as simulated during the first cycle of our validation, where there was a significant difference in volumetric wear values measured with the gravimetric method and optical scanning method, probably due to the plastic deformation process.

Because there is a wide selection of THRs on the market, some cups are nonspherical in their original geometry as produced by the manufacturers; other cups are originally spherical but can be deformed later. Nonsphericity of the cups is one of the limitations of the presented method and opens up the possibilities for further research aimed at developing an evaluation algorithm to correct the manufacturing tolerance and the nonspherical shape of the cup.

Despite these shortcomings, the 3D optical method is a fast and effective measurement method that simplifies further data processing. It is particularly suitable for the analysis of PE acetabular cups where the volumetric wear is more significant than in the case of metal and ceramic bearing components.

## Conclusion

This article presents a new method of determining volumetric wear using an optical 3D scanner. This method was demonstrated on 13 extracted UHMWPE acetabular cups with various ranges of wear.

The study consists of three parts: (1) description of the optical method used for volumetric wear analysis, (2) validation of the methodology, and (3) application of methodology on the extracted acetabular cups.

1. The optical 3D scanner was used to investigate the volume loss of an acetabular cup. This method is less time consuming than the conventionally used CMM method. Another advantage of the method is the ability to develop a complex geometry built on a large number of points. This approach enables us to reconstruct the most accurate original geometry. A comparison of the extracted cup scans with models of their original geometry reconstructed on the basis of these scans can determine the volumetric wear for PE acetabular cups with satisfying results. The obtained data can be further processed by CAD software.
2. The optical scanning method was validated with the gravimetric method as defined by the standard ISO 14242-2 *(5)*. The mean difference between the methods in quantifying the volume for three cups was −0.0040, −0.0021, and −0.0029 g. Repeatability of the scanning method was 0.005 mm on the evaluated diameter.

3. This method was demonstrated on a series of 13 extracted UHMWPE acetabular cups with known clinical history. Here, all components showed volumetric wear that exceeds the uncertainty of measurement. This method allows for an efficient analysis of acetabular cups.

Basically, there are contact and noncontact methods of volumetric wear measurement. Selection of the most suitable wear measurement method usually depends on various characteristics of the measured samples. This article introduces a new optical scanning method using the ATOS Triple Scan and evaluates its advantages and disadvantages in the context of the conventional CMM method.

Previous research shows that CMM enables more accurate measurements suitable for metal and ceramic components. This article suggests that the scanning method enables more efficient data collection and a more variable geometry processing, which is particularly useful for PE extracted acetabular cups.

## Acknowledgements

The authors thank A. Přikryl for optical scanning of acetabular cups and V. Trulíková for help with editing the article.

## Funding

This research was carried out under the project NETME CENTRE PLUS (LO1202) with financial support from the Ministry of Education, Youth and Sports under the National Sustainability Programme I. This research was also supported by the project "The Influence of Joint Fluid Composition on Formation of Lubricating Film in THA" (NT/14267-3/2013) financed by the Internal Grant Agency of the Ministry of Health of the Czech Republic.

## References

(1) Kurtz, S., Ong, K., Lau, E., Mowat, F., and Halpern, M. (2007), "Projections of Primary and Revision Hip and Knee Arthroplasty in the United States from 2005 to 2030," *Journal of Bone and Joint Surgery*, **89**(4), pp 780–785.

(2) Gallo, J., Goodman, S. B., Konttinen, Y. T., and Raska, M. (2013), "Particle Disease: Biologic Mechanisms of Periprosthetic Osteolysis in Total Hip Arthroplasty," *Innate Immunity*, **19**(2), pp 213–224.

(3) Patel, A., Pavlou, G., Mujica-Mota, R. E., and Toms, A. D. (2015), "The Epidemiology of Revision Total Knee and Hip Arthroplasty in England and Wales: A Comparative Analysis with Projections for the United States. A Study Using the National Joint Registry Dataset," *Bone & Joint*, **97**(8), pp 1076–1081.

(4) Affatato, S., Zavalloni, M., Taddei, P., Di Foggia, M., Fagnano, C., and Viceconti, M. (2008), "Comparative Study on the Wear Behaviour of Different Conventional and Cross-Linked Polyethylenes for Total Hip Replacement," *Tribology International*, **41**(8), pp 813–822.

(5) International Organization for Standardization (ISO) 14242-2. (2000), "Implants for Surgery—Wear of Total Hip-Joint Prostheses," Geneva, Switzerland.

(6) Bills, P. J., Racasan, R., Underwood, R. J., Cann, P., Skinner, J., Hart, A. J., Jiang, X., and Blunt, L. (2012), "Volumetric Wear Assessment of Retrieved Metal-on-Metal Hip Prostheses and the Impact of Measurement Uncertainty," *Wear*, **274–275**, pp 212–219.

(7) Bills, P., Blunt, L., and Jiang, X. (2007), "Development of a Technique for Accurately Determining Clinical Wear in Explanted Total Hip Replacements," *Wear*, **263**(7–12), pp 1133–1137.

(8) Martell, J. M., Leopold, S. S., and Liu, X. L. (2000), "The Effect of Joint Loading on Acetabular Wear Measurement in Total Hip Arthroplasty," *Journal of Arthroplasty*, **15**(4), pp 512–518.

(9) Kothari, M., Bartel, D. L., and Booker, J. F. (1996), "Surface Geometry of Retrieved McKee-Farrar Total Hip Replacements," *Clinical Orthopaedics and Related Research*, **329**, pp S141–S147.

(10) International Organization for Standardization (ISO) 10360-2. (2009), "Geometrical Product Specifications (GPS)—Acceptance and Reverification Tests for Coordinate Measuring Machines (CMM)," Geneva, Switzerland.

(11) Becker, A. and Dirix, Y. (2009), "Wear Measurements on Retrieved Metal-on-Metal Bearings: A High Accuracy 3D Measurement Approach," *Proceedings of the 55th Annual Meeting of the Orthopaedic Research Society*, Poster No. 2270, Smith & Nephew Orthopaedics AG: Aarau, Switzerland.

(12) Lord, J. K., Langton, D. J., Nargol, A. V. F., and Joyce, T. J. (2011), "Volumetric Wear Assessment of Failed Metal-on-Metal Hip Resurfacing Prostheses," *Wear*, **272**(1), pp 79–87.

(13) Rossler, T., Mandat, D., Gallo, J., Hrabovsky, M., Pochmon, M., and Havranek, V. (2009), "Optical 3D Methods for Measurement of Prosthetic Wear of Total Hip Arthroplasty: Principles, Verification and Results," *Optics Express*, **17**(15), pp 12723–12730.

(14) Pochmon, M., Rossler, T., Mandat, D., Gallo, J., and Hrabovsky, M. (2007), "Verification of Abrasion Measurement of Juncture Implants Using Fourier Profilometry, "*15th Czech-Polish-Slovak conference on Wave and Quantum Aspect of Contemporary Optics*, 9780819467485, p. 6609.

(15) Zou, L., Samarawickrama, D. Y. D., Jovanovski, V., and Shelton, J. C. (2001), "Measurements of Sequential Impressions of Acetabula Cups from a Total Hip Joint Replacement Using a Non-Contact Measurement System," *International Journal of Machine Tools and Manufacture*, **41**(13–14), pp 2023–2030.

(16) Yun, H. H., Shon, W. Y., Yoon, J. R., Yang, J.-H., and Lim, D.-S. (2012), "Reliability of a PowerPoint Method for Wear Measurement After Total Hip Arthroplasty: A Retrieval Study Using 3-Dimensional Laser Scanning," *The Journal of Arthroplasty*, **27**(8), pp 1530–1537.

(17) Dougherty, P. S. M., Srivastava, G., Onler, R., Ozdoganlar, O. B., and Higgs, C. F., III. (2015), "Lubrication Enhancement for UHMWPE Sliding Contacts through Surface Texturing," *Tribology Transactions*, **58**(1), pp 79–86.

(18) Choudhury, D., Ghosh, S., Ali, F., Vrbka, M., Hartl, M., and Krupka, I. (2015), "The Influence of Surface Modification on Friction and Lubrication Mechanism under a Bovine Serum Lubricated Condition," *Tribology Transactions*, **59**, pp 1–28.

(19) Milosev, I., Kovac, S., Trebse, R., Levasic, V., and Pisot, V. (2012), "Comparison of Ten-Year Survivorship of Hip Prostheses with Use of Conventional Polyethylene, Metal-on-Metal, or Ceramic-on-Ceramic Bearings," *Journal of Bone and Joint Surgery*, **94**(19), pp 1756–1763.

(20) Williams, P. A., Yamamoto, K., Masaoka, T., Oonishi, H., and Clarke, I. C. (2007), "Highly Crosslinked Polyethylenes in Hip Replacements: Improved Wear Performance or Paradox?," *Tribology Transactions*, **50**(2), pp 277–290.

(21) GOM mbH. Available at: http://www.gom.com/metrology-systems/3d-scanner.html. (accessed October 16, 2015).

(22) VDI/VDE2634-3. (2008), "Optical 3D-Measuring Systems-Multiple view systems based on area scanning," Fachbereich Fertigungsmesstechnik: Dusseldorf, Germany.

(23) Palousek, D., Omasta, M., Koutny, D., Bednar, J., Koutecky, T., and Dokoupil, F. (2015), "Effect of Matte Coating on 3D Optical Measurement Accuracy," *Optical Materials*, **40**, pp 1–9.

(24) Uddin, M. S. (2014), "Wear Measurement and Assessment of Explanted Cross-Linked PE Acetabular Cups Using a CMM," *Tribology Transactions*, **57**(5), pp 767–777.

(25) McKellop, H. A., Campbell, P., Park, S. H., Schmalzried, T. P., Grigoris, P., Amstutz, H. C., and Sarmiento, A. (1995), "The Origin of Submicron Polyethylene Wear Debris in Total Hip-Arthroplasty," *Clinical Orthopaedics and Related Research*, **311**, pp 3–20.

(26) Vrbka, M., Nečas, D., Hartl, M., Křupka, I., Urban, F., and Gallo, J. (2015), "Visualization of Lubricating Films between Artificial Head and Cup with Respect to Real Geometry," *Biotribology*, **1–2**, pp 61–65.

(27) Dumbleton, J. H., Manley, M. T., and Edidin, A. A. (2002), "A Literature Review of the Association between Wear Rate and Osteolysis in Total Hip Arthroplasty," *Journal of Arthroplasty*, **17**(5), pp 649–661.

(28) Ottink, K., Barnaart, L., Westerbeek, R., van Kampen, K., Bulstra, S., and van Jonbergen, H. P. (2015), "Survival, Clinical and Radiological Outcome of the Zweymuller SL/Bicon-Plus Total Hip Arthroplasty: A 15-Year Follow-Up Study," *Hip International*, **25**(3), pp 204–208.

(29) Ilchmann, T., Lüem, M., Pannhorst, S., and Clauss, M. (2012), "Acetabular Polyethylene Wear Volume after Hip Replacement: Reliability of Volume Calculations from Plain Radiographs," *Wear*, **282–283**, pp 69–75.

(30) Carmignato, S., Spinelli, M., Affatato, S., and Savio, E. (2011), "Uncertainty Evaluation of Volumetric Wear Assessment from Coordinate Measurements of Ceramic Hip Joint Prostheses," *Wear*, **270** (9–10), pp 584–590.

(31) Lu, Z. and McKellop, H. A. (2014), "Accuracy of Methods for Calculating Volumetric Wear from Coordinate Measuring Machine Data of Retrieved Metal-on-Metal Hip Joint Implants," *Proceedings of the Institution of Mechanical Engineers - Part H: Journal of Engineering in Medicine*, **228**(3), pp 237–249.

(32) Dai, X. S., Omori, H., Okumura, Y., Ando, M., Oki, H., Hashimoto, N., and Baba, H. (2000), "Serial Measurement of Polyethylene Wear of Well-Fixed Cementless Metal-Backed Acetabular Component in Total Hip Arthroplasty: An over 10 Year Follow-Up Study," *Artificial Organs*, **24**(9), pp 746–751.

(33) Uddin, M. S. and Zhang, L. C. (2013), "Predicting the Wear of Hard-on-Hard Hip Joint Prostheses," *Wear*, **301**(1–2), pp 192–200.

(34) International Organization for Standardization (ISO)/IEC98-3. (2008), "Uncertainty of Measurement," Geneva, Switzerland.

(35) McKellop, H. A. (2007), "The Lexicon of Polyethylene Wear in Artificial Joints," *Biomaterials*, **28**(34), pp 5049–5057.

(36) Shankar, S. and Nithyaprakash, R. (2014), "Effect of Radial Clearance on Wear and Contact Pressure of Hard-on-Hard Hip Prostheses Using Finite Element Concepts," *Tribology Transactions*, **57**(5), pp 814–820.

Journal of the Mechanical Behavior of Biomedical Materials 79 (2018) 314–323

Contents lists available at ScienceDirect

Journal of the Mechanical Behavior of Biomedical Materials

journal homepage: www.elsevier.com/locate/jmbbm

# Mechanical wear and oxidative degradation analysis of retrieved ultra high molecular weight polyethylene acetabular cups

Dipankar Choudhury[a,b], Matúš Ranuša[c,*], Robert A. Fleming[a], Martin Vrbka[d], Ivan Křupka[d], Matthew G. Teeter[e], Josh Goss[a,b], Min Zou[a,b,**]

[a] Department of Mechanical Engineering, University of Arkansas, Fayetteville, AR, USA 72701
[b] Center for Advanced Surface Engineering, University of Arkansas, Fayetteville, AR, USA 72701
[c] Faculty of Mechanical Engineering, Brno University of Technology, Technická 2896/2, 616 69 Brno, Czech Republic
[d] Central European Institute of Technology (CEITEC), Brno University of Technology, Brno, Czech Republic
[e] Medical Biophysics and Surgery, Schulich School of Medicine & Dentistry, Western University, 339 Windermere Road, London, Ontario, Canada, N6A 5A5

ARTICLE INFO

*Keywords:*
Retrieved prosthesis
Wear
Oxidative degradation
Plasticity index
Micro-CT
Raman spectroscopy
Nanoindentation

ABSTRACT

The number of revision joint replacements has been increasing substantially over the last few years. Understanding their failure mechanism is extremely important for improving the design and material selection of current implants. This study includes ten retrieved and four new mildly cross-linked ultra-high molecular weight polyethylene (UHMWPE) acetabular liners. Among them, most of the prostheses (n = 5) were reported to be revised and replaced due to aseptic loosening, followed by painful joint (n = 2), dislocation (n = 1), intra articular ossification (n = 1), combination of wear (liner) and osteolysis (stem) (n = 1). Surface deviations (wear, material inflation and roughness), oxidative degradation and change of material properties were measured using micro-computed tomography (micro-CT) scan, 3D laser scanning microscopy, raman spectroscopy and nanoindentation, respectively. Prostheses having eccentric worn areas had much higher linear wear rates (228.01 ± 35.51 μm/year) compared to that of centrically worn prostheses (96.71 ± 10.83 μm/year). Oxidation index (OI) showed similar trends to the surface penetration depth. Among them, sample 10 exhibited the highest OI across the contact area and the rim of the cup liner. It also had the lowest hardness/elasticity ratio. Overall, wear and creep, oxidative degradation and reduced hardness/elasticity ratio all contributed to the premature failure of the UHMWPE acetabular cup liners.

## 1. Introduction

Ultra-high molecular weight polyethylene (UHMWPE) is a common bearing material in the acetabular components used in total hip arthroplasty (2017; Steinberg, 2014). It contributes to the good performance features such as absorbing impact loadings and giving low frictional sliding (Ge et al., 2009; Kurtz, 2009). Typically, a UHWMPE liner is placed in a titanium alloy shell to form the acetabular cup component of the implant. The stiffness of the acetabular cup component, when measured by rim compression, is less than when a metal or ceramic cup liner is used. It has been suggested acetabular cup components with lower stiffness provide a more uniform load distribution on the pelvis compared with that of stiffer components and this is a possible further advantage of using UHMWPE (Small et al., 2013).

Cup liners made from UHMWPE can suffer from higher wear rates than when other liner materials are used (such as metals or ceramics). These wear rates are still low enough to avoid immediate problems after hip replacement surgery. However, as found in one wear simulator study (Goldsmith et al., 2000), they can be as much as 100 times higher than that of metal-on-metal hip implant systems. Over time, these UHMWPE wear rates change the overall conformity of the articular joint and affect the contact mechanics and wear mechanisms (Dowson et al., 2004; Goldsmith et al., 2000). Also, more significantly, this wear rate results in an accumulation of wear particles into the periprosthetic tissues. The contacting surface of the UHMWPE components also suffers from creep. Creep is a permanent deformation, which occurs due to rearrangement of the positions of the polyethylene molecules and could result in an increasing hardness, stiffening and embrittlement.

To improve the wear resistance of virgin UHWMPE, cross-linking of its microstructure can be performed. In the retrieved and new cup liners of the present study, this was done by a γ-irradiation process in a nitrogen atmosphere (25–45 kGy/$N_2$ sterilized). The nitrogen atmosphere

* Corresponding author.
** Corresponding author at: Department of Mechanical Engineering, University of Arkansas, Fayetteville, AR, USA 72701.
*E-mail addresses:* Matus.Ranusa@vut.cz (M. Ranuša), mzou@uark.edu (M. Zou).

https://doi.org/10.1016/j.jmbbm.2018.01.003
Received 1 December 2017; Accepted 3 January 2018
Available online 06 January 2018
1751-6161/ © 2018 Elsevier Ltd. All rights reserved.

prevents oxygen from combining with the free radicals at the ends of the chains that were cut by the irradiation process, and thus cross-linking occurs without oxidation. However, the oxidative process can initiate after the irradiation process; and in the presence of the lipids in the body fluid, the oxidation accelerates. It is to be noted that, the extent of cross-linking is considered to be mild when 25–45 kGy irradiations are applied.

Current literature (Peers et al., 2015; Xiong and Xiong, 2012) reports that using highly cross-linked polyethylene (HXLPE, 50–100 kGy γ-irradiated with various strategies for reducing free radicals) significantly reduces wear (Kurtz et al., 2010). Bragdon et al. (2007) reported that the use of "HXLPE substantially improved the prognosis of patients after THA (total hip arthroplasty) up to 13 years as judged by clinical scores, incidence of osteolysis, and polyethylene wear measurements". Furthermore, a recent study of total knee arthroplasty by de Steiger et al. (Steinberg, 2014) found a lower revision rate when cross-linked polyethylene ($\geq$ 50 kGy with various strategies to reduce free radicals) was used compared with the mildly cross-linked polyethylene ($\leq$ 50 kGy versions identified above), but noted that this was only for a smaller subset of implant designs and patient groups. In addition, HXLPE cup liners that were infused with vitamin E demonstrated further improvements against oxidation (Puppulin et al., 2016). However, very long term clinical data for HXLPE are still not available. Moreover, the older versions of UHMWPE (25 − 45 kGy/$N_2$ sterilized) may still find some applications in knee replacements (Sakellariou et al., 2013) and a large number of patients still have older version of polyethylene in acetabular and tibia liners (Fulin et al., 2016; Pokorny et al., 2012). Hence, the wear and degradation of the older version of polyethylene remains a topic of interest.

The wear and surface degradation of acetabulum component of an artificial hip joint have very complex mechanisms, where mechanical wear, creep and oxidative degradation could happen simultaneously and also accelerate each other. A comprehensive mapping (locations and level) of wear, creep and oxidation of the retrieved prosthesis might provide insight into the mechanisms and processes of surface degradation. Besides surface degradation, changing mechanical properties, such as hardness and modulus of elasticity, are key indicators for contact and wear mechanisms. For example, a higher ratio of hardness and modulus of elasticity with lower wear when surface coatings are applied to orthopaedics implants (Ching et al., 2014). For the retrievals of the present study, oxidation causes hardening and embrittlement of UHMWPE and so the, ratio of hardness to modulus of elasticity changes over time. The changed mechanical properties can be precisely measured using nanoindentation (Briscoe et al., 1998; Cakmak et al., 2012).

Radiographic, gravimetric, volumetric and optical techniques are available for mapping mechanical wear and creep. A few examples of the techniques involved are: a) 3D profiler (Govind et al., 2015; Ranusa et al., 2017; Ranuša et al., 2016), b) coordinate measuring machine (CMM) (Spinelli et al., 2009; Uddin et al., 2016) and c) micro–computer topography (micro-CT) (RAD, 2015; Teeter et al., 2011). These techniques can map wear/creep volume and the measurement accuracy is related to the number of detected points. Micro-CT is a non-destructive technique (NDT) that can provide precise and accurate volumetric measurements along with quantifiable three-dimensional surface deviation maps for the entire retrieved prosthesis surface (Teeter et al., 2011).

On the other hand, advanced NDT for measuring oxidation are: scanning electron microscopy (SEM) with Energy Dispersive Spectroscopy (EDS) (Costa et al., 2002; Salahshoor and Guo, 2014), Raman spectroscopy (Puppulin et al., 2016), transmission electron microscopy (TEM) (Hellmann et al., 2015), and Fourier transform infrared spectroscopy (FTIR) (Pezzotti et al., 2007). Raman spectroscopy is a very powerful tool, easy to operate and affordable compared to EDS and TEM. Moreover, Raman can also assess the complex microstructural changes at the microscopic scale giving the fraction of crystalline phase in the polyethylene (Pezzotti et al., 2007). This enables Raman spectroscopy to detect chemical distortion caused by creep deformation and oxidation, which cannot be achieved by FTIR.

Pezzotti et al. (2007, 2011) developed and validated a protocol for separately measuring the contributions to the dimensional change in acetabular cups arising from creep and wear without any destructive sample manipulation. They considered the integrating peaks around $I_{1293}$, $I_{1305}$ and $I_{1414}$ $cm^{-1}$ as the main Raman spectra for measuring oxidation index and orthorhombic crystalline phase fraction. Puppulin et al. (2016) conducted a similar study which included various cross-linked UHMWPE cups. The study mapped oxidation indices and crystalline fraction in the depth direction and along the material subsurface. The results revealed the effects of γ-ray irradiation and vitamin E blended on the oxidation indices of HXLPE cups for total joint replacement.

One of the key limitations of these published NDT studies on wear and oxidation analysis was their reliance on a single measurement technique and the lack of surface mapping. For example, almost all of the wear studies only considered mechanical wear rate and the remaining studies considered only Raman spectra based studies. As noted by Kumakura et al. (2009) and Pezzotti et al., (2017), orthopaedics implants undergo both mechanical and chemical wear, and it is essential to conduct a combined study to map wear and creep followed by an oxidation and crystalline study. Puppulin et al. (2016) and Pezzotti et al. (2007) predicted an ideal wear-zone and conducted their Raman analyses, but Jasty et al. (1997) showed that the wear at the articulating surface was characterized by a highly worn polished area superiorly and a less worn area inferiorly, separated by a transition ridge, in all components, depending on the host patient gait patterns, surgical technique and accuracy. Thus, it is important to identify the wear-zone through mapping to accurately measure wear rates and relate them to wear mechanisms.

The main purpose of the present study was to examine the relationships between hip implant failures and features of their retrieved polyethylene cups such as the location of the wear and creep on the cup along with chemical and mechanical changes in material properties. Therefore, we measured surface deviations (material added to or removed from the original surface), roughness, oxidation indices and ratios of hardness to elastic modulus of the retrieved polyethylene liners along with the same measurements of new polyethylene liners to provide a baseline. Following clinical observations, the reasons for retrieval were classified into three subgroups (Table 1): group-1: aseptic loosening, group-2: pain in the joint, and group-3: other (variety of other reasons). The surface deviations were mapped with micro-CT because of its time-efficiency, easy post-processing of the measurement data and precision. Based on the surface deviation map, the targeted areas were identified and Raman analyses were conducted. Finally, nanoindentation was utilized for measuring the hardness and modulus of elasticity of selected samples, which were also used to provide some validation for the crystalline outcomes from the Raman spectra.

## 2. Materials and methods

### 2.1. New and retrieved prostheses

A total of four new and ten retrieved polyethylene cup liners from Bicon-plus acetabular cup components (Plus Endoprothetik AG, Rotkreuz, Switzerland; later Smith and Nephew, USA) were studied. All of the cup liners were made from compression molded GUR 1020 UHMWPE according to International Organization for Standardization (ISO-5834-2) and American Society for Testing and Materials (ASTM-F648). The irradiation dose (applied in a $N_2$ environment) was between 25 and 37 kGy (Milosev et al., 2012). All the cup liners had inner surface radius of 14 mm. The cup components were implanted using cementless fixation.

**Table 1**
Demographic data for the ten retrieved ultra-high molecular weight polyethylene components.

| *Sample No.* | *Gender, age of patient at extraction (years)* | *Weight of patient (kg)* | *Duration in situ (years)* | *Size of the cup (outer/inner diameter – mm)* | *Reason for original surgery* | *Description of revision* |
|---|---|---|---|---|---|---|
| Group - 1: revision mainly due to aseptic loosing and wear | | | | | | |
| 1 | F, 70 | 75 | 7.36 | 40/28 | Primary Arthrosis | Replacement of cup |
| 2 | F, 60 | 70 | 9.71 | 40/28 | Primary Arthrosis | Replacement of THR |
| 3 | M, 60 | 92 | 11.47 | 42/28 | Primary Arthrosis | Replacement of cup |
| 4 | M, 70 | 78 | 10.60 | 36/28 | Primary Arthrosis | Replacement of cup |
| 5 | F, 67 | 80 | 15.24 | 38/28 | Post dysplastic coxarthrosis | Replacement of THR |
| Group - 2: revision mainly due to pain | | | | | | |
| 6 | F, 73 | 85 | 12.32 | 36/28 | Primary Arthrosis | Replacement of liner |
| 7 | F, 63 | 56 | 4.95 | 40/28 | Primary Arthrosis | Replacement of cup |
| Group - 3: Other - sample 8: dislocation; sample 9: Articular ossification; sample 10: combination of wear (liner) and osteolysis (stem) | | | | | | |
| 8 | F, 70 | 80 | 0.10 | 36/28 | Primary Arthrosis | Replacement of head and cup |
| 9 | M, 59 | 105 | 6.72 | 36/28 | Primary Arthrosis | Removal of ossification, replacement of cup |
| 10 | M, 57 | 100 | 16.76 | 42/28 | Primary Arthrosis | Replacement of liner |

### 2.2. Clinical Observations

The retrieved prostheses were obtained at revision surgeries between 2015 and 2016 and their survival time in vivo was on average 9.52 years (range: 0.1–16.76 years), with a standard deviation (SD) of 4.69 years. Reasons for the revision surgeries include aseptic loosening, pain, articular ossification and wear of the cup liner. After the prostheses extraction, all of the UHMWPE cup liners were mechanically cleaned, immersed in a disinfectant for 24 h, and then sterilized routinely for 2 h. All retrieved cups were obtained with a written informed patient consent, and the study was approved by the local Ethics Committee (as a part of the project NT11049-5 Ministry of Health, Czech Republic).

### 2.3. Surface deviation measurement

Each UHMWPE cup liner was individually scanned at 50-μm resolution using a laboratory cone beam micro-CT scanner (Explore Vision 120, GE Healthcare). Each scan took approximately 95 min and included 1200 views in 0.3° increments, with 10 frames per view on average. The X-ray tube voltage was set to 90 kVp with a current of 40 mA (Teeter et al., 2010). Scans were reconstructed at the full 50-μm isotropic resolution. The reconstructed scans of the liners were analysed with 3D micro-CT analysis software (MicroView v2.2, GE Healthcare). A region-growing algorithm was applied to the cup liner area, and the resulting geometry was converted to a temporary region of interest (ROI). Everything outside of the ROI was set to a background value of −1000 Hounsfield units (HU). HU values can provide a calibrated description of a material relative to water (0 HU), with air defined to be −1000 HU (Badea et al., 2008). Isosurface rendering was then performed for a new ROI encompassing the entire scan volume, with a threshold of −664 HU at the highest possible surface quality and no decimation. The resulting 3D volume of each cup liner was saved in a stereolithographic file format (STL).

After the measurement, the data were post-processed using the software GOM Inspect (GOM mbH) (GOB, 2016). For further analysis, only the articulating surface and its close surroundings of the rim were necessary. The backside of liners was neglected because it was only plastically deformed without any substantial material loss. A custom software was first used to appropriately align the geometry of the each acetabular liner to a consistent coordinate system in three directions. The rim of the cup, which showed the best compliance with the original geometry, was used as a base plane. However, for the antiluxation liners, the outer edge was used (Ranuša et al., 2016). Reference holes on the surface of the rim (Fig. 1) were used for positioning of the cups. A new liner was set as reference geometry. This liner was of the same type as all the retrieved liners, with nominal inner surface radius of 14 mm. Any variation in the manufacturing techniques would cause an error in the calculated deviation. Manufacturing variability of the liner geometry was estimated to be ± 0.02 mm (Teeter et al., 2010).

### 2.4. Raman analysis

Confocal Raman microscope (inVia™, Renishaw) was used to characterize the microstructures of the UHMWPE liners in terms of variation in the orthorhombic crystalline phase fraction and oxidation indices. The excitation source has a 785 nm wavelength, yielding a power of approximately 1.5 W, with an exposing time of 30 s and a spot size of ~ 100 μm in diameter. The generated Raman spectra (800–2000 $cm^{-1}$) were processed in the Origin software (2017) and the integrated peaks were measured around 1293, 1305, and 1414 $cm^{-1}$ Raman shift: $I_{1293}$, $I_{1305}$, and $I_{1414}$. It is noted that $I_{1293}$ and $I_{1305}$ of the Raman bands of UHMWPE associated with $–CH_2–$ bond wagging, whereas $I_{1414}$ represents $–CH_2–$ twisting vibrations (Pezzotti et al., 2007). The volume fraction of orthorhombic crystalline phase and the oxidation index were calculated based on the following equations (Kumakura et al., 2009; Pezzotti et al., 2007).

$$\alpha_c = \frac{I_{1414}}{0.14(I_{1293} + I_{1305})} \quad (1)$$

$$OI = \exp\{1.19\, x\, tan\left[14.26\left(\frac{I_{1414}}{I_{1293}+I_{1305}} - 0.26\right)\right] - 0.13\} \quad (2)$$

The Raman investigations were conducted in two different phases. In the first phase, a 5× lens was used due to the curvature (~ 28 mm diameter) of the prosthesis cup liners. A schematic view of such measurement is shown in the Fig. 2. A total of nine (9) points on each liner were measured, as described in the Fig. 2(a). Point-1 is in the center region (C-1), three points are located around the apex of the articulating surface (P-1-1, P-2-1, P-3-1), three points are on the side wall (P-1–2, P-2-2, P-3-2) and the last three points are located in the rim of a cup (P-1–3, P-2–3 and P-3-3).

In the second phase, 1 mm-diameter cylindrical shaped specimens from the wear/creep area (P-3-1) of selected prostheses (new, 1, and 7–10) were prepared using a biopsy punch. The specimens were also suitable to be used for the nanoindentation measurement. The Raman analyses were performed on the specimen using a 20 × lens. The laser power and exposing time were kept same in both phases. At least five readings were carried out for each of the points.

### 2.5. Surface roughness and mechanical property analysis

The average roughness (Ra) and root mean square roughness (Rq)

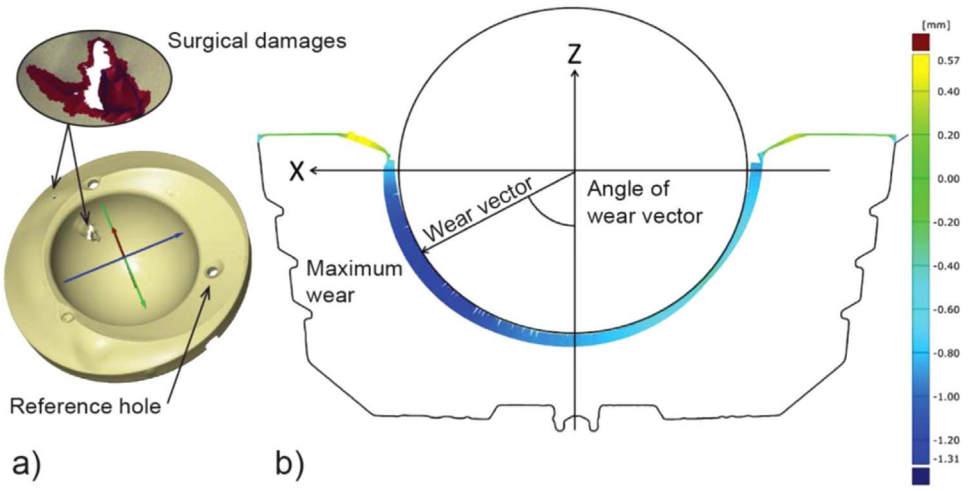


**Fig. 1.** Method of wear measurement: (a) a retrieved cup showing reference hole, and surgical damages and (b) mapping surface deviation using GOM Inspect software.

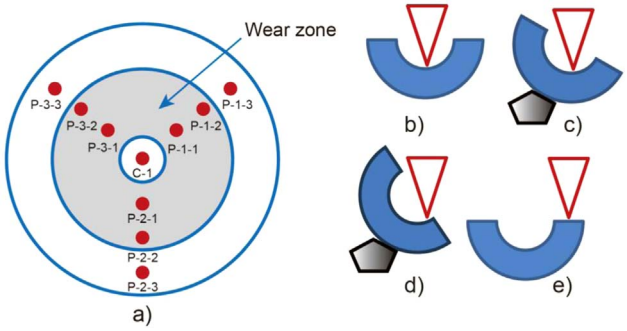


**Fig. 2.** The schematic diagram for confocal Raman (non-destructive) assessments of oxidation index in UHMWPE for phase-1: (a) the locations of measuring spots, (b) at the center point (C-1), (c) at the ideal wear zone (P-1-1), (d) at the side wall (P-1–2), and (e) at the rim of a cup (P-1–3). In the case of (c) and (d), a support block was used to tilt the cup in order to get a perpendicular position of the focused laser.

were measured using a laser scanning confocal microscope (LSCM, VK-X260K, Keyence, USA). Nanoindentation measurements (mechanical properties and surface roughness) were performed on the 1 mm-diameter specimens. Since biopsy punching is a destructive procedure, only a few samples were selected for the nanoindentation: sample 1 from group 1, sample 7 from group 2, samples 8–10 from group 3 (each sample of this group failed due to a different mechanism) and the new sample. The hardness and modulus of elasticity were measured using an instrumented nanoindenter (TriboIndenter, Hysitron Inc. Minneapolis, MN) with a diamond Berkovich tip having a 100 nm tip radius. Normal loads of 500 μN were chosen for the nanoindentation with 5 indentation tests under the same test conditions (Choudhury et al., 2017; Jee and Lee, 2010; Tavares et al., 2003).

## 3. Results

### 3.1. Surface deviation analysis

The mapped surface deviation spectra across the acetabular liners for the group-1 are shown in the Fig. 3. The spectra that have positive values indicates material inflation and negative values indicates penetration (wear/creep) on the retrieved liners. Material inflation is a material gain and sometimes it indicates small precision errors in the micro-CT assessment of surface deviation but it can be legitimate because material can be pushed around on the surface. Interestingly, most of the wear/creep areas were eccentric but a few were centric and this did not seem to be correlated to their demographic data or to clinical observations. However, this type of wear pattern can be caused by lower activity of patient. The direction of eccentric penetration relative to the axis of liner was indicated by the wear vector (Fig. 1b). Within the group 1, samples 1–3 had mostly centric wear/creep areas; on the other hand, samples 4–5 had obviously eccentric wear/creep areas. Importantly, the influence of the eccentric applied loads is enormous (Fig. 3). For example, the sample 1 had a linear penetration rate of −81.47 μm/year with a centric wear/creep area, while the sample 4 had linear penetration rate of −233.08 μm/year with an eccentric wear/creep area, although both of samples were implanted to patients with very similar body weight. The trend was very similar to the samples 2 and 3 with centric wear/creep areas and lower penetration rate compared to the sample 5 with eccentric worn area and significantly higher penetration rate. It is noted that among the centric worn areas, body weight was not found to be a dominating factor — sample 2 (weight of host patient: 70 kg) had higher penetration rate: −92.72 μm/year compare to that of sample 1: −81.47 μm/year (weight of host patient: 75 kg). Samples 2 and 3 have a severe material inflation at the rim areas. These inflations could be result of oxidation and displacement during creeping and/or thermally distortion during high friction (Bergmann et al., 2001; Pezzotti, 2017).

The mapped surface deviation spectra across the cup liners for group 2 and 3 are described in the Figs. 4 and 5, respectively. The primary reason of revision for group 2 was pain in the joint. The x-ray images showed that the sample 6 was stable but the sample 7 was loosened. The penetration spectrum of sample 6 revealed a fairly centric worn area and linear wear rate was −107.16 μm/year. On the other hand, sample 7 had an obviously eccentric worn area, along with a combination of higher penetration rate (−137.43 μm/year) and a significant sign of material inflation (≈ + 50 μm/year) within the contact area. It is noted that the sample 7 failed within 5 years after implantation, although the host patient weighted only 56 kg.

Within group 3, sample 9 which failed due to articular ossification, revealed similar wear features: eccentric worn area (wear rate −119.04 μm/year) and material inflation (≈ + 60 μm/year). Sample 8 failed due to dislocation. Fig. 8(a) shows that its material inflation (+800 μm) was significantly higher than the penetration depth (−230 μm) in the duration of 1.2 months. High amount of distortion (mainly fracture thus positive surface deviation) happened during the dislocation, confirmed by clinical observation. Finally, sample 10, which had the longest durability among the experiment samples, failed due to the wear of the cup liner resulting in osteolysis around the stem. It revealed an eccentric wear track and a penetration rate (−260.71 μm/year). Few of the retrieved cups such as samples 2, 3 and 6 had a substantial amount of distortion at the rim of cup.

Surface roughness of the experimental samples is described in Table 2, which provides some interesting indications. For example, the

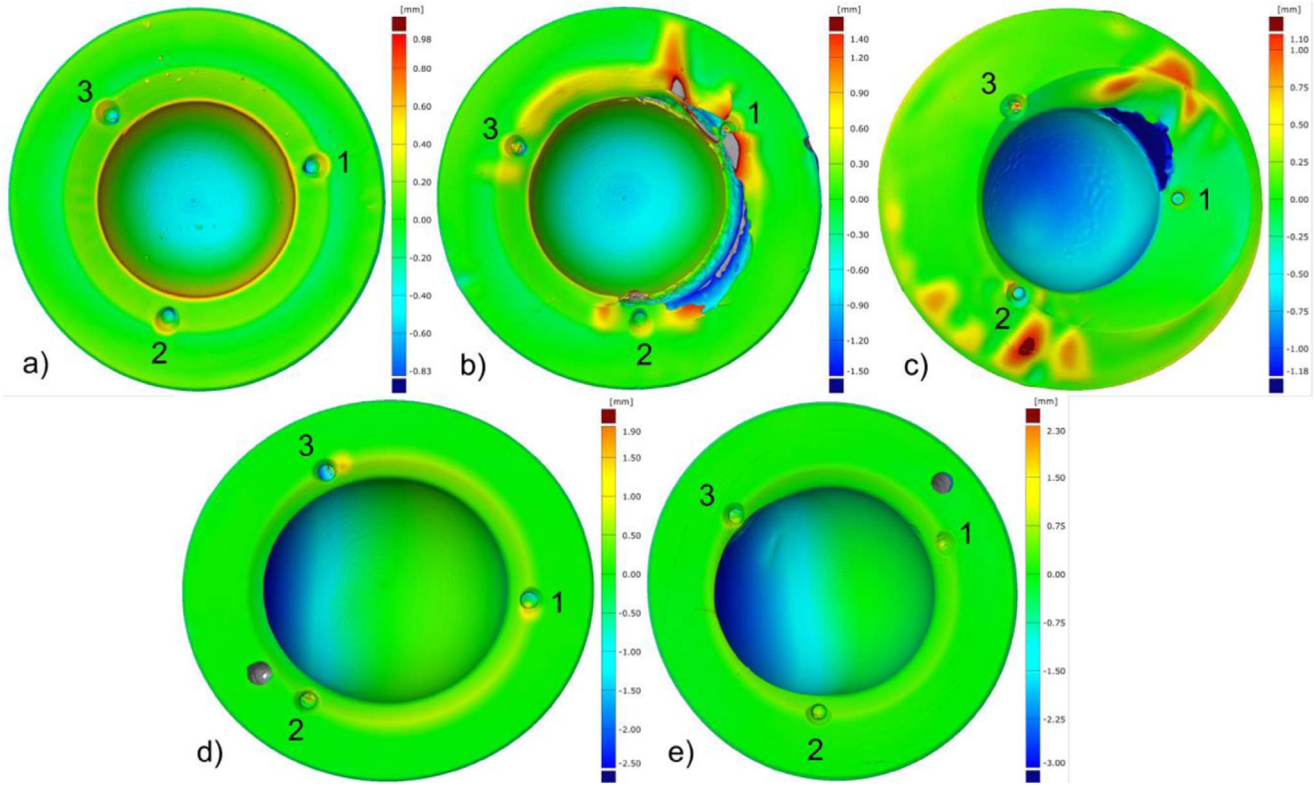


**Fig. 3.** Mapped Surface deviation (mm): (a) sample 1, (b) sample 2, (c) sample 3, (d) sample 4 and (e) sample 5. Positive values refer to material inflation and negative values refer to material wear. Numbers 1, 2 and 3 are the reference points.

new sample has a relatively rougher surface (1.96 ± 0.42 μm), which was a result of shallow grooves (Fig. 6a). The shallow groves were formed during the molding process of polyethylene. On the other hand, samples with centric wear area had higher surface roughness compared to the samples with ecentric wear area. For example, P-3-1 of the sample 1 had much higher roughness (1.55 ± 0.29 μm) compared to that in the same location of sample 4 (0.43 ± 0.08 μm) and 5 (0.49 ± 0.16 μm). The higher roughness of the eccentric worn area is due to less wear. On the other hand, the trends are completely different for samples 8 and 9. Sample 9 had eccentric wear but exhibited one of the rougher surface (3.05 ± 0.56 μm) followed by sample 8 (2.57 ± 0.49 μm, centric worn area). This phenomenon matched with their failure mechanisms: the sample 8 failed due to dislocation and the sample 9 failed due to ossification. It is obvious that during dislocation, the cup had to rub through uneven surfaces, as a result, the roughened topography yielded. Similarly, an ossification refers to grow of an ossified tissue on the surface. The microscopic images of a new sample and samples 2, 4, 8, 9 and 10 are shown in the Fig. 6. The surface topography of samples 8 and 9 are clearly distinguished from the other topographies, showing large surface damage and reflecting higher roughness and failure mechanisms. Therefore, both the penetration rate and changes in surface roughness are highly dependent on the type of wear (centric or eccentric) and the failure mechanism (aseptic loosening, dislocation and bone remodeling). Within the aseptic loosening group 1, eccentric wear showed a higher linear wear rate, while centric wear track showed the relatively higher surface roughness.

### 3.2. Oxidation Index

The measured oxidation indices of the groups 1, 2 and 3 are presented in the Fig. 7(a), (b) and (c), respectively. The new sample had consistent oxidation indices (0.46 ± 0.03) across the surface (ten depicted points in Fig. 2(a). It is noted that the new sample had around one year of shelf-life, thus its crystallinity changed as well as the oxidation index (Tavares et al., 2003). According to Puppulin et al. (2016), the oxidation index (OI) increased over time after γ radiation,

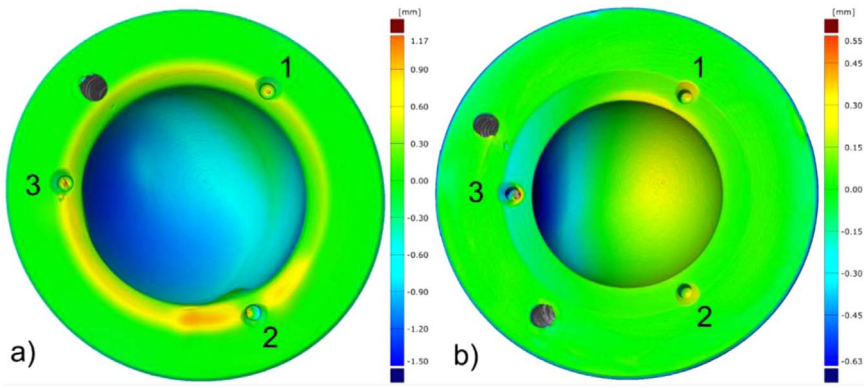


**Fig. 4.** Mapped Surface deviation (mm): (a) sample 6 and (b) sample 7. Positive values refer to material inflation and negative values refer to material wear. Numbers 1, 2 and 3 are the reference points.

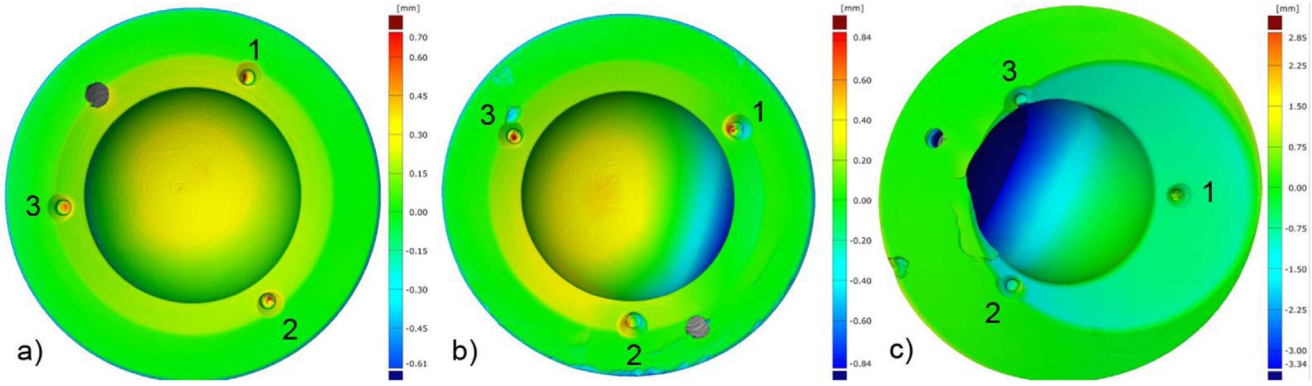


**Fig. 5.** Mapped Surface deviation (mm): (a) sample 8, (b) sample 9, and (c) sample 10. Positive values refer to material inflation and negative values refer to material wear. Numbers 1, 2 and 3 are the reference points.

**Table 2**
Surface roughness of new and retrieved UHMWPE Cups.

| *Samples No.* | *Ra (μm)* | *SD (μm)* | *Rz (μm)* | *SD (μm)* | *Angel of wear vector (deg)* | *Linear wear rate (μm/year)* |
|---|---|---|---|---|---|---|
| New | 1.96 | 0.42 | 2.52 | 0.54 | – | – |
| 1 | 1.55 | 0.29 | 2.08 | 0.32 | 1.41 | −81.47 |
| 2 | 1.50 | 0.25 | 1.83 | 0.27 | 2.04 | −92.72 |
| 3 | 0.66 | 0.16 | 0.83 | 0.18 | 44.60 | −95.02 |
| 4 | 0.43 | 0.08 | 0.57 | 0.10 | 83.24 | −233.08 |
| 5 | 0.49 | 0.16 | 0.57 | 0.17 | 69.28 | −190.24 |
| 6 | 0.77 | 0.12 | 1.07 | 0.27 | 53.53 | −107.16 |
| 7 | 0.65 | 0.16 | 0.87 | 0.18 | 74.00 | −137.43 |
| 8 | 2.57 | 0.49 | 3.24 | 0.57 | 89.11 | −2209.21 |
| 9 | 3.05 | 0.56 | 3.81 | 0.65 | 77.34 | −119.04 |
| 10 | 1.01 | 0.21 | 1.30 | 0.24 | 69.44 | −260.71 |

irrespective of depth (up to 8 mm). The oxidation indices at the center region (C-1) of the liners of group 1 were 0.71, 0.93, 1.13, 0.50 and 0.98, respectively. These values are significantly higher than that of new samples (0.46) with the exception of sample 4. Interestingly, within the group 1, sample 3 exhibited higher OI (1.13), which is synchronized with the worn area pattern and penetration depth — higher penetration depth (≈ 1 mm), followed by sample 5 (wear depth ≈ 0.75 mm and OI (0.98).

Similarly, within group 2, OIs for sample 6 at the center region (C-1) was higher than that of sample 7, which is consistent with their wear tracks. On the other hand, within group 3, the center point of sample 9 showed a nearly similar value to that of a new sample, what reflects its material inflation and failure mechanism. The mechanism involved bone remodeling, thus surface topography changed though the material inflation and underneath UHMWPE had no/little chemical degradation. Sample 10 showed a significantly higher oxidation index (1.28) in the center. In summary, the oxidation indices at center region are very consistent with their penetration depths, for example, samples 6 and 10 had the most penetration depth and so were their oxidation indices. The scenario is also very similar in the ideal wear zone (P-1-1, P-2-1, and P-3-1). For example, the depth of the worn area (5c) and magnitudes of oxidation indices (Fig. 7c) of sample-10 followed a similar trend: P-1-1 < P-2-1 < P-3-1 and P-1–2 < P-2-2 < P-3-2.

The rim areas of the cup (P-1–3, P-2–3, and P-3-3) were mainly in contact with surrounding tissues thus should be oxidized without being subjected to sliding. The oxidation profiles for the rim areas revealed that sample 3 had the highest OI followed by sample 2. The OIs of the side wall (P-1–2, P-2-2, and P-3-2) were subjected to more complex mechanisms, influenced by both of tribo-corrosion and the surrounding tissues. From the oxidation profiles, it can be clearly identified that all of the retrieved samples at the contacting side wall and the rim regions have higher oxidation indices compared to that of a new sample. Among them, sample 10 was found to have significantly higher OIs. It is worth noting that sample 10 had a longer survival period and implanted to a much heavier host patient (16.76 years and 100 kg).

### 3.3. Changes in material properties

The Modulus of elasticity and hardness are key material parameters that play vital roles in contact mechanics and tribology. The implanted cup liners were subjected to a good number of cyclic loading; therefore it is important to evaluate changes in the modulus of elasticity and hardness. Fig. 8 shows the modulus of elasticity (E), hardness (H) and the H/E ratios for the selected samples. The E and H of the new sample were 1.06 MPa and 45.48 MPa, respectively, which are very similar to other published results (Sobieraj and Rimnac, 2009). Remarkably, most of the retrieved cups had higher H and E than those of a new sample. The trends of E and H are as follow: sample 10 ≥ sample 1 ≥ sample 9 ≥ samples 7 ≥ sample 8 ≥ new samples. Most of these values have a correlate well with their mapped surface deviation spectra at P-3-1 (Figs. 3–5). For example, sample 10, which has the highest penetration depth showed highest hardness (43.26% higher than that of a new sample), and sample 8, which demonstrated only material inflation, had the lowest hardness (very similar to new sample), among the retrieved prostheses.

It has been observed that despite of the increased hardness and elasticity, the ratio of the hardness/elasticity of the new sample (42.72) is higher than that of the retrieved prostheses. Particularly, the samples (1 & 10) that had a significant penetration depth, have much lower ratios (38.31 and 31.30, respectively) compared to that of the new sample. The percentages of orthorhombic phase and oxidation indices of these samples are also much correlated to the nanoindentation results. It is worth noting that OIs are representative of mechanical and chemical wear and the percentage of orthorhombic phase is an indicator of material hardness and stiffness. The OIs in Fig. 9 for the slotted samples show that all retrieved samples have a higher magnitude, particularly, samples 1 and 10. It was also surprising to see that sample 9 had a high standard deviation and sample 8 showed two different phenomenon, distinguished by the different regions, specified as bright area and dark area.

## 4. Discussion

Understanding the failure mechanisms is important for reducing the revision rate of acetabulum components. Wear and resultant wear debris are the most dominating factors for such revisions (Clarke and Gustafson, 2000; Nine et al., 2014). Wear have complex mechanisms, and it can be dominantly influenced by the oxidation and material stiffening (Kurtz, 2009; Pezzotti et al., 2007; Wang et al., 1997) along

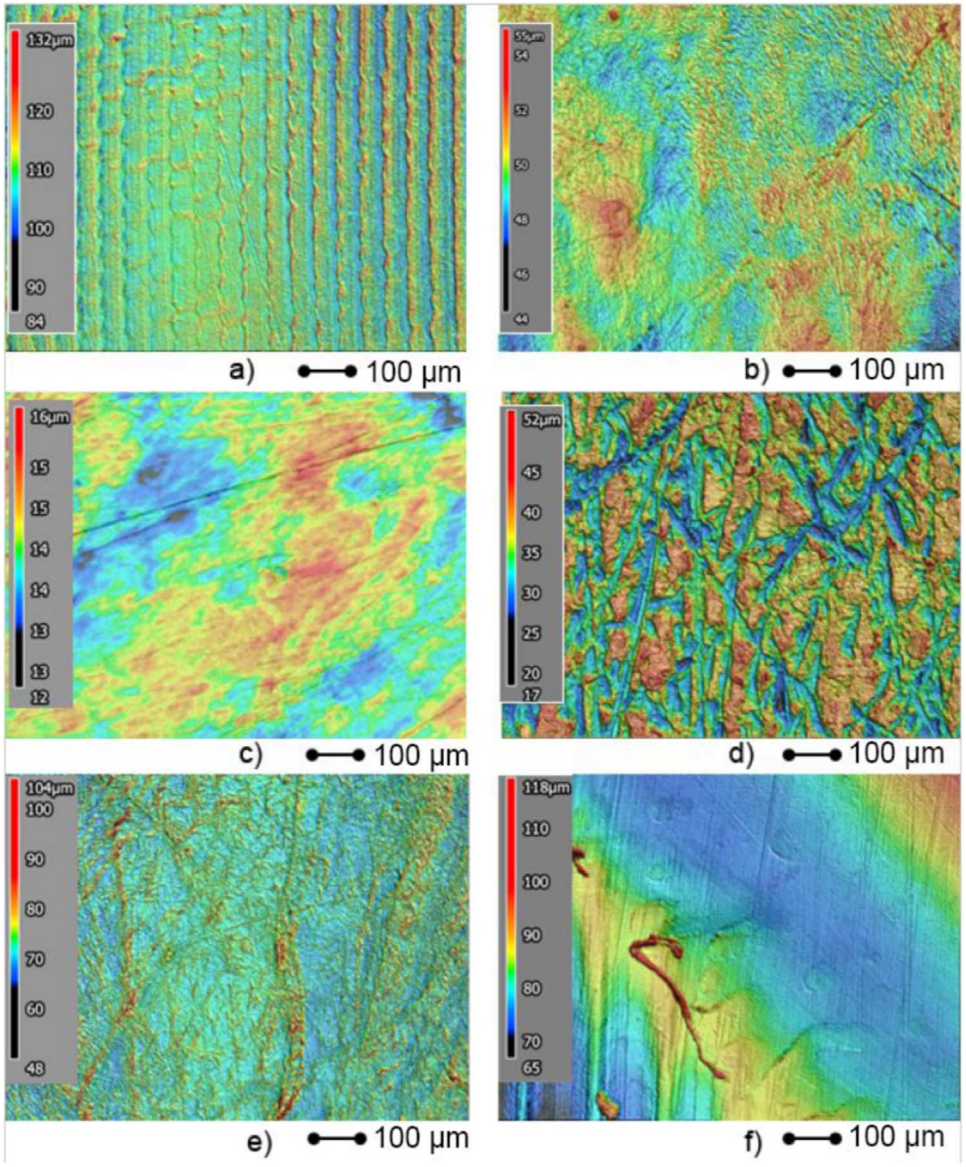


**Fig. 6.** Surface topography of UHMWPE cups: (a) new sample, (b) sample 2, (c) sample 4, (d) sample 8, (e) sample 9 and (f) sample 10.

with mechanical wear due to cyclic loading. Therefore, in this study, we have mapped the surface deviation spectra using the micro-CT, evaluated the OIs and the fraction of orthorhombic phases using the micro-Raman, and measured the changed material properties such as hardness, modulus of elasticity and the ratio of hardness and elasticity using nanoindention.

All of the new and retrieved prosthesis were made of the same material (mildly cross-linked UHMWPE) and were sterilized between a

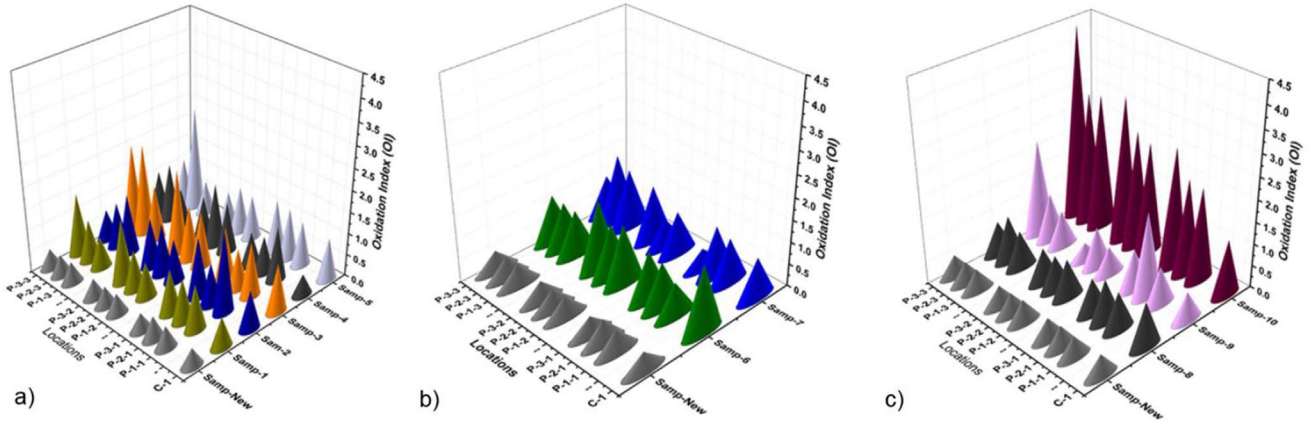


**Fig. 7.** Oxidation index for the retrieved samples: (a) group 1, (b) group 2, and (c) group 3.

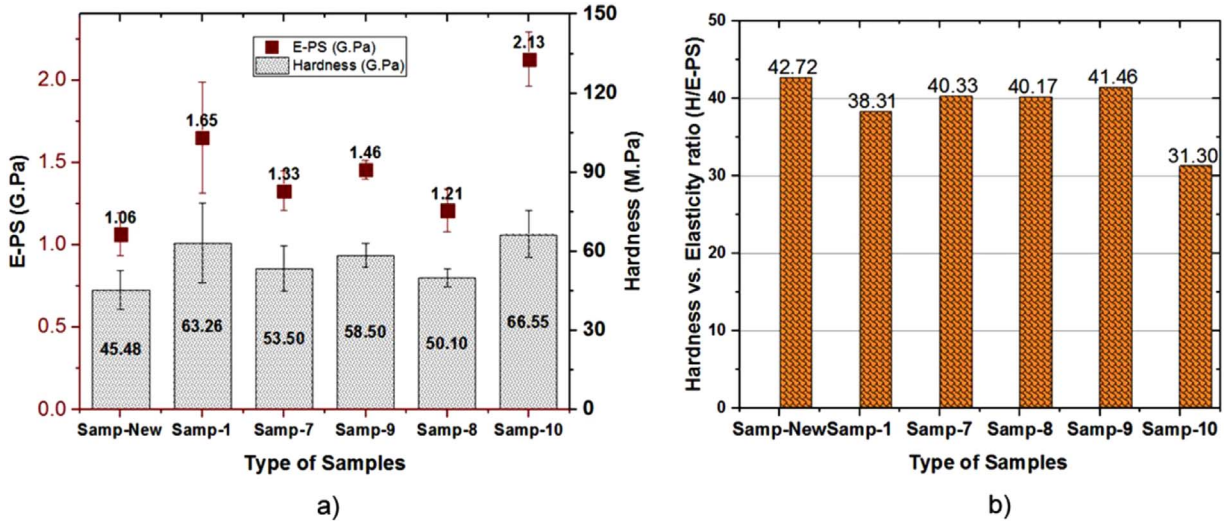


**Fig. 8.** Mechanical properties of selected samples: (a) hardness (H) and modulus of elasticty (E), and (b) ratio of hadness Vs. Ealsticty (H/E-PS).

minimum of 25 kilogray (kGy) and a maximum of 37 kGy gamma ray. The clinical observation for the retrieved prostheses provided important indication of possible failure mechanisms. For example, sample 9, which failed due to articular ossification, had certainly different failure mechanism than that of sample 8, which failed due to dislocation. Moreover, within a similar failure mechanism, there are a number of variables such as the body weight, the pattern of gaits, and the diverse liner and cup thickness. Despite these variables and the diverse failure mechanisms, the wear spectra showed that the penetration rates were significantly higher for the samples that had eccentric worn areas, excluding sample 8, which is just slightly eccentric. Jasty et al. (1997) concluded similar trends where worn areas were eccentric to the apex of the liner. In this study, 5 out of 10 retrieved cup liners were found to have eccentric worn area. Overall, the average penetration rate was −146.32 μm/year (SD 65.77 μm/year), which is very similar to the results of Ottink, et al.(2015) (−120 μm/year) and Ranuša et al. (2016) (−180 μm/year). However, the rate is much lower than the rate that was observed by Kurtz et al. (2010) (−1100 μm/year). Remarkably, none of the previous articles (Kurtz et al., 2010; Ottink et al., 2015; Ranuša et al., 2016) categorically acknowledged that the linear wear rate were influenced by the centricity of loading. In addition, a number of the samples (7–9) had predominated material inflations instead of penetration depth, which could be the result of displaced materials, especially during the compressive loading and thermal expansion due to high friction .

The surface profile analysis showed some important information on the wear mechanism. The surface image of the new samples confirmed that it has some groove type pattern (Li and Burstein, 1994), and as a result, relatively high roughness was revealed (Ra: 1.96 ± 0.41 μm and Rz: 2.52 ± 0.41). The groove type surface textures resulted from the molding procedure of the UHMWPE. Among the retrieved prostheses, the worn area of sample 8 showed a severe distortion of surface, and resulted in a higher surface roughness (Ra: 2.57 ± 0.49 μm and Rz: 3.24 ± 0.56). Similarly, sample 9, which was subject to ossification, showed a much higher surface roughness (Ra: 3.05 ± 0.56 μm and Rz: 3.81 ± 0.65). Both samples 8 and 9 had significant material inflations due to their failure mechanisms, which were also confirmed by their surface topography (Fig. 5(a) and (b)). The other samples (#1–6 and 10), had relatively smoother surface topography within the wear tracks (P-3-1). This phenomenon indicates an abrasive wear-polishing mechanism in these samples (Jasty et al., 1997). However, a closer look at the surface topographical images showed that there was something beyond the abrasive wear-polishing. For example, sample 10 had an interface of abrasive wear-polishing and original molding mark.

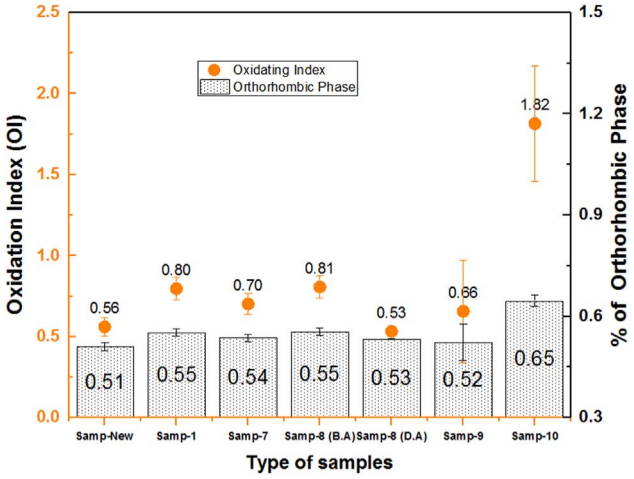


**Fig. 9.** Oxidation indices and percentages of orthorhombic phase for selected samples, B.A: bright area and D.A: dark area.

The Raman analysis was actually an additional measurement that confirmed the oxidative degradation alongside mechanical wear. A number of studies used confocal Raman spectroscopy as a non-destructive tool for measuring chemical degrading of highly cross-linked Polyethylene (HXLPE) liners at a microscopic level (Kumakura et al., 2009; Pezzotti et al., 2007). Among these analysis, oxidation index (OI) and volume fraction of orthorhombic phase ($\alpha_c$) are very significant, since both of them are closely related to the oxidative degradation due to tribo-corrosion process (Sobieraj and Rimnac, 2009). Pizzotti et al. (Kumakura et al., 2009) mentioned that when a oxidative degradation of HXLPE proceeds by chain scission (reaction with oxygen or lipids), a stiffening of the molecular chain occurs. As a result, both hardening and embrittlement occurs to the HXLPE liners at the micro-structure level. The chain scission can be detected by the ratio between the overall degree of crystallinity and an orthorhombic phase (Eq. 1), $\alpha_c$. OI is related to $\alpha_c$ but enables prediction of a precise degree of oxidative degradation (Eq. (2)).

In our Raman analysis, a 785 nm wavelength laser was used, which is different from other published articles (Puppulin et al., 2016). The Raman spectra were very clear (low noise) and peaks around the 1305 and 1414 $cm^{-1}$ were clearly identified. Typical Raman spectra for a new sample and sample 10 are shown in the Fig. 10. The OIs all over the new sample were very consistent (0.41–0.54) and very similar to other published data (0.44–0.52 for remodeled HXLPE and 28 days of

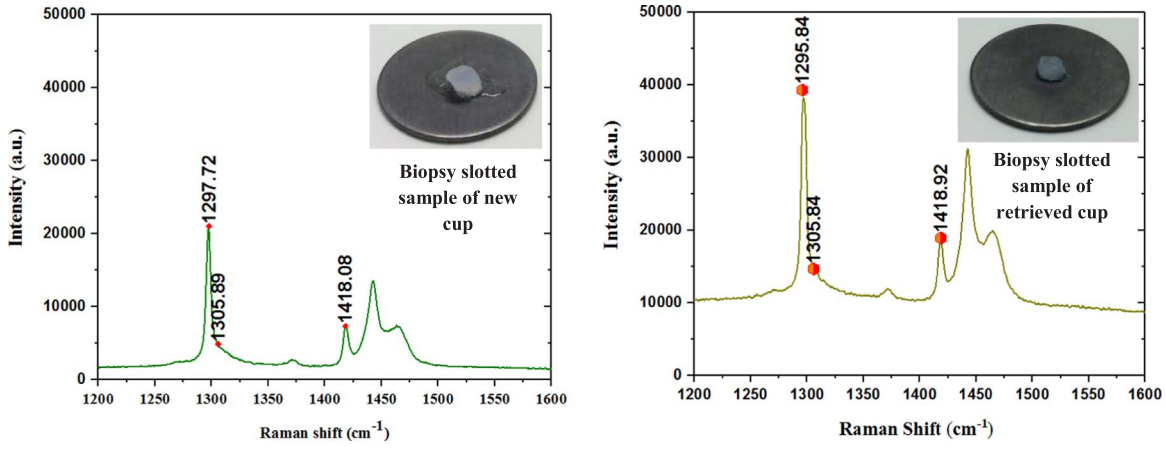


**Fig. 10.** Raman spectra for UHMWPE: (a) new sample and (b) sample 10. The spectra around 1305 ($I_{1305}$) represent crystallinity phase and the spectra around 1418 represent the orthorhombic phase ($I_{1418}$).

accelerate aging) (Pezzotti et al., 2007; Puppulin et al., 2016). Interestingly, almost all of the retrieved samples had an increased OI across the contacting (both wear and non-wear) zones and at the rim of the cup liners. Among them, sample 10 demonstrated the maximum OIs, especially at P-3-2 location where the OI became as high as 4. It is noted that, P-3-2 location of sample 10 had the highest penetration depth (−3.34 mm). The obtained result is consistent with the published work of Pezzotti et al. where the OI were reported to be 3–7 (Pezzotti et al., 2007). Similarly, samples 3, 7 and 10 with eccentric worn area, showed higher OIs (≥ 2.0) in their corresponded wear zones. Even most of OIs for non-wear zone of the retrieved prosthesis were higher than that of new samples. This confirmed that oxidative degradation occurred all over the retrieved prosthesis; however, the intensities of OI were higher mainly in the wear and rim areas.

Although the OI and $\alpha_c$ can indicate the mechanical degradations such as hardening and embrittlement (Pezzotti et al., 2007), hardness and modulus of elasticity were also measured using nanoindentation on the surface of the samples (indentation depth is below 2 μm). Sample 10 was 1.46 times harder and 1.99 times stiffer than the new sample (from nanoindentation measurement). The comparison was 3.25 times oxidative and 1.27 times higher $\alpha_c$ from Raman analysis. On the other hand, sample 8 (bright part) was 1.14 times harder and 1.10 times stiffer than the new sample. The comparison was 1.44 times oxidative and 1.08 times higher $\alpha_c$ from Raman analysis.

A number of studies showed that the ratio of the hardness to elastic modulus is a key material property that is related to tribological performance (Ching et al., 2014). In our study, we found that a new sample has a higher ratio compared to all retrieved components; particularly sample 10 which had the lowest ratio. From the ratios, it is also confirmed that the retrieved prostheses had degraded mechanical properties. Therefore, this study recommended that retrieved prostheses suffered from a combination of mechanical wear (eccentricity of load was the dominating factor), material inflation, oxidative degradation and reduced ratio of hardness to elastic modulus.

## 5. Conclusion

In this study, ten retrieved and four new conventional UHWMPE cups liners were examined in terms of surface deviation, oxidative degradation and changes in material properties. It can be concluded that eccentrically worn track was the one of the most denominating factor for higher penetration rate. In addition, material inflations were formed in the few samples: rim areas of sample 2 and 3, and contact areas of sample 8 and 9. The oxidation indices showed a clear sign of chemical degradation in the retrieved prosthesis, and these are mostly correlated with wear depth. Furthermore, hardening and stiffening were identified in these prostheses. In conclusion, implanted prostheses faced simultaneous mechanical wear, material inflation, oxidative degradation and lower hardness vs. elasticity ratio, thus all these matters need to be taken into account during new prosthesis design and material selection.

## Acknowledgements

Funding support for this work was provided by the University of Arkansas with partial support from the US National Science Foundation (NSF) through Center for Advanced Surface Engineering under Grant No. OIA-1457888 and the Arkansas EPSCoR Program, ASSET III. We thank the Arkansas Biosciences Institute and the University of Arkansas for major equipment funding support. This research was also carried out under the project LTAUSA17150 with financial support from the Ministry of Education, Youth and Sports of the Czech Republic and by CEITEC 2020 (LQ1601) with financial support from the Ministry of Education, Youth and Sports of the Czech Republic under the National Sustainability Programme II. The authors express thanks to Prof. J.B.Medley for help with editing the manuscript and Prof. A. Malshe for the helping with the Raman Spectroscopy.

## References

2017. Canadian Joint Replacement Registry, Canadian Institute for Health Information., Canada.
Badea, C.T., Drangova, M., Holdsworth, D.W., Johnson, G.A., 2008. In vivo small-animal imaging using micro-CT and digital subtraction angiography. Phys. Med. Biol. 53, R319–R350.
Bergmann, G., Graichen, F., Rohlmann, A., Verdonschot, N., Van Lenthe, G., 2001. Frictional heating of total hip implants. Part 2: finite element study. J. Biomech. 34, 429–435.
Bragdon, C.R., Greene, M.E., Freiberg, A.A., Harris, W.H., Malchau, H., 2007. Radiostereometric analysis comparison of wear of highly cross-linked polyethylene against 36-vs 28-mm femoral heads. J. Arthroplast. 22, 125–129.
Briscoe, B., Fiori, L., Pelillo, E., 1998. Nano-indentation of polymeric surfaces. J. Phys. D: Appl. Phys. 31, 2395.
Cakmak, U.D., Schöberl, T., Major, Z., 2012. Nanoindentation of polymers. Meccanica 47, 707–718.
Clarke, I.C., Gustafson, A., 2000. Clinical and hip simulator comparisons of ceramic-on-polyethylene and metal-on-polyethylene wear. Clin. Orthop. Relat. Res. 379, 34–40.
Costa, L., Jacobson, K., Bracco, P., Del Prever, E.B., 2002. Oxidation of orthopaedic UHMWPE. Biomaterials 23, 1613–1624.
Dowson, D., Hardaker, C., Flett, M., Isaac, G.H., 2004. A hip joint simulator study of the performance of metal-on-metal joints: Part II: design. J. Arthroplast. 19, 124–130.
Fulin, P., Pokorny, D., Slouf, M., Nevoralova, M., Vackova, T., Dybal, J., Kasprikova, N., Landor, I., 2016. Analysis of oxidative damage to components removed from Beznoska/Poldi total hip replacements. Acta Chir. Orthop. Et. Traumatol. Cechoslov. 83, 155–162.

Ge, S., Wang, S., Huang, X., 2009. Increasing the wear resistance of UHMWPE acetabular cups by adding natural biocompatible particles. Wear 267, 770–776.
GOB, 2016. GOM mbH, ATOS - Industrial 3D Scanning Technology.
Goldsmith, A., Dowson, D., Isaac, G., Lancaster, J., 2000. A comparative joint simulator study of the wear of metal-on-metal and alternative material combinations in hip replacements. Procd. Inst. Mech. Eng. Part H: J. Eng. Med. 214, 39–47.
Govind, G., Henckel, J., Hothi, H., Sabah, S., Skinner, J., Hart, A., 2015. Method for the location of primary wear scars from retrieved metal on metal hip replacements. BMC Musculoskelet. Disord. 16, 173.
Hellmann, R., Cotte, S., Cadel, E., Malladi, S., Karlsson, L.S., Lozano-Perez, S., Cabié, M., Seyeux, A., 2015. Nanometre-scale evidence for interfacial dissolution–reprecipitation control of silicate glass corrosion. Nat. Mater. 14, 307–311.
Ching, H.A., Choudhury, D., Nine, M.J., Osman, N.A.A., 2014. Effects of surface coating on reducing friction and wear of orthopaedic implants. Sci. Technol. Adv. Mater. 15, 014402.
Choudhury, D., Lackner, J., Fleming, R.A., Goss, J., Chen, J., Zou, M., 2017. Diamond-like carbon coatings with zirconium-containing interlayers for orthopedic implants. J. Mech. Behav. Biomed. Mater. 68, 51–61.
Jasty, M., Goetz, D.D., Bragdon, C.R., Lee, K.R., Hanson, A.E., Elder, J.R., Harris, W.H., 1997. Wear of polyethylene acetabular components in total hip arthroplasty. An analysis of one hundred and twenty-eight components retrieved at autopsy or revision operations. J. Bone Jt. Surg. Am. 79, 349–358.
Jee, A.-Y., Lee, M., 2010. Comparative analysis on the nanoindentation of polymers using atomic force microscopy. Polym. Test. 29, 95–99.
Kumakura, T., Puppulin, L., Yamamoto, K., Takahashi, Y., Pezzotti, G., 2009. In-depth oxidation and strain profiles in UHMWPE acetabular cups non-destructively studied by confocal Raman microprobe spectroscopy. J. Biomater. Sci., Polym. Ed. 20, 1809–1822.
Kurtz, S.M., 2009. UHMWPE Biomaterials Handbook: Ultra High Molecular Weight Polyethylene in Total Joint Replacement and Medical Devices. Academic Press.
Kurtz, S.M., Medel, F.J., MacDonald, D.W., Parvizi, J., Kraay, M.J., Rimnac, C.M., 2010. Reasons for revision of first-generation highly cross-linked polyethylenes. J. Arthroplast. 25, 67–74.
Li, S., Burstein, A.H., 1994. Ultra-high molecular weight polyethylene. The material and its use in total joint implants. JBJS 76, 1080–1090.
Milosev, I., Kovac, S., Trebse, R., Levasic, V., Pisot, V., 2012. Comparison of Ten-Year Survivorship of Hip Prostheses with Use of Conventional Polyethylene, Metal-on-Metal, or Ceramic-on-Ceramic Bearings. J. Bone Jt. Surg.-Am. Vol. 94A, 1756–1763.
Nine, M.J., Choudhury, D., Hee, A.C., Mootanah, R., Osman, N.A.A., 2014. Wear debris characterization and corresponding biological response: artificial hip and knee joints. Materials 7, 980–1016.
Ottink, K., Barnaart, L., Westerbeek, R., van Kampen, K., Bulstra, S., van Jonbergen, H.-P., 2015. Survival, clinical and radiological outcome of the Zweymüller SL/Bicon-Plus total hip arthroplasty: a 15-year follow-up study. Hip Int. 25.
Peers, S., Moravek, J.E., Budge, M.D., Newton, M.D., Kurdziel, M.D., Baker, K.C., Wiater, J.M., 2015. Wear rates of highly cross-linked polyethylene humeral liners subjected to alternating cycles of glenohumeral flexion and abduction. J. Shoulder Elb. Surg. 24, 143–149.
Pezzotti, G., 2017. Raman spectroscopy of biomedical polyethylenes. Acta Biomater.
Pezzotti, G., Kumakura, T., Yamada, K., Tateiwa, T., Puppulin, L., Zhu, W., Yamamoto, K., 2007. Confocal Raman spectroscopic analysis of cross-linked ultra-high molecular weight polyethylene for application in artificial hip joints. J. Biomed. Opt. 12, 014011–014011-014014.
Pezzotti, G., Takahashi, Y., Takamatsu, S., Puppulin, L., Nishii, T., Miki, H., Sugano, N., 2011. Non-destructively differentiating the roles of creep, wear and oxidation in long-term in vivo exposed polyethylene cups. J. Biomater. Sci., Polym. Ed. 22, 2165–2184.
Pokorny, D., Slouf, M., Fulin, P., 2012. Current knowledge on the effect of technology and sterilization on the structure, properties and longevity of UHMWPE in total joint replacement. Acta Chir. Orthop. Et. Traumatol. Cechoslov. 79, 213–221.
Puppulin, L., Miura, Y., Casagrande, E., Hasegawa, M., Marunaka, Y., Tone, S., Sudo, A., Pezzotti, G., 2016. Validation of a protocol based on Raman and infrared spectroscopies to nondestructively estimate the oxidative degradation of UHMWPE used in total joint arthroplasty. Acta Biomater. 38, 168–178.
RAD, E.M., 2015. Volumetric Wear Assessment and Characterization of Striated Pattern of Retrieved UHMWPE Tibial Inserts. Rush University.
Ranusa, M., Gallo, J., Hobza, M., Vrbka, M., Necas, D., Hartl, M., 2017. Wear and roughness of bearing surface in retrieved polyethylene bicon-plus cups. Acta Chir. Orthop. Et. Traumatol. Cechoslov. 84, 159–167.
Ranuša, M., Gallo, J., Vrbka, M., Hobza, M., Paloušek, D., Křupka, I., Hartl, M., 2016. Wear analysis of extracted polyethylene acetabular cups using a 3D optical scanner. Tribol. Trans. 1–11.
Sakellariou, V.I., Sculco, P., Poultsides, L., Wright, T., Sculco, T.P., 2013. Highly cross-linked polyethylene may not have an advantage in total knee arthroplasty. HSS J. ® 9, 264–269.
Salahshoor, M., Guo, Y., 2014. Biodegradation control of magnesium-calcium biomaterial via adjusting surface integrity by synergistic cutting-burnishing. Procedia CIRP 13, 143–149.
Small, S.R., Berend, M.E., Howard, L.A., Tunç, D., Buckley, C.A., Ritter, M.A., 2013. Acetabular cup stiffness and implant orientation change acetabular loading patterns. J. Arthroplast. 28, 359–367.
Sobieraj, M., Rimnac, C., 2009. Ultra high molecular weight polyethylene: mechanics, morphology, and clinical behavior. J. Mech. Behav. Biomed. Mater. 2, 433–443.
Spinelli, M., Carmignato, S., Affatato, S., Viceconti, M., 2009. CMM–based procedure for polyethylene non-congruous unicompartmental knee prosthesis wear assessment. Wear 267, 753–756.
Steinberg, M.E., 2014. Total hip replacement arthroplasty-past, present and future. Univ of Penns Ortho J 19.
Tavares, A.C., Gulmine, J.V., Lepienski, C.M., Akcelrud, L., 2003. The effect of accelerated aging on the surface mechanical properties of polyethylene. Polym. Degrad. Stab. 81, 367–373.
Teeter, M.G., Naudie, D.D., McErlain, D.D., Brandt, J.-M., Yuan, X., MacDonald, S.J., Holdsworth, D.W., 2011. In vitro quantification of wear in tibial inserts using micocomputed tomography. Clin. Orthop. Relat. Research® 469, 107–112.
Teeter, M.G., Naudie, D.D.R., Charron, K.D., Holdsworth, D.W., 2010. Three-dimensional surface deviation maps for analysis of retrieved polyethylene acetabular liners using micro-computed tomography. J. Arthroplast. 25, 330–332.
Uddin, M., Mak, C., Callary, S., 2016. Evaluating hip implant wear measurements by CMM technique. Wear 364, 193–200.
Wang, A., Sun, D., Yau, S.-S., Edwards, B., Sokol, M., Essner, A., Polineni, V., Stark, C., Dumbleton, J., 1997. Orientation softening in the deformation and wear of ultra-high molecular weight polyethylene. Wear 203, 230–241.
Xiong, L., Xiong, D., 2012. The influence of irradiation dose on mechanical properties and wear resistance of molded and extruded ultra high molecular weight polyethylene. J. Mech. Behav. Biomed. Mater. 9, 73–82.

Journal of the Mechanical Behavior of Biomedical Materials 87 (2018) 30–39

Contents lists available at ScienceDirect

Journal of the Mechanical Behavior of Biomedical Materials

journal homepage: www.elsevier.com/locate/jmbbm

# UHMWPE acetabular cup creep deformation during the run-in phase of THA's life cycle

Jakub Zeman[a], Matúš Ranuša[a,*], Martin Vrbka[a], Jiří Gallo[b], Ivan Křupka[a], Martin Hartl[a]

[a] Faculty of Mechanical Engineering, Brno University of Technology, Technická 2896/2, 616 69 Brno, Czech Republic
[b] Department of Orthopaedics, University Hospital Olomouc, Faculty of Medicine and Dentistry, Palacky University, I. P. Pavlova 6, 775 20 Olomouc, Czech Republic

ARTICLE INFO

*Keywords:*
UHMWPE
Creep deformation
Run-in-phase
Inclination angle
Optical scanning
Scanning Electron Microscopy

ABSTRACT

Ultra-high molecular polyethylene (UHMWPE) is one of the most used materials of the acetabular liners in total tip arthroplasty (THA). Polyethylene has good tribological properties and biocompatibility. However, the lifetime of polyethylene implants is limited by wear related complications. Polyethylene material released into the periprosthetic environment induces osteolysis that can be followed by implant loosening. Wear of cup is influenced mainly by orientation of the cup in pelvis, by initial geometry before the material degradation and by tribological parameters. Aim of this study is to focus on the run-in-phase of the liner which is predictive for future life cycles of liner. Creep deformations of liners for 30°, 45°, 60° inclination angles surgically recommended for the positioning in pelvis were analyzed by the optical scanning method. Load tests were performed for 50,000 cycles. Creep deformations and surface changes were analyzed at each 10,000 cycles. The results showed that liners with 60° inclination angle had higher creep deformations. Penetration of femoral head was 0.04–0.05 mm and occupied bearing area was around 77%. The smallest creep was measured for the 45° angle. However, deformation in the superior quadrant of acetabular rim, which is vulnerable for potential fracture of a liner, was identified in this case. Topography of the surface bearing was also observed during the run-in-phase. The surface was smoothened and showed multidirectional scratches caused by the influence of third body particles. This phase was followed by early delamination. Flakes sized approximately 5–20 μm were observed on the UHMWPE surface. This is similar to the'flake' shape wear debris extracted in vivo. Detailed analysis of run-in phase of loading of modern polyethylene implants can help to distinguish between their creep deformation and true degradation. The latter contributes strongly to the development of wear related complications associated with THAs limiting substantially their time in service.

## 1. Introduction

The main factor limiting longevity of metal on polyethylene (MoP) hip replacement is wear of the Ultra High Molecular Weight Polyethylene (UHMWPE) acetabular cup. Mutual motion of bearing surfaces of the THA, identified as multidirectional cross shear motion (Turell et al., 2003), causes deliberation of polyethylene particles from an articulating surface.

As it has been stated in multiple studies (Gallo et al., 2017; Gibon et al., 2017; Ingham and Fisher, 2000), deliberated polyethylene particles of critical sizes 0,3–10 μm (Green et al., 1998) can cause inflammatory biological reaction causing osteolysis of the bone that surrounds components of the THA. This can eventually lead to aseptic loosening of the THA requiring its imminent surgical revision.

Thus, there is a consistent effort to reduce wear rate of UHMWPE cups, to increase THA's lifespan and to minimize the need for a revision surgery. There has been a notable progress in material development in the form of second (XLPE) and third (Vitamin E doped XLPE) generations of UHMWPE that show better wear resistance. Besides the material development, there are numerous studies focusing on other factors affecting wear rates of THA in vivo, such as acetabular cup orientation in human body (Korduba et al., 2014; Scheerlinck, 2014).

Spatial orientation of acetabular cup in patient's body is determined by anteversion and inclination angles. There are surgically recommended intervals for both of these angles being 5–25° for anteversion and 30–50° for inclination (Bobman et al., 2016). Altering the inclination angle significantly affects the properties of the contact area. Increasing the inclination angle shifts the area of contact pressure closer towards the acetabular rim, while decreasing its overall size and increasing its maximal value of contact pressure (Hua et al., 2016).

* Corresponding author.
*E-mail address:* matus.ranusa@vut.cz (M. Ranuša).

https://doi.org/10.1016/j.jmbbm.2018.07.015
Received 22 May 2018; Received in revised form 9 July 2018; Accepted 10 July 2018
Available online 12 July 2018
1751-6161/ © 2018 Elsevier Ltd. All rights reserved.

While influence of the acetabular orientation on the contact stress is well documented, a direct relationship between the contact pressure properties and wear mechanism is not yet fully understood. Older studies found no significant correlation between higher wear rates and higher inclination angles (Del Schutte et al., 1998; Patil et al., 2003). On the other hand, some more recent studies showed decreasing wear rates with increased inclination angles (Halma et al., 2014; Korduba et al., 2014; Rijavec et al., 2014). There are also generally higher wear rates when measured with radiography than obtained by simulator wear tests (Kang et al., 2003).

These rather significant differences between numerous studies could be caused by multiple factors. For example, simulator studies with strictly controlled conditions do not take into account loose third body particles of bone void fillers (Cowie et al., 2016) or bone cement. There are also different approaches to wear measurement. The radiographic method, used in clinical practice, displays head's penetration as result of wear and plastic deformation (creep) of polyethylene acetabular cup. This analysis is less accurate and determines only the linear wear (Ebramzadeh et al., 2003). It is also difficult to identify released polyethylene apart from creep plastic deformation of a liner using this method. In vitro volumetric measurements are on the other hand performed using various methods such as gravimetry, coordinate-measuring machine (Lord et al., 2011; Uddin, 2014) or optical methods (Choudhury et al., 2018; Ranuša et al., 2016; Zou et al., 2001). These methods are used on retrieved cups or during in vitro simulator wear tests. The key difference is that gravimetric methods show solely physical loss of liners material, caused by abrasion, adhesion and fatigue which are subsequent to hip articulation (Affatato et al., 2008), whereas analysis of liners surface (Ranuša et al., 2017) shows complex information about combined wear and creep processes. Gravimetry bears the problem of joint fluid soak which needs to be accounted for, surface analysis on the other hand presents the challenge of distinguishing material loss of the liner from its creep behavior.

Creep behavior of polyethylene acetabular cup has been observed in multiple computational studies, hip simulator studies and clinical studies on retrieved THAs. It has been stated in the computational studies (Bevill et al., 2005; Liu et al., 2012; Penmetsa et al., 2006), that major part of the creep deformation occurs in the very first phase of the acetabular wear, when bearing surfaces are adjusting to each other. The creep deformation changes spherical geometry of acetabular cup and alters contact area of the THA implants. While there is the Finite Element Method (FEM) analysis for the initial phase of wear, it involves certain simplifications regarding the creep model, loading and kinematic conditions and surface geometry. Moreover, there is lack of in vitro data on the initial wear. Hip simulator studies (Affatato et al., 2017; Galvin et al., 2010) are mainly focused on long term wear testing and first measurements of articulating surfaces are usually carried out far beyond the initial run-in phase of the THA. Creep in the run-in phase was observed in vivo on early retrieved THAs (Muratoglu et al., 2004). Authors concluded, that creep degradation was predominant in this phase. Surface texture changes caused by creep degradation affect tribological properties (friction, wear intensity) of the MoP bearing in pin on plate configuration (Niemczewska-Wójcik and Piekoszewski, 2017).

The aim of this study is therefore to observe creep degradation of polyethylene acetabular cups during the run-in phase. For the first time, measurements in this phase are based on in-vitro hip simulator testing. Changes of surface geometry validate the existing simplified FEM analysis (Bevill et al., 2005; Liu et al., 2012). Measurement of the creep deformation depth could improve the accuracy of head penetration measurements using radiography and thus narrow the gap between in vivo and in vitro wear rate measurements. The study also helps to clarify the impact of the plastic deformation of cups on the tribological characteristics of hip implants as well as the impact of the cup orientation on the wear rate. The surface texture of bearing surfaces is observed together with the friction coefficient to describe the run-in phase of the wear cycle more closely.

## 2. Materials and methods

The run-in phase was observed on Polyethylene-on-Metal hip replacement using acetabular cup components (B-Braun, Aesculap AG et Co. KG, Germany) paired with corresponding CrCoMo femoral heads from the same manufacturer. All of the cup liners were made from compression molded GUR 1020 UHMWPE – Chirulen, according to International Organization for Standardization (ISO-5834-2). The irradiation dose (applied in a $N_2$ environment) was between 25 and 37 kGy (Milošev et al., 2012). The inner surface radius of all cup liners was 14 mm. The outer shape of cups was also spherical with diameters varying between 58 mm and 60 mm, similar liner wall thickness was chosen because it was identified as factor influencing the creep deformations. The cup components were intended for cemented fixation. Brand new samples of these components, commonly used in clinical practice, were used in this study. Acetabular cups were placed in high strength resin (Dentacryl, SpofaDental a.s., Czech Republic) simulating placement in bone cement.

Three physiological orientations with different inclination angles were tested each with test sample number of n = 1. Inclinations of 30°; 45° and 60° were chosen to represent the whole surgically recommended inclination interval. Anteversion angle was the same in all three tested replacements to isolate the influence of inclination. The chosen anteversion was 15° approximately in the middle of the recommended interval.

The tested hip replacements were subjected to physiological loading and motions using the hip simulator. The simulator was fully servo-driven and featured uniaxial load and two motion axes. The physiological load was applied via spring compression using twin peak 3000 N load gait cycle with 1 Hz frequency according to the ISO 14242-1.

The orientation of the two motion axes relative to the load line was chosen to simulate Flexion-Extension (applied on the femoral head, range $-18°/+25°$) and Inner-Outer rotation (applied on the acetabular cup, range $-10°/+2°$) motions. Lack of the third motion (Abduction-Adduction) axis specified in ISO 14242-1 was compensated by a phase shift of F/E and I/O sinusoidal motion curves by 90° in comparison to ISO 14242-1 (Fig. 1).

The elliptical motion of the bearing surfaces, causing multi-directional shear stress typical for the physiological load (Turell et al., 2003) was maintained in this way. It has been also stated (Ali et al., 2016) that replacing Abduction-Adduction axis with phase shift of other two axes does not have notable impact on wear rates and deformations of an acetabular cup while simulating the gait cycle (Fig. 2).

The hip replacement components were submerged in model-synovial fluid during simulator testing. The fluid was based on PBS solution with addition of Albumin (28 mg/ml) and γ-globulin (9.4 mg/ml) proteins. During the testing, the whole containment with flooded hip

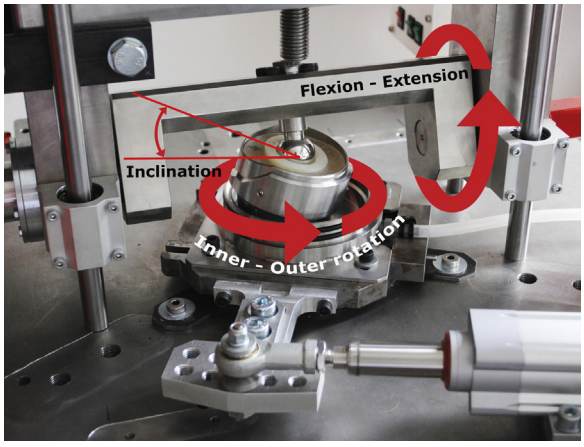


**Fig. 1.** The kinematic of hip joint simulator.

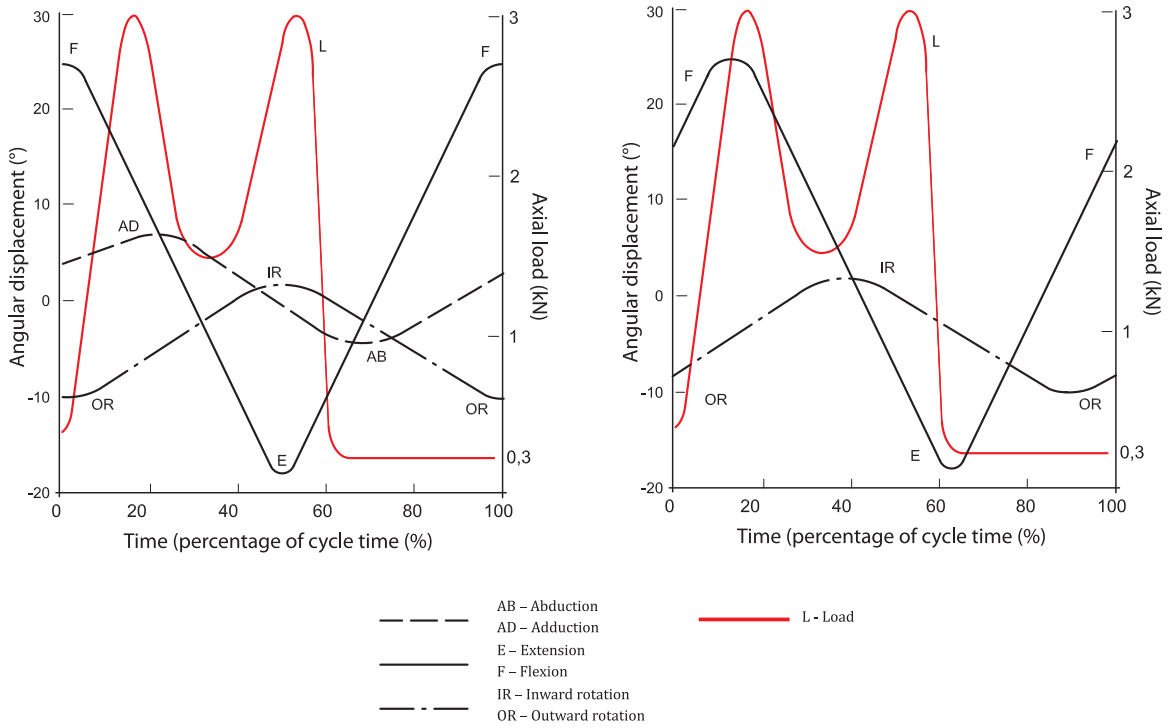


**Fig. 2.** Variation with time of angular movement and load to be applied to the femoral test specimen.

articulating components was heated to 37 °C with accuracy of ± 2 °C according to the ISO 14242-1 using heating elements in the containment's bed. This heating design was notably less complicated than commercially used circulating systems with external heating chamber and peristaltic pump ensuring smaller fluid temperature fluctuations during testing. A fresh batch of fluid was prepared for each test sample and used for the whole duration of the samples testing. The whole test period of each sample was shorter than the recommended lifespan of the fluid disclosed in ISO 14242-1.

The simulator ran for total of 50,000 gait cycles with series of measurements in the initial brand-new state and then after every 10,000 gait cycles to observe development of cup wear and deformations (Fig. 3). The test interval was chosen to cover the initial run-in phase with a quick development of an early creep whereas volumetric loss of UHMWPE in this period is negligible.

Measurement of friction coefficient as well as evaluation of surface texture changes of both components followed right after each testing segment. The friction coefficient was measured on a pendulum simulator (Vrbka et al., 2015) with the articulating pair being the joint between stationary and winging frame of the pendulum and calculated from curve of slowdown of pendulum oscillations. The components were oriented in the same way as in the hip simulator while the swinging motion of pendulum had the same orientation as F/E motion with an amplitude of 16°. The model-synovial fluid was transferred from the hip simulator (and heated in the similar matter) as well to match the conditions during the loading period on the hip simulator. The friction coefficient was measured 5 times at each stage of each tested cup. Condition of a cup's bearing surface was observed by optical microscopy while femoral head was inspected on an optical interferometry profilometer (Bruker Contour GT-X8). Optical profilometry measurements in multiple positions of the head allowed to create a Ra roughness map of the heads surface (Fig. 4). The degradation of both articulating components was also assessed using Scanning Electron Microscopy (SEM) for a detailed view of the surface changes. The combined back-scattering electron detection and secondary electron emission detection methods were used as well as gold sputter deposition (< 25 nm layer) on the cups surface to prevent charging of the cup and severe artifacts on the resulting images.

Cup deformations measurements were always delayed by 12 h after the simulator testing period to allow the elastic part of creep deformations to relax. This approach should ensure that only the permanent creep deformations were measured. The measurement was based on an active fringe projection and triangulation using the 3D scanning method. Using this approach ensures that the measurements are not dependent on environmental factors during the measurements (GOM mbH). For measurement of the acetabular cups, the reference points with a diameter of 0.8 mm were positioned on the non-measured surface. The measurement was carried out with MV170 lenses with a measurement volume of 170 × 130 × 130 mm calibrated in a small object arrangement. The lenses complied with standard (VDI/VDE2634-3, 2014). Parameters of scanning method and conditions of measurement including calibration are shown in Table 1 (Ranuša et al., 2016; Palousek et al., 2015).

As this method requires a matte surface finish of the scanned object, the semi-glossy finish of the bearing surface was covered with a matte coating. A solution of $TiO_2$ in isopropyl alcohol (1:12 ratio) was applied using an airbrush gun. The thickness of such coating was previously stated to be less than 0.003 mm. After the acetabular cups were 3D scanned at each stage of testing, the 3D scans were transferred from a point cloud to meshes and then were compared to reference geometry as the initial brand-new state of the cups. A map of spatial surface deviations between the initial state and each testing stage was created. The matte coating was then thoroughly removed from the acetabular cup by multi-stage cleaning process based on ISO 14242-2 ensuring removal of loose $TiO_2$ particles from the cups surface. This process also served as overall cleaning of the samples before starting a new stage of simulator testing. The procedure of geometry validation is detailed described in previous research (Ranuša et al., 2016). Validation process was performed on 3 new acetabular cups in 8 stages of partial wear. Wear was performed by articulating metal head on hip pendulum simulator. Wear rate corresponded with wear rate in human body (range 51.80–1119.70 $mm^3$). Gravimetric and scanning method was compared and a result of measurement was recalculated by density. Final accuracy of method was between 2.2 and 4.2 $mm^3$. Repeatability of method

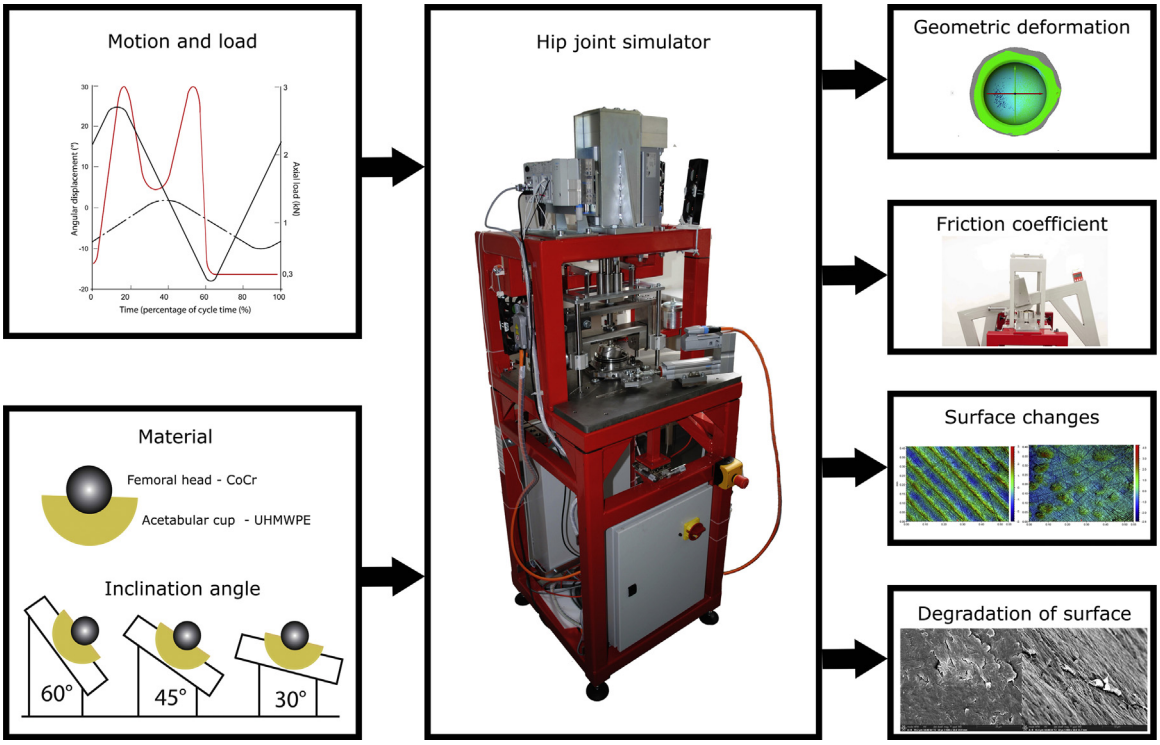


**Fig. 3.** Scheme of valuation algorithm.

was declared as 0.005 mm. Validation of method was also mentioned in study (Dold et al., 2014) where was used for acetabular shell measurement.

## 3. Results

### 3.1. Deformation of cup's bearing surface

Three main deformation regions of cup's bearing surface could be distinguished. The first one being region affected directly by head's penetration with most profound compression deformations. Position of this oval-shaped region was aligned with direction of applied force, moving closer to the superior quadrant of acetabular rim with increasing inclination angle. Though even in case of 60° inclination specimen, being the highest tested inclination, this deformation region did not involve cup's rim itself. The maximal measured penetration of femoral head into acetabular cup ranged from 0.03 mm to 0.05 mm at 50,000 cycles being slightly more profound in 30° and 60° inclination specimens than in the 45° inclination specimen (Fig. 5).

**Table 1**
Accuracy of used scanning method.

| *Parameters of 3D scanning method and ATOS III Triple scan* | |
|---|---|
| Repeatability of method (Ranuša et al., 2016) | 0.005 mm |
| Point distance of measured points on surface | 0.055 mm |
| Camera pixels | 2 × 8 Mpx |
| Image Sensor KAI-08050 resolution | 3296 × 2472 px |
| Calibration results (170 × 130 × 130 mm) | 0.001 mm |
| Angles of cameras | 27.2° |
| Temperature | 24 °C |
| Diameter of reference points | 0.8 mm |

The region of most profound deformations was surrounded by region of shallow compression deformations ranging up to the inferior quadrant of the cup's rim. The development of compressive deformation

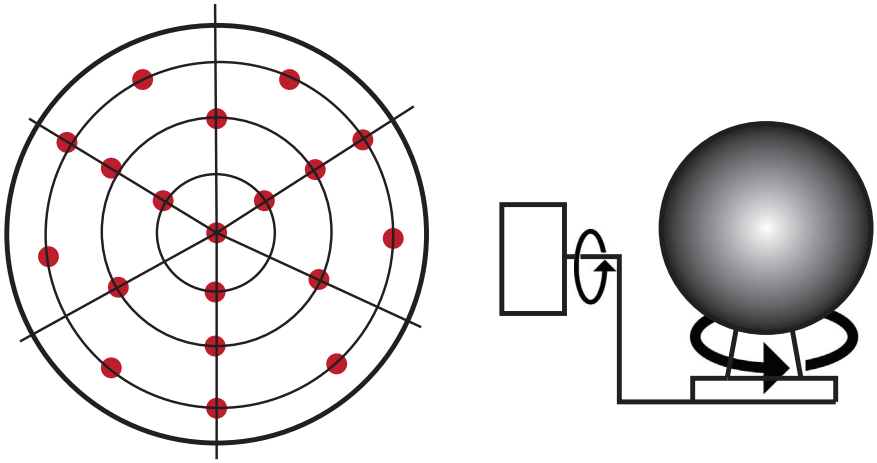

**Fig. 4.** Pattern of measured on femoral head in polar coordinate system.

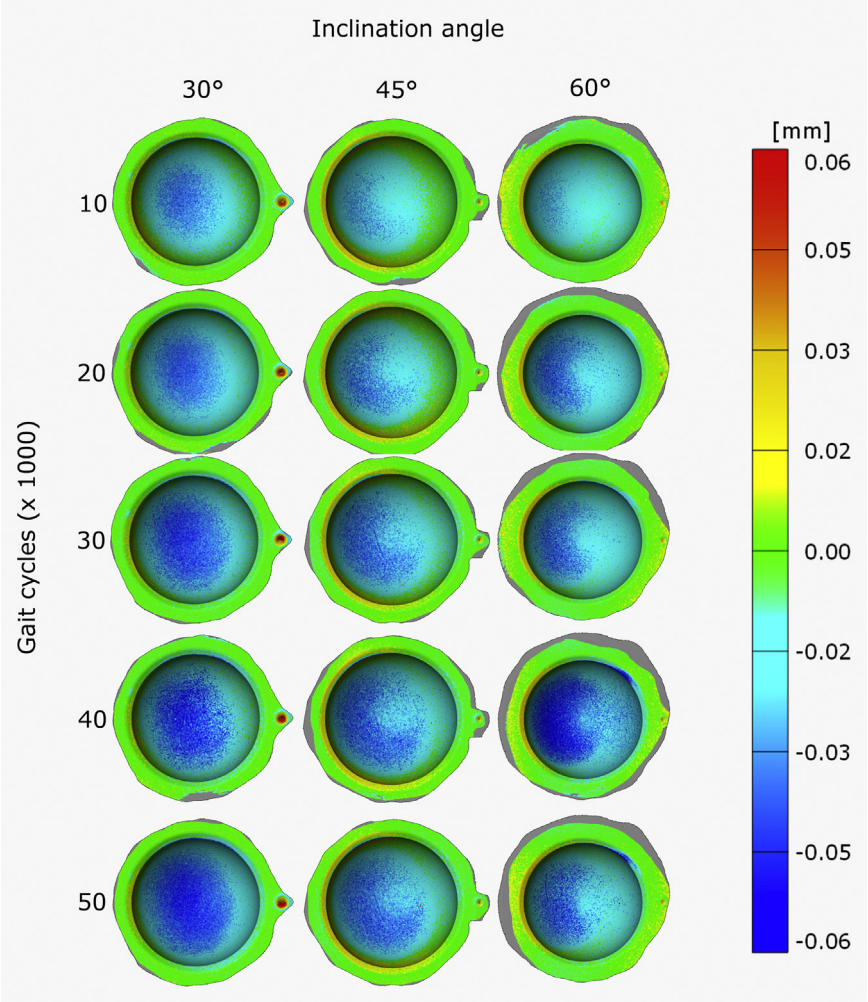


**Fig. 5.** Deformation regions of cup's bearing surface.

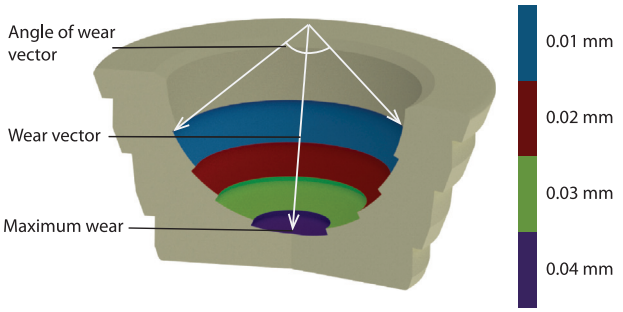


**Fig. 6.** Pattern of measured on femoral head in polar coordinate system.

took place in the first 20,000–40,000 gait cycles depending on the acetabular inclination. After this initial period, there was no significant increase of area or depth of the compressed zone (Fig. 6). The 60° inclination specimen showed the largest area affected by compressive deformation, occupying 77% of the cups bearing surface. The smallest compressed area was on the other hand observed on the 45° inclination specimen occupying only 51% of the cups bearing surface (Fig. 7).

The third region of deformation was located in the posterior-superior quadrant of acetabular rim (Fig. 8). While the previous two regions showed compression deformations this area was on contrary elevated above the reference geometry. The area affected by elevation was considerably smaller than in case of compression deformation. Position of the elevated area depended on the inclination angle, similarly as in case of the first mentioned region. The elevated area included part of rim and front face of acetabular cup in case of all three specimens. With increasing inclination angle the area spread more to the front face of the cup. Maximal elevation ranged from 0.02 mm to 0.03 mm. In contrast with compressive deformations, the elevation area was considerably bigger in case of mid inclination specimen (45°) than in uttermost inclination specimens, occupying 16% of the bearing surface. The elevated area of the 30° and 60° inclination specimens was considerably smaller, occupying 4–6% of the bearing surface. Development of elevation deformation was even steeper than in case of the compressive deformation. The whole deformed volume was measured after the first 10,000 gait cycles, with minimal increase of elevation afterwards.

### 3.2. Degradation of bearing surfaces

Brand new acetabular cups had spherical articulating surface with distinctive circular marks from manufacturing process. During the first 10,000–20,000 gait cycles were these marks evened out to smooth finish via articulating with femoral head. Development of fine multidirectional scratches was observed up to 50,000 gait cycles via optical microscopy replacing the initial structure of the cup's bearing surface. The smoothened zone was aligned with load applied during testing and covered the approximate area of the previously mentioned first region of the most profound deformations. In contrast to that, fine scratching was developed in considerably larger area going beyond the smoothened region.

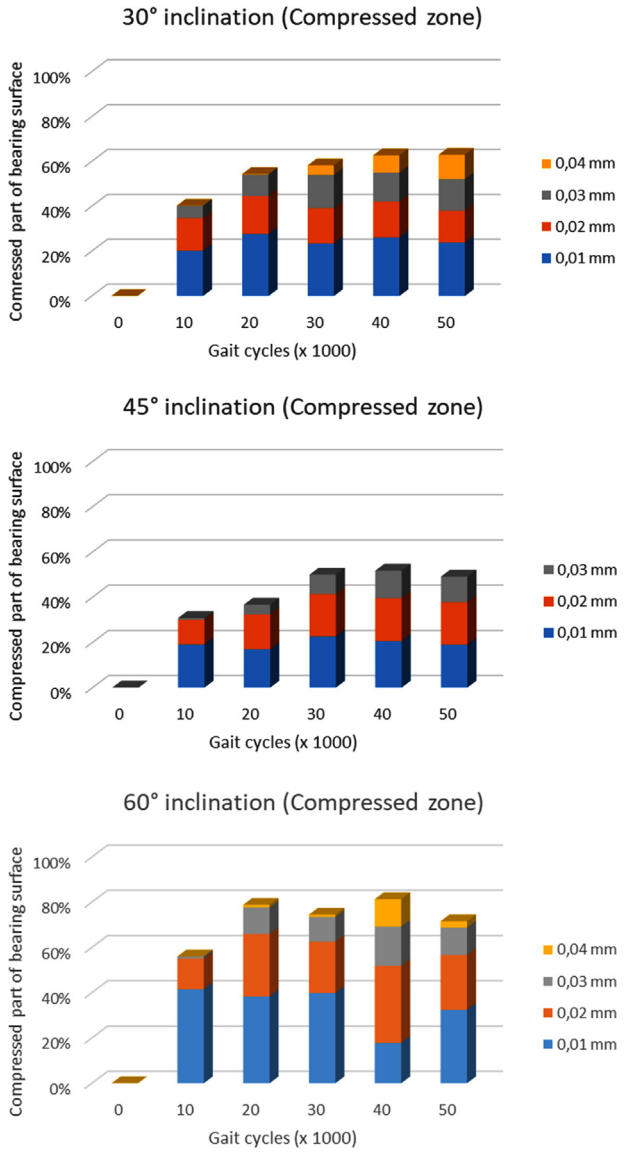


**Fig. 7.** Depth of the compressed zone.

A state of femoral head's surface during the testing was assessed by measuring the surface roughness at each 10,000-gait cycle stage of testing. Two main trends could be distinguished between the three tested specimens. The two higher inclination angle specimens (45° and 60°) showed similar steady increase of roughness from average Ra of 10.2–11.2 nm at initial measurement to the final measurement Ra of 12.7–13.0 nm. The main factor contributing to surface degradation was development of occasional fine multi-directional scratching similar to one observed on cups' surface, in addition small pits on the head's surface were observed. This kind of surface degradation resembles carbide wear pattern where fine scratching is caused by third body particles in form of carbides deliberating from head's surface (Wong et al., 2013). On the contrary the lowest inclination angle specimen (30°) showed decrease of the initial roughness from Ra 9.0 nm to Ra 7.7 nm during the first 20,000 gait cycles. There was no notable change of the roughness in the following 30,000 tested gait cycles and there were almost no fine scratches compared to the remaining specimens. Overall changes in Ra were insignificant, being well under the 20 nm Ra threshold to affect wear rates or joint friction significantly (Sorimachi et al., 2009; Wong et al., 2013).

In-depth observation of cup's surface via SEM after finishing 50,000 gait cycles showed various kinds of surface structure and its degradation (Fig. 9). The non-deformed areas showed persisting circular machining marks from cups manufacturing process. At the edges of the compressed area, there was apparent smoothing of machining marks and development of abrasive degradation of the surface in form of previously mentioned multidirectional scratching. There was apparent adhesive degradation in form of flaking of the plasticity-induced damage layer, in the area of deepest compressive deformations, previously marked as smoothened. While no notable delamination of the cup's surface was observed after the tested 50,000 cycles, the complete detachment of the partly severed flakes of the damage layer was likely to be imminent. Moreover the size of flakes of approximately 5–20 μm is similar to the'flake' shape wear debris extracted in vivo (Hongtao et al., 2011).

### 3.3. Friction coefficient

The most significant changes of friction coefficient were measured in the first 10,000 gait cycles. In the initial brand-new state, all three specimens had similar average friction coefficient ranging from 0.136 to 0.156. In case of 30° and 45° inclination specimens, there was a notable increase of friction coefficient ranging from 0.163 to 0.171. The third specimen of 60° inclination on the contrary showed decrease of friction coefficient from 0.149 to 0.129 during the first 10,000 gait cycles. After these 10,000 gait cycles, friction coefficients of all three specimens stabilized and showed no significant changes during the rest of tested period. The 45° showed the highest friction coefficient ranging from 0.163 to 0.171 for the rest of the test period. The friction coefficient of 30° specimen was slightly lower ranging from 0.152 to 0.164. The 60° inclination specimen showed by far the lowest friction coefficient ranging from 0.129 to 0.140 (Fig. 10). There was no correlation between development of friction coefficient and slight changes of the heads surface roughness leading to assumption that friction coefficient is not susceptible to such minor changes of femoral head's roughness. Inverse proportionality was however found between the area of compressive deformations and coefficient of friction. This suggests that larger contact areas with smaller maximal contact stress is beneficial for reducing the friction coefficient.

## 4. Discussion

The measured maximal depths of compressive creep deformation (0.04–0.05 mm) are generally on the lower end of those predicted by previous studies (0.032–0.09 mm) carried out on cups with similar inner diameter and shell thickness (Bevill et al., 2005; Liu et al., 2012; Penmetsa et al., 2006). This supports usage of creep model parameters taken over from static creep tests for purpose of creep depth measurements. Neglecting the elastoplastic nature of creep deformations in favour of purely plastic creep model, however, could be the cause of the slightly more profound deformations of these analyses compared to this study.

The bearing surface area affected by deformation was on contrary notably larger than in previous studies. This could be caused by omitting the cross-shear factor in creep model in previous FEM studies. Only in study (Liu et al., 2012) was made first attempt to include cross shear loading to creep model and indeed the surface area affected by creep deformations was closest to the one observed in this study. In case of simulator studies there was also usually no mutual motion of bearing surfaces at all to isolate the creep from wear, but those focused mainly on depth of creep deformation rather than size of affected area.

Gait cycle loading, according to ISO 14242 used in this study is cyclic with minimally loaded "swing" phase taking nearly 40% of the cycle and potentially allowing some elastic strain relaxation in a short-term horizon. In addition, our study's testing design with short periods of 10,000 gait cycles and 12-h relaxation intermissions were closer to the real-life usage of the hip joint and allowed additional relaxations between stages of simulator loading. The relaxation periods allowed not

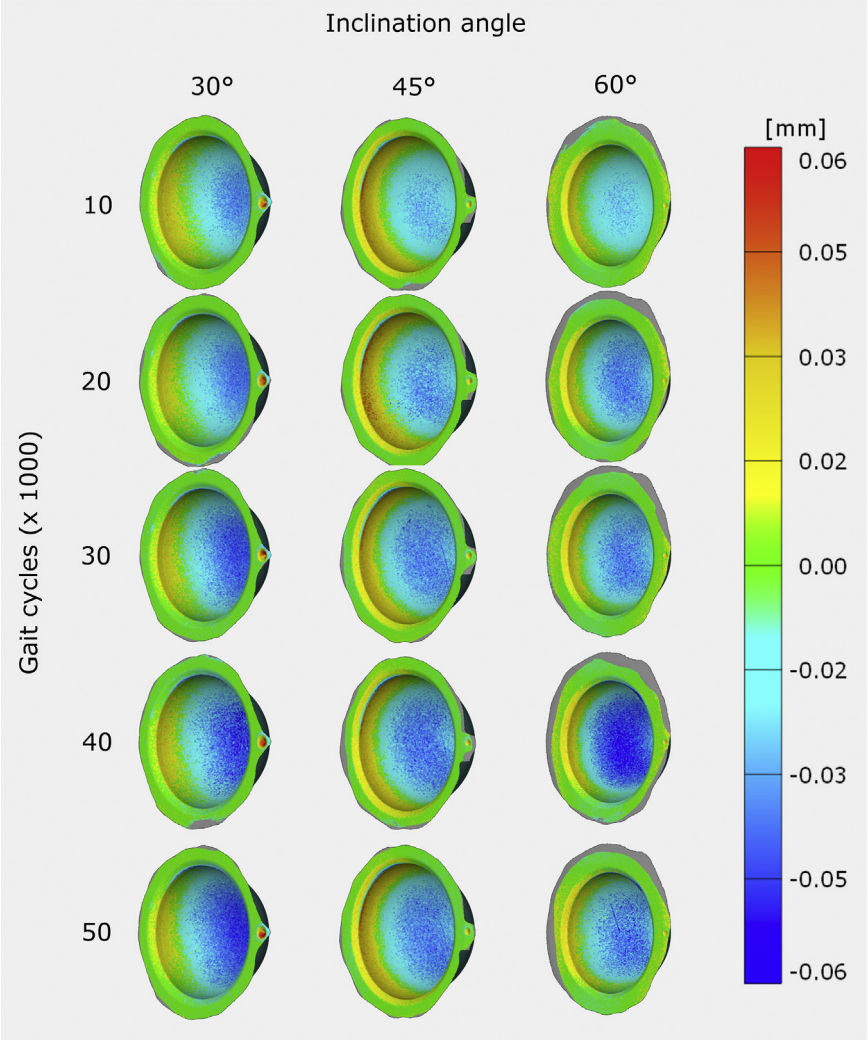


**Fig. 8.** Posterior-superior quadrant of acetabular rim.

only to observe just the irreversible plastic creep deformation, but cyclic applying and relaxing of the elastic strain could enhance the process of strain-induced recrystallization of UHMWPE and enhance lamellae alignment perpendicularly to the applied load (Meyer and Pruitt, 2001). The increased crystallinity and aligned crystalline phase increase the elastic modulus hence improve the creep resistance. On the other hand, an increased elastic modulus increases maximal value of the Hertz contact stress, making the acetabular cup prone to fracture and delamination.

This theory is supported by rather steep development of creep deformations compared to previous studies. Measured deformations fully developed in first 20,000 gait cycles in case of 60° inclination sample, in 30,000 gait cycles in case of 45° inclination sample and in 40,000 cycles in case of 30° inclination sample. After this period of initial development, the creep deformation stagnated with no significant growth in either depth of penetration or size of the affected area. Therefore, the correlation can be found between the pace of creep development and the inclination angle. This is probably caused by a higher maximal contact stresses at higher inclination angle as the head's coverage decreases (Patil et al., 2003).

The area of elevated superior quadrant of acetabular rim was not previously addressed thoroughly. The location of the elevated part of the rim is aligned with predicted distribution of contact stress predicted by previous FEM study (Hua et al., 2016). On the other hand, this area was not addressed as elevated in any of the previous creep studies. This elevation was presumably consequent to compressive stress caused by femoral head which tended to relax in direction of the least head coverage being the acetabular rim and therefore pushed the acetabular rim towards the femoral head. This elevated rim decreases the radial clearance of the hip replacement and it is highly probable that it carries a part of contact load as at least the 45° inclination sample tested in this study showed marks of wear similar to the compressed area. However, it is not full clear why was the elevation most significant in the mid inclination sample. It is possible that the orientation of the elevation was aligned towards the acetabular rim as the weak spot. On the other hand, the 30° inclination angle was oriented more towards the bearing surface and the 60° inclination sample towards the front face of the cup. It is interesting to note that the borderline of elevated region is very similar to the acetabular rim fractures that occurred in clinical practice. The deformed elevated rim can be one of the causes of this phenomenon because in nonstandard situations, when the vector of reactionary force in hip joint points towards the superior quadrant, an extensive load is carried solely by the elevated region, which represents only a fraction of the cup's normal bearing surface.

Coefficient of friction measurements show that the bearing surfaces adjust to each other within the first 10,000 gait cycles. The process involves evening out the machining marks of the acetabular cup, thus decreasing the initial roughness of the cups bearing surface and also steep initial creep deformations of the cups bearing surfaces. The period of first 10,000 gait cycles therefore shows notable friction coefficient

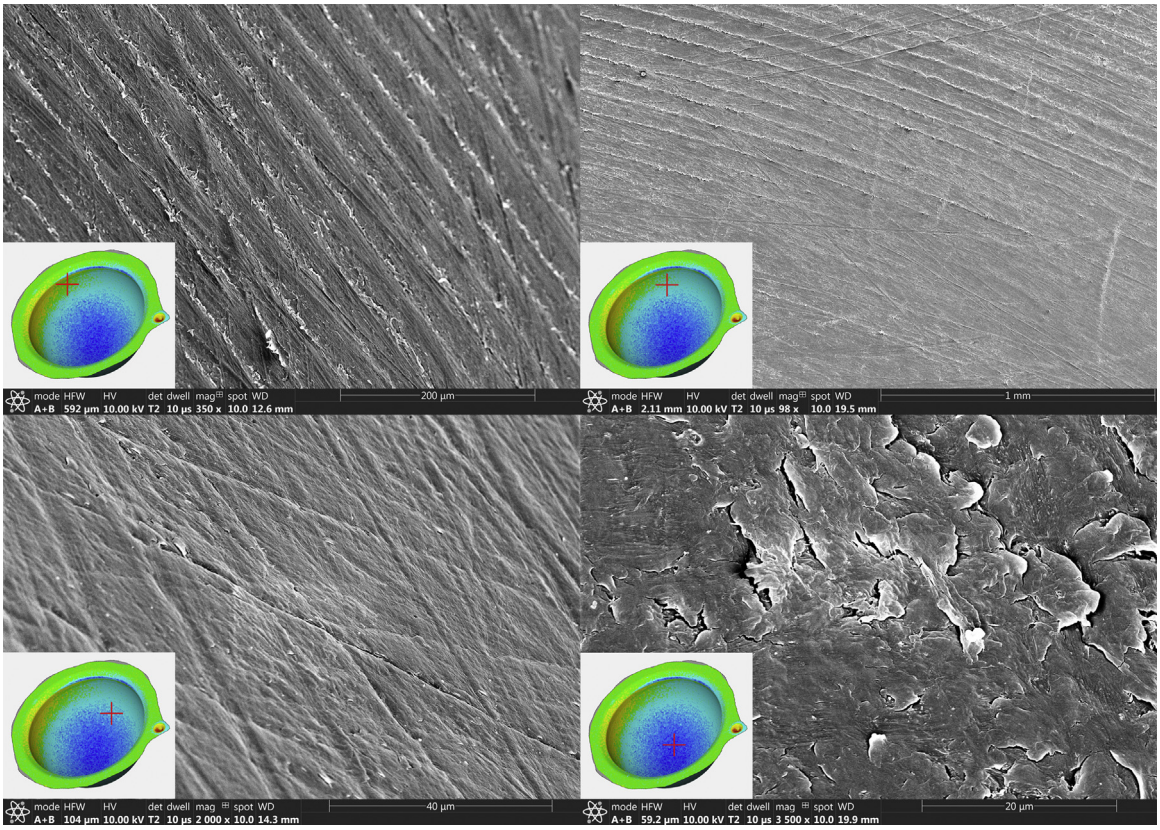


**Fig. 9.** Observation of cup's surface via SEM.

changes (Fig. 10). After this period, the coefficient of friction shows no significant changes, which suggests, that from the biotribology point of view is run in phase completed in the first 10,000 gait cycles.

After smoothening of the surface, an initial phase of abrasive degradation occurs, caused by harder particles released presumably from the head. The particles were identified by the SEM on the head's surface in smaller amounts, possibly due to leaking particles from contact area caused by lubricants. Alternatively, the particles could had been removed during preparations of sample together with the $TiO_2$ matte coating. Further development of abrasive degradation is not that important with no significant changes of roughness on the observed areas and with no significant changes of the friction coefficient.

Beginning of the delamination of polyethylene cup in pressured areas was in form of partly severed flakes and that was demonstrated via the SEM measurements after the first 50,000 cycles (Fig. 9.). Therefore, the first significant load of the periprosthetic environment by polyethylene particles is imminent shortly after the period tested in this study. This early sign of delamination may be consequent to cyclic deformation/relaxation induced morphological changes of polyethylene as mentioned before.

This study has its limitations. Conventional polyethylene cups were used as test samples, while nowadays XLPE acetabular cups are more common. Process of the crosslinking itself doesn't affect creep mechanism, not nearly as much as wear resistance though (Estok et al., 2005; Takahashi et al., 2016). There are however parameters affecting creep such as head/cup size and thickness of liner which were not considered in this study. While this study provides a baseline for creep measurements in the run-in phase, it would be beneficial to carry out more extensive measurements with cups of different inner diameters, different liner thicknesses and from different manufacturers in the future.

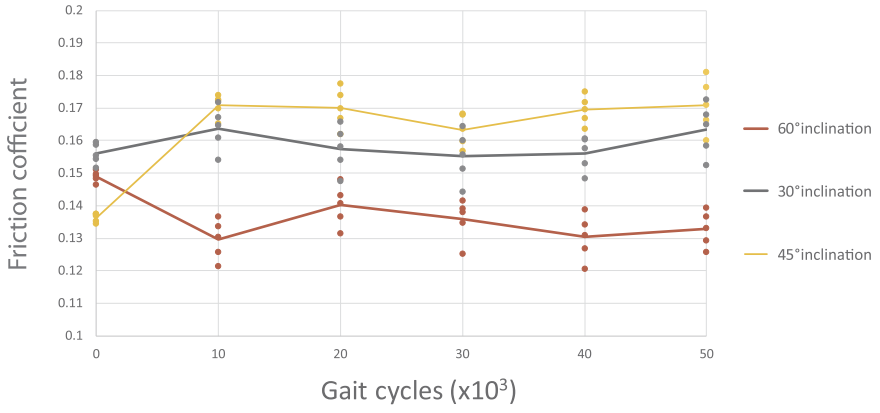


**Fig. 10.** Friction coefficient development.

## 5. Conclusion

The present study examines three effects: the effect of cup position on (1) deformation of the cups' bearing surface, (2) degradation of the bearing surface, and (3) friction coefficient development. The results show that:

1. The initial plastic transformation of liner geometry is strongly influenced by the inclination angle of the liner in pelvis. Angles around 45° showed the smallest deformation, as supported by FEM studies depicting the contact stress distribution. The deformation then increases with both the increasing and decreasing angle. On the other hand, the 45° inclination angle showed significantly larger elevated areas of the rim, with rim being one of the s main weak spots, where liner fractures occur frequently.
2. Roughness of the liners' surface was smoothed in the initial phase and subsequently scratches caused by third body particles released from metallic head occurred. Creep deformation development period was observed for up to 40,000 gait cycles. Flake-shaped delamination of the surface and first material loosening followed afterwards. The size of flakes of approximately 5–50 μm is similar to the'flake' shape wear debris extracted in vivo.
3. Friction coefficient of the THA components was changing during the first 10,000 cycles. After this phase, the friction coefficient values showed no significant changes. The inclination angle of 45° showed the highest friction coefficient (from 0.163 to 0.171) and the inclination angle of 60° showed the lowest friction coefficient (from 0.129 to 0.140).

## Acknowledgements

This research was carried out under the project LTAUSA17150 with financial support from the Ministry of Education, Youth and Sports of the Czech Republic.

## References

Affatato, S., Zanini, F., Carmignato, S., 2017. Quantification of wear and deformation in different configurations of polyethylene acetabular cups using micro X-ray computed tomography. Materials 10, 259. https://doi.org/10.3390/ma10030259.

Affatato, S., Zavalloni, M., Taddei, P., Di Foggia, M., Fagnano, C., Viceconti, M., 2008. Comparative study on the wear behaviour of different conventional and cross-linked polyethylenes for total hip replacement. Tribol. Int. 41, 813–822. https://doi.org/10.1016/j.triboint.2008.02.006.

Ali, M., Al-Hajjar, M., Partridge, S., Williams, S., Fisher, J., Jennings, L.M., 2016. Influence of hip joint simulator design and mechanics on the wear and creep of metal-on-polyethylene bearings. Proc. Inst. Mech. Eng. H 230, 389–397. https://doi.org/10.1177/0954411915620454.

Bevill, S.L., Bevill, G.R., Penmetsa, J.R., Petrella, A.J., Rullkoetter, P.J., 2005. Finite element simulation of early creep and wear in total hip arthroplasty. J. Biomech. 38, 2365–2374. https://doi.org/10.1016/j.jbiomech.2004.10.022.

Bobman, J.T., Danoff, J.R., Babatunde, O.M., Zhu, K., Peyser, K., Geller, J.A., Gorroochurn, P., Macaulay, W., 2016. Total hip arthroplasty functional outcomes are independent of acetabular component orientation when a polyethylene liner is used (e3). J. Arthroplast. 31, 830–834. https://doi.org/10.1016/j.arth.2015.10.022.

Cowie, R.M., Carbone, S., Aiken, S., Cooper, J.J., Jennings, L.M., 2016. Influence of third-body particles originating from bone void fillers on the wear of ultra-high-molecular-weight polyethylene. Proc. Inst. Mech. Eng. Part H J. Eng. Med. 230, 775–783. https://doi.org/10.1177/0954411916651461.

Dold, P., Bone, M.C., Flohr, M., Preuss, R., Joyce, T.J., Deehan, D., Holland, J., 2014. Validation of an optical system to measure acetabular shell deformation in cadavers. Proc. Inst. Mech. Eng. Part H-J. Eng. Med. 228, 781–786. https://doi.org/10.1177/0954411914546562.

Del Schutte J., H., Lipman, A.J., Bannar, S.M., Livermore, J.T., Ilstrup, D., Morrey, B.F., 1998. Effects of acetabular abduction on cup wear rates in total hip arthroplasty. J. Arthroplast. 13, 621–626. https://doi.org/10.1016/S0883-5403(98)80003-X.

Ebramzadeh, E., Sangiorgio, S.N., Lattuada, F., Kang, J.-S., Chiesa, R., McKellop, H.A., Dorr, L.D., 2003. Accuracy of measurement of polyethylene wear with use of radiographs of total hip replacements. J. Bone Jt. Surg. Am. 85–A, 2378–2384.

Estok, D.M., Bragdon, C.R., Plank, G.R., Huang, A., Muratoglu, O.K., Harris, W.H., 2005. The measurement of creep in ultrahigh molecular weight polyethylene: a comparison of conventional versus highly cross-linked polyethylene. J. Arthroplast. 20, 239–243. https://doi.org/10.1016/j.arth.2004.08.008.

Gallo, J., Juranova, J., Svoboda, M., Zapletalova, J., 2017. Excellent AUC for joint fluid cytology in the detection/exclusion of hip and knee prosthetic joint infection. Biomed. Pap. – Olomouc 161, 310–319. https://doi.org/10.5507/bp.2017.021.

Galvin, A.L., Jennings, L.M., Tipper, J.L., Ingham, E., Fisher, J., 2010. Wear and creep of highly crosslinked polyethylene against cobalt chrome and ceramic femoral heads. Proc. Inst. Mech. Eng. Part H J. Eng. Med. 224, 1175–1183. https://doi.org/10.1243/09544119JEIM741.

Gibon, E., Córdova, L.A., Lu, L., Lin, T.-H., Yao, Z., Hamadouche, M., Goodman, S.B., 2017. The biological response to orthopedic implants for joint replacement. II: polyethylene, ceramics, PMMA, and the foreign body reaction. J. Biomed. Mater. Res. Part B Appl. Biomater. 105, 1685–1691. https://doi.org/10.1002/jbm.b.33676.

GOM, b.r. GOM mbH. ATOS – Industrial 3D Scanning Technology.

Green, T.R., Fisher, J., Stone, M., Wroblewski, B.M., Ingham, E., 1998. Polyethylene particles of a 'critical size' are necessary for the induction of cytokines by macrophages in vitro. Biomaterials 19, 2297–2302. https://doi.org/10.1016/S0142-9612(98)00140-9.

Halma, J.J., Señaris, J., Delfosse, D., Lerf, R., Oberbach, T., van Gaalen, S.M., de Gast, A., 2014. Edge loading does not increase wear rates of ceramic-on-ceramic and metal-on-polyethylene articulations. J. Biomed. Mater. Res. Part B Appl. Biomater. 102, 1627–1638. https://doi.org/10.1002/jbm.b.33147.

Hongtao, L., Shirong, G., Shoufan, C., Shibo, W., 2011. Comparison of wear debris generated from ultra high molecular weight polyethylene in vivo and in artificial joint simulator. Wear 271, 647–652. https://doi.org/10.1016/j.wear.2010.11.012.

Hua, X., Li, J., Jin, Z., Fisher, J., 2016. The contact mechanics and occurrence of edge loading in modular metal-on-polyethylene total hip replacement during daily activities. Med. Eng. Phys. 38, 518–525. https://doi.org/10.1016/j.medengphy.2016.03.004.

Choudhury, D., Ranusa, M., Fleming, R.A., Vrbka, M., Krupka, I., Teeter, M.G., Goss, J., Zou, M., 2018. Mechanical wear and oxidative degradation analysis of retrieved ultra high molecular weight polyethylene acetabular cups. J. Mech. Behav. Biomed. Mater. 79, 314–323.

Ingham, E., Fisher, J., 2000. Biological reactions to wear debris in total joint replacement. Proc. Inst. Mech. Eng. Part H J. Eng. Med. 214, 21–37. https://doi.org/10.1243/0954411001535219.

Kang, J.S., Park, S.R., Ebramzadeh, E., Dorr, L.D., 2003. Measurement of polyethylene wear in total hip arthroplasty – accuracy versus ease of use. Yonsei Med. J. 44, 473–478.

Korduba, L.A., Essner, A., Pivec, R., Lancin, P., Mont, M.A., Wang, A., Delanois, R.E., 2014. Effect of acetabular cup abduction angle on wear of Ultrahigh-Molecular-weight polyethylene in hip simulator testing. Am. J. Orthop. 43, 466–471.

Liu, F., Fisher, J., Jin, Z., 2012. Computational modelling of polyethylene wear and creep in total hip joint replacements: effect of the bearing clearance and diameter. Proc. Inst. Mech. Eng. Part J J. Eng. Tribol. 226, 552–563. https://doi.org/10.1177/1350650112441908.

Lord, J.K., Langton, D.J., Nargol, A.V.F., Joyce, T.J., 2011. Volumetric wear assessment of failed metal-on-metal hip resurfacing prostheses. Wear 272, 79–87. https://doi.org/10.1016/j.wear.2011.07.009.

Meyer, R.W., Pruitt, L.A., 2001. The effect of cyclic true strain on the morphology, structure, and relaxation behavior of ultra high molecular weight polyethylene. Polymer 42, 5293–5306. https://doi.org/10.1016/S0032-3861(00)00626-1.

Milošev, I., Kovač, S., Trebše, R., Levašič, V., Pišot, V., 2012. Comparison of ten-year survivorship of hip prostheses with use of conventional polyethylene, metal-on-metal, or ceramic-on-ceramic bearings. J. Bone Jt. Surg. 94, 1756–1763. https://doi.org/10.2106/JBJS.J.01858.

Muratoglu, O.K., Greenbaum, E.S., Bragdon, C.R., Jasty, M., Freiberg, A.A., Harris, W.H., 2004. Surface analysis of early retrieved acetabular polyethylene liners. J. Arthroplast. 19, 68–77. https://doi.org/10.1016/j.arth.2003.08.003.

Niemczewska-Wójcik, M., Piekoszewski, W., 2017. The surface texture and its influence on the tribological characteristics of a friction pair: metal–polymer. Arch. Civ. Mech. Eng. 17, 344–353. https://doi.org/10.1016/j.acme.2016.10.011.

Palousek, D., Omasta, M., Koutny, D., Bednar, J., Koutecky, T., Dokoupil, F., 2015. Effect of matte coating on 3D optical measurement accuracy. Opt. Mater. 40, 1–9. https://doi.org/10.1016/j.optmat.2014.11.020.

Patil, S., Bergula, A., Chen, P.C., Colwell, C.W., D'Lima, D.D., 2003. Polyethylene wear and acetabular component orientation. J. Bone Jt. Surg. 85, 56–63.

Penmetsa, J.R., Laz, P.J., Petrella, A.J., Rullkoetter, P.J., 2006. Influence of polyethylene creep behavior on wear in total hip arthroplasty. J. Orthop. Res. 24, 422–427. https://doi.org/10.1002/jor.20042.

Ranuša, M., Gallo, J., Hobza, M., Vrbka, M., Nečas, D., Hartl, M., 2017. Wear and roughness of bearing surface in retrieved polyethylene Bicon-Plus cups. Acta Chir. Orthop. Traumatol. Cech. 84, 159–167.

Ranuša, M., Gallo, J., Vrbka, M., Hobza, M., Paloušek, D., Křupka, I., Hartl, M., 2016. Wear analysis of extracted polyethylene acetabular cups using a 3D optical scanner. Tribol. Trans. 60, 437–447. https://doi.org/10.1080/10402004.2016.1176286.

Rijavec, B., Košak, R., Daniel, M., Kralj-Iglič, V., Dolinar, D., 2014. Effect of cup inclination on predicted contact stress-induced volumetric wear in total hip replacement. Comput. Methods Biomech. Biomed. Eng. 5842, 1–6. https://doi.org/10.1080/10255842.2014.916700.

Scheerlinck, T., 2014. Cup positioning in total hip arthroplasty. J. Bone Jt. Surg. 98, 108–116. https://doi.org/10.2106/JBJS.N.00753.

Sorimachi, T., Clarke, I.C., Williams, P.A., Gustafson, A., Yamamoto, K., 2009. Third-body abrasive wear challenge of 32 mm conventional and 44 mm highly crosslinked polyethylene liners in a hip simulator model. Proc. Inst. Mech. Eng. Part H J. Eng. Med. 223, 607–623. https://doi.org/10.1243/09544119JEIM562.

Takahashi, Y., Tateiwa, T., Shishido, T., Masaoka, T., Kubo, K., Yamamoto, K., 2016. Size and thickness effect on creep behavior in conventional and vitamin E-diffused highly crosslinked polyethylene for total hip arthroplasty. J. Mech. Behav. Biomed. Mater.

62, 399–406. https://doi.org/10.1016/j.jmbbm.2016.05.020.
Turell, M., Wang, A., Bellare, A., 2003. Quantification of the effect of cross-path motion on the wear rate of ultra-high molecular weight polyethylene. Wear 255, 1034–1039. https://doi.org/10.1016/S0043-1648(03)00357-0.
Uddin, M.S., 2014. Wear measurement and assessment of explanted cross-linked PE acetabular cups using a CMM. Tribol. Trans. 57, 767–777. https://doi.org/10.1080/10402004.2014.911398.
VDI/VDE2634-3, 2014. VDI/VDE 2634 Part 3, Optical 3D-measuring Systems, Part 3 – Multiple View Systems Based on Area Scanning. Fachbereich Fertigungsmesstechnik, Düsseldorf, pp. 20.
Vrbka, M., Nečas, D., Bartošík, J., Hartl, M., Křupka, I., Galandáková, A., Gallo, J., 2015. Determination of a friction coefficient for THA bearing couples. Acta Chir. Orthop. Traumatol. Cech. 82, 341–347.
Wong, W.W., Clarke, I.C., Donaldson, T.K., Burgett, M., 2013. Surface roughness of retrieved femoral heads in CoCr-polyethylene hip bearings – a retrieval assessment with 11–17 years follow-up, pp. 45–48.
Zou, L., Samarawickrama, D.Y., Jovanovski, V., Shelton, J., 2001. Measurements of sequential impressions of acetabula cups from a total hip joint replacement using a non-contact measurement system. Int. J. Mach. Tools Manuf. 41, 2023–2030. https://doi.org/10.1016/S0890-6955(01)00067-0.

# 7 CONCLUSION

Total hip replacement surgery is a standard treatment of degenerated or damaged hip joints with numbers of primary arthroplasties increasing every year. At the same time, revision surgeries caused by failed implants are increasing too; with wear being the main factor limiting the longevity of the artificial implants. Wear analysis is one of the most important sources of knowledge on the tribological processes. Complicated tribological mechanisms involving interaction of materials, lubrication, structural surface changes and geometry modifications contribute to the wear rate.

These processes are mostly investigated by in vitro testing on new samples as defined by international standards. However, this approach entails many simplifications, such neglecting the effects of lubrication and surrounding tissues and tendons or simulating the kinematic cycle by a simple gait cycle, excluding more complex movements such as jumping or walking up the stairs.

These limitations of analysis on new samples led researchers to study implants retrieved during the revision surgeries which served in the real environments. This type of analysis attempts to reconstruct processes occurring in human body during the lifecycle of the implant.

The first part of this thesis focused on measuring methods for wear analysis. Particularly, the coordinate measuring method was described in a greater detail. The coordinate measuring method was found to be used mostly for hard materials such as metal-on-metal or ceramics-on-ceramics implants. Procedures of the coordinate measuring method are described in international standards providing the advantage of comparable results across the CMM studies. An alternation of the coordinate measuring method, where the touching probe of the CMM device is replaced by an optical laser sensor was introduced as well. The method provides high resolution images. However, it is limited in its application for polyethylene liners due to a complicated reconstruction of the surface geometries with extensive surface damages.

Recent years showed first attempts to use optical methods such as laser scanner or x-ray imaging such as microCT. These new, innovative methods can contribute to a more complex wear analysis. However, there are still number or problems to be resolved, such as time efficiency, resolution of the images or post-processing of the collected data. Basic principles of these methods inspired our new approach to wear analysis.

Article A
The main goal of this thesis was to introduce a new approach to determination of volumetric wear of polyethylene liners using optical scanning methods and to evaluate this new approach in the context of the existing research.

In Appendix A we expanded the surface analysis with investigations of roughness changes across articulating surface of liners.

We found that positioning of a liner in human body can influence wear rate as well as type of changes in its surface structures. Several higher abduction angles showed impact on stability of the cup and its survival time in situ after the THR. We found that the higher was the abduction angle, the higher was the wear rate, especially for abduction angles above 50 degrees. However, the relationship between the wear rate of retrieved polyethylene liners and their survival time in situ was not clearly linear. This suggests shows the possibility of other factors influencing the wear. Several types of surface structure changes such as delamination, pitting, plastic deformation and abrasive/adhesive type of wear were found across all samples. The study is limited by low number of a single-type liners used for measurements and analysis.

Article B
A new group of retrieved samples showed changing mechanical and chemical properties such as roughness, hardness, elasticity and oxidation index with increasing wear rate. Oxidation index was significantly higher compared to a new sample and values varied across the surface. Modulus of elasticity and hardness on surface were also higher (hardness vs. elasticity ratio was lower) compared to a new polyethylene liner.

Article C

The article C investigated relationship between the acetabular cup positioning in pelvis and development of plastic deformation. Three new liners positioned in three various inclination angles chosen according to surgical requirement were investigated in their run-in phase. Results showed that the initial plastic deformation of liner geometry was strongly influenced by the inclination angle of the liner in pelvis. We found the smallest plastic deformation at the angle of 45 degrees. At higher and lower angles, the plastic deformation increased. The friction coefficient changed during the first 10 000 cycles of the simulated gait and varied with different angles. Flake shaped delamination of the surface and first material loosening followed the plastic deformation.

The main contribution of the thesis can be summarized into the following points:

- New approach of volumetric wear investigation by the optical scanning method was developed and demonstrated.
- Analysis of 23 retrieved liners was performed to identify linear and volumetric wear. The identified wear scare region was analysed by surface analysis. We found four elementary types of wear mechanisms as a delamination, plastic deformation, abrasive/adhesive and scoring occurring together with the remaining unworn areas of the original geometry.

- Mechanical changes and chemical degradation such as plastic deformations, increased oxidation index and decreasing hardness vs elasticity ratio were observed in retrieved liners.
- We confirmed experimentally the results of FEM studies predicting the contact stress distribution in relation to inclination angle. We found the smallest plastic deformations at angles around 45 degrees. At the same time these angles showed significantly larger elevated areas of the rim, with rim being one of the main weak spots, where liner fractures occur frequently.

Regarding the scientific questions and hypotheses, our findings can be summarized in following concluding remarks:

H1: The optical method will be able to approximate the original surface geometry with a better accuracy than current methods that use new lines for approximation of the original geometry and hence will be more accurate in determining the wear – in correlation with the gravimetric measurements.

*The optical scanning method was validated using the gravimetric method on new samples. The new samples were worn in 6 cycles and the resulting deviation between the methods was* 2.2 – 4.3 $mm^3$*. This method is less time consuming than the conventionally used CMM method. Another advantage of the method is the ability to develop a complex geometry built on a large number of points. This approach enables us to reconstruct the most accurate original geometry.* ***(Hypothesis H1 was confirmed).***

H2: Retrieved polyethylene liners that survived longer time in situ will show lower rate of material loss per year with no extensive changes of their surface structures.

*Relationship between the wear rate of retrieved polyethylene liners and their survival time in situ was not clearly linear. Changes of surface structures such as delamination were found both in samples with higher and lower wear rate. Several samples with abrasive/adhesive type of wear showed higher wear without extensive changes of surface structures. We defined the change of surface structure as extensive in cases when: (1) the surface roughness of the respective area was higher than the surface roughness of the unworn parts of the retrieved lines and (2) the area did not show scoring caused by manufacturing machines.* ***(Hypothesis H2 was falsified).***

H3: Retrieved liners with lower abduction angle will have lower wear rate and lower plastic deformations due to decreasing contact pressure in the articulating area.

*We tested the hypothesis on new samples during their simulated run-in phase. We found the smallest plastic deformation at the abduction angle of 45*

*degrees. At higher and lower angles, the plastic deformation increased.* ***(Hypothesis H3 was falsified).***

# 8 LIST OF PUBLICATIONS

## 8.1 Papers published in journals with impact factor

RANUŠA, M., J. GALLO, M. VRBKA, M. HOBZA, D. PALOUŠEK, I. KŘUPKA and M. HARTL. Wear Analysis of Extracted Polyethylene Acetabular Cups Using a 3D Optical Scanner. *Tribology Transaction,* 2017, 60(3), 437–447.

RANUŠA, M., J. GALLO, M. VRBKA, M. HOBZA, D. PALOUŠEK, I. KŘUPKA and M. HARTL. Wear Analysis of Extracted Polyethylene Acetabular Cups Using a 3D Optical Scanner. *Tribology and Lubrication Technology,* 2018, 74(6), 68–84.
(Same article published in different journal)

RANUŠA, M., J. GALLO, M. HOBZA, M. VRBKA, D. NEČAS, and M. HARTL. Wear and Roughness of Bearing Surface in Retrieved Polyethylene Bicon-Plus Cups. *Acta Chirurgiae Orthopaedicae et Traumatologiae Cechoslovaca,* 2017, 84(3), 159–167.

CHOUDHURY, D., M. RANUŠA, R. A. FLEMING, M. VRBKA, I. KŘUPKA, M. G. TEETER, J.GOSS and M. ZOU. Mechanical wear and oxidative degradation analysis of retrieved ultra-high molecular weight polyethylene acetabular cups. *Journal of the Mechanical Behavior of Biomedical Materials,* 2018, 79, 314-323.

ZEMAN, J., M. RANUŠA, M. VRBKA, J. GALLO, I. KŘUPKA and M. HARTL. UHMWPE Acetabular Cup Creep Deformation during the Run-in Phase of THA's Life Cycle. *Journal of the Mechanical Behavior of Biomedical Materials,* 2018, 87, 30-39.

## 8.2 Conference abstracts

HOBZA, M. and M. RANUSA. Zhodnocení typu a míry otěru u extrahovaných jamek Bicon. XXIII. Mezinárodní sympozium FREJKOVY DNY, 2015, Brno, Czech Republic.

RANUSA, M., M. VRBKA, I. KŘUPKA and M. HARTL. M. Development and Validation of an Optical Scanning Method for Volumetric Wear Analysis*. The 17*$^{th}$ *Nordic Symposium on Tribology - NORDTRIB 2016*, 2016, Hämeenlinna, Finland.

RANUSA, M., M. VRBKA, J. GALLO, I. KŘUPKA and M. HARTL. Influence of acetabular cup inclination on wear of UHMWPE liner. 6$^{th}$ *World Tribology Congress (WTC)*, 2017, Beijing, China.

RANUSA, M., M. VRBKA, J. GALLO, I. KŘUPKA and M. HARTL. Influence of Positioning Retrieved Acetabular Liners in Vivo on the Wear Rate Determined by optical scanning. 2$^{th}$ Czech-Japan Tribology Workshop, 2017, Takamatsu, Japan

RANUSA, M., J. ZEMAN, M. VRBKA, J. GALLO, I. KŘUPKA and M. HARTL. Effects of Polyethylene Acetabular Liner Orientation on Run-in-Phase Deformation. 4th International Conference on BioTribology, Montreal, Canada.

# 9 LITERATURE


1. OECD, *Health at a Glance 2017*. OECD Publishing.
2. Registry, N.J., *National Joint Registry for England, Wales and Northern Ireland*, in *14th Annual Report*. 2017. p. 202.
3. Pramanik, S., A.K. Agarwal, and K. Rai, *Chronology of total hip joint replacement and materials development.* Trends in Biomaterials & Artificial Organs, 2005. **19**(1): p. 15-26.
4. Turell, M., A. Wang, and A. Bellare, *Quantification of the effect of cross-path motion on the wear rate of ultra-high molecular weight polyethylene.* Wear, 2003. **255**(7): p. 1034-1039.
5. ISO14242-2, *ISO 14242-2, Implants for surgery-Wear of total hip-joint prostheses*, in *Part 2 - Methods of measurement*. 2000, ISO copyright office: Switzerland, CH-1211 Geneva 20. p. 5.
6. Tsai, T.-Y., et al., *In-vivo 6 degrees-of-freedom kinematics of metal-on-polyethylene total hip arthroplasty during gait.* Journal of Biomechanics, 2014. **47**(7): p. 1572-1576.
7. Pokorny, D., et al., *New Metod for Quantification of UHMWPE Wear Particles around Joint Replacements.* Acta Chirurgiae Orthopaedicae Et Traumatologiae Cechoslovaca, 2009. **76**(5): p. 374-381.
8. Zolotarevova, E., et al., *Distribution of polyethylene wear particles and bone fragments in periprosthetic tissue around total hip joint replacements.* Acta Biomaterialia, 2010. **6**(9): p. 3595-3600.
9. Shibo, W., et al., *Wear behaviour and wear debris characterization of UHMWPE on alumina ceramic, stainless steel, CoCrMo and Ti6Al4V hip prostheses in a hip joint simulator.* Journal of Biomimetics, Biomaterials, and Tissue Engineering, 2010. **7**(1): p. 7-25.
10. Dumbleton, J.H., M.T. Manley, and A.A. Edidin, *A literature review of the association between wear rate and osteolysis in total hip arthroplasty.* Journal of Arthroplasty, 2002. **17**(5): p. 649-661.
11. Oparaugo, P.C., et al., *Correlation of wear debris-induced osteolysis and revision with volumetric wear-rates of polyethylene: A survey of 8 reports in the literature.* Acta Orthopaedica, 2001. **72**(1): p. 22-28.
12. Heisel, C., M. Silva, and T.P. Schmalzried, *Bearing surface options for total hip replacement in young patients.* Journal of Bone and Joint Surgery-American Volume, 2003. **85A**(7): p. 1366-1379.

13. Oral, E., W. Ghali Bassem, and K. Muratoglu Orhun, *The elimination of free radicals in irradiated UHMWPEs with and without vitamin E stabilization by annealing under pressure.* Journal of Biomedical Materials Research Part B: Applied Biomaterials, 2011. **97B**(1): p. 167-174.
14. Kurtz, S.M., *UHMWPE Biomaterials Handbook: Ultra High Molecular Weight Polyethylene in Total Joint Replacement and Medical Devices: Third Edition*. UHMWPE Biomaterials Handbook: Ultra High Molecular Weight Polyethylene in Total Joint Replacement and Medical Devices: Third Edition. 2015: Elsevier Inc. 1-815.
15. Martell, J.M. and S. Berdia, *Determination of polyethylene wear in total hip replacements with use of digital radiographs.* Journal of Bone and Joint Surgery - Series A, 1997. **79**(11): p. 1635-1641.
16. Ebramzadeh, E., et al., *Accuracy of measurement of polyethylene wear with use of radiographs of total hip replacements.* Journal of Bone and Joint Surgery-American Volume, 2003. **85A**(12): p. 2378-2384.
17. Rahman, L., J. Cobb, and S. Muirhead-Allwood, *Radiographic methods of wear analysis in total hip arthroplasty.* Journal of the American Academy of Orthopaedic Surgeons, 2012. **20**(12): p. 735-743.
18. DeFisher, S. and E.M. Fess, *Comparison of contact and non-contact asphere surface metrology devices.* Optifab 2013, 2013. **8884**.
19. Hall, R.M., *Biomechanics - Radiographic measurement of wear in total hip arthroplasty.* Current Orthopaedics, 1998. **12**(3): p. 202-208.
20. Goldvasser, D., et al., *A New Technique for Measuring Wear in Total Hip Arthroplasty Using Computed Tomography.* Journal of Arthroplasty, 2012. **27**(9): p. 1636-1640.e1.
21. Jedenmalm, A., et al., *A new approach for assessment of wear in metal-backed acetabular cups using computed tomography: A phantom study with retrievals.* Acta Orthopaedica, 2008. **79**(2): p. 218-224.
22. Olivecrona, H., et al., *A new technique for diagnosis of acetabular cup loosening using computed tomography: Preliminary experience in 10 patients.* Acta Orthopaedica, 2008. **79**(3): p. 346-353.

23. D'Antonio, J., W. Capello, and R. Ramakrishnan, *Second-generation Annealed Highly Cross-linked Polyethylene Exhibits Low Wear*. Vol. 470. 2011. 1696-704.
24. Livermore, J., D. Ilstrup, and B. Morrey, *Effect of femoral head size on wear of the polyethylene acetabular component.* Journal of Bone and Joint Surgery - Series A, 1990. **72**(4): p. 518-528.
25. Krismer, M., et al., *EBRA: A method to measure migration of acetabular components.* Journal of Biomechanics, 1995. **28**(10): p. 1225-1236.
26. Ilchmann, T., et al., *Acetabular polyethylene wear volume after hip replacement: Reliability of volume calculations from plain radiographs.* Wear, 2012. **282–283**(0): p. 69-75.
27. McCalden, R.W., et al., *Current concepts review - Radiographic methods for the assessment of polyethylene wear after total hip arthroplasty.* Journal of Bone and Joint Surgery-American Volume, 2005. **87A**(10): p. 2323-2334.
28. Selvik, G., *Roentgen stereophotogrammetric analysis.* Acta Radiologica, 1990. **31**(2): p. 113-126.
29. Bragdon, C.R., et al., *Experimental assessment of precision and accuracy of radio stereometric analysis for the determination of polyethylene wear in a total hip replacement model.* Journal of Orthopaedic Research, 2002. **20**(4): p. 688-695.
30. Hu, X.Q., C.M. Han, and R.J.K. Wood, *A geometric method to measure the wear of hip joint.* Wear, 2011. **271**(11–12): p. 2775-2781.
31. Joyce, T.J., et al., *Quantification of self-polishing in vivo from explanted metal-on-metal total hip replacements.* Tribology International, 2011. **44**(5): p. 513-516.
32. Joyce, T.J., D.J. Langton, and A.V.F. Nargol, *A study of the wear of explanted metal-on-metal resurfacing hip prostheses.* Tribology International, 2011. **44**(5): p. 517-522.
33. Becker, A. and Y. Dirix. *Wear measurements on retrieved metal-on-metal bearings: a high accuracy 3D measurement approach*. in *Proceedings of the 55th Annual Meeting of the Orthopaedic Research Society*. 2009.
34. Morris, B., et al., *Quantifying the wear of acetabular cups using coordinate metrology.* Wear, 2011. **271**(7–8): p. 1086-1092.
35. Bills, P., L. Blunt, and X. Jiang, *Development of a technique for accurately determining clinical wear in explanted total hip replacements.* Wear, 2007. **263**(7–12): p. 1133-1137.

36. Galvin, A., et al., *Comparison of wear of ultra-high molecular weight polyethylene acetabular cups against surface-engineered femoral heads.* Proceedings of the Institution of Mechanical Engineers Part H-Journal of Engineering in Medicine, 2008. **222**(H7): p. 1073-1080.
37. Wang, L., et al., *THE DETERMINATION OF THE VOLUMETRIC WEAR FOR SURGICALLY RETRIEVED HIP IMPLANTS BASED ON CMM*. 2015.
38. Lord, J.K., et al., *Volumetric wear assessment of failed metal-on-metal hip resurfacing prostheses.* Wear, 2011. **272**(1): p. 79-87.
39. Carmignato, S., et al., *Uncertainty evaluation of volumetric wear assessment from coordinate measurements of ceramic hip joint prostheses.* Wear, 2011. **270**(9–10): p. 584-590.
40. ISO/IEC98-3, *ISO/IEC Guide 98-3, Uncertainty of measurement*, in *Part 3: Guide to the expression of uncertainty in measurement (GUM:1995)*. 2008: Switzerland, CH-1211 Geneva 20. p. 120.
41. Uddin, M.S., *Wear Measurement and Assessment of Explanted Cross-Linked PE Acetabular Cups Using a CMM.* Tribology Transactions, 2014. **57**(5): p. 767-777.
42. Chen, H.W., et al., *Volume computation for tomographic images in assessing polyethylene wear and pelvic osteolysis after total hip arthroplasty using a 3-D image reconstruction-related method*, in *2003 Ieee Nuclear Science Symposium, Conference Record, Vols 1-5*, S.D. Metzler, Editor. 2004, Ieee: New York. p. 2968-2969.
43. Bowden, A.E., S.M. Kurtz, and A.A. Edidin, *Validation of a micro-CT technique for measuring volumetric wear in retrieved acetabular liners.* Journal of Biomedical Materials Research - Part B Applied Biomaterials, 2005. **75**(1): p. 205-209.
44. Teeter, M.G., et al., *Three-Dimensional Surface Deviation Maps for Analysis of Retrieved Polyethylene Acetabular Liners Using Micro-Computed Tomography.* Journal of Arthroplasty, 2010. **25**(2): p. 330-332.
45. Zou, L., et al., *Measurements of sequential impressions of acetabula cups from a total hip joint replacement using a non-contact measurement system.* International Journal of Machine Tools and Manufacture, 2001. **41**(13–14): p. 2023-2030.
46. Rossler, T., et al., *Optical 3D methods for measurement of prosthetic wear of total hip arthroplasty: principles, verification and results.* Optics Express, 2009. **17**(15): p. 12723-12730.
47. Tuke, M., et al., *3D linear and volumetric wear measurement on artificial hip joints-Validation of a new methodology.* Precision

Engineering-Journal of the International Societies for Precision Engineering and Nanotechnology, 2010. **34**(4): p. 777-783.
48. Yun, H.H., et al., *Reliability of a PowerPoint Method for Wear Measurement After Total Hip Arthroplasty: A Retrieval Study Using 3-Dimensional Laser Scanning.* The Journal of Arthroplasty, 2012. **27**(8): p. 1530-1537.
49. Dorr, L.D. and Z. Wan, *Ten years of experience with porous acetabular components for revision surgery.* Clinical Orthopaedics and Related Research, 1995(319): p. 191-200.
50. McKellop, H.A., *The lexicon of polyethylene wear in artificial joints.* Biomaterials, 2007. **28**(34): p. 5049-5057.
51. Puloski, S.K.T., et al., *Tibial post wear in posterior stabilized total knee arthroplasty - An unrecognized source of polyethylene debris.* Journal of Bone and Joint Surgery-American Volume, 2001. **83A**(3): p. 390-397.
52. Sychterz, C.J., et al., *Wear polyethylene cups in total hip arthroplasty - A study of specimens retrieved post mortem.* Journal of Bone and Joint Surgery-American Volume, 1996. **78A**(8): p. 1193-1200.
53. Lee, C.S., et al., *Dynamic mechanical behavior of ultra-high molecular weight polyethylene irradiated with gamma rays.* Macromolecular Research, 2004. **12**(1): p. 141-143.
54. Meyer, R.W. and L.A. Pruitt, *The effect of cyclic true strain on the morphology, structure, and relaxation behavior of ultra high molecular weight polyethylene.* Polymer, 2001. **42**(12): p. 5293-5306.
55. Bevill, S.L., et al., *Finite element simulation of early creep and wear in total hip arthroplasty.* Journal of Biomechanics, 2005. **38**(12): p. 2365-2374.
56. Penmetsa, J.R., et al., *Influence of polyethylene creep behavior on wear in total hip arthroplasty.* Journal of Orthopaedic Research, 2006. **24**(3): p. 422-427.
57. Estok, D.M., et al., *The measurement of creep in ultrahigh molecular weight polyethylene - A comparison of conventional versus highly cross-linked polyethylene.* Journal of Arthroplasty, 2005. **20**(2): p. 239-243.
58. Affatato, S., N. Freccero, and P. Taddei, *The biomaterials challenge: A comparison of polyethylene wear using a hip joint simulator.* Journal of the Mechanical Behavior of Biomedical Materials, 2016. **53**: p. 40-48.

59. Edidin, A.A., et al., *Mechanical behavior, wear surface morphology, and clinical performance of UHMWPE acetabular components after 10 years of implantation.* Wear, 2001. **250**(1–12): p. 152-158.
60. Kurtz, S.M., et al., *Assessment of surface roughness and waviness using white light interferometry for short-term implanted, highly crosslinked acetabular components*, in *Crosslinked and Thermallly Treated Ultra-High Molecular Weight Polyethylene for Joint Replacements*, S.M. Kurtz, R.A. Gsell, and J. Martell, Editors. 2004. p. 41-56.
61. Trommer, R.M., et al., *Multi-Scale Evaluation of Wear in UHMWPE-Metal Hip Implants Tested in a hip Joint Simulator.* Biotribology, 2015. **4**: p. 1-11.
62. ISO14242-1, *ISO 14242-1, Implants for surgery-Wear of total hip-joint prostheses*, in *Part 1 - Loading and displacement parameters for wear-testing machines and corresponding environmental conditions for test*. 2000, ISO copyright office: Switzerland, CH-1211 Geneva 20. p. 5.
63. Wang, A. and G. Schmidig, *Ceramic femoral heads prevent runaway wear for highly crosslinked polyethylene acetabular cups by third-body bone cement particles.* Wear, 2003. **255**: p. 1057-1063.
64. Scheerlinck, T., *Cup positioning in total hip arthroplasty.* Acta Orthopaedica Belgica, 2014. **80**(3): p. 336-347.
65. Hua, X.J., et al., *The contact mechanics and occurrence of edge loading in modular metal-on-polyethylene total hip replacement during daily activities.* Medical Engineering & Physics, 2016. **38**(6): p. 518-525.
66. Patil, S., et al., *Polyethylene wear and acetabular component orientation.* Journal of Bone and Joint Surgery - Series A, 2003. **85**(SUPPL. 4): p. 56-63.
67. Halma, J.J., et al., *Edge loading does not increase wear rates of ceramic-on-ceramic and metal-on-polyethylene articulations.* Journal of Biomedical Materials Research - Part B Applied Biomaterials, 2014. **102**(8): p. 1627-1638.
68. Korduba, L.A., et al., *Effect of acetabular cup abduction angle on wear of ultrahigh-molecular-weight polyethylene in hip simulator testing.* American journal of orthopedics (Belle Mead, N.J.), 2014. **43**(10): p. 466-471.

69. Kang, J.S., et al., *Measurement of polyethylene wear in total hip arthroplasty - Accuracy versus ease of use.* Yonsei Medical Journal, 2003. **44**(3): p. 473-478.
70. Bills, P.J., et al., *Volumetric wear assessment of retrieved metal-on-metal hip prostheses and the impact of measurement uncertainty.* Wear, 2012. **274–275**(0): p. 212-219.
71. ISO14242-3, *ISO 14242-3, Implants for surgery-Wear of total hip-joint prostheses*, in *Part 3 - Loading and displacement parameters for orbital bearing type wear testing machines and corresponding environmental conditions for test*. 2000, ISO copyright office: Switzerland, CH-1211 Geneva 20. p. 5.
72. GOM. *GOM mbH, ATOS - Industrial 3D Scanning Technology*. Available from: http://www.gom.com/metrology-systems/3d-scanner.html.
73. VDI/VDE2634-3, *VDI/VDE 2634 Part 3, Optical 3D-measuring systems*, in *Part 3 - Multiple view systems based on area scanning*. 2014, Fachbereich Fertigungsmesstechnik. p. 20.
74. Palousek, D., et al., *Effect of matte coating on 3D optical measurement accuracy.* Optical Materials, 2015. **40**: p. 1-9.
75. Pezzotti, G., et al., *Confocal Raman spectroscopic analysis of cross-linked ultra-high molecular weight polyethylene for application in artificial hip joints.* Journal of biomedical optics, 2007. **12**(1): p. 014011-014011-14.
76. Kumakura, T., et al., *In-depth oxidation and strain profiles in UHMWPE acetabular cups non-destructively studied by confocal Raman microprobe spectroscopy.* Journal of Biomaterials Science, Polymer Edition, 2009. **20**(12): p. 1809-1822.
77. Milosev, I., et al., *Comparison of Ten-Year Survivorship of Hip Prostheses with Use of Conventional Polyethylene, Metal-on-Metal, or Ceramic-on-Ceramic Bearings.* Journal of Bone and Joint Surgery-American Volume, 2012. **94A**(19): p. 1756-1763.
78. Vrbka, M., et al., *Visualization of lubricating films between artificial head and cup with respect to real geometry.* Biotribology, 2015. **1–2**(0): p. 61-65.
79. Ottink, K., et al., *Survival, clinical and radiological outcome of the Zweymuller SL/Bicon-Plus total hip arthroplasty: a 15-year follow-up study.* Hip International, 2015. **25**(3): p. 204-208.
80. Hallan, G., S.A. Lie, and L.I. Havelin, *High wear rates and extensive osteolysis in 3 types of uncemented total hip arthroplasty - A review of the PCA, the Harris Galante and the profile/tri-lock*

*plus arthroplasties with a minimum of 12 years median follow-up in 96 hips.* Acta Orthopaedica, 2006. **77**(4): p. 575-584.
81. Samad, M.A. and S.K. Sinha, *Mechanical, thermal and tribological characterization of a UHMWPE film reinforced with carbon nanotubes coated on steel.* Tribology International, 2011. **44**(12): p. 1932-1941.
82. Brazier, B.G. and J.W. Mesko, *Superior rim fracture of a vitamin E-infused highly cross-linked polyethylene (HXLPE) liner leading to total hip arthroplasty revision.* Arthroplasty Today, 2018.

# 10 LIST OF FIGURES AND TABLES

# 11 LIST OF SYMBOLS AND ABBREVIATIONS

| | |
|---|---|
| 3D | Three dimensional |
| AHP | Artificial Hip Profiler |
| CoC | Ceramic on Ceramic |
| CT | Computer Tomography |
| DoF | Degree of Freedom |
| EBRA | Einzel Bild Röntgen Analyse |
| FEM | Finite Elements Method |
| MoM | Metal on Metal |
| MoP | Metal on Polyethylene |
| OECD | Organisation for Economic Cooperation and Development |
| PE | Polyethylene |
| RSA | Radiostereometric Analysis |
| SO | Small Object |
| STL | Stereolithographic file format |
| SD | Standard Deviation |
| THR | Total Hip Replacement |

# 12 APPENDIX A

**Wear and Roughness of Bearing Surface in Retrieved Polyethylene Bicon-Plus Cups**

RANUŠA, M., J.GALLO, M.HOBZA, M.VRBKA, D.NEČAS, and M. HARTL. Wear and Roughness of Bearing Surface in Retrieved Polyethylene Bicon-Plus Cups. *Acta Chirurgiae Orthopaedicae et Traumatologiae Cechoslovaca,* 2017, 84(3), 159–167.

*(Short English Version)*

**INTRODUCTION**

4,755 Bicon-Plus cups in total were implanted in the Czech Republic by the end of the December 2016. Some of them required revision surgery, while the most frequent reason of failure was polyethylene wear and aseptic loosening. This study focuses on surface analysis of retrieved polyethylene Bicon-Plus cups and on determination of the roughness of their bearing surfaces.

**MATERIAL AND METHODS**

Patients

We have studied 13 Bicon-plus implants extracted from 13 patients with total hip replacements during revision surgeries between years 2010 and 2016. The implants were made of the newest generation of high molecular polyethylene, the compression molded GUR 1020 (Ticona) produced according to the Standard ISO 5834-2. The implants were gamma-radiated (2,5 Mrad; 1 rad = 0,01 Gy) sterilized while sealed in a threefold pouch in a nitrogen atmosphere. The polyethylene were mechanically cleaned immediately after the extraction and sterilized in the Sekusept Aktiv solution (Ecolab GmbH, Düsseldorf, Německo) and later were dried and archived at standard room temperatures.

Wear measurement method

Wear of the articulating surfaces of the extracted polyethylene liners was measured using the optical scanning method and the ATOS Triple Scaner, produced by the GOM company. The method is described in detail in the study *Wear Analysis of Extracted Polyethylene Acetabular Cups Using a 3D Optical Scanner* presented in this disertation.

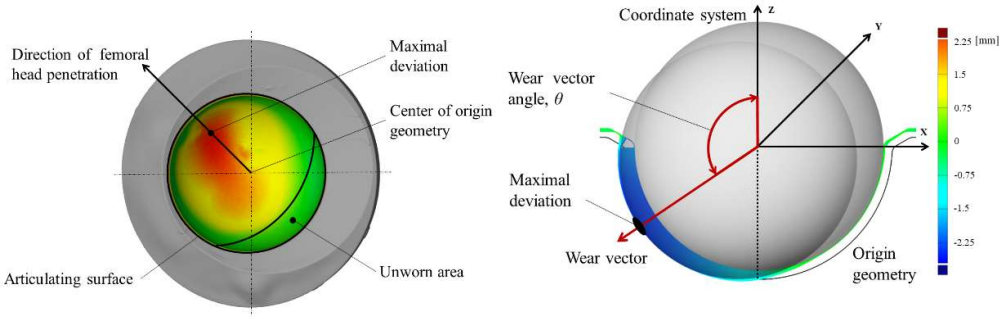


Roughness measurement method

The 3D optical profiler contour GT-X8 (Bruker, USA) was used to measure the surface roughness of the extracted implants. The measurements were based on the phase shifting interferometry technique. The measuring method allowed topography measurements with resolution down to 0,1 nm. The surface was scanned with lenses allowing 20-times zoom of the measured surface of 0,22 $mm^2$. The commercial machine was customized by installing a rotational stage allowing to position the samples in a polar coordinate system. Measurements resulted in creating a roughness map for each implant. Each quarter of the cup was measured at 19 defined points evenly distributed across the defined coordinate map. In sum, 76 roughness values were measured for each of the extracted implants. Ranges of roughness typical for different wear modes were determined. Three types of areas with distinctive surface roughness were recognized after analysing the surface morphology. Areas showing scoring from the manufacturing machines were identified as residual unworn areas showing no or only negligible wear. These areas showed roughness values that were lower than the roughness values of new cups, suggesting occurrence of certain surface smoothening as a result of articulation movements. The other two areas described the worn parts of the cups and the parts that are roughened with parallel striation caused by the cup/head contact. Waved surface with eventual delamination caused by plastic deformation was also observed. The measured surface roughness was described by the roughness parameter Ra, an arithmetic average value determined by deviations from the central line. The roughness values were sorted into several roughness ranges.

**RESULTS**

Surface wear

The average linear wear of the soft cup was 0,13 mm/year (SD = 0,06 mm/year). The average value of the volumetric wear was 44,37 $mm^3$/year (SD = 32,45 $mm^3$/year ). The measured data were compared with the clinical data of the patients. Graph describes relationship between the linear wear rate and the implants' survival time in situ. On a basic level, we would expect that the wear would increase proportionally with the survival time in situ. However, graph shows that the relationship is not

clearly linear. Relationship between the wear rate, survival time in situ and the body mass index (BMI) was examined in a similar way.

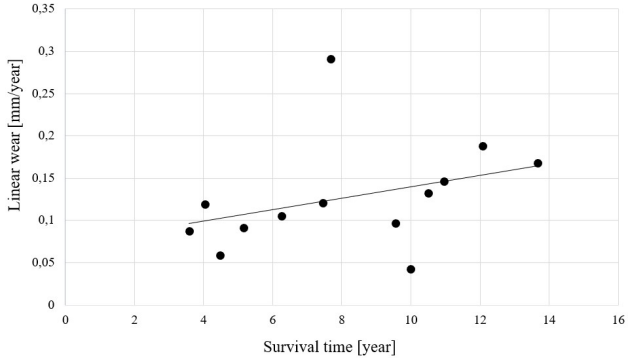


| No. | Size | Linear wear [mm] | Linear wear rate [mm/year] | Angle of wear vector [°] | Volumetric wear [mm³] | Volumetric wear rate [mm³/year] |
|---|---|---|---|---|---|---|
| 01 | 4/28 | 2,27 | 0,19 | 63,4 | 1119,7 | 92,66 |
| 02 | 5/28 | 1,39 | 0,13 | 59,3 | 528,97 | 50,38 |
| 03 | 4/28-Antilux. | 0,43 | 0,04 | - | 99,81 | 9,98 |
| 04 | 4/28 | 1,60 | 0,15 | 13,8 | 752,02 | 68,63 |
| 05 | 6/28 | 0,66 | 0,11 | - | 170,98 | 27,36 |
| 06 | 4/28 | 0,48 | 0,12 | 42,6 | 162,63 | 40,24 |
| 07 | 5/28 | 0,90 | 0,12 | - | 299,66 | 40,18 |
| 08 | 4/28-Antilux. | 2,24 | 0,30 | 59,3 | 966,92 | 125,85 |
| 09 | 3/28 | 2,29 | 0,17 | 53,0 | 584,86 | 42,79 |
| 10 | 5/28-Antilux. | 0,26 | 0,06 | 62,9 | 69,46 | 15,55 |
| 11 | 4/28-Antilux. | 0,47 | 0,09 | 20,8 | 152,98 | 29,66 |
| 12 | 7/28 | 0,31 | 0,09 | 33,1 | 51,80 | 14,46 |
| 13 | 4/28 | 0,92 | 0,10 | 67,8 | 182,05 | 19,06 |

Surface roughness

Surface topography of the extracted cups was measured on points evenly distributed across the whole articulating surface. The total roughness was defined as an arithmetic mean value of the measured values. The values were then ordered according to the frequency of their occurrence and assigned to categories defining several different modes of wear. This approach led to identification oh three different wear modes: (1) surfaces smoothened by the abrasive adhesive wear, (2), areas showing scoring from the manufacturing machines and (3) surfaces with plastic deformations.

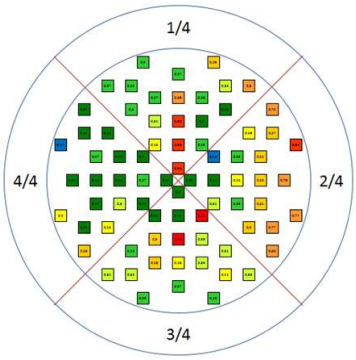


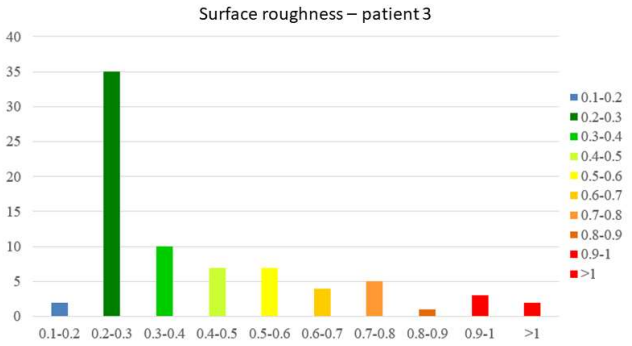


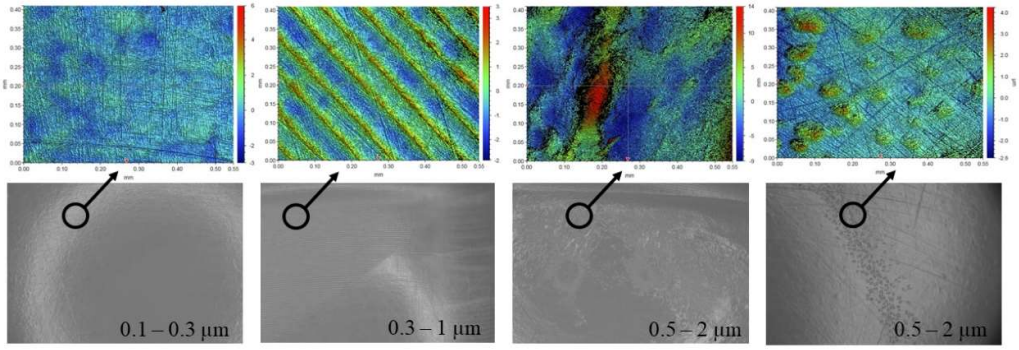


| Patient | Roughness [µm] | Roughness of articulating surface [µm] | | | | | | | | Type of wear |
|---|---|---|---|---|---|---|---|---|---|---|
| | | 0,1 – 0,3 | 0,3 – 0,4 | 0,4 – 0,5 | 0,5 – 0,6 | 0,6 – 0,7 | 0,7 – 0,8 | 0,9 - 1 | 1 < | |
| | | Smooth. | | | | | | | | |
| | | | Recognizable unworn area | | | Significant unworn area | | | | |
| | | | | | Plastic deformation, significant damages | | | | | |
| 01 | 0,33 | **58 %** | 17 % | | 12 % | | | | | Smoothening, unworn area, fatigue |
| 02 | 0,53 | **30 %** | 14 % | 18 % | | | | | | Smoothening, unworn area, fatigue |
| 03 | 0,42 | **46 %** | 13 % | | 9 % | | | | | Smoothening, unworn area, fatigue |
| 04 | 1,46 | | | | 9 % | 14 % | | | **55 %** | Smoothening, plastic deformation |
| 05 | 0,42 | **43 %** | 18 % | | | | | | 11 % | Smoothening, unworn area, fatigue |
| 06 | 0,46 | | 30 % | **37 %** | 24 % | | | | | Smoothening, unworn area, plastic deformation, cracks |
| 07 | 0,75 | | 18 % | 13 % | | | | | **26 %** | Smoothening, unworn area, plastic deformation, cracks |
| 08 | - | | | | | | | | | Delamination, edge damages |
| 09 | 0,63 | **34 %** | 33 % | | | | | | 28 % | Smoothening, unworn area, delamination |
| 10 | 0,70 | | | 13 % | **37 %** | 28 % | | | | Smoothening, unworn area, plastic deformation, delamination, edge damages |
| 11 | 0,45 | 20 % | **25 %** | 24 % | | | | | | Smoothening, unworn area, |
| 12 | 0,37 | 25 % | **53 %** | | | 9 % | | | | Smoothening, unworn area, delamination, edge damages |
| 13 | 0,51 | 41 % | **22 %** | | | | | 21 % | | Smoothening, unworn area |

**DISCUSSION**

Geometrical and topographical changes of the articulating surfaces were analyzed on 13 extracted Bicon implants with an average survival time in situ of 8,1 years (SD 3,2 years). The results were compared with the clinical data of the patients.

One of the analyzed parameters was the wear rate of the implants, defined as head/cup penetration speed in mm/year or $mm^3$/year. We found that the average linear wear rate were higher than 0,1 mm/year with prevalent abrasive/adhesive mode of wear. Other authors used radiographic methods and observed linear wear rates higher than 0,1 mm/year, too. This value is usually associated with a higher probability of osteolysis and aspetic loosening. In other words, the implant resisted osteolysis despite having met the basic conditions for this type of body reaction. Despite this, we recommend regular check and examinations of patients with Bicon-Plus cups, especially after the 10th year of the total hip replacement surgery.

The results clearly show increasing wear with longer survival time in situ. However, the relationship is not linear. That might be caused by a higher number of abrasive particles causing higher friction or higher surface wear in form of micro-cracks and oxidative degeneration of the polyethylene. However, it is necessary to note that data from 13 samples are not sufficient for making strong conclusions.

The highest deviations from the linear trend of the relationship between the wear rate and the survival time in situ were observed in patients with lower abduction angles of the implants. However, even these cups were positioned under abduction angles between 30° - 50°, recommended by other studies for the lowest wear of the articulating surfaces. Abduction angles outside this range lead to higher wear rates or cup fractions.

The analysis was supplemented with comparison of topographies of the articulating surfaces. Samples with the most frequent occurrence of roughness values between 0,1 – 0,3 µm are worth mentioning. These roughness values are typical for surfaces with extensive surface smoothening (compared to the roughness of the new cups) caused by articulating movements.
The smoothening effect is the result of the abrasive/adhesive wear with occurrence of parallel striation caused by the contact between the cup and the head. The polyethylene articulated with ceramic heads in our set. This type of wear was observed only in patients who did not suffer cup loosening and in several cases avoided micro scars – pitting or extensive surface delamination. The phenomenon was observed in implants with an average survival time in situ of 10,5 years (SD 2,5 years). However, plastic deformation and delamination can be related also to cup loosening. With this type of failure, changes of load direction can be assumed, eventually leading to collision of the cup's rim with the femoral head as was the case for several our patients. Another correlation identified in cups with prevalent roughness of 0,1 – 0,3 µm was a relatively large wear vector angle as measured by

the optical scanning method. Implants with the longest survival time in situ that did not loosened showed an average wear vector angle of 56,8° (SD 2,1°).

**CONCLUSION**

This paper analyses morphology of extracted Bicon-Plus cups. We found a relatively high wear rate of abrasive/adhesive wear mode. The relationship between wear and survival time in situ was not clearly linear, suggesting that other parameters might play role in the polyethylene wear. Despite this, we recommend regular check and examinations of patients with Bicon-Plus cups, especially after the 10th year of the total hip replacement surgery. Survival time of the implant in situ was also influenced by its position in the pelvis. It seemed to be a more important factor than were the other characteristics of the patients. Optical measurements showed influence of the wear vector on surface topography. The roughness was lower at higher angles, impacting mainly the stability of the cup and its survival time after the total hip replacement surgery.

PŮVODNÍ PRÁCE
ORIGINAL PAPER

# Opotřebení a drsnost artikulačního povrchu u extrahovaných polyetylenů jamky Bicon-Plus

## Wear and Roughness of Bearing Surface in Retrieved Polyethylene Bicon-Plus Cups

**M. RANUŠA[1], J. GALLO[2], M. HOBZA[2], M. VRBKA[1], D. NEČAS[1], M. HARTL[1]**

[1] Ústav konstruování, Fakulta strojního inženýrství, Vysoké učení technické v Brně
[2] Ortopedická klinika, Lékařská fakulta, Univerzita Palackého v Olomouci a Fakultní nemocnice Olomouc

## ABSTRACT

PURPOSE OF THE STUDY

By 7th December 2016, 4,755 Bicon-Plus cups in total were implanted in the Czech Republic. Some of them have been continuously re-operated, while the most frequent reason of failure is polyethylene wear and aseptic loosening. The present study is focused on surface analysis of retrieved polyethylene Bicon-Plus cups and the determination of the roughness of their bearing surfaces.

MATERIAL AND METHODS

In this study, we had 13 high molecular weight polyethylene cups with the average time *in situ* of 8.11 years (3.6–13.7, SD 3.2) before the retrieval. The study population was composed of 3 men, 10 women, with the mean age of 53.31 years. An optical scanning method, based on the principle of active triangulation, was used to determine wear rate. The rate of wear was identified by means of an obtained scan subsequently processed with the use of the GOM Inspect software. The roughness of surfaces was analysed with the application of Contour GT-X8 profiler using the principle of phase shifting interferometry. Measurements of surface topography of the retrieved cups were performed on the entire bearing surfaces. For the individual surface changes, a typical range of surface roughness, describing the particular wear character, was determined. By means of morphology analysis of the tested implants, three areas were identified: unworn area; area representing the worn part of the cup; and the area roughened by parallel grooving. The total surface roughness was evaluated as an arithmetic mean of the measured values. Subsequently, the values were sorted based on frequency and were classified into categories defining the particular wear mechanisms.

RESULTS

Wear rate of the retrieved acetabular cups was evaluated based on the wear direction vector and the size of linear wear. The average linear wear was equal to 0.13 mm/year (ranging from 0.26 to 2.29 mm/year), and the mean value of total volumetric material loss was 44.37 $mm^3$/year (the range being from 51.80 to 1,119.7 $mm^3$/year). Using the optical profilometer, a map of roughness distribution of the individual cups was obtained. For each implant, 76 values of roughness were evaluated. With the respect to average roughness, the samples were sorted to various categories describing: surface polishing; abrasive-adhesive wear; surfaces with preserved grooving; substantial plastic deformation.

DISCUSSION

The results clearly showed an increase of wear depending on implant survival; however, the tendency is not linear. This fact can be attributed to a larger amount of abrasive particles, causing an increase of wear or occurrence of surface wear in terms of micro cracks and oxidation degradation of polyethylene. This study indicates that geometry, positioning, and cup alignment during the implantation have a fundamental impact on the cup durability. Further correlation, which was observed in the case of the cup with prevailing roughness in the range from 0.1 to 0.3 μm, is a relatively wide wear vector angle determined with the use of the optical method. Considering the implants with the longest survival time with no loosening of the acetabular cup, the mean angle of direction vector was 56.8° (SD 2.1°).

CONCLUSIONS

The present study provides the results of morphology analysis of the retrieved Bicon-Plus cups. In general, relatively high wear rate, mainly of abrasive-adhesive character was identified. The dependence between wear and implant *in situ* longevity was not clearly linear, which suggests the influence of other parameters on the polyethylene wear rate. An important role of implant positioning on survival was also revealed. Moreover, it seems that it can be a more important parameter than the characteristics of the patient.

**Key words:** total hip arthroplasty, Bicon-Plus cup, retrieval analysis, surface analysis, wear measurement, roughness, deformation, survivorship.

Tento článek vznikl v rámci projektu LO1202 za finanční podpory MŠMT v rámci programu NPU I a v rámci projektu IGA MZ ČR 16-31852A a IGA_LF_2017_021.

## ÚVOD

Bikonická titanová šroubovací jamka byla uvedena do praxe koncem roku 1993 (Bicon-Plus®; Plus Orthopedics AG, Rotkreuz, Switzerland). Charakteristickým konstrukčním rysem této jamky jsou tenký plášť, lamelární závity a dvojitý kónus, který v porovnání s jednoduchým kónusem, například u jamky Alloclassic, šetří kost při frézování acetabula. Jamka má verzi standardní a tzv. porózní s rozšířeným povrchem zdrsnělého titanu. Podle firemních údajů jí bylo implantováno několik set tisíc. V literatuře lze nalézt studie s 10- a víceletým sledováním tohoto implantátu s výbornými klinickými výsledky a vynikajícím přežitím k 10. roku od operace (20, 28, 37). V české literatuře se jí věnovalo několik autorských týmů (2, 5, 24). Implantát se stále používá, a proto má smysl věnovat se výzkumu jeho výsledků.

Jamku Bicon používáme na naší klinice nepřetržitě od roku 1998 v primární a revizní indikaci, v posledních letech s polyetylenem RexPol (s vysokým stupněm síťování). V poslední době se setkáváme s aseptickým uvolněním implantátů, které jsme operovali v první dekádě tohoto století. Setkali jsme se také několikrát s její frakturou. Měření otěru polyetylenu se věnujeme dlouhodobě, vyvinuli jsme postupně kontaktní (9) i bezkontaktní metody (27) ke stanovení jeho míry na extrahovaných jamkách. Cílem této studie bylo změřit opotřebení extrahovaných polyetylenů u jamek Bicon-Plus a stanovit drsnost jejich artikulačního povrchu.

*Obr. 1. Aseptické uvolnění jamky Bicon.*

## MATERIÁL A METODIKA

### Pacienti

V letech 2010 až 2016 jsme reoperovali 51 jamek Bicon-Plus. Důvod k reoperaci byl 46x aseptický (aseptické uvolnění včetně centrální migrace jamky (obr. 1), opotřebení polyetylenu, periprotetické zlomeniny) a 5x byla kyčel reoperována pro infekci. Do studie s měřením extrahovaného polyetylenu jsme mohli zařadit 13 vyjmutých komponent od 13 pacientů, kterým jsme extrahovali polyetylenovou vložku TEP kyčle s jamkou Bicon-Plus. U ostatních byl povrch polyetylenu při vyprošťování z kovové části jamky buď výrazně poškozen, anebo se jamku nepodařilo archivovat podle níže uvedeného protokolu. Základní informace o pacientech shrnuje tabulka 1.

*Tab. 1. Základní klinické informace o pacientech*

| Číslo pacienta | Pohlaví | Rok narození | BMI | Strana | Datum implantace | Věk v době implantace | Primární diagnóza | Abdukční úhel [°] | Přežití implantátu [roky] | Stabilita implantátu | Důvod revize |
|---|---|---|---|---|---|---|---|---|---|---|---|
| 01 | m | 1947 | 24,24 | pravá | 9. 1. 2003 | 55 | PA | 50,6 | 12,08 | 1 | PPFF |
| 02 | ž | 1963 | 19,23 | pravá | 15. 4. 2001 | 37 | PD | 35,5 | 10,5 | 1 | asymptomatické, uvolnění dříku |
| 03 | ž | 1957 | 27,55 | levá | 5. 4. 2002 | 45 | PA | 35,7 | 10 | 1 | bolesti |
| 04 | ž | 1952 | 24,01 | pravá | 30. 9. 2002 | 50 | PA | 48 | 10,96 | 2 | bolesti |
| 05 | m | 1960 | 32,51 | pravá | 8. 11. 2005 | 45 | AVN | 46,4 | 6,25 | 0 | bolesti |
| 06 | ž | 1936 | 34,38 | pravá | 13. 1. 2010 | 73 | PA | 46 | 4,04 | 2 | bolesti |
| 07 | m | 1940 | 30,86 | levá | 4. 1. 2006 | 66 | PA | 48 | 7,46 | 1 | bolesti |
| 08 | ž | 1966 | 21,05 | levá | 15. 1. 2003 | 36 | PD | 34 | 7,68 | 2 | fraktura pláště jamky |
| 09 | ž | 1950 | 23,31 | pravá | 3. 3. 2000 | 50 | PA | 51 | 13,67 | 0 | bolesti |
| 10 | ž | 1960 | 26,77 | pravá | 7. 4. 2010 | 49 | PD | 35,5 | 4,47 | 2 | bolesti |
| 11 | ž | 1944 | 26,96 | levá | 13. 1. 2009 | 64 | PA | 63 | 5,16 | 2 | bolesti |
| 12 | ž | 1933 | 22,04 | pravá | 14. 2. 2007 | 73 | PA | 40 | 3,58 | 2 | bolesti |
| 13 | ž | 1951 | 29,05 | levá | 3. 10. 2001 | 50 | PA | 39 | 9,55 | 1 | bolesti |

*m = muž, ž = žena; * 0 = obě komponenty stabilní, 1 = stabilní jamka, nestabilní dřík, 2 = uvolněná jamka; AVN = avaskulární nekróza hlavice femuru; BMI = body mass index; PA = primární artróza; PD = postdysplastická artróza; PPFF = periprotetická fraktura femuru.*

### Polyetylenová vložka do jamky Bicon-Plus

Acetabulární vložka z vysokomolekulárního polyetylenu GUR 1020 (Ticona) byla vyrobena technologií „compression molded“ podle normy ISO 5834-2. Sterilizace probíhala gama zářením (2,5 Mrad; 1 rad = 0,01 Gy) v inertním prostředí dusíku. Zámek vložky fungoval výborně. Polyetylenová vložka artikulovala s keramickou hlavicí.

### Extrakce a archivování

Extrahované polyetyleny byly ihned po vyjmutí z těla mechanicky očištěny a sterilizovány v roztoku Sekusept Aktiv (Ecolab GmbH, Düsseldorf, Německo). Po vysušení a zabalení byly jamky archivovány za standardní pokojové teploty. Následně byly poslány do laboratoře spoluautorů k měření otěru.

### Metodika měření otěru

Pro stanovení otěru u artikulačních povrchů extrahovaných polyetylenových vložek byla použita optická skenovací metoda (21). Měření bylo realizováno s využitím skeneru ATOS Triple Scan od společnosti GOM. Princip metody je založený na aktivní triangulaci. Analyzovaný objekt je nasvícený úzkopásmovým modrým světlem, přičemž se využívá takzvaná proužková projekce. Využívaná technologie se nazývá „blue light technology“. Jednou z výhod této technologie je nezávislost na okolních světelných podmínkách (10). Obrazce promítané na objekt jsou snímány dvěma kamerami, které jsou uloženy ve skenovací hlavě. Ze získaných obrazů a na základě znalosti úhlu mezi snímacími kamerami je možné pomocí triangulačních algoritmů získat prostorové souřadnice jednotlivých bodů na skenovaném objektu

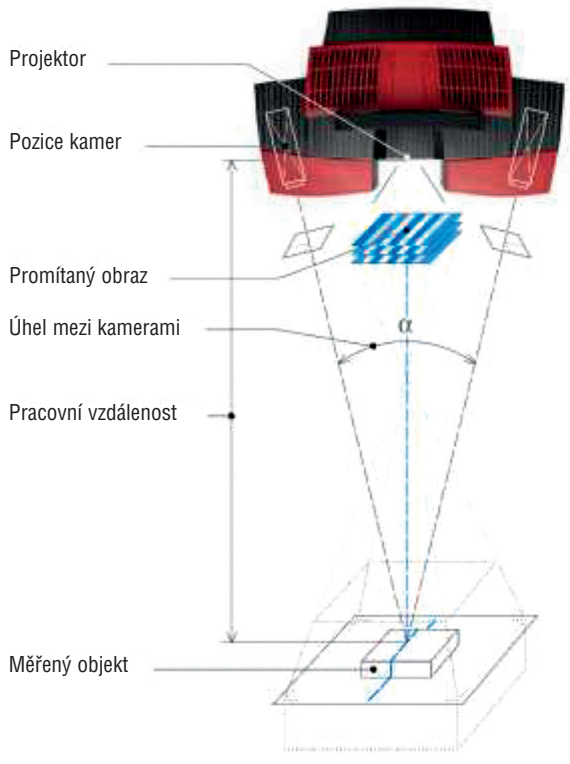


*Obr. 2. Schéma principu optického skenovaní.*

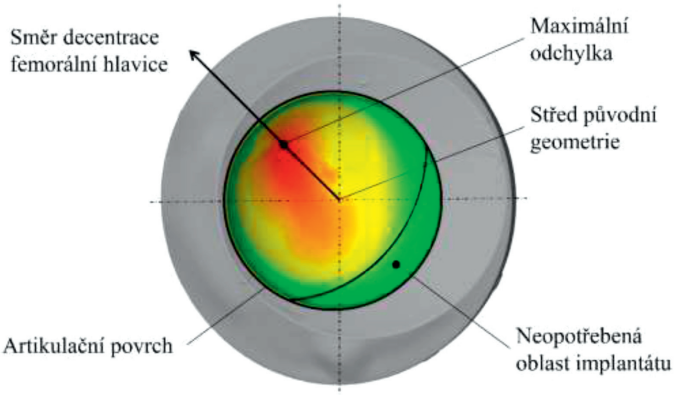


*Obr. 3. Odchylková mapa opotřebení extrahovaného implantátu.*

(obr. 2). Výsledkem skenovacího procesu je tak získání velkého počtu bodů na povrchu objektu. V případě skenování acetabulární jamky s průměrem 28 mm je na jejím artikulačním povrchu získáno přibližně 200 000 bodů. Hustota bodů poskytuje možnost přesnější vizualizace povrchu.

Následně jsou data polygonizována za pomoci software GOM Inspect, čímž je získána geometrie povrchu jamky. Tuto geometrii je možné dále editovat. V prvním kroku byla odstraněna všechna poškození způsobená chirurgem při explantaci, která do objemového úbytku jamky v těle pacienta nesmí být započítána. V dalším kroku byla odstraněna nadbytečná data, jako je například okolí analyzované jamky. K analýze byl zachovaný jen artikulační povrch explantátu a jeho blízké okolí. Následně jsou povrchová data transformována na objemové těleso.

Získaná geometrie byla následně proložená ideální koulí, takzvaným primitivem, o nominálním průměru odpovídajícím průměru neopotřebované části jamky. Tím bylo možné stanovit odchylky od ideální geometrie v jednotlivých směrech, a následně tak definovat neopotřebovanou oblast acetabulární jamky a směr nárůstu opotřebení. Na základě definovaného neopotřebovaného povrchu byla softwarově vytvořena rekonstrukce původní geometrie implantátu (obr. 3).

Model skenu extrahovaného implantátu byl následně porovnán s rekonstruovanou původní geometrií. Tímto postupem je možné stanovit množství úbytku materiálu v těle pacienta, směr nárůstu opotřebení a velikost decentrace femorální hlavice. Jedním z parametrů, který definuje rozsah opotřebení, je směrový vektor opotřebení, často také označovaný jako vektor decentrace, který je určen maximální odchylkou opotřebené artikulační oblasti vůči původní geometrii. Tento vektor svírá s vertikální osou jamky (osa z) takzvaný úhel vektoru decentrace (obr. 4), (26).

### Metodika měření drsnosti

Pro stanovení drsnosti povrchu extrahovaných jamek byl využit profilometr Contour GT-X8 od společnosti Bruker. Optický profilometr pracuje na principu interferometrie s řízenou změnou fáze. Profilometr využívá vlnovou délku světla pro porovnání optických drah světla mezi analyzovaným povrchem a referenčním po-

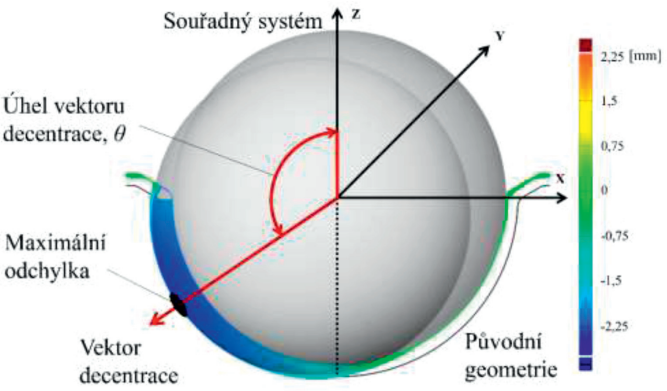


*Obr. 4. Stanovení vektoru decentrace femorální hlavice.*

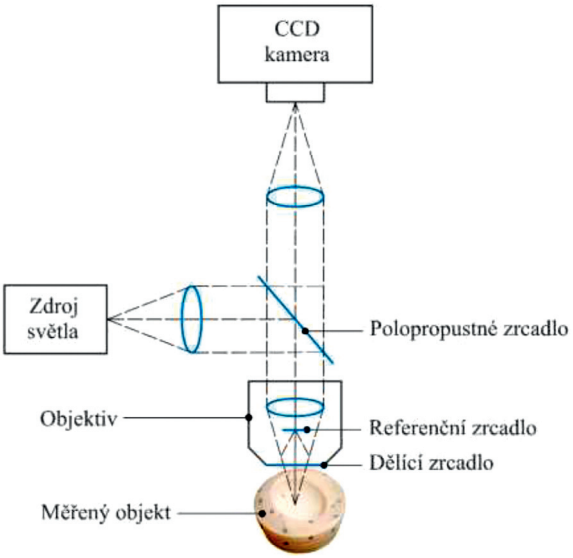


*Obr. 5. Schéma principu optické profilometrie.*

vrchem. Vyzařovaný světelný paprsek je rozdělen, přičemž jedna jeho část se odrazí od testovaného povrchu po průchodu objektivem a druhá část se odrazí od referenčního zrcadla. Na základě interference paprsků je možné následně vyhodnotit topografii povrchu, přičemž výsledný interferogram (obrazec interferujících paprsků) je snímaný CCD kamerou (obr. 5).

Metoda poskytuje měření topografie povrchu s rozlišením až 0,1 nm. Pro skenování povrchu byl použit objektiv s 20násobným zvětšením snímané plochy o velikosti 0,22 mm$^2$, což je dostatečné pro účely námi prováděných měření. U acetabulární jamky o průměru 28 mm docházelo při měření drsnosti v určitých bodech ke kolizi mezi jamkou a objektivem. Nutností tak bylo měřené jamky rozřezat na čtyři části a po měření data následně složit do komplexní mapy popisující topografii povrchu. Pro definici jednotlivých měřených bodů na povrchu jamky byl navržený polohovací přípravek umožňující natočení vzorku do konkrétní definované polohy, přičemž se využívá takzvaný polární souřadnicový systém.

Výsledkem měření na optickém profilometru je mapa rozložení drsností u jednotlivých explantátů. U každé čtvrtiny jamky bylo provedeno měření v 19 definovaných místech rovnoměrně rozložených podle stanovené souřadnicové mapy měření (obr. 6). Celkem tak bylo získáno 76 hodnot drsností pro každý extrahovaný implantát.

U jednotlivých povrchových změn bylo na základě struktury povrchu stanoveno typické rozmezí drsností popisující konkrétní charakter opotřebení. Analýzou morfologie povrchu testovaných náhrad byly stanoveny tři oblasti lišící se úrovní drsnosti povrchu. Jednu z oblastí lze popsat jako neopotřebenou. V této oblasti jsou jasně viditelné stopy po výrobním nástroji. Povětšinou se přitom jeví jako neopotřebované, případně bylo pozorováno jen jejich velmi omezené opotřebení. Drsnost této oblasti dosahuje hodnot nižších, než bylo naměřeno u jamek před opotřebením, což naznačuje, že v důsledku artikulace náhrady došlo k určitému vyhlazení povrchu (6, 13). Další dvě oblasti popisují opotřebenou oblast jamky a oblast zdrsněnou paralelním rýhováním způsobeným kontaktem jamky s povrchem hlavice. Z pozorování opotřebené oblasti bylo identifikováno zvlnění povrchu jamky a případná delaminace, která je přisuzována plastické deformaci (30). Měřená drsnost povrchu jamek byla popsána parametrem drsnosti Ra, tedy střední aritmetickou úchylkou profilu. Jednotlivé hodnoty drsnosti u každého explantovaného vzorku byly zařazené do rozmezí drsností (obr. 6).

## VÝSLEDKY

### Opotřebení povrchu

Na základě měření za pomoci optické skenovací metody byl u třinácti extrahovaných acetabulárních jamek stanoven směrový vektor opotřebení, velikost lineárního opotřebení a celkový objemový úbytek materiálu. Výsledky těchto parametrů jsou uvedeny v tabulce 2.

*Tab. 2. Geometrická analýza extrahovaných implantátů*

| Číslo pacienta | Velkost implantátu | Lineární opotřebení [mm] | Lineární opotřebení [mm/rok] | Úhel vektoru opotřebení [°] | Objemové opotřebení [mm$^3$] | Objemové opotřebení [mm$^3$/rok] |
|---|---|---|---|---|---|---|
| 01 | 4/28 | 2,27 | 0,19 | 63,4 | 1119,7 | 92,66 |
| 02 | 5/28 | 1,39 | 0,13 | 59,3 | 528,97 | 50,38 |
| 03 | 4/28-Antilux. | 0,43 | 0,04 | - | 99,81 | 9,98 |
| 04 | 4/28 | 1,60 | 0,15 | 13,8 | 752,02 | 68,63 |
| 05 | 6/28 | 0,66 | 0,11 | - | 170,98 | 27,36 |
| 06 | 4/28 | 0,48 | 0,12 | 42,6 | 162,63 | 40,24 |
| 07 | 5/28 | 0,90 | 0,12 | - | 299,66 | 40,18 |
| 08 | 4/28-Antilux. | 2,24 | 0,30 | 59,3 | 966,92 | 125,85 |
| 09 | 3/28 | 2,29 | 0,17 | 53,0 | 584,86 | 42,79 |
| 10 | 5/28-Antilux. | 0,26 | 0,06 | 62,9 | 69,46 | 15,55 |
| 11 | 4/28-Antilux. | 0,47 | 0,09 | 20,8 | 152,98 | 29,66 |
| 12 | 7/28 | 0,31 | 0,09 | 33,1 | 51,80 | 14,46 |
| 13 | 4/28 | 0,92 | 0,10 | 67,8 | 182,05 | 19,06 |

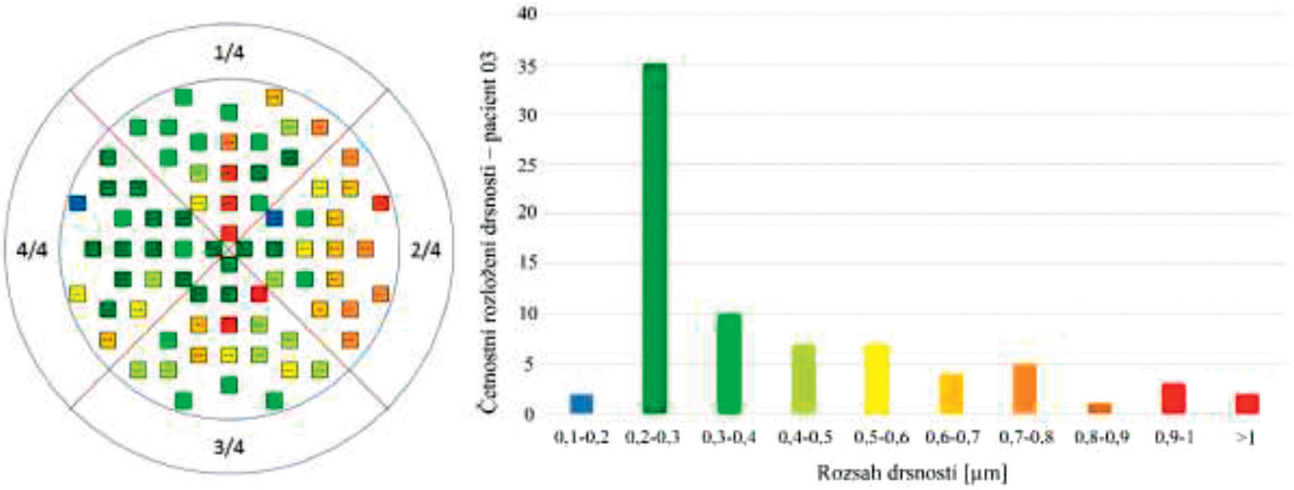


*Obr. 6. Měření drsnosti povrchu – pacient 03.*

Měření bylo u každého vzorku třikrát zopakováno a z naměřených hodnot byl stanoven aritmetický průměr. Průměrná rychlost lineárního otěru u měřených jamek byla 0,13 mm/rok (směrodatná odchylka, angl. standard deviation (SD) = 0,06 mm/rok). Průměrná hodnota objemového otěru byla 44,37 $mm^3$/rok (SD = 32,45 $mm^3$/rok). Získaná data byla porovnána s klinickými daty jednotlivých pacientů. Graf 1 popisuje závislost rychlosti lineárního opotřebení v závislosti na době přežití implantátu v těle pacienta. Na elementární úrovni lze očekávat, že opotřebení bude narůstat přímo úměrně s časem, po který je implantát přítomný v těle pacienta. Na základě výsledků uvedených v grafu 1 se však ukazuje, že závislost mezi rychlostí otěru a délkou používání implantátu lineární není. Podobně jsme stanovili závislost mezi rychlostí otěru, délkou implantátu in situ a body mass indexem (BMI), (graf 2, 3).

## Drsnost povrchu

Měření topografie povrchu na extrahovaných jamkách bylo realizované rovnoměrně po celém artikulačním povrchu. Celková drsnost povrchu byla stanovena aritmetickým průměrem naměřených hodnot. Následně byly hodnoty seřazeny podle četnosti a byly zařazeny do kategorie definující jednotlivé mechanismy opotřebení (tab. 3). Tímto způsobem je možné definovat vzorky, u kterých došlo k výraznému vyhlazení povrchu abrazivně adhezním opotřebením (obr. 7a), povrchy se zachovanými rýhami po výrobním nástroji (obr. 7b) a vzorky s výrazným plastickým poškozením (obr. 7c).

## DISKUSE

U souboru 13 vzorků extrahovaných implantátů Bicon s průměrnou délkou přežití 8,1 roku (SD 3,2 roku) byly analyzovány geometrické a topografické změny artikulačních povrchů. Získané výsledky byly následně hodnoceny v porovnání s dostupnými klinickými daty pacientů.

*Graf 1. Závislost lineárního opotřebení na době přežití implantátu*

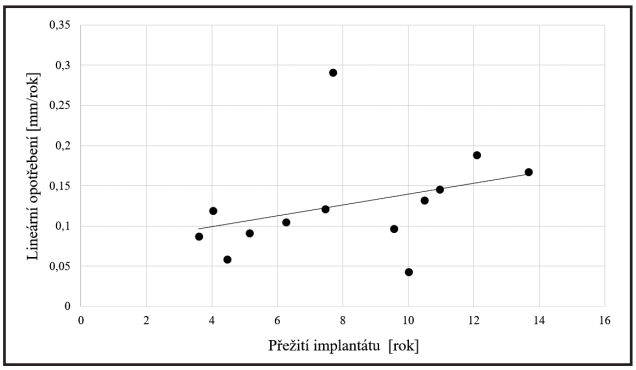


*Graf 2. Závislost objemového opotřebení na BMI*

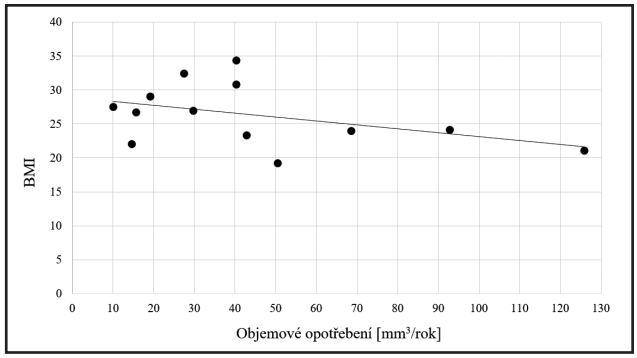


*Graf 3. Závislost přežití implantátu na BMI*

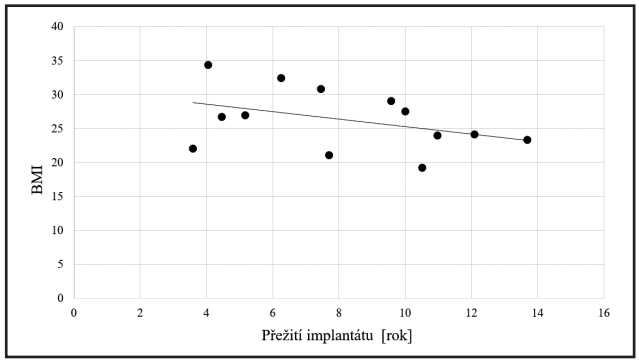

*Tab. 3. Vyhodnocení drsností artikulačních povrchů u extrahovaných jamek*

| Číslo pacienta | Průměrná drsnost [μm] | Drsnost artikulujícího povrchu [μm] 0,1–0,3 | 0,3–0,4 | 0,4–0,5 | 0,5–0,6 | 0,6–0,7 | 0,7–0,8 | 0,9–1 | 1 < | |
|---|---|---|---|---|---|---|---|---|---|---|
| | | Vyhlaz. | | | | | | | | |
| | | | Znatelné rýhy po nástroji | | | Výrazné rýhy po nástroji | | | | |
| | | | | | Plastické deformace, znatelné poškození | | | | | |
| 01 | 0,33 | **58 %** | 17 % | | 12 % | | | | | Vyhlazení, stopy po obrábění, pitting |
| 02 | 0,53 | **30 %** | 14 % | 18 % | | | | | | Vyhlazení, stopy po obrábění, pitting |
| 03 | 0,42 | **46 %** | 13 % | | 9 % | | | | | Vyhlazení, stopy po obrábění, pitting |
| 04 | 1,46 | | | | 9 % | 14 % | | | **55 %** | Vyhlazení, výrazné plastické deformace |
| 05 | 0,42 | **43 %** | 18 % | | | | | | 11 % | Vyhlazení, stopy po obrábění, počátek pittingu |
| 06 | 0,46 | | 30 % | **37 %** | 24 % | | | | | Vyhlazení, stopy po obrábění, plastické deformace, trhliny |
| 07 | 0,75 | | 18 % | 13 % | | | | | **26 %** | Vyhlazení, stopy po obrábění, plastické deformace, trhliny |
| 08 | – | | | | | | | | | Delaminace povrchu, hranové poškození |
| 09 | 0,63 | **34 %** | 33 % | | | | | | 28 % | Vyhlazení, stopy po obrábění, delaminace povrchu |
| 10 | 0,70 | | | 13 % | **37 %** | 28 % | | | | Vyhlazení, stopy po obrábění, plastické deformace, delaminace, hranové poškození |
| 11 | 0,45 | 20 % | **25 %** | 24 % | | | | | | Vyhlazení, stopy po obrábění |
| 12 | 0,37 | 25 % | **53 %** | | | 9 % | | | | Vyhlazení, stopy po obrábění, delaminace, hranové poškození |
| 13 | 0,51 | 41 % | **22 %** | | | | | 21 % | | Vyhlazení, stopy po obrábění |

Jednou z porovnávaných veličin je rychlost lineárního opotřebení implantátu stanovená jako rychlost vnoření femorální hlavice do polyetylenové jamky vyjádřená v mm/rok, případně $mm^3$/rok. Z literatury i z vlastní zkušenosti víme, že hodnocený implantát má vynikající přežití (tab. 4), (12, 16, 20, 29, 31, 37). V naší práci jsme zjistili průměrnou rychlost otěru polyetylenu vyšší než 0,1 mm/rok a převážně abrazivně adhezní typ otěru. Také další autoři změřili na rentgenových snímcích rychlost otěru vyšší než 0,1 mm/rok (tab. 5), což by měla být hodnota sdružená s vyšší pravděpodobností výskytu periprotetické osteolýzy a aseptického uvolnění (4). Jinými slovy, tento implantát se zjevně dokázal ubránit rozvoji osteolýzy, přestože základní podmínka rozvoje této reakce byla splněna. Přesto doporučujeme pacienty s jamkou Bicon-Plus a starším polyetylenem pravidelně kontrolovat, a to zejména po desátém roce od operace.

Z výsledků je jasně pozorovatelný nárůst opotřebení s délkou přežití implantátu, kdy se však nejedná o závislost lineární (graf 1). Tento jev může být způsobený vyšším počtem abrazivních částic způsobujících zvýšení tření, případně výskyt povrchového opotřebení ve formě mikrotrhlin a oxidační degradace polyetylenu (6, 7). Procesy opotřebení může ovlivňovat dále také různá velikost a tvar otěrových částic (36). Je však třeba zdůraznit, že bylo analyzováno pouze 13 vzorků, což nemusí být pro vyvození jasných závěrů dostatečné množství. Nejvyšší odchylky od lineárního trendu nárůstu opotřebení v porovnání s dobou přežití byly pozorovány u pacientů

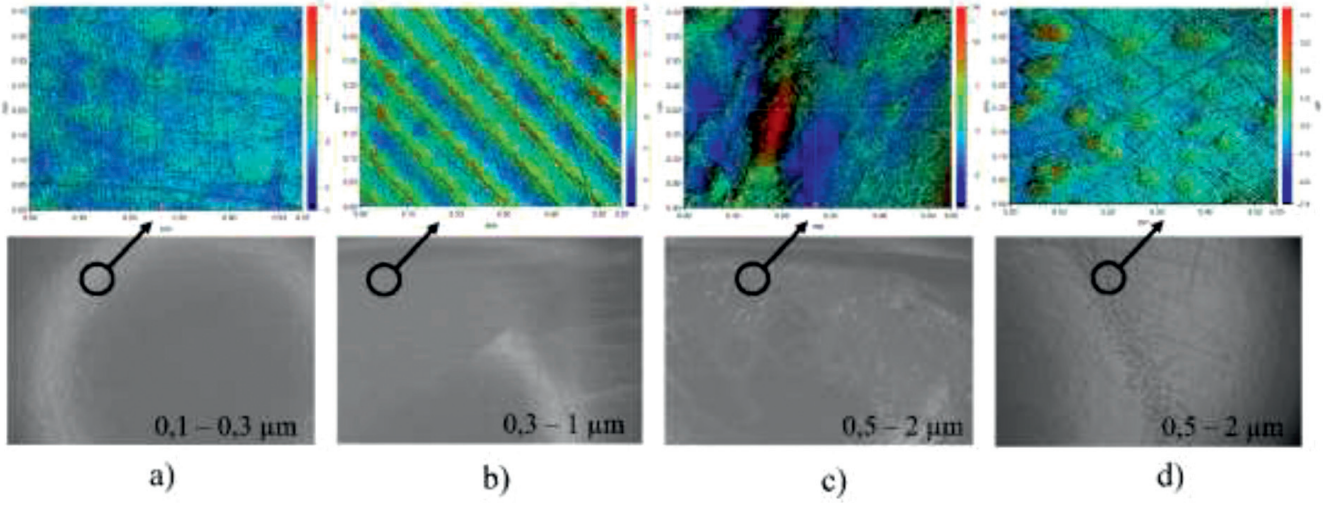


*Obr. 7. Typy opotřebení na explantovaných vzorcích.*

*Tab. 4. Přehled studií referujících přežití TEP Bicon-Plus*

| Autor | Počet kyčlí | Délka sledování (roky) | Přežití k 10. roku od operace | Výskyt AU | Výskyt PPOL |
|---|---|---|---|---|---|
| Zweymuller, 2007 | 232 | 10 | 99,3 % (96,9 – 99,8 %) *# | 0 | 1/232; 0,43 % |
| Veen, 2016 | 125 | 7 | 99,2 % # ** | 1/125; 0,80 % | – |
| Topolovec, 2014 | 587 | 11 | 96,1 % (94,3 – 97,9 %) *# | 13/587; 2,21 % | 13/587; 2,21 %§ |
| Milošev, 2012 | 200 | 10 | 98,4 % (96,6 – 100 %) *# | 1/200; 0,5 % | 0 § |
| Korovessis, 2011 | 153 | 11 | 97,5 % (94,0 – 99,0 %) * | 4/153; 2,61 % | 6,54 % |
| Schmolders, 2016 | 81 | 13,5 | 96,8 % (90,5 – 98,9 %) *# | 4/81; 4,94 % | 12/81; 14,81 % |
| Ottink, 2015 | 218 | 14,4 | 97 % (0,95 – 0,99 %) *# | 7/218; 3,21 % | – |

*AU = aseptické uvolnění, PPOL = periprotetická osteolýza, # = reoperace z jakéhokoliv důvodu, * = v závorce je uveden 95% interval spolehlivosti, ** = přežití k 7. roku, § = osteolýza hodnocena jen u revidovaných pacientů.*

*Tab. 5. Rychlost otěru polyetylenu u jamky Bicon-Plus*

| Autor | Počet kyčlí | Délka sledování (roky) | Kloubní pár | Průměr hlavičky | Metoda měření | Lineární otěr (mm) | Lineární otěr (mm/R) |
|---|---|---|---|---|---|---|---|
| Zweymuller, 2007 | 232 | 10 | Ker-PE | ? | Hall | 1,33 ± 0,66 | 0,13 |
| Ottink, 2015 | 218 | 14,4 | Ker-PE | 32 mm | Rogan-Delft software | 1,80 | 0,12 |
| Korovessis, 2011 | 153 | 11 | Ker-PE | 28 mm | Diagnostic PRO Advantage | – | 0,059 ± 0,06 |

*Ker = keramika; PE = polyetylen; R = rok; ? = není explicitně uvedeno.*

s menším abdukčním úhlem náhrady, přičemž však i u těchto jamek je hodnota abdukčního úhlu v rozsahu 30°–50°, kdy by na základě studií (14, 15, 35) mělo docházet k nejmenšímu opotřebení artikulační vložky. Uložení mimo optimální rozsah je spjato s vyšší rychlostí otěru, případně s poškozením jamky frakturou.

Mnohem méně víme o reálném rozložení a velikosti síly působící na kloub při zátěži a o způsobu zatěžování jednotlivými pacienty. Tento fakt do velké míry ovlivňuje přežití náhrady v důsledku opotřebení, případně jejího uvolnění. Doposud však nebyla publikována práce, která by porovnávala reálné parametry zatěžování kloubní soustavy při běžných aktivitách v souvislosti s objemovým opotřebením implantátu. Jedná se pouze o simulace jednotlivých stavů za pomoci numerických metod. Tato studie se snaží poukázat na fakt, že geometrie, poloha a způsob uložení jamky při její implantaci mají zásadní vliv na její životnost. Dalšími parametry, které rovněž nelze opomenout, je konkrétní materiálová kombinace, případně velikost implantátu (33).

Následně byla data rozšířena o porovnání topografie artikulačního povrchu. U těchto výsledků je nutné poukázat na vzorky, kde byla zaznamenána největší četnost drsností v rozsahu 0,1–0,3 μm (tab. 3). Tato hodnota drsnosti je vykazována u povrchů, kde došlo v důsledku proběhlé artikulace k výraznému vyhlazení povrchu oproti drsnosti dosažené při výrobě jamky. Jde přitom o mechanismus abrazivně adhezního opotřebení s přítomností významných paralelních rýh od kovové femorální hlavice (25). V našem souboru však polyetylen artikuloval s keramickou hlavičkou. Toto opotřebení bylo pozorováno výhradně u pacientů, kde nedošlo k uvolnění jamky, a ve vícero případech předcházelo vzniku mikrotrhlin – pittingu (obr. 7d) či odlupování větších povrchových vrstev (obr. 7c). Tento jev je možné pozorovat u implantátů s průměrnou dobou přežití 10,5 roku (SD 2,5 roku). Avšak plastická deformace a delaminace materiálu mohou souviset také s uvolněním jamky. U tohoto typu selhání je možné předpokládat změny směru zatěžování, které mohou způsobovat tento důsledek a případně vést až ke kolizi okraje jamky s krčkem femorální hlavice, což se projevilo u některých našich pacientů (konkrétně u pacientů č. 08, 10, 12). Změna rozložení tlaku vlivem natočení vložky je popsána v několika studiích (11, 23).

Další korelací, která je identifikována u jamek s převažující drsností v rozsahu 0,1–0,3 μm, je poměrně velký úhel vektoru opotřebení stanovený za pomoci optické metody. U implantátů s nejdelší dobou přežití, u kterých současně nedošlo k uvolnění acetabulární jamky, byl stanovený průměrný úhel směrového vektoru 56,8° (SD 2,1°). Tyto výsledky jsou unikátní, a nemůžeme je proto porovnat s literárními údaji. Z hlediska biotribologických procesů vyplývajících z pozorování je přežití implantátu spojené tedy i se strukturou povrchu. V běžných podmínkách, kdy je implantát uložený do těla v rozmezí doporučovaných abdukčních úhlů, a za předpokladu stability implantátu dochází k rovnoměrnému opotřebení a vyhlazování povrchu.

Metody schopné testovat parametry konkrétního souboru extrahovaných implantátů můžeme v uvedeném kontextu chápat jako nezbytné analytické nástroje pro zpětné hodnocení procesů opotřebení TEP kyčle. Z hlediska geometrie náhrady hraje dále velmi podstatnou roli i velikost průměrové vůle. Studie (1) se zabývala vlivem velikosti vůle na koeficient tření mezi povrchy, kdy byl pozorován trend snižujícího se tření se snižující se vůlí mezi komponentami. Stejné chování bylo popsáno i v další literatuře (3), kdy byl zaznamenán pokles opotřebení u dvojic s menší vůlí. Tento efekt byl pozorován jak v případě 36 mm, tak 54 mm implantátu. S ohledem na vliv průměru tak autoři konstatovali, že velikost implantátu by měla být co možná největší při zachování co možná nejmenší průměrové vůle. V této souvislosti je

třeba také zmínit problematiku mazání, která má bezpochyby na opotřebení implantátů zásadní vliv. Z tohoto pohledu je rozhodující především tloušťka mazacího filmu (32) a adsorpce proteinů na třecí povrchy (22). Přitom bylo v literatuře poukázáno na fakt, že utváření proteinového mazacího filmu mezi komponentami náhrady je ovlivněno jak materiálovou kombinací (18, 19), tak geometrií (34), a především pak velikostí náhrady a průměrovou vůlí (17). Rovněž je třeba vzít v úvahu složení synoviální kapaliny, která se liší v závislosti na mnoha faktorech, jako je pohlaví, věk, zdravotní stav apod. (8).

Pokud jde o limitace provedené studie, je třeba zmínit zejména malý soubor analyzovaných implantátů. Dále by bylo nepochybně vhodné doplnit povrchové analýzy o stanovení oxidačního indexu extrahovaných polyetylenů. Tuto metodu však v současné době nemáme k dispozici.

## ZÁVĚR

V této práci předkládáme výsledky morfologické analýzy extrahovaných jamek Bicon-Plus. Zjistili jsme relativně vysokou rychlost otěru, který byl převážně abrazivně adhezního typu. Závislost mezi otěrem a délkou implantátu *in situ* nebyla jednoznačné lineární, což ukazuje na vliv dalších parametrů na rychlost opotřebení polyetylenu. Přesto doporučujeme pacienty s tímto implantátem pravidelně sledovat, zvláště po 10. roce od operace. Důležitý vliv na celkové přežití implantátu má také jeho poloha po implantaci. Zdá se dokonce, že jde o významnější parametr, nežli jsou charakteristiky pacienta. Z optických měření je možné pozorovat vliv směrového vektoru opotřebení na topografii povrchu. Při vyšších úhlech byla celková stanovená drsnost menší, což se projevilo hlavně na stabilitě jamky, a tím i na jejím přežití po implantaci.

### Literatura

1. Brockett CL, Harper P, Williams S, Issac GH, Dwyer-Joyce RS, Jin Z, Fisher J. The influence of clearance on friction, lubrication and squeaking in large diameter metal-on-metal hip replacements. J Mater Sci Mater M. 2008;19:1575–1579.
2. Cichy Z. [Treatment of dysplastic acetabulum using total hip arthroplasty: our intermediate-term results]. Acta Chir Orthop Traumatol Cech. 2006;73:340–344.
3. Dowson D, Hardaker C, Flett M, Isaac GH. A hip joint simulator study of the performance of metal-on-metal joints – Part II: Design. J Arthroplasty. 2004;19:124–130.
4. Dumbleton JH, Manley MT, Edidin AA. A literature review of the association between wear rate and osteolysis in total hip arthroplasty. J Arthroplasty. 2002;17:649–661.
5. Dungl P, Stedry V, Hajny P. [Medium-term Experience with Zweymuller's Bicon Plus Cup in the Treatment of Postdysplastic Osteoarthritits of the Hip Joint.]. Acta Chir Orthop Traumatol Cech. 2000;67:88–92.
6. Edidin AA, Rimnac CM, Goldgber VM, Kurtz SM. Mechanical behavior, wear surface morphology, and clinical performance of UHMWPE acetabular components after 10 years of implantation. Wear. 2001;250:152–158.
7. Fulín P, Pokorný D, Šlouf M, Nevoralová M, Vacková T, Dybal J, Kaspřiková N, Landor I. [Analysis of Oxidative Damage to Components Removed from Beznoska/Poldi Total Hip Replacements]. Acta Chir Orthop Traumatol Cech. 2016;83:155–162.
8. Galandáková A, Ulrichová J, Langová K, Hanáková A, Vrbka M, Hartl M, Gallo J. Characteristics of synovial fluid required for optimization of lubrication fluid for biotribological experiments. J Biomed Mater Res Part B Appl Biomater. 2016.
9. Gallo J, Havranek V, Cechova I, Zapletalova J. Wear measurement of retrieved polyethylene ABG 1 cups by universal-type measuring microscope and X-ray methods. Biomed Pap Med Fac Univ Palacky Olomouc Czech Repub. 2006;150:321–326.
10. GOM. GOM mbH, ATOS - Industrial 3D Scanning Technology. Available at: http://www.gom.com/metrology-systems/3d-scanner.html.
11. Korhonen RK, Koistinen A, Konttinen YT, Santavirta SS, Lappalainen R. The effect of geometry and abduction angle on the stresses in cemented UHMWPE acetabular cups - Finite element simulations and experimental tests. Biomed Eng Online. 2005;4:32.
12. Korovessis P, Repantis T, Zafiropoulos A. High medium-term survivorship and durability of Zweymuller-Plus total hip arthroplasty. Arch Orthop Traum Su. 2011;131:603–611.
13. Kurtz SM, Turner J, Herr M, Edidin AA, Rimnac CM. Assessment of surface roughness and waviness using white light interferometry for short-term implanted, highly crosslinked acetabular components. In: Kurtz SM, Gsell, RA, Martell, J, (eds). Crosslinked and thermally treated ultra-high molecular weight polyethylene for joint replacements. ASTM International, West Conshohocken, 2004, pp 41–56.
14. Little NJ, Busch CA, Gallagher JA, Rorabeck CH, Bourne RB.Acetabular Polyethylene Wear and Acetabular Inclination and Femoral Offset. Clin Orthop Relat R. 2009;467:2895–2900.
15. McBride A, Flynn J, Miller G, Barnes M, Mackie S. Body mass index and acetabular component position in total hip arthroplasty. ANZ J Surg. 2013;83:171–174.
16. Milosev I, Kovac S, Trebse R, Levasic V, Pisot V. Comparison of ten-year survivorship of hip prostheses with use of conventional polyethylene, metal-on-metal, or ceramic-on-ceramic bearings. J Bone Joint Surg Am. 2012;94:1756–1763.
17. Nečas D, Vrbka M, Urban F, Křupka I, Hartl M. The effect of lubricant constituents on lubrication mechanisms in hip joint replacements. J Mech Behav Biomed. 2016;55:295–307.
18. Nečas D, Vrbka M, Křupka I, Hartl M, Galandáková A. Lubrication within hip replacements - Implication for ceramic-on-hard bearing couples. J Mech Behav Biomed. 2016;61:371–383.
19. Nečas D, Vrbka M, Urban F, Křupka I, Hartl M. The effect of lubricant constituents on lubrication mechanisms in hip joint replacements. J Mech Behav Biomed. 2015;55:295–307.
20. Ottink K, Barnaart L, Westerbeek R, van Kampen K, Bulstra S, van Jonbergen HP. Survival, clinical and radiological outcome of the Zweymuller SL/Bicon-Plus total hip arthroplasty: a 15-year follow-up study. Hip Int 2015;25:204–208.
21. Palousek D, Omasta M, Koutny D, Bednar J, Koutecky T, Dokoupil F. Effect of matte coating on 3D optical measurement accuracy. Opt Mater. 2015;40:1–9.
22. Parkes M, Myant C, Cann PM, Wong JSS. The effect of buffer solution choice on protein adsorption and lubrication. Tribol Int. 2014;72:108–117.
23. Patil S, Bergula A, Chen PC, Colwell JR, CW, D'Lima DD. Polyethylene wear and acetabular component orientation. J Bone Joint Surg A. 2003;85:56–63.
24. Pavelka T, Linhart M, Houček P. [Hip joint arthroplasty following surgical treatment of acetabular fracture]. Acta Chir Orthop Traumatol Cech. 2006;73:268–274.
25. Pruitt LA, Chakravartula AM. Mechanics of biomaterials: Fundamental principles for implant design. Cambridge University Press, New York, 2011.
26. Ranuša M, Gallo J, Vrbka M, Hobza M, Paloušek D, Křupka I, Hartl M. Wear analysis of extracted polyethylene acetabular cups using a 3D optical scanner. Tribol Trans. 2017;60:437–447.
27. Rossler T, Mandat D, Gallo J, Hrabovsky M, Pochmon M, Havranek V. Optical 3D methods for measurement of prosthetic wear of total hip arthroplasty: principles, verification and results. Opt Express. 2009;17:12723-12730.
28. Schmolders J, Amvrazis G, Pennekamp PH, Strauss AC, Friedrich MJ, Wimmer MD, Rommelspacher Y, Wirtz DC, Wallny T. Thirteen year follow-up of a cementless femoral stem and a threaded

acetabular cup in patients younger than fifty years of age. Int Orthop. 2017;41:39–45.
29. Topolovec M, Milosev I. A comparative study of four bearing couples of the same acetabular and femoral component: a mean follow-up of 11.5 years. J Arthroplasty. 2014;29:176-180.
30. Trommer RM, Maru MM, Oliveira Filho WL, Nykanen VPS, Gouvea CP, Archanjo BS, Martins Ferreira EH, Silva RF, Achete CA. Multi-scale evaluation of wear in UHMWPE-metal hip implants tested in a hip joint simulator. Biotribology. 2015;4:1–11.
31. Veen EJ, Schrier JC, Van'T Riet E, Breslau MJ, Barnaart AF. Outcome of the cementless Zweymuller BICON-PLUS Cup and SL-PLUS stem in the very elderly individuals. Geriatr Orthop Surg Rehabil. 2016;7:74–80.
32. Vrbka M, Návrat T, Křupka I, Hartl M, Šperka P, Gallo J. Study of film formation in bovine serum lubricated contacts under rolling/sliding conditions. P I Mech Eng J-J Eng Tribol. 2013;227:459–475.
33. Vrbka M, Nečas D, Bartošiík J, Hartl M, Křupka I, Galandáková A, Gallo J. [Determination of a friction coefficient for THA bearing couples]. Acta Chir Orthop Traumatol Cech. 2015;82:341–347.
34. Vrbka M, Nečas D, Hartl M, Křupka I, Urban F, Gallo J. Visualization of lubricating films between artificial head and cup with respect to real geometry. Biotribology. 2015;1–2:61–65.
35. Wan Z, Boutary M, Dorr LD. The Influence of Acetabular Component Position on Wear in Total Hip Arthroplasty. J Arthroplasty. 2008;23:51–56.
36. Zolotarevova E, Entlicher G, Pavlova E, Slouf M, Pokorny D, Vesely F, Gallo J, Sosna A. Distribution of polyethylene wear particles and bone fragments in periprosthetic tissue around total hip joint replacements. Acta Biomater. 2010;6:3595–3600.
37. Zweymuller KA, Steindl M, Schwarzinger U. Good stability and minimal osteolysis with a biconical threaded cup at 10 years. Clin Orthop Relat Res. 2007;463:128–137.

**Korespondující autor:**
prof. MUDr. Jiří Gallo, Ph.D.
Ortopedická klinika LF UP a FNOL
I. P. Pavlova 6
779 00 Olomouc
E-mail: jiri.gallo@volny.cz